FLORIDA INTERNATIONAL UNIVERSITY

Miami, Florida

IMPROVED SAMPLING, PRE-CONCENTRATION, AND DETECTION OF HIDDEN EXPLOSIVES AND ILLICIT DRUGS BY A NOVEL SOLID PHASE MICROEXTRACTION GEOMETRY COUPLED TO ION MOBILITY SPECTROMETRY

A dissertation submitted in partial fulfillment of the

requirements for the degree of

DOCTOR OF PHILOSOPHY

in

CHEMISTRY

by

Patricia Diaz

2010

To: Dean Kenneth Furton
College of Arts and Sciences

This dissertation, written by Patricia Diaz, and entitled Improved Sampling, Pre-Concentration, and Detection of Hidden Explosives and Illicit Drugs by a Novel Solid Phase Microextraction Geometry Coupled to Ion Mobility Spectrometry, having been approved in respect to style and intellectual content, is referred to you for judgment.

We have read this dissertation and recommend that it be approved.

Yong Cai

Kenneth Furton

John Landrum

Wenzhi Li

Jose Almirall, Major Professor

Date of Defense: March 11, 2010

The dissertation of Patricia Diaz is approved.

Dean Kenneth Furton
College of Arts and Sciences

Interim Dean Kevin O'Shea
University Graduate School

Florida International University, 2010

DEDICATION

To my dad, Vicente Guerra, with all my love.

ACKNOWLEDGMENTS

I would first like to extend my deepest gratitude to Dr. José Almirall, my major professor, for believing in me ever since I began work at his laboratory as an undergraduate researcher, and for continually challenging me for the better. As Dr. Almirall's student, I had many unique opportunities to present at conferences around the country, where I was able to interact with the scientific community, build networks, and mature as a scientist. I am eternally grateful for all the knowledge he has imparted, his example of work ethic, and his support and encouragement throughout the years. I would like to thank Dr. Sigalit Gura whom I have had the privilege of conducting research with while she was on sabbatical. I gained so much from her expertise, but most of all I gained a friend. I would like to thank my committee members, Dr. John Landrum, Dr. Yong Cai, Dr. Wenzhi Li and Dr. Kenneth Furton, for all their insightful contributions to the research and for always being available and eager to help. Dr. John Landrum provided valuable advice on the characterization of the La (dihed) complex. Past committee members, Dr. Alberto Sabucedo, Dr. Eric Crumpler, and Dr. Jiandi Zhang are also acknowledged. I would like to thank Thao Dang for help with the synthesis of La (dihed) and Dr. Stainslaw Wnuk for allowing me to use his laboratory. Ya Li Hsu and Dr. Yaru Song are thanked for their help with the NMR and DI-MS, respectively. I would like to thank my many past and present lab mates, especially Dr. Jeannette Perr, Hanh Lai, Tatiana Trejos, Dr. Maria Mendoza, Sayuri Umpierrez, Dr. Waleska Castro, Dr. Benjamin Naes, Howard Holness, Wen Fan and Mimy Young. My friends Paola Prada, Lucy Yehiayan, and Urooj Khan have helped make my time at FIU both fun and intellectually stimulating. I would also like to thank my husband, Jorge Diaz, and my precious family for all their love and

support. This work has been funded by the National Institutes of Justice, a grant from Sensor Concepts and Applications, a doctoral fellowship from the Kauffmann Foundation and the Dissertation Year Fellowship from the University Graduate School.

ABSTRACT OF THE DISSERTATION

IMPROVED SAMPLING, PRE-CONCENTRATION, AND DETECTION OF HIDDEN EXPLOSIVES AND ILLICIT DRUGS BY A NOVEL SOLID PHASE MICROEXTRACTION GEOMETRY COUPLED TO ION MOBILITY SPECTROMETRY

by

Patricia Diaz

Florida International University, 2010

Miami, Florida

Professor: José Almirall, Major Professor

The 9/11 Act mandates the inspection of 100 % of cargo shipments entering the U.S by 2012 and 100 % inspection of air cargo by March 2010. So far, only 5% of inbound shipping containers are inspected thoroughly while air cargo inspections have fared better at 50 %. Government officials have admitted that these milestones cannot be met since the appropriate technology does not exist. This research presents a novel planar solid phase microextraction (PSPME) device with enhanced surface area and capacity for collection of the volatile chemical signatures in air that are emitted from illicit compounds for direct introduction into ion mobility spectrometers (IMS) for detection. These IMS detectors are widely used to detect particles of illicit substances and do not have to be adapted specifically to this technology. For static extractions, PDMS and sol-gel PDMS PSPME devices provide significant increases in sensitivity over conventional fiber SPME. Results show a 50-400 times increase in mass detected of piperonal and a 2-4 times increase for TNT. In a blind study of 6 cases suspected to contain varying

amounts of MDMA, PSPME-IMS correctly detected 5 positive cases with no false positives or negatives. One of these cases had minimal amounts of MDMA resulting in a false negative response for fiber SPME-IMS. A La (dihed) phase chemistry has shown an increase in the extraction efficiency of TNT and 2,4-DNT and enhanced retention over time. An alternative PSPME device was also developed for the rapid (seconds) dynamic sampling and preconcentration of large volumes of air for direct thermal desorption into an IMS. This device affords high extraction efficiencies due to strong retention properties under ambient conditions resulting in ppt detection limits when 3.5 L of air are sampled over the course of 10 seconds. Dynamic PSPME was used to sample the headspace over the following: MDMA tablets (12-40 ng detected of piperonal), high explosives (Pentolite) (0.6 ng detected of TNT), and several smokeless powders (26-35 ng of 2,4-DNT and 11-74 ng DPA detected). PSPME-IMS technology is flexible to end-user needs, is low-cost, rapid, sensitive, easy to use, easy to implement, and effective.

TABLE OF CONTENTS

CHAPTER		PAGE
1.	STATEMENT OF THE PROBLEM	1
1.1	Security Concerns	1
1.1.1	Explosives	2
1.1.2	Illicit Drugs	5
1.2	Research Approach in Response to Current Needs	6
1.3	Project Goals and Hypotheses	7
2.	EXPLOSIVES AND ILLICIT DRUGS	9
2.1	Chemistry of Explosives	9
2.1.1	Propellants	10
2.1.2	Military Explosives	13
2.2	Chemistry of Illicit Drugs	15
2.2.1	Cocaine	15
2.2.2	Marijuana	17
2.2.3	MDMA	18
2.3	Field Analysis of Explosives	20
2.3.1	Biological Detection	21
2.3.2	Chemical Detection	22
3.	VOLATILE CHEMICAL SIGNATURES	24
3.1	Definition of Volatile Chemical Signatures	24
3.2	Volatile Chemical Signatures of Explosives	25
3.3	Volatile Chemical Signatures of Drugs	26
3.4	Delivery Methods for Volatile Chemical Signatures	28
4.	SOLID PHASE MICROEXTRACTION	30
4.1	Theory of Solid Phase Microextraction	30
4.1.1	Historical Aspects of SPME	30
4.1.2	Thermodynamics	31
4.1.3	Kinetics	32
4.2	Practical Aspects of Sampling	33
4.2.1	Extraction Modes	35
4.2.2	Dynamic Sampling	37
4.2.3	Method Development	38
4.3	Phase Chemistry	40
4.3.1	Sol-gel Coating Technology	40
4.3.1.1	Chemical Reactions in the Sol-gel Process	42
4.3.1.2	Sol-gel SPME Coatings	44
4.3.2	La (dihed) Phase Chemistry	46
4.3.3	Characterization of Polymer Products	49
4.3.3.1	Scanning Electron Microscopy	49

4.3.3.2 ^{1}H Nuclear Magnetic Resonance Spectroscopy 50
4.3.3.3 Direct-Infusion Mass Spectrometry 51
4.3.3.4 Infrared Spectroscopy 52
4.4 Solid Phase Microextraction for Explosives and Illicit Drug Sampling 52
4.4.1 Explosives Sampling 52
4.4.2 Drug Sampling 53

5. ION MOBILITY SPECTROMETRY 55
5.1 Theory of Ion Mobility Spectrometry 55
5.1.1 Ion Chemistry 57
5.1.2 IMS Response 59
5.2 Forensic Applications of Ion Mobility Spectrometry 60
5.3 IMS Modifications to Improve Contraband Detection 60
5.3.1 Sampling Improvements 61
5.3.2 Operating Condition Optimization 66

6. METHODOLOGY 67
6.1 Development of Planar SPME (PSPME) Devices for Static Extractions 67
6.1.1 Preparation of the Substrate 67
6.1.2 Coating Techniques 68
6.1.2.1 Dip-Coating 68
6.1.2.2 Spin-Coating 69
6.1.3 Preparation of the Coating Solutions 71
6.1.3.1 Sol-gel PDMS 71
6.1.3.2 PDMS by a Chlorine-Terminated PDMS Route 72
6.1.3.3 Sylgard® 184 PDMS 73
6.1.3.4 Activated Charcoal/ Sylgard 184® PDMS 73
6.1.3.5 Activated Charcoal/Sol-Gel PDMS 74
6.1.3.6 La (dihed) 74
6.1.4 Characterization of Final PSPME Products 78
6.1.4.1 Scanning Electron Microscopy 78
6.1.4.2 IMS Plasmagram Blanks 78
6.1.4.3 Classical Methods 78
6.1.4.4 Fourier Transform-Infrared Spectroscopy 79
6.1.4.5 Direct Infusion- Mass Spectrometry 79
6.1.4.6 ^{1}H Nuclear Magnetic Resonance Spectroscopy 80
6.2 Validation Experiments for Static PSPME 80
6.2.1 IMS Detection 80
6.2.2 Performance Comparison of the SPME Fiber, PDMS, and Sol-gel PDMS PSPME Devices Using TNT as the Target Analyte 82
6.2.2.1 Quantitation of TNT Using Response Curves 82
6.2.2.2 Determination of Equilibrium Extraction Time and Recovery 83
6.2.2.3 Extraction Efficiency Experiments at Equilibrium 83
6.2.2.4 Study of TNT Adsorption to Vessel Walls 83

6.2.3 Comparison of Sol-Gel PDMS PSPME and Fiber SPME for Sampling Piperonal 84
6.2.3.1 Gas Chromatography- Mass Spectrometry (GC/MS) 84
6.2.3.2 IMS Operating Conditions 84
6.2.3.3 SPME-IMS Sampling 85
6.2.3.4 SPME-IMS Quantitation 85
6.2.3.5 SPME-IMS Limit of Detection (LOD) and Linear Dynamic Range (LDR) Determinations 86
6.2.3.6 Piperonal IMS Response Curve 86
6.2.3.7 Method Development for PSPME-IMS of Piperonal 87
6.2.3.8 Sampling Real MDMA Cases at a Local Crime Laboratory 87
6.2.4 Performance of PSPME for Other Volatile Chemical Signatures 88
6.2.5 Performance of PSPME for the Smokeless Powder Volatile Chemical Signatures 89
6.2.5.1 Smokeless Powder Volatile Chemical Signature IMS Response Curves 89
6.2.5.2 Concentration Study for 2,4-DNT 90
6.2.5.3 Determination of Equilibrium Extraction Time 90
6.2.5.4 Sampling of Unburned Smokeless Powders 90
6.2.6 PSPME Static Sampling of TNT from a Large Volume Vessel 91
6.2.7 Comparison of Planar La (dihed) SPME Devices with Control Planar Sol-gel and PDMS Devices for the Extraction of TNT and 2,4-DNT 92
6.2.7.1 Aging Study 92
6.2.7.2 Coating Study 92
6.2.7.3 La (dihed)/ Sol-gel PDMS 93
6.3 Development of Dynamic PSPME 93
6.3.1 Preparation of Dynamic PSPME Devices 93
6.3.2 Coating Method Development 94
6.3.3 Characterization of Final Dynamic PSPME Devices 95
6.3.4 Handheld Sampler 95
6.3.5 Volatile Chemical Signature Standards for Dynamic PSPME Sampling 97
6.3.5.1 Spike on Manufacturer Provided Filters 97
6.3.5.2 Controlled Odor Mimic Permeation Systems (COMPS) 98
6.4 Validation Experiments for Dynamic PSPME 99
6.4.1 Dynamic PSPME Retaining Capability Studied By Analyte Solution Spiking 100
6.4.2 Dynamic PSPME Retaining Capability Studied By COMPS Vapor Source 101
6.4.3 Dynamic PSPME LOD 101
6.4.2 Application of Dynamic PSPME-IMS for Screening of Illicit Compounds 102

7. RESULTS AND DISCUSSION 104
7.1 Development of PSPME Devices for Static Extractions 104
7.1.1 Sol-gel PDMS 105
7.1.2 PDMS PSPME Via a Chlorine-terminated PDMS Route 109
7.1.3 Sylgard® 184 by Dow 111
7.1.4 Activated Charcoal in PDMS Formulations 113

7.1.5 La (dihed) 115
7.1.5.1 Structure Determination 115
7.1.5.2 La (dihed) SPME Coatings 126
7.1.6 Summary of PSPME Devices Developed 134
7.2 Validation Experiments for Static PSPME 134
7.2.1 Performance Comparison of the SPME Fiber, PDMS, and Sol-gel PDMS PSPME Devices Using TNT as the Target Analyte 134
7.2.1.1 Quantitation of TNT Using Response Curves 134
7.2.1.2 Determination of Equilibrium Extraction Time and Recovery 135
7.2.1.3 Extraction Efficiency Experiments at Equilibrium 139
7.2.1.4 Study of TNT Adsorption to Vessel Walls 140
7.2.2 Comparison of Sol-Gel PDMS PSPME and Fiber SPME for Sampling Piperonal 142
7.2.2.1 SPME-IMS Sampling 142
7.2.2.2 SPME-IMS Quantitation 144
7.2.2.3 SPME-IMS Limit of Detection (LOD) and Linear Dynamic Range (LDR) Determinations 146
7.2.2.4 Piperonal IMS Response Curve 146
7.2.2.5 Method Development for PSPME-IMS of Piperonal 148
7.2.2.6 Sampling Real MDMA Cases at a Local Crime Laboratory 154
7.2.3 Performance of PSPME for Other Volatile Chemical Signatures 159
7.2.4 Performance of PSPME for the Smokeless Powder Volatile Chemical Signatures 162
7.2.4.1 Smokeless Powder Volatile Chemical Signature IMS Response Curves 162
7.2.4.2 Concentration Study for 2,4-DNT 165
7.2.4.3 Determination of Equilibrium Extraction Time 166
7.2.4.4 Sampling of Unburned Smokeless Powders 167
7.2.5 PSPME Static Sampling of TNT from a Large Volume Vessel 169
7.2.6 Comparison of Planar La (dihed) SPME Devices with Control Planar Sol-gel and PDMS Devices for the Extraction of TNT and 2,4-DNT 171
7.2.6.1 Aging Study 171
7.2.6.2 Coating Study 172
7.3 Development of Dynamic PSPME 176
7.3.1 Coating Method Development 178
7.3.2 Characterization of Final Dynamic PSPME Devices 186
7.3.3 Volatile Chemical Signature Standards for Dynamic PSPME Sampling 188
7.3.3.1 Spike on Manufacturer Provided Filters 188
7.3.3.2 Controlled Odor Mimic Permeation Systems (COMPS) 191
7.4 Validation Experiments for Dynamic PSPME 193
7.4.1 Dynamic PSPME Retaining Capability Studied by Analyte Solution Spiking 193
7.4.2 Dynamic PSPME Retaining Capability Studied by COMPS Vapor Source 198
7.4.3 Dynamic PSPME LOD 203
7.4.4 Application of Dynamic PSPME- IMS for Screening of Illicit Compounds 204

8. CONCLUSIONS 209
8.1 Static PSPME 209
8.2 Dynamic PSPME 211
8.3 PSPME Terminology 212
8.4 Implications of PSPME-IMS for Security 214
8.5 Future Directions 214

REFERENCES 216

APPENDICES 227

VITA 230

LIST OF TABLES

TABLE PAGE

Table 1: Common Military and Commercial Explosive Compositions 14

Table 2: Classification of Compounds Based on Volatility 24

Table 3: Commercially Available Fiber Coatings 38

Table 4: Operating Conditions of IMS Instruments and SPME-IMS Interface 81

Table 5: Detection of Volatile Chemical Signatures from Real Case Samples Using Dynamic PSPME-IMS 100

Table 6: IR Band Interpretation 119

Table 7: Recovery of TNT Calculated from Response Curves 139

Table 8: Extraction Efficiencies Measured by PSPME Device and SPME Fiber Inside Gallon-Sized Cans Containing 2 μg and 5 μg of Piperonal 153

Table 9: IMS Analysis Response Curves 191

Table 10: Detection of Target Analytes from Real Case Samples Using the Dynamic PSPME-IMS Method 205

LIST OF FIGURES

FIGURE PAGE

Figure 1: Energetic Compounds in Smokeless Powders 11

Figure 2: Smokeless Powder Morphology: A) Ball, B) Tube, C) Rod, D) Disc 12

Figure 3: Common Military Explosives and Their Vapor Pressures at 25°C 13

Figure 4: Chemical Structures of Cocaine and Methyl Benzoate 16

Figure 5: The Decarboxylation of Δ^9-tetrahydrocannabinolic Acid to THC 18

Figure 6: Structures of the: A) Amphetamine Drugs and B) MDMA Precursors 19

Figure 7: Volatile Chemical Signatures of the Appropriate Parent Compounds and Vapor Pressures 28

Figure 8: Boundary Layer Model 33

Figure 9: Commercial SPME Fiber Sampler 34

Figure 10: Extraction Modes of SPME 35

Figure 11: Schematic of Processes in an Ion Mobility Spectrometer 55

Figure 12: The Dip-Coating Process 69

Figure 13: The Spin-Coating Process 70

Figure 14: Image of the Spin Coater Used with the Glass Substrate in Place on the Chuck 71

Figure 15: Large Volume Static Sampling for TNT from Pentolite 91

Figure 16: Dynamic Sampling By Dynamic PSPME and Manufacturer Provided Filter 96

Figure 17: Dynamic sampling at Distance (h (cm)) Above an Emitting Source (i) 97

Figure 18: Fiber to Planar SPME 104

Figure 19: Sol-gel: Dip-coating Processes 106

Figure 20: Dehydration Resulting in –M-O-M'- Bonds 107

Figure 21: The Sol-gel PDMS PSPME Device 109

Figure 22: Surface and Coating Thickness of the PDMS PSPME Device 111

Figure 23: Explosive Standards for LIBS Experiments in Sylgard® 184 PDMS 112

Figure 24: Coating Thickness of Sylgard 184 ® PDMS on Glass 112

Figure 25: SEM Image (Low Vacuum) of CAR/ PDMS Fiber 113

Figure 26: SEM Image (LV) of Activated Charcoal Particles 114

Figure 27: Activated Charcoal/ PDMS PSPME Devices 114

Figure 28: Ligand Structure Showing Enol and Keto Tautomers of H_2 (dihed) 115

Figure 29: ^1H NMR Spectrum of the H_2 (dihed) Ligand 116

Figure 30: $[La_2\ Dihed_3 \cdot 4H_2O]_n$, $[La_2\ (C_{18}H_6O_4F_{14})_3 \cdot 4H_2O]_n$ Structure 117

Figure 31: Overlaid IR Spectra of H_2 (dihed) and the La (dihed) Complex 118

Figure 32: Negative Ion Mass Spectrum of H_2 (dihed) Ligand 120

Figure 33: Negative Mass Spectrum of the La (dihed) Complex 121

Figure 34: Negative Mass Spectrum of the La (dihed) Complex from 1900-2000 m/z 122

Figure 35: ^1H NMR (160 scans) of the La (dihed) Complex 123

Figure 36: ^1H NMR of the La (dihed) Complex at 50 °C 124

Figure 37: Temperature Effects on Control La (dihed) PSPME Devices 127

Figure 38: Temperature Effects on La (dihed) Coated PDMS PSPME Devices 128

Figure 39: Temperature Effects on La (dihed) Coated Sol-gel PDMS PSPME Devices 129

Figure 40: Coating Thickness of La (dihed) 129

Figure 41: Images of the Sol-gel PDMS PSPME Device (A) and La (dihed)/ PDMS PSPME Device (B) 131

Figure 42: Plasmagrams of the Blank La (dihed)/ Sol-gel PDMS PSPME Device..... 132

Figure 43: Equilibrium Extraction Time Curves for A) Sol-gel PDMS PSPME B) PDMS PSPME and C) PDMS SPME Fiber 137

Figure 44: Extraction Efficiencies of the Three SPME Devices Tested for TNT 140

Figure 45: Effects of Adsorption of TNT to Vessel Walls 141

Figure 46: Piperonal Extraction Time Curve 143

Figure 47: Equilibrium Time Curve for Piperonal 144

Figure 48: A) GC-MS Response Used for B) SPME-IMS Quantitation 145

Figure 49: IMS Response Curves for the Piperonal A) Monomer and B) Dimer Product Ions 147

Figure 50: Piperonal Detected Following Extraction with A) the PSPME Device and B) the SPME Fiber 149

Figure 51: Equilibrium Extraction Curves for Piperonal by the PSPME Device and the SPME Fiber 152

Figure 52: Extraction Time Curves Generated Using Confirmed MDMA Tablets..... 156

Figure 53: Response v. Number of MDMA Tablets Sampled..... 156

Figure 54: Blind Case Study Results for A) Monomer and B) Dimer Product Ions 158

Figure 55: PSPME-IMS of the Volatile Chemical Signatures 2,4-DNT, 4-NT, and Cyclohexanone..... 161

Figure 56: DPA Response Curve 162

Figure 57: 2,4-DNT Response Curve 163

Figure 58: IMS Analysis: 1 µl of 42 and 250 ppm 2,4-DNT (n=5) in Different Solvents Spiked on Manufacturer Provided Filters. 164

Figure 59: EC Response Curve 164

Figure 60: Equilibrium Curves for EC and DPA 167

Figure 61: Mass Detected of DPA from Smokeless Powders Using PSPME-IMS 168

Figure 62: IMS Plasmagram Following PSPME Sampling of Red Dot Smokeless Powder 169

Figure 63: 3-D IMS Plasmagram for the Static Large Volume Sampling of TNT 170

Figure 64: Results for the Aging of 2,4-DNT and TNT 172

Figure 65: La (dihed) on Sol-gel PDMS Coating Parameter Effects on the Extraction and Detection of 2,4-DNT and TNT 174

Figure 66: La (dihed) on PDMS Coating Parameter Effects on the Extraction and Detection of 2,4-DNT and TNT 175

Figure 67: Fiberglass Screen Exposed to Various Corrosive Procedures 177

Figure 68: SEM Images of Sol-gel PDMS on Different Substrates 178

Figure 69: Spin Speeds Tested by Deposting 1 mL of Coating Solution on Substrate and Spinning for 1 min at 0, 200, 1000, and 2000 rpm. 179

Figure 70: 100 mg of Hogdon H322 Smokeless Powder- Immediate or Aged 181

Figure 71: IMS plasmagram of Backgrounds Obtained From Blank Dynamic PDMS Devices Created Using Various Spin Programs 182

Figure 72: Aging study of TNT on the Surface of Manufacturer Provided Filters and Dynamic PSPME Devices Created Using Various Spin Programs 184

Figure 73: IMS Plasmagrams of Both the PSPME Device and Manufacturer Filter Blanks 185

Figure 74: SEM Images of the Glass Fiber Filter and the Dynamic PSPME Device.... 187

Figure 75: Dissipation Rates of Volatile Chemical Signatures in COMPS Devices 193

Figure 76: Retention Capability Study by Spiking Standard Solution of the Analytes onto the PSPME Surface Device Followed by Clean Air Pumping. 197

Figure 77: Mass of Piperonal Detected When Dynamically Sampling a COMPS Device for 30 s at Different Sampling Heights 199

Figure 78: Retention Capability Study and Sampling Time Optimization by Dynamically Sampling Vapors of Analytes Emitted from COMPS Bags 202

Figure 79: Sample IMS Plasmagrams Following Dynamic PSPME Sampling of Illicit Drugs and Explosives 208

LIST OF ABBREVIATIONS AND ACRONYMS

1,3-DE-1,3-DPU	1,3-diethyl-1,3-diphenyl urea, ethyl centralite
DMNB	2,3-dimethyl-2,3-dinitro butane
1,3-DNB	1,3-dinitrobenzene
Tetryl	2,4,6-trinitrophenylmethylnitramine
TNT	2,4,6-trinitrotoluene
2,4-DNT	2,4-dinitrotoluene
2,6-DNT	2,6-dinitrotoluene
2-E-1-hexanol	2-ethyl-1-hexanol
MDMA	3,4-methylenedioxymethamphetamine
MD-P2P	3,4-methylenedioxy-phenyl-2-propanone
4-NT	4-nitrotoluene
AC	Activated Charcoal
a.m.u.	Atomic Mass Unit
CW	Carbowax
CAR/PDMS	Carboxen Polydimethyl Siloxane
COMPS	Controlled Odor Mimic Permeation Systems
CSA	Controlled Substances Act
CBP	Customs and Border Protection
DHS	Department of Homeland Security
DPA	Diphenylamine
DI-MS	Direct Infusion Mass Spectrometry

DVB	Divinyl Benzene
ECD	Electron Capture Detector
ESI	Electrospray Ionization
EC	Ethyl Centralite, 1,3-diethyl-1,3-diphenyl urea
EGDN	Ethylene Glycol Dinitrate
FT-IR	Fourier Transform Infrared Spectroscopy
GC	Gas Chromatography
GC/MS	Gas Chromatography Mass Spectrometry
GA	Genetic Algorithm
GFP	Green Fluorescence Protein
HPLC	High Pressure Liquid Chromatography
RDX	Hexahydro-1,3,5-trinitro-s-triazine
IED	Improvised Explosive Device
IR	Infrared Detector
IMS	Ion Mobility Spectrometer or Ion Mobility Spectrometry
La (dihed)	$[La_2 (C_{18}H_6O_4F_{14})_3 \cdot 4H_2O]_n$
LOD	Limit of Detection
LDR	Linear Dynamic Range
LC	Liquid Chromatography
MS	Mass Spectrometer or Mass Spectrometry
m/z	Mass to Charge Ratio
MTMOS	Methyl Trimethoxysilane

μg	Microgram
ng	Nanogram
NIST	National Institute of Standards and Technology
NC	Nitrocellulose
NG	Nitroglycerin
(BMA/OH-TSO)	*o*-poly(butyl methacrylate/hydroxy terminated silicone oil)
H_2 (dihed)	*p*-di(4,4,5,5,6,6,6-heptafluoro-1,3-hexanedionyl)benzene
^{1}H NMR	Proton Nuclear Magnetic Resonance
HMX	Octahydro-1,3,5,7-tetranitro-1,3,4,5-tetrazocine
PETN	Pentaerythritol Tetranitrate
pg	Picogram
PSPME	Planar Solid Phase Microextraction
PA	Polyacrylate Resin
Cl-PDMS	Chlorine-terminated Polydimethylsiloxane
PDMS	Polydimethylsiloxane
PEG	Polyethylene glycol
PMHS	Poly(methylhydrosiloxane)
PTFE	Polytetrafluoroethylene
limonene	R-(+)-limonene
SEM	Scanning Electron (Microscopy or Microscope)
S/N	Signal to Noise Ratio
SPE	Solid Phase Extraction

SPME	Solid Phase Microextraction
SPME-IMS	Solid Phase Microextraction-Ion Mobility Spectrometry
SOP	Standard Operating Procedure
TMOS	Tetramethoxysilane
TLC	Thin Layer Chromatography
TATP	Triacetone Triperoxide
TFA	Trifluoroacetic Acid
TEEM	Tunable Electron Energy Monochromator
TSA	Transportation Security Administration
UV	Ultraviolet
vt-PDMS	Vinyl-terminated Polydimethylsiloxane
VOC	Volatile Organic Compound
WMD	Weapons of Mass Destruction

CHAPTER 1. STATEMENT OF THE PROBLEM

"The world is a dangerous place to live; not because of the people who are evil, but because of the people that don't do anything about it."

Albert Einstein

1.1 Security Concerns

The United States Government is tasked with protecting its citizens and the homeland from terrorist attacks. Following the 1995 bombing of the Murrah Federal Building in Oklahoma City, OK, the Anti-Terrorism and Effective Death Penalty Act **[1]** was enacted. This law requires the tagging of all explosives in order to facilitate discovery of an explosive device before detonation, and banned the sale of un-tagged explosives. A taggant is a solid or liquid substance that produces a vapor that, when added into the explosive, makes the explosive easily detectable by instruments and trained canines. Requirements for a taggant are that it must be inexpensive and have a sufficiently long half-life while not affecting the detonation or deflagration properties of the explosive. The taggant currently used in the U.S. is 2,3-dimethyl-2,3-dinitrobutane (DMNB) **[2]**. Although the explosive used in the 1995 bombing, an improvised mixture of ammonium nitrate (fertilizer) and fuel oil, would not have been tagged if this law were in place earlier because the single components are not considered explosive, the requirement serves as a much needed preventative measure and likely helped ease public concerns.

1.1.1 Explosives

The dangers of explosives in the hands of terrorists are well known and this prompted the creation of the tagging system currently in place. Smokeless powders, propellants not considered explosives for tagging purposes, are important to national security since they can be tempting to use as the filler in improvised explosive devices such as pipe bombs (IEDs) by individuals with ill-will. This is because smokeless powders, along with black powders (another propellant), are readily accessible in gun shops and sporting clubs. It is reported that around 3.5 million individuals use these substances in the United States **[3]** who either prefer to load their own ammunition by hand and/or operate muzzle loading handguns for hunting or reenactments **[4]**. In general, a pipe bomb consists of a few simple components: the propellant, a container for the propellant, and an initiation system to start the burning of the propellant within the container. When sufficient pressure builds up within the container, the device explodes. Nails or tacks could be added to worsen the effects of the shrapnel ejected upon explosion. The most notable incidents of the use of pipe bombs in terrorist attacks have been the Centennial Park bombing at the 1996 Olympics in Atlanta, GA and the devices mailed by the Unabomber. The Bureau of Alcohol, Tobacco and Firearms reported that there were 448 total significant incidents in the U.S. involving smokeless powder and black powder IED explosions from 1992 to 1994, killing 27 people and injuring 199 others **[4]**. Improvements in the preemptive detection of smokeless powder pipe bombs are necessary to deter possible terrorists from using this easily attainable explosive material and to help in the pre-blast discovery of these explosives.

The terrorist attacks of September 11, 2001 heightened national concerns about threats posed to the homeland by weapons of mass destruction (WMD). The 9/11 Commission was gathered to determine the intelligence gaps that enabled these attacks and to identify ways to improve security for the prevention of future terrorism incidents. In 2007, a bill, known as the 9/11 Act was approved by Congress and signed into law in order to meet the recommendations given by the 9/11 Commission in 2004 **[5]**.

The law mandated that 50 % of domestic and in-bound air passenger cargo be screened by February 2009, a milestone that has been reached **[6]**. The Transportation Security Administration (TSA) has been able to meet this deadline largely because there are 85 canine teams specifically assigned to screening of air cargo at airports in the US with the highest cargo volume and 460 additional canine teams that each spend at least 25 % of their work day in the cargo environment **[6]**.

The next step is to meet the goal of screening 100 % of air cargo by March 2010. Recently, Ed Kelley, director of the TSA, the agency with the authority to enforce the regulation, testified to Congress that he did not expect the mandate could be met for in bond air cargo. He provided the following written statement as to why this was not feasible **[7]**.

"One of the challenges we face is the limitations of the currently available technology -- specifically, the effectiveness of existing technology for detecting explosives in cargo, its operational feasibility, and its general availability for deployment to the industry to meet the mandate of the 9/11 Act."

Requiring domestic and international airlines to meet the demand for 100 % screening would severely impede the flow of commerce without the proper technology available for this purpose.

In another facet of transportation-related mandates included in the 9/11 Act, the director of the Department of Homeland Security (DHS), Janet Napolitano informed lawmakers on December 2, 2009, that her department would not be meeting the 2012 deadline for 100 % screening of the 10 million shipping containers that enter the U.S. annually. She explained that in order to implement the 100 percent scanning requirement by the 2012 deadline, technologies would be needed that do not currently exist and many ports would have to be redesigned. If screening was expanded with available technology **[8]** that involves large and expensive X-ray or gamma ray scanners to generate an image of the contents of the container and that the screener reviews for anomalies, cargo flow would be significantly reduced driving up consumer costs without in her opinion, bringing additional security benefits **[9]**. In reality, it was reported in May 2002, that the costs associated with U.S. port closures resulting from a detonated explosive or WMD could amount to $1 trillion, assuming economic fallout due to the changes it would cause in the ability of the U.S. to trade **[8]**.

The strategy in place designed to meet this daunting task is outlined in the Container Security Initiative, implemented by U.S. Customs and Border Protection (CBP) which began shortly after the 9/11 attacks. This plan has deployed equipment at 58 ports around the world to help scan incoming cargo for contraband weapons. The Secure Freight Initiative further compartmentalizes the task by scanning cargo at the five ports that have

the highest potential for the smuggling nuclear-weapon materials **[10]**. Despite the efforts in place, approximately only 5 % of cargo entering the U.S. from the largest ports is thoroughly screened **[11]**.

1.1.2 Illicit Drugs

The drug trade also poses a threat to U.S. national security. The Coast Guard is the lead federal agency for maritime law enforcement and drug interdiction **[12],** accounting for 52% of all U.S. government seizures each year **[13]**. The Coast Guard Drug Removal Statistics reveal that for the 2010 fiscal year alone, 9,454 lbs. of marijuana and a staggering 24,590.3 lbs. of cocaine were seized and removed **[14]**. From the fiscal year 1997 to present 806, 469 lbs. of cocaine and 333, 285 lbs. of marijuana have been seized by the Coast Guard **[13]**.

The previous statistics that reveal information about only one segment of the drug war, demonstrate the enormity of the problem the U.S. faces. But the problem of drug addiction although individual to the addicted person also has large scale implications. The illicit drug, 3,4-methylenedioxymethamphetamine, MDMA, is both a stimulant and psychedelic that causes an energizing effect, distorts time and perception, and enhances enjoyment from tactile experiences. As such, this drug is more commonly known to users as 'ecstacy.' The use of MDMA affects the brain adversely, with the worst effect being the loss of nerve endings that contain serotonin observed in as little as two weeks of abuse. In a recent survey, 11 million people over the age of 12, report to have used MDMA in their lifetimes **[15]**. Currently, this drug can be presumptively identified using the Marquis color test. A purple-blue color is obtained for MDMA but it may be confused

with the indigo color obtained for the opiates by the same test. Thin layer chromatography is also used but the results can be confused with other amphetamines **[16].** A rapid sensitive screening technique for MDMA is necessary that will minimize incorrect detections and false negatives.

1.2 Research Approach in Response to Current Needs

The U.S. Government has identified certain deficiencies with regards to the detection of explosives/WMD and drugs. These can be summarized into three recommendations for technology aimed at detecting contraband items:

1) The technology must be effective at detecting explosives and drugs in cargo.
2) The technology must be operationally feasible. This means it must have a low total cost to implement (technology, maintenance, consumable products, and change in security infrastructure). The analysis must be fast so as not to slow down the flow of commerce.
3) The technology must be available for deployment to the security industry.

In regards to the first recommendation, the trace detection problem for national security in reality has little to do with the detectors available to detect drugs and explosives. The main detector used in this dissertation in fact has extremely low detection limits, on the order of picograms (pg) **[17]**.The central issue, rather, is the problem of sample collection. Air cargo holds and shipping containers have a large volume and attempting to sample this amount for trace particles is like looking for a needle in a haystack. It is proposed that the sampling methodology utilize vapors emitted from the contraband, like

trained canine teams do, to increase detection probabilities. Furthermore, because of the large volume of air in containers, vapors likely will not build up sufficient vapor pressure over even extended periods of time **[18]**, whereby and efficient pre-concentration and sampling device becomes necessary.

The latter two requirements can be easily met by the research described herein which aims to provide an efficient, rapid sampling and pre-concentration device that is easily adaptable to existing detectors deployed in the security field.

1.3 Project Goals and Hypotheses

The first project goal is to alter the cylindrical geometry of the solid phase microextraction fiber into a planar geometry. The SPME fiber, in the static sampling mode, has previously been shown to improve the detection limits of IMS alone by allowing vapor sampling as opposed to particle sampling **[19]**.

The first hypothesis is that changing the geometry of SPME:

1) increases the surface area and capacity for the pre-concentration and sampling (extraction) of previously identified volatile chemical signatures of drugs and explosives.

2) allows direct introduction of the sampling device into existing desorbers of ion mobility spectrometry instruments (IMS) which are accepted and widely used detectors for explosives, drugs and their volatile chemical signatures, thus eliminating the need for fabricating interfaces for each instrument model.

The second project goal is to alter the planar geometry of SPME such that it enables flow of the air of a suspect area through the sampling media. This would allow mass transfer by fluid flow and decrease the boundary layer associated with static sampling thereby allowing sampling of large volumes of air in a short time.

The second hypothesis is that developing a dynamic SPME sampling device:

1) will enable open air dynamic sampling of trace amount of volatile chemical signatures emitted from drugs and explosives in short sampling times.

2) would allow canine detection to be simulated more closely when the device is coupled to fast detection (s) by IMS. This hypothesis will be tested by dynamically sampling the same permeation sources used to calibrate the trained canines, with planar SPME.

The third project goal is to alter the conventional extraction phase (coating) of the SPME device.

As such, the final hypothesis is that additional benefits beyond those achieved by changing the geometry of the SPME fiber can be observed by implementing and developing coatings for planar SPME that will afford higher capacity and affinity for the targeted volatile chemical signatures.

CHAPTER 2. EXPLOSIVES AND ILLICIT DRUGS

2.1 Chemistry of Explosives

Simply defined, an explosion is an event in which a large amount of energy is suddenly released. This occurs in order to relieve accumulated pressure and return the surrounding medium to atmospheric pressure.

There are three types of explosions: mechanical, chemical, and nuclear. A mechanical explosion occurs when gas builds up in a container to the point where the container bursts. For example, the explosion of a steam boiler is considered mechanical. A chemical explosion is the result of a rapid release of gas from a chemical reaction. This reaction occurs when a composition (the explosive) in a metastable state, undergoes an almost instantaneous (one-hundredth of a second) exothermic transformation or decomposition without the participation of external reactants, such as atmospheric oxygen, since a chemical explosive contains both an oxidizer and a fuel. The fuel is carbon and hydrogen while the oxidizer is typically nitrogen and oxygen bonded in groups such as NO, NO_2, and NO_3. The reaction occurs when nitrogen and oxygen separate and recombine with the fuel releasing large amounts of hot gases. Sensitizers can also be included in the explosive composition to enhance the ease of initiation. A chemical explosive must be packed but does not necessarily require confinement. Lastly, a nuclear explosion is produced from the energy released following the splitting of an atom or the fusion of atoms. The energy produced from this type of explosion is a billion times greater than that of a chemical explosion **[20]**. In this section, the characteristics of

chemical explosives will be described with special focus on propellants and military explosives.

The reactions produced by chemical explosions can be high or low order. Propellants are low explosives that deflagrate, meaning they burn particle to particle at sub-sonic speeds in the material. The direction of flow of the reaction products in a low order explosion is opposite to the propagation of the disturbance. While low explosives are initiated by ignition, high explosives such as military explosives are initiated by shock and detonate. In a detonation the energy that initiates and sustains the reaction is transmitted to the material that has yet to react, as a shock wave moving at speeds greater than the speed of sound with respect to the undisturbed material. As a result of the much greater speed, temperature, and pressure, of the reaction **[21]**, a detonation causes destruction on a much larger scale than a deflagration.

2.1.1 Propellants

Propellants are used to accelerate the projectile in a weapon to its full velocity as it exits the barrel. Smokeless powders are the propellants of most relevance to this study. Smokeless powders were developed to replace black powder, another propellant that was subject to accidental initiations **[22]**. The ingredients in black powders are sulfur, charcoal and potassium nitrate, the reaction produces solid product which can be as much as 60% residue of KNO_3 and other salts. Smokeless powders greatly reduced the black smoke produced after the firing of a weapon that utilized black powders.

The nitration reaction of cellulose to produce nitrocellulose (NC) enabled the production of smokeless powders. This is known as a single base smokeless powder since the only energetic compound is NC. The double base smokeless powder was invented by Alfred Nobel in 1888 consisting of nitroglycerine (NG), produced by the nitration of glycerin, added as a reactive solvent to NC, creating a gel. Triple base powders contained NC and NG with added nitroguanidine, to reduce muzzle flash, and are used almost exclusively in high caliber weapons. Figure 1 shows the structures of the energetic compounds in smokeless powders.

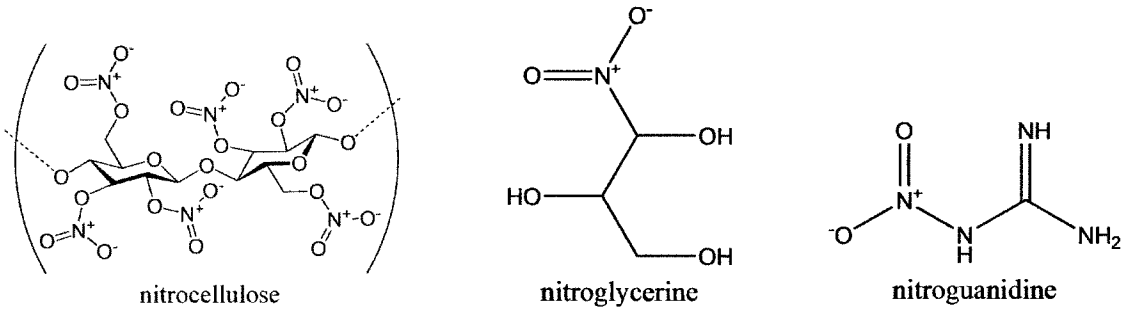

Figure 1. Energetic Compounds in Smokeless Powders

Smokeless powders contain the following additives in their formulation: stabilizers, flash suppressants and plasticizers. Stabilizers prevent the nitrocellulose and nitroglycerine from decomposing by neutralizing nitric and nitrous acids that can catalyze further decomposition of the energetic compound. Diphenylamine (DPA), methyl centralite, and ethyl centralite (EC) are common stabilizers. Plasticizers reduce the need for volatile solvents necessary to colloid nitrocellulose; they soften the propellant, and reduce hygroscopicity. Some plasticizers include NC, dibutyl phthalate, 2,4-dinitrotoluene (2,4-DNT), ethyl centralite, and triacetin. The plasticizer 2,4-DNT is produced by the nitration

of toluene. The exterior of the smokeless powder granules are coated with deterrents that improve burn characteristics of the powder by reducing ignitability and initial flame temperature, as well reducing the initial burn rate on the granule surface. Both 2,4-DNT and EC are also considered deterrents. Burn characteristics can also be controlled by altering the shape of the particle. Dyes can also be added to the formulation to help in identification of smokeless powders **[23]**, of which the best example is Red Dot, a brand that contains a small concentration of discrete red granules mixed in with black granules.

The morphology of the particles is also helpful in the preliminary identification of smokeless powders. The various geometries include: balls, discs, perforated discs, tubes, rods and lamels and result from the various manufacturing processes of the powders. Figure 2 shows an image of various morphologies of the powders used in this research.

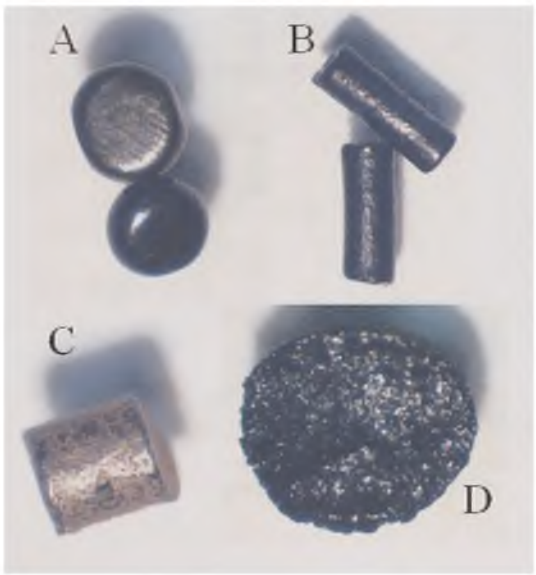

Figure 2. Smokeless Powder Morphology: A) Ball, B) Tube, C) Rod, D) Disc

In general, most tube and cylindrical powders are single-base while disc, ball, and aggregate powders are double-base **[21]**.

2.1.2 Military Explosives

Most military explosives are organic high explosives. They can be separated into groups by their compound class, either aromatic nitro ($C\text{-}NO_2$), nitrate esters ($C\text{-}O\text{-}NO_2$), or nitramines ($C\text{-}N\text{-}NO_2$) **[24]**. Several military explosives are included in figure 3 along with their vapor pressures at 25°C.

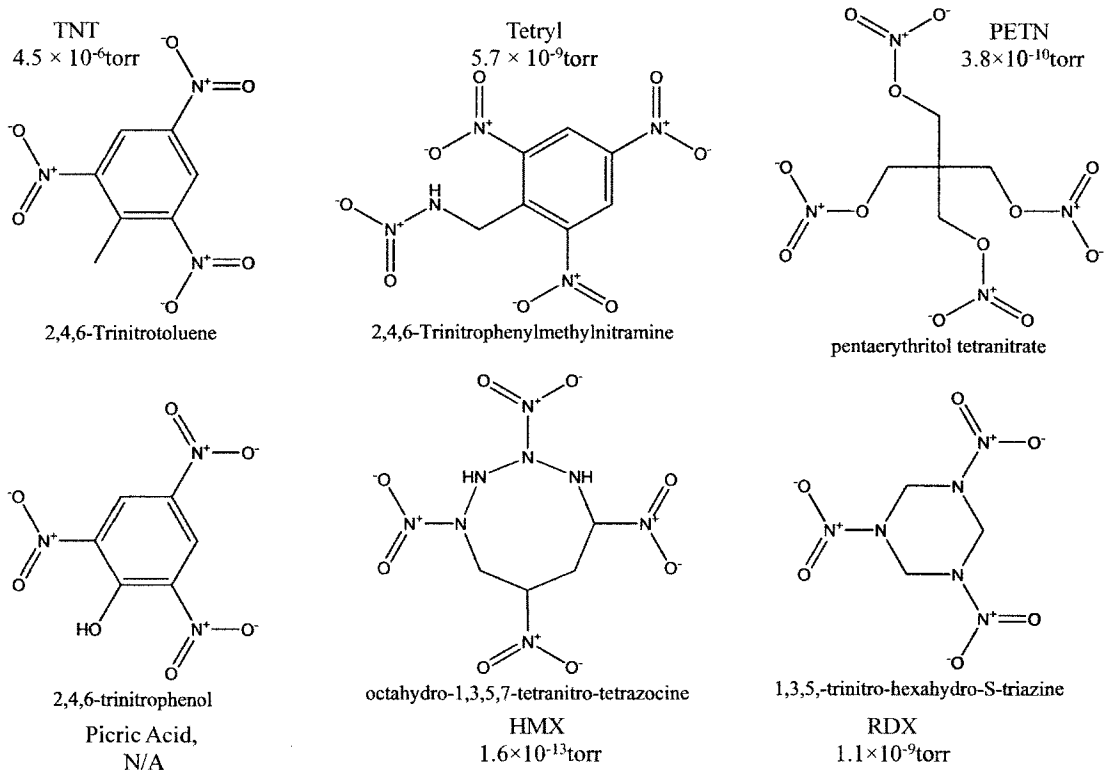

Figure 3. Common Military Explosives and Their Vapor Pressures at 25°C [25,26]

Table 1. Common Military and Commercial Explosive Compositions [27]

Explosive	Components
Composition B	RDX + TNT
Composition C-3	RDX + TNT + DNT + Tetryl + NC
Composition C-4	RDX + plasticizers
Commercial detonation cord	PETN
Pentolite	PETN + RDX
Tetrytol	Tetryl + TNT
Torpex	TNT + RDX + Al

The aromatic nitro explosives include picric acid and 2,4,6-trinitrotoluene (TNT). Picric acid was the most popular choice of shell fill by military forces during the 1900s. It was later replaced by TNT since this explosive was easier to cast in the necessary shape as compared to picric acid. The explosive, pentaerythritol tetranitrate (PETN) is a nitrate ester used in detonating cords and blasting caps. It is a white crystalline solid that can be made into sheets or any desired shape by combining it with plasticizers. It can also be mixed with TNT to make the commercial explosive Pentolite **[28]**. Tetryl (2,4,6-trinitrophenylmethylnitramine) falls under the category of nitramine explosives. Tetryl can be mixed with TNT, allowing the casting of Tetryl into munitions rather than pressing. The explosives, RDX, (1,3,5- trinitro-hexahydro-S-triazine) and HMX (octahydro-1,3,5,7-tetranitrotetrazocine) are also nitramine explosives, and have replaced Tetryl for military operations. Lastly, polymer bonded explosives are mixtures/ combinations of the organic military explosives blended with binders, plasticizers, and/

or aluminum. They afford high mechanical strength, insensitivity to shock and temperature, high detonation velocities, etc **[22]**. Table 1 contains some common explosive compositions that are relevant to this discussion.

2.2 Chemistry of Illicit Drugs

In the United States, the Drug Enforcement Administration is tasked with enforcing the Controlled Substances Act (CSA) **[29]**. This law was enacted in 1970 in order to regulate the manufacture, importation, possession, distribution and use of specific chemical substances **[30]**. The CSA regulates five classes of drugs: narcotics, depressants, stimulants, hallucinogens, and anabolic steroids. There are five schedules (I-V) of controlled substances based on potential for abuse, level of physical and psychological dependence, and medical acceptance **[31]**.

The following section is intended to provide a brief overview of the chemistry and analysis of cocaine and marijuana, illicit drugs that were identified in Chapter 1 as being smuggled on a large scale into the United States. Information about the most heavily abused club drug **[31]**, 3,4-methylenedioxymethamphetamine (MDMA), is also included since it was the subject of several experiments in this dissertation research.

2.2.1 Cocaine

Cocaine is a Schedule II drug since it has a high potential for abuse that may lead to severe psychological or physical dependence, but has a currently accepted medical use under severe restrictions.

Cocaine (figure 4A) is derived from the coca leaf *Erythroxylum* sp. which grows in the Andean Highland region of South America. More specifically, it is produced from alkaloids extracted from the plant *Erythroxylum coca.* The leaf itself can be chewed or coca paste can be made from which cocaine is subsequently produced.

One way coca paste is made is by wetting coca leaves in dilute sulfuric acid and crushing them. The water-soluble sulfate salts of the alkaloids are then extracted with kerosene. The aqueous layer is basified with ammonia, lime or sodium carbonate, thereby precipitating the alkaloids. Another route involves basifying the leaves with sodium or potassium carbonate and crushing them. The alkaloids are extracted with kerosene and dilute aqueous sulfuric acid is used to collect the alkaloids as the sulfate salts. The aqueous layer is basified and the alkaloids are precipitated **[16]**. Hydrochloric acid is added to the precipitate to produce cocaine hydrochloride. The cocaine is 75-85% pure, is scraped into a powder once dried and is compressed into one-kilogram bricks and packaged for distribution **[31]**.

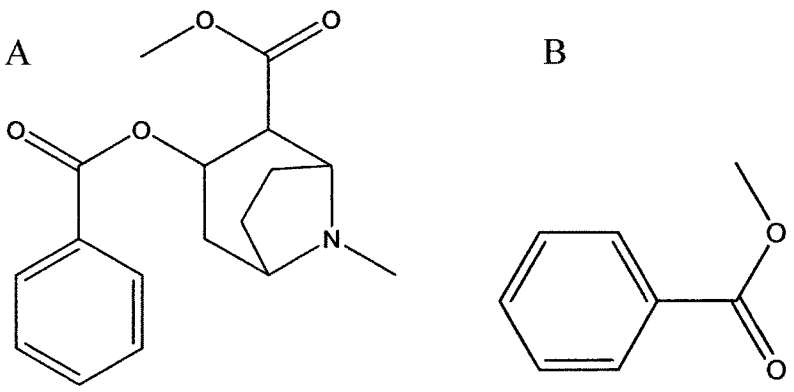

cocaine methyl benzoate

Figure 4. Chemical Structures of: A) Cocaine and B) Methyl Benzoate

Studies have shown that exposure of cocaine hydrochloride to normal ambient conditions will produce methyl benzoate (figure 4B) as a degradation product. Specifically, dissipation rate of 1.89 ng min^{-1} of methyl benzoate at room temperature with 0 % relative humidity was observed after one hour. A dissipation rate of 62 ng min^{-1}at 40 °C with 80 % relative humidity, was observed upon agitation by additional airflow **[32]**. This signifies that methyl benzoate, which has a very high vapor pressure, 0.38 Torr at 25 °C **[33]**, is expected to be available for sampling from typical cargo containers, which are exposed to humid conditions and fluctuating temperatures during loading and transport.

2.2.2 Marijuana

Marijuana, or *Cannabis sativa* L. is classified as a Schedule I drugs since it has a high potential for abuse, no acceptable medical use, and can cause severe physical and psychological dependence.

Cannabis sativa L. is one of the oldest cultivated plants because of its many uses. Oil can be produced from the seeds, while the stalk can be used to make ropes and fabric known as hemp. The psychoactive effects due to the compound Δ^9-tetrahydrocannaninol (THC), present in marijuana resin, are also a reason for continued cultivation. This compound (figure 5), a cannabinoid, is formed in surface features known as the glandular trichomes. A flowering female plant contains visibly larger number of these glandular trichomes and as such, a greater concentration of THC **[16]**.

The leaf material of marijuana contains about 1 wt% THC while the flowering material contains about 3.5 wt% **[34]**. Resin obtained by rubbing the plants against another surface

2-10% while the highest concentration of THC (10-30 wt%) can be found in hash oil, which is producing by extracting the cannabinoids from the plant material using an organic solvent, by refluxing. The solvent is evaporated, leaving behind the concentrated oil **[16]**.

The most popular and most efficient method of ingestion is by smoking the cannabis product since heating it above 100 °C causes Δ^9-tetrahydrocannabinolic acid (figure 5) to thermally decarboxylate to THC, thus increasing the total concentration of the psychoactive component, producing a stronger "high"**[35]**.

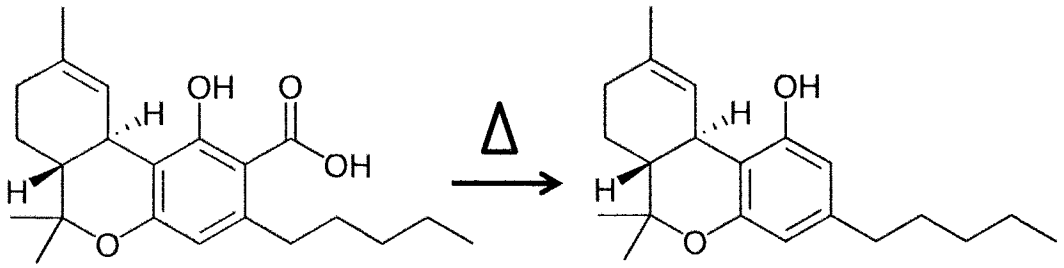

Δ^9-tetrahydrocannabinolic acid Δ^9-tetrahydrocannabinol

Figure 5. The Decarboxylation of Δ^9-tetrahydrocannabinolic Acid to THC

2.2.3 MDMA

The club drug, MDMA, also known as ecstacy, belongs to the drug class of amphetamines (shown in figure 6A). It is a Schedule I drug since it has a high potential for abuse, no acceptable medical use, and can cause severe physically and psychological dependence. MDMA is normally found in tablet form **[36]** with typical dose in the range of 75- 125 mg **[16]**.

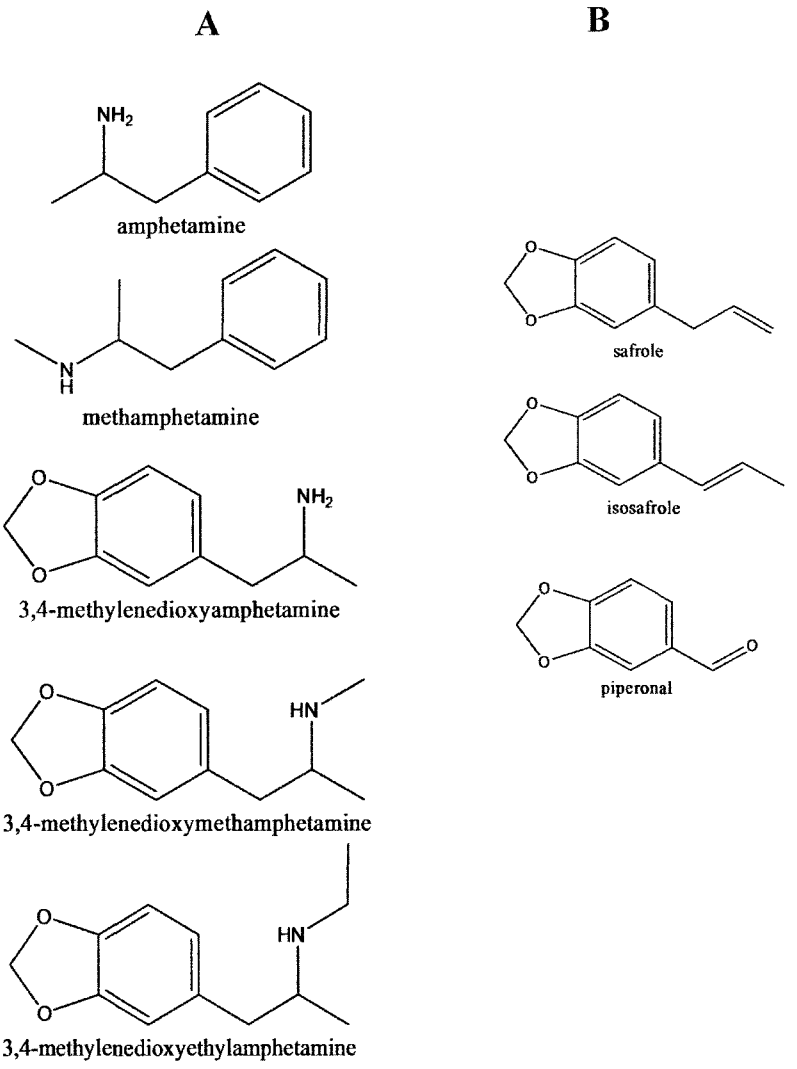

Figure 6. Structures of the: A) Amphetamine Drugs and B) MDMA Precursors

Numerous syntheses of MDMA have been reported in the literature **[37, 38, 39, 40]**, but all routes start with one of three compounds, safrole, isosafrole, or piperonal **[36]** shown in figure 6B. The precursors safrole, and isosafrole share the methylenedioxy moiety whereas piperonal is the derived aldehyde.

2.3 Field Analysis of Explosives and Illicit Drugs

Trace detection involves the determination of a very small chemical signal produced by as little as only a few molecules. There are two scenarios that require a trace detection approach. First, residues of the main explosive or the parent drug can remain on surfaces as a result of from a primary transfer from the hands of people preparing an explosive device or packaging illegal drugs for transport/ shipment. An even smaller amount would remain following a secondary transfer. For example, a third party coming into contact with the handler(s) of contraband may have traces transferred onto his/her person or belongings. An alternate scenario, would be a hidden explosive device or drugs concealed in extensive packaging. Although there may be a bulk amount of the contraband contained, a trace amount may remain on the outside or may cross the barrier in which it is concealed. There is a large body of research that details the structure of the compounds that are emitted by (in the gas phase), and are characteristic of the energetic material or the illicit drug (see Chapter 3). When attempting to screen, locate and identify (definitively or presumptively) these trace particulates or vapors, extremely sensitive detection devices are required.

The varieties of detectors available for this purpose employ optical, biological, and chemical means. Some examples of optical detectors are portable Raman spectroscopy for drug detection **[41, 42]**, other various forms of Raman spectroscopy for explosives detection **[43, 44]**, and optical fluorescence, a technique that employs UV radiation to decompose the explosive producing fragments that fluoresce **[45]**. This technique provides remote detection (2.5 m) of TNT. Optical techniques generally suffer from the

high cost and fragility of the instrumentation, a relatively large sample size required as compared to other trace detection techniques, and long analysis times to obtain high signal to noise ratios. The focus in the following sections is placed on biological and chemical trace detectors.

2.3.1 Biological Detection

There are many sensitive biological detectors for the trace detection of drug and explosive contraband. Some of these include trained canines **[24, 27, 36]**, honey bees **[46]** and plants **[47]**. Detection by trained canines is largely based on their exemplar olfaction capabilities. Olfaction is the detection of a chemical signal (an odor/scent) in the environment that produces a response in the nervous system **[48]**.

Canines are ultra-mobile sampling and detection devices that can locate explosive and drug odors because of the unique flow system of their nose. In the process of sniffing, air jets are created that prevent disturbance of the scent source, agitate surrounding particles that can then be inspired and sensed, and entrains the surrounding air to the air current surrounding the nose, further aiding in olfaction. An extensive review of canine olfaction and their unique flow system can be found elsewhere **[48]**. Canines have excellent detection limits that depend on the target compound and have been reported as 500 ppt (part per trillion) for 2,4-DNT and 2,3-dimethyl-2,3-dinitrobenzene (DMNB), a taggant. The detection limits are in the 10 ppb (part per billion) range for NG and methyl benzoate, a degradation product of cocaine **[49]**.

Detector dogs require constant training on the substances they routinely detect and recertification for quality assurance; they have an operational time of 20 min with 40 min breaks depending on conditions, for a whole 8 h day **[24]**. They also can have varied responses for the same compound since individual detector dog teams are trained on differing amounts of target compound, but this can likely be remedied by implementing uniform training aids **[50]**.

The latter two biological detectors, honey bees and plants are not as widely used in the detection of drugs and explosives as are detector dog teams. The honey bees collect TNT and other chemical contaminants in the environment while pollinating plants. They carry these substances back to the hive and the honey and honeycombs are analyzed for the presence of these substances. The disadvantages of this method include the large expense in training the bees and relatively short lifetime of the hives **[46]**. The role of plants as detectors is limited to the TNT explosive. They have been mutated to contain a receptor gene that makes them fluoresce in the presence of TNT in the soil. They can help in the remediation of soils contaminated with chemical munitions. The detection limits of this detector are not yet known and since it only works in the presence of TNT, it fails to detect the multitude of explosives available for illicit purposes.

2.3.2 Chemical Detection

The premier chemical detector for the field analysis of drugs and explosives is the ion mobility spectrometer (IMS) (further discussed in Chapter 5), since it is fast (analysis in s), can detect both drugs and explosives at atmospheric pressure, is portable, easy to use, has extremely low detection limits (pg levels **[17]**) and is affordable (~$40,000). Other

chemical detectors include electronic noses that mimic canine olfaction **[51]**. They accomplish this through a system of chemical sensing and pattern recognition. Targeted chemicals are presented to the sensing system producing a signature or fingerprint for each chemical. A database is created of all the signatures, and then the pattern recognition system is used to detect the chemicals after analysis. Gas chromatography (GC), mass spectrometry (MS), and IMS are also considered electronic noses provided they are portable, lightweight, and sensitive to the target chemicals **[52]**.

CHAPTER 3. VOLATILE CHEMICAL SIGNATURES

Trained canines are accepted by the general public as the ultimate detection and locating device for contraband substances, such as drugs and explosives, human cadavers, missing persons, etc. This is because of their acute sense of smell, or olfaction. Olfaction is defined as the sensory detection of an odor **[48]**, or a chemical mixture of volatile compounds that stimulates the olfactory neurons **[53]**. For olfaction to occur, the source of this volatile chemical mixture need not be present **[48]**. This has major implications since it means that the parent compound, such as the specific drug or explosive is not necessarily what is being detected by trained canines. In fact, research described in this chapter shows that canine detection mainly involves the sensing of vapor substances, or molecules in the gas phase.

3.1 Definition of Volatile Chemical Signatures

For a substance to be in the gas phase it must possess sufficient vapor pressure. Table 2 shows the classification of substances based on their vapor pressures as volatile, semi-volatile, or non-volatile (particles).

Table 2. Classification of Compounds Based on Volatility

Classification	Vapor Pressure (Torr)	Boiling Point (°C)
Volatile	>0.1	<100
Semi-volatile	0.1 to 10^{-7}	100-325
Non-volatile	<10^{-7}	>325

Relatively volatile explosives such as EGDN (ethylene glycol dinitrate), NG, or TNT have vapor pressures at 25°C of 4.8×10^{-2} torr, 2.3×10^{-4} torr and 4.5×10^{-6} torr, respectively, making them available in air for direct detection by a chemical and biological detector. Other organic explosives of security interest such as RDX, HMX, and PETN have very low vapor pressures, 1.1×10^{-9} torr, 1.6×10^{-13} torr, 3.8×10^{-10} torr, respectively, and are not available in the headspace. This essentially makes vapor sampling impossible, yet trained dogs can easily detect these explosives because they utilize volatile chemical signatures of explosive mixtures to reliably located them under difficult field conditions **[27]**.

A volatile chemical signature is being defined for this research as a compound, or a mixture of compounds that has been demonstrated to produce an olfactory response by a trained canine, and/or has been detected in the headspace above its respective parent compound by an instrumental technique, and persists for a period of time in order to allow its detection.

3.2 Volatile Chemical Signatures of Explosives

Canine trials have elucidated several odor volatile chemical signatures of explosives. For example, TNT and cast explosives share 2,4-dinitrotoluene (2,4- DNT) as a volatile chemical signature **[27]**. For the polymer-bonded explosives such as Composition C-4, 2-ethyl-1-hexanol elicited canine response, while the primary explosive RDX produced none.

The low explosives, smokeless powders, contain stabilizers such as diphenylamine (DPA), ethyl centralite (N,N-diethyl diphenyl urea), methyl centralite and deterrents such

as butyl phthalate, 2,4-DNT. These additives are useful in the characterization and identification of the source of these explosives **[54]** and have even been detected in gunshot and post-blast residues **[55,56,57]**. Despite confirmation of the presence of these volatile chemical signatures in the headspace of smokeless powders and residues, dogs showed little or no interest in these compounds during dog trials **[58]**.

Headspace sampling using solid phase microextraction (SPME, described in Chapter 4) has helped to identify many explosive volatile chemical signatures. The presence of cyclohexanone **[3]** and 2-ethyl-1-hexanol **[24,59]**, in the headspace of plastic cast explosives has been confirmed.

The successful extraction of the volatile chemical signatures of TNT from simulated buried mines has been reported by using SPME **[60]**. The explosive, TNT was detectable from various soils and at different temperatures all at or below 23°C by sampling of the headspace above the soil. The compounds 2,4-DNT, 1,3-dinitrobenzene (1,3-DNB), and TNT were detected and although99% of the explosive composition of the mines was TNT, the analytes 2,4-DNT and 1,3-DNB predominated in the headspace. This further demonstrates that targeting volatile chemical signatures as a means of identifying the presence of explosives is feasible. Baez et al. sampled vapors emitted from TNT crystals buried in soil and found that TNT and 2,4-DNT predominated in the headspace **[61].**

3.3 Volatile Chemical Signatures of Drugs

The detection of drugs by seeking the parent compounds is also problematic for the same reason, but canine detection of these illicit drugs is based upon volatile chemical

signatures **[36, 62, 63]**. For example, cocaine detection by canine olfaction is accomplished by targeting methyl benzoate, a decomposition product, not cocaine itself **[36, 63]**.

In the case of MDMA, its high polarity and low vapor pressure make SPME extraction of the tablets ineffective. Fortunately, the high vapor pressure of one of the starting materials in the synthesis of this drug, piperonal (1.0 mmHg at 87 °C), enables headspace SPME sampling. Through canine trials as well as SPME-GC/MS analysis, the volatile chemical signatures of MDMA have been identified as piperonal and 3,4-methylenedioxy-phenyl-2-propanone (MD-P2P) **[36, 62]**. Instrumental analysis of SPME extracts of another drug, marijuana, revealed α-pinene & β-pinene, limonene, as volatile chemical signatures **[64]**.

Figure 7 includes the structures and vapor pressures of the volatile chemical signatures of importance to this dissertation research.

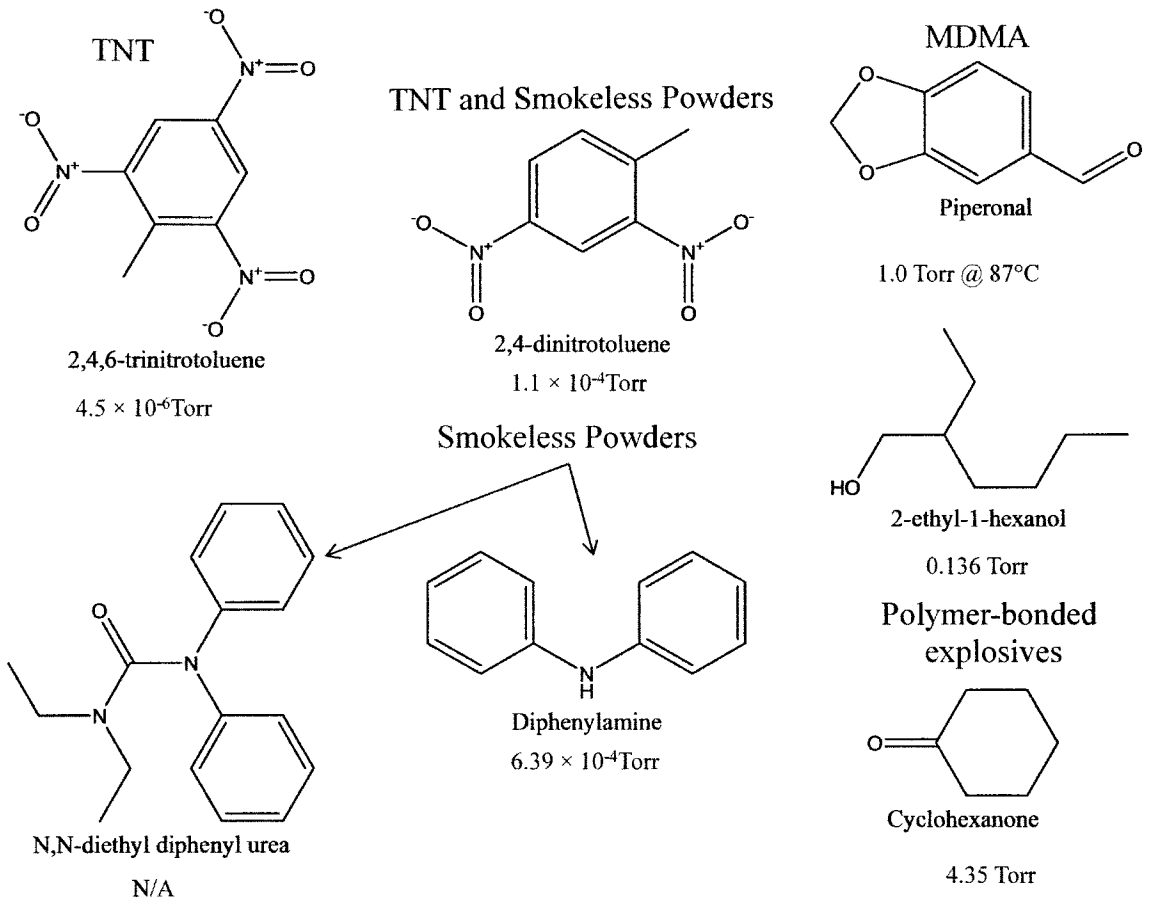

Figure 7. Volatile Chemical Signatures of the Appropriate Parent Compounds and Vapor Pressures. The values listed are at 25 °C unless otherwise stated [59, 26, 65].

3.4 Delivery Methods for Volatile Chemical Signatures

With the body of knowledge gained from canine and headspace analysis of illicit drugs and explosives, the next stage was to create calibration standards for certification of detector dogs. Controlled Odor Mimic Permeation Systems (COMPS) **[27, 50,66]** were developed for this purpose, and enable quantitation of the maximal mass of the volatile chemical signatures in air available for sampling by a trained canine or an instrumental technique. These COMPS devices differ from currently available gas generating systems

[67,68] in portability since they are lightweight, do not require any power to operate, are very inexpensive, and as opposed to a type of finite gas generating system**[69]**, they provide a continuous vapor source. Piperonal COMPS devices have recently been reported as a vapor source for the determination of canine detection sensitivity in the detection of MDMA **[50]**.

CHAPTER 4. SOLID PHASE MICROEXTRACTION

4.1 Theory of Solid Phase Microextraction

Solid Phase Microextraction (SPME) is a solvent-free, sampling, extraction, pre-concentration, and sample introduction technique that absorbs or adsorbs analytes onto a small volume of non-volatile polymeric coating or solid sorbent phase spread on a solid support. Mass transfer of the analytes occurs the moment the coated fiber comes into contact with the sample **[70]**, and is influenced by the attraction of the analytes to the phase based on the principle of "like dissolves like."

4.1.1 Historical Aspects of SPME

The inception of solid phase microextraction dates back to 1987 **[71]**. At this time, the Pawliszyn group was conducting work on laser desorption/fast gas chromatography (GC), which was inhibited by the long sample preparation times relative to the separation and analyses times. Optical fibers were already being used to transmit laser light energy to the GC, so as a clever sample preparation technique, sections of the fibers were dipped in the solution containing the analytes, the solvent was evaporated and the fiber was introduced into the GC with analyte desorption via a laser pulse. A subsequent study **[72]** focused mainly on confirming the usefulness of this sampling approach and showed that both polar and non-polar analytes were extracted from aqueous samples. The only issue was the loss of head pressure at the column, since for introduction of the fiber, opening of the injector was required. This problem was corrected by incorporating the coated fibers into a Hamilton 7000 series microsyringe resulting in the first SPME device, as the

analytical community knows it **[73]**. Since then, SPME has become a widely used sample preparation technique, employed for a wide range of applications and has even been the subject of several recent reviews **[74, 75, 76]**.

4.1.2 Thermodynamics

The mass extracted onto the coating (n) is mediated by several parameters including the equilibrium constants described by equation 1, temperature, coating chemistry, sample volume and coating volume and the initial concentration in the headspace available for sampling.

$$n = \frac{K_{fs} V_f V_s C_0}{K_{fs} V_f + V_s} \quad \textbf{(Equation 1)}$$

The fiber/coating matrix distribution constant is K_{fs}, V_f is the volume of the coating, V_s is the sample volume, and C_0 is the initial concentration of the analyte of interest in the sample. When the sample volume is large ($V_s >> K_{fs} V_f$) then equation 1 can be simplified to equation 2, providing a direct quantitative relationship between the amount extracted and the initial concentration of the analyte in the matrix:

$$n = K_{fs} V_f C_0 \quad \textbf{(Equation 2)}$$

The utility of SPME for field sampling is evident because based on equation 2, the amount of extracted drug, explosive or volatile chemical signature will correspond directly to the initial concentration of the analyte in the matrix without dependency on the volume of the sample **[70]**.

4.1.3 Kinetics

Studying kinetics can help the analyst optimize extraction conditions by elucidating ways to increase the speed of extraction. Agitation is the main route to accomplish this and in an ideal scenario the molecules in the sample phase, be it the headspace or the actual sample matrix as in direct immersion, move very rapidly with respect to the SPME phase. In this manner, the analytes in the sample all have equal access to the SPME coating. With these perfect agitation conditions, the equilibrium time (equation 3) is the time it takes for 95% of the equilibrium amount of a given analyte in a sample to be extracted by the coating,

$$t_e = t_{95\%} = \frac{2(b-a)^2}{D_f} \quad \textbf{(Equation 3)}$$

where b is the fiber coating outer radius, a is the fiber coating inner radius, and D_f is the analyte diffusion coefficient in the fiber coating. The equation can be used in the method development process to estimate the minimum amount of time it will take to reach equilibrium. In reality, the fluid in contact with the fiber surface is always stationary regardless of how well the analyst agitates the sample. Like a gradient, the further away from the fiber surface, the greater the fluid motion until bulk flow in the sample is reached. To model this behavior, the space closest to the fiber surface is considered a zone of defined thickness where no convection of molecules occurs. On the other hand, perfect agitation occurs beyond this depletion zone. Figure 8, illustrates this boundary layer model, while equation 4 represents a correction for determining equilibrium time under less than perfect agitations conditions.

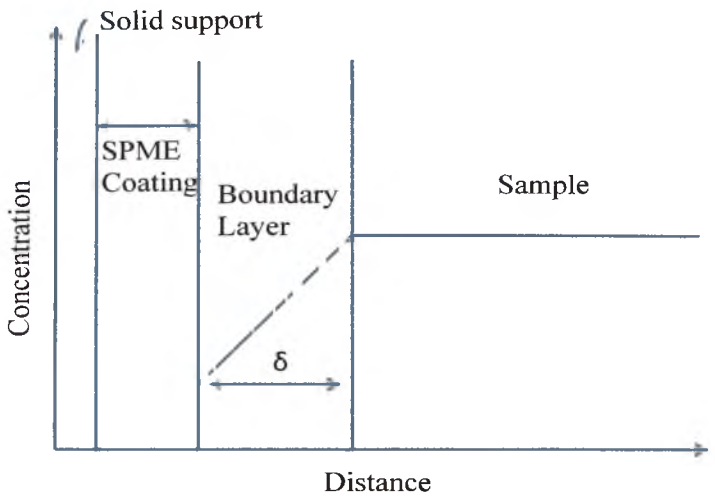

Figure 8. Boundary Layer Model

$$t_e = t_{95\%} = 3\frac{\delta K_{fs}(b-a)}{D_s} \quad \textbf{(Equation 4)}$$

This equation factors in both the analyte's diffusion coefficient, D_s, in the sample fluid as well as K_{fs} rather than simply considering D_f. The thickness of the boundary layer (δ) is also accounted for, and is determined by agitation conditions and fluid viscosity [77]. By minimizing this zone, extraction rates can be increased.

4.2 Practical Aspects of Sampling

This small volume of sorbent is generally coated onto fused silica or metal fibers. These delicate coated fibers are housed in a syringe in the commercial configuration available from Supelco. A schematic of the complete sampling system is shown in figure 9.

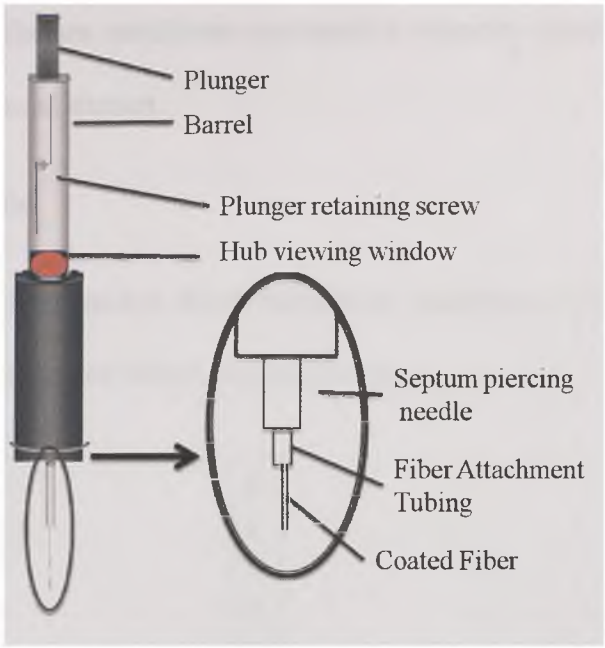

Figure 9. Commercial SPME Fiber Sampler from Supleco

There are several theoretical SPME configurations besides the fiber including: stir-bar, disk/membrane, particles suspended in the sampling media, in-tube SPME with sampling media flowing through (similar to GC and HPLC stationary phases), and vessel walls **[77]**. One of the main advantages of SPME is the ability to develop/ select the appropriate geometry depending on the sample considerations for the particular matrix in which the desired analyte resides. Examples of effective varied geometries are stir-bar sorptive extraction **[78]** that is useful for the analysis of biological matrices **[79]**, and thin-film microextraction **[80]**.These have been developed to increase capacity for absorption by increasing the surface area of the extraction phase.

The complete SPME process requires extraction, transfer, and desorption **[81]**. Extraction begins when the SPME device is exposed to the sample. The analyte mass accumulates

over time until equilibrium conditions are reached whereby extraction for longer time does not afford additional extract.

4.2.1 Extraction Modes

There are three extraction modes: direct immersion, headspace, and membrane-protected extractions, and are illustrated below (see figure 10).

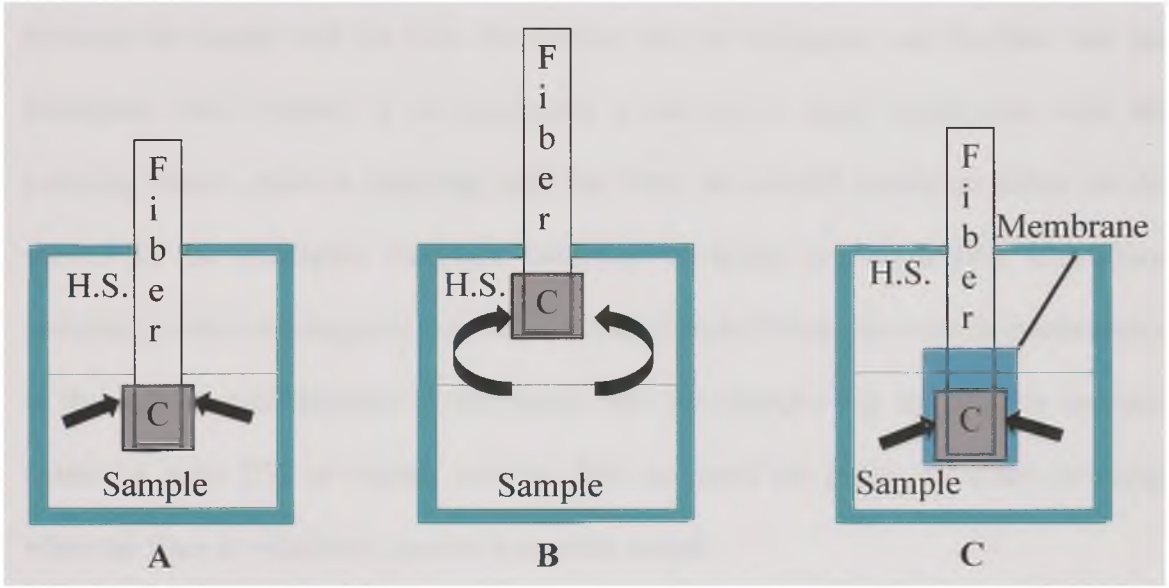

Figure 10. Extraction modes of SPME (H.S. - sample headspace): A) direct immersion, B) headspace and C) membrane-protected [77]

For direct immersion, shown in figure 10A, the SPME fiber is directly inserted into the sample and the analytes are immediately transported to the coating. Agitation such as stirring or movement of the sample vial can be used to further expedite the absorption/ adsorption of molecules by moving them near the SPME phase thus preventing depletion of the boundary layer. Agitation techniques are generally not required for gaseous samples since air convection is considered sufficient.

When conducting headspace sampling, shown in figure 10B, the analytes are removed from the headspace by the fiber, with further extraction originating from the sample matrix. The rate-determining step is the speed with which the sample matrix replenishes the headspace concentration. This process is fastest for volatile compounds but can be aided by agitation and/or increasing the temperature of extraction for the determination of semi-volatile analytes. This process continues until multi-phase equilibrium is reached between the sample and the fiber, the sample and the headspace, and the fiber and the headspace. For volatiles, if the headspace is allowed to reach equilibrium with the sampling matrix prior to sampling with the fiber, the overall extraction times can be shorter for the headspace technique compared to direct immersion **[77]**. Headspace sampling is also advantageous since the fiber is protected from non-volatile interferences in the matrix, modifications of the matrix like pH changes that are used to increase extraction rates **[77]** or organic solvents that can swell the phase and cause stripping when the fiber is withdrawn into the protective needle.

The membrane-protected technique, shown in figure 10C, was created to build upon strategies for protecting the delicate SPME fiber from very dirty matrices. The technique is in-line with utilizing headspace sampling for volatile compounds instead of direct immersion, but is aimed at providing analysts with a technique for the determination of analytes with insufficient volatility to use the headspace technique. Obviously, the extraction rates are slower since the analytes must diffuse through the membrane prior reaching the SPME fiber, but the use of agitation techniques and extremely thin membranes help alleviate this slight disadvantage **[77]**.

Under any extraction mode, after the analytes have been collected, they are desorbed from the coated fiber into the analytical instrumentation by thermal desorption into the high temperature injection liner of a GC or by a solvent for HPLC **[82]**.

4.2.2 Dynamic Sampling

The discussion of SPME thus far has been limited to static sampling, or exposure of the extraction phase to the sample while allowing the analytes to passively diffuse into the phase without increasing the diffusion rate via external techniques beyond the agitation methods described earlier. Dynamic sampling is an alternate mode of SPME sampling achieved by exposing a SPME fiber to a stream of gas, typically air, containing volatile and semi-volatile compounds which can be absorbed or adsorbed onto the fiber's coating. One downside of dynamic SPME fiber sampling is the long extraction time necessary when sampling open air **[83]**, although it may be reduced to 1 hr with the aid of an air pump **[84]**. Instead Larroque, et al., collected open air samples in bulbs of various volumes and sampled statically with SPME for periods of over 10 hr **[85]**. Augusto, et. al developed a rapid dynamic air SPME sampling method for detection of volatile organic compounds (VOC's) using a modified hairdryer **[86]**. Although sampling was possible in 30 s because of the decrease in boundary layer resulting from the constant agitation at critical air speeds, the fibers placed in the slit of the modified hairdryer likely suffered from increased fragility due to the air turbulence. All the previously mentioned dynamic SPME sampling methods are still limited in terms of capacity by the surface area of the fiber geometrical configuration. A recently reported SPME device with increased surface area due to the helical carboxen/ polydimethylsiloxane (CAR/PDMS) phase wound

between two glass tubes, has shown improvement in extraction of VOC's when compared to conventional SPME fiber dynamic sampling **[87]**. These dynamic sampling methods still depend on the fiber configuration for introduction into the analytical instrumentation.

4.2.3 Method Development

There are several steps involved when developing a SPME method. The first step is selecting the fiber coating. The others are described elsewhere, with some more important than others **[77]**. There is a wide range of commercially available fibers for the purposes of method development that exhibit various polarities, coating thicknesses, and coating types. These are listed in Table 3.

Table 3. Commercially Available Fiber Coatings [20]

Fiber Coating	Desorption Temp. (°C)	Coating Type	Polarity
Bare fused silica	270	Adsorbent	Unknown
7-μm PDMS	270	Absorbent	Non polar
30-μm PDMS	270	Absorbent	Non polar
100-μm PDMS	270	Absorbent	Non polar
85-μm Polyacrylate	290	Absorbent	Polar
PDMS-DVB SF	260	Adsorbent	Bipolar
CW-DVB SF	260	Adsorbent	Polar
DVB- Carboxen SF	270	Adsorbent	Bipolar
Carboxen-PDMS SF	340	Adsorbent	Bipolar

Based on the principle of "like dissolves like," the polarity of the coating is chosen to be closest to the analytes targeted for extraction from the sample matrix. The coating thickness is chosen to be the thinnest amount that enables equilibrium to be reached the fastest, and desorption to be complete, while still retaining sensitivity. The thicker a SPME coating is, the more capacity for extraction/retention, but the drawbacks include longer sampling times and higher desorption temperatures required. The coating type determines the method of extraction as absorption or adsorption. Absorptive coatings extract by partitioning of the sample into and out of a liquid polymeric coating until equilibrium is reached. This process has been compared to how a sponge absorbs liquid **[88]**. Since absorbent materials are films, there are no active sites that molecules compete for to occupy. The retention of analytes on an absorbent coating is mostly determined by the film thickness. The size of the analyte and polarity also affect retention, but not as much as the film thickness.

Adsorptive coatings, sometimes referred to as solid coatings, are designed for the extraction of very small and volatile molecules. These coatings extract by physically interacting with the molecules; they have pores of varying sizes (micropores and mesopores) that trap the analytes and retain them until high temperature or a solvent is used to remove them from the coating and also provide a large surface area for extraction. Medium sized molecules can also be retained if the coating has large pores (mesopores). The solid coating can be dispersed in a polymeric medium as is the case with Carboxen-PDMS Stableflex. This PDMS polymer coating helps to attach the solid particles to the fiber core as well as enhances selectivity based on its polarity **[88]**.With the presence of

the pores that enable physical interaction with the sample molecules and trapping, competition is observed for the available active sites at capacity. A diligent analyst will monitor effects of displacement over time to determine the optimal extraction conditions for the desired analyte(s).

4.3 Phase Chemistry

Much effort has been devoted to altering and developing new SPME coatings **[89]**. This is because phase chemistry affects extraction outcomes (mass uptake rate, percent recovery, etc.) for a desired analyte. In this section, a coating technique using sol-gel technology will be described thoroughly. A polymer coating based on rare earth ß-diketonate complexes recently employed for SPME in the determination of TNT **[90]** will also be described, as it is potentially a viable alternative extraction phase for this research.

4.3.1 Sol-gel Coating Technology

The sol-gel process first involves the formation of a suspension of colloidal particles known as the sol. A sol is defined as a colloid (a mechanical mixture where one substance is dispersed evenly throughout another) **[91]**, consisting of solid particles dispersed in a liquid medium. The sol is then converted to a gel, whereby the solid particles become connected by chemical treatment. The gel is then dried and sintered to form a ceramic product **[92]**, for example.

Utilization of the sol-gel process to create inorganic and hybrid organic-inorganic polymers affords many advantages **[93]**. The sol-gel technique allows these polymers of

tailored chemistry to be synthesized in various forms depending on the desired end-use. Dense thin films, fibers, powders, dense ceramics, monoliths and uniformly sized particles, can be produced by various processing and drying techniques (coating, extruding, conventional drying, supercritical drying, grinding, sintering, etc.) **[94]**. These customized materials, are formed under very mild conditions, such as lower temperatures of preparation, and can even be made in-situ or in "one pot." This stems from the compatibility of the ingredients that facilitate thorough mixing. Since these products originate from raw materials of known origin, the final product has better purity and homogeneity than glass and ceramics produced traditionally. By enabling the creation of hybrid organic-inorganic polymers, selectivity, stationary phase stability, and overall performance of chromatographic separations can be improved. Improvements in chromatographic stationary phase stability are due to high thermal resistance the sol-gel polymer, thereby reducing column bleed when conducting separations at extremely high temperatures, and high pH stability when exposed to mobile phases ranging from the most acidic to the most basic. The siloxane bond (Si-O-Si) at the surface of traditional stationary phases hydrolyzes at pH values greater than 8 and this reaction is expedited further at high temperatures **[95]**. Lastly, and what is likely the largest contributor to the ever increasing popularity of the sol-gel process as a method for creating new materials aimed at a wide range of scientific and engineering applications, is that the structure and properties of the polymers synthesized can be designed by keenly selecting the precursors and building blocks for the sol-gel reactions **[93]**.

4.3.1.1 Chemical reactions in the sol-gel process

There are generally 2 main steps in the sol-gel process. First, simple, sol-gel active precursors are converted into the sol, or an intermediate colloidal state consisting of solid nanometer sized particles in a liquid medium. Next, the sol solution is converted, through another set of reactions into a three-dimensional polymeric network with solvent filled pores. This is called the gel.

For a sol-gel reaction to proceed, there are several building blocks that are required. One or more precursors are necessary and are typically metal alkoxides $M(OR)_x$. One or more sol-gel active polymers act as the stationary phase. Another sol-gel active polymer known as the deactivating reagent is used to encap (derivatize) residual silanol groups. The deactivating reagent should have a similar structure to the stationary phase so as not to alter the overall absorptive properties **[96]**. A solvent such as methylene chloride is required to disperse the ingredients. An acid or base catalyst, and water, the hydrolysis reagent are also necessary **[93]**.

The chemical reactions that take place in a sol-gel process are first, the precursor(s) are hydrolyzed, then polycondensation of the hydrolyzed products occurs. The condensation and hydrolysis products react with the sol-gel active species that include the deactivation reagent and the stationary phase. As the condensation reactions are occurring the viscosity of the solution gradually increases and the nanometer sized particles that have been created agglomerate in a rigid three-dimensional network. Lastly, the sol-gel polymer product reacts with the activated silica surface of the glass or a metal activated surface such as titanium **[93]**.

The choice of catalyst can affect the final structure of the sol-gel product formed. When base is used as a catalyst, electron donating –OR groups are removed. The monomers are almost completely hydrolyzed so cross-linking begins at an early stage even though original precursor remains. The resulting condensed particulate matter makes up the porous sol-gel polymer structure since the condensation reactions occur faster than the relatively slow hydrolysis step **[97]**. Under acidic conditions, the precursors are converted into the silanol hydrolysis product very rapidly leading to highly branched linear polymers by virtue that the hydrolysis of the precursors occurs much faster than the condensation reactions **[98]**. Protonation of silanol species is less favorable since one electron donating alkoxy group has already been removed, making the second hydrolysis step is much slower. As a result, polycondensation reactions occurs between Si-OH and Si-OR groups of partially or non-hydrolyzed products. The terminal Si-OR groups that result are more reactive both inductively and stearically, thus long linear polymers are formed. These linear polymers can become entangled, or crosslinked after hydrolysis of the Si-OR moieties **[93]** affording added stability under conditions of extreme heat or pH. The precursor, if chosen carefully, can minimize the undesirable effects of cracking from stress and shrinkage that occur during the drying step. Shrinkage and cracking is observed when the gel applied to the substrate results in a thick (greater than 0.5 μm) film **[99]**. The coherent force within a thick film causes drying of the film in a direction parallel to the substrate surface rather than perpendicular to the surface as seen in thin films **[100]**.

Since coating thicknesses beyond 0.5 μm can be required for a particular application, a way to minimize these structural defects was necessary. Rather than using the popular

precursor TMOS, tetramethoxysilane, alkyl derivatives of TMOS can be used **[101,102]** since they ultimately lead to a more open bed structure of the sol-gel and thus the stress is minimized during the drying step **[102]**when compared to using TMOS. The alkyl derivative, methyl trimethoxysilane (MTMOS) satisfies these requirements and was first used by Chong, et.al. **[101]**as the precursor in their sol-gel process.

4.3.1.2 Sol-gel SPME Coatings

Sol-gel coating technology was used for the first time in the preparation of solid phase microextraction fibers **[101]**.The use of sol-gel SPME extraction phases is fueled by a number of disadvantages traditional commercially available SPME fibers possess **[93]**. The SPME fibers normally have low operating temperature limits (240 °C -280 °C). Desorption of strongly attracted analytes off the SPME fiber extraction device may require higher temperatures than the particular operating limit. In these cases, increasing the temperature despite the reported limits would result in damage to the fiber, decomposition of the SPME phase with possible contamination of the analytical instrument, and at best, reduce overall lifetimes of the fiber. Also, the fiber is extremely fragile and can easily break, the coating may inadvertently be stripped off, and the phase can easily swell in organic solvents, and degrade when exposed to extreme pH conditions. These problems originate from the SPME extraction phase not being covalently bonded to the substrate, which is typically the fused silica fiber or titanium rod. The sol-gel process affords high temperature (300 °C- 450°C) **[103]**, solvent and pH stability **[104]**, and can provide very thin coatings that facilitate desorption. The phase chemistry can be tailored to extract specific analytes, increasing selectivity of the

analytical process. Furthermore, an extraction phase consisting of nano-sized particles created during the sol-gel process, affords additional surface area and capacity when compared to a glassy film of PDMS.

Many novel SPME coatings based on sol-gel technology have been developed since it first was introduced as a way of coating fibers **[101]** and thus the topic is the subject of a recent review **[93]**. An *o*-poly(butyl methacrylate/OH-TSO) (BMA/OH-TSO) coating has been developed that enabled the extraction of mustard gas, 2-chloroethyl ethyl sulfide, a chemical warfare agent from the soil with low detection limits (ng g^{-1}) and good reproducibility (2.2%) **[105]**. Another study produced three different forms of vinyl crown ether phases to preferentially extract organophosporus pesticides from foods **[106]**. These workers used vinyl crown ethers with different cavity sizes and benzyl substitutions to determine which was best for this target analyte, while strongly attaching this coating to the substrate via a sol-gel process. Vinyl crown ether coatings exhibit medium polarity because of the cavity structure and strong electronegative effect of heteroatoms on the ring. This provides unique selectivity for polar compounds such as the pesticides in question. They concluded that the benzo-15-crown-5 coating exhibited the greatest extraction efficiency since there is one benzyl group on its crown ether ring and its electron distribution not symmetrical. This is because of the P/ π conjugation between the benzyl group and the oxygen atoms connected to the benzyl group, which result in a bigger dipole moment. This made it the most polar of all the phases studied. Other SPME phases developed based on sol–gel include polyethylene glycol (PEG) **[107]** and hydroxyfullerene **[108]** fibers for extraction of polar and non-polar compounds. It is

evident just from these few examples that any strongly attached coating with desired extraction capabilites and high operating temperature limits can be developed for SPME sampling just by using sol-gel technology and the appropriate precursors that will result in a coating chemistry containing moieties chosen to preferentially extract the desired compounds.

4.3.2 La (dihed) Phase Chemistry

Since before 1967, it has been accepted that the rare earth chelates of ß-diketones, especially the tris complexes, showed promise as stationary phases for gas chromatography **[109]**. There was the issue of hydration in compounds that affected the thermal stability of some of the complexes **[110]**, but this was successfully addressed by using a sterically hindered ligand **[111]**. Furthermore, by employing highly electronegative fluorinated ligands, a water molecule may be hydrogen bonded to an electronegative site on the ligand shell instead of being coordinated with the metal center **[112, 113]**. As a result, thermal stability is increased, since the possibility of hydrolysis of the complex is decreased **[109]**.

With these potential setbacks resolved, the use of ß-diketonate chelates of the lanthanide mixed with liquid stationary phases was further explored **[114, 115]**. Later, pre-analytical columns were prepared containing a sorbent based on a lanthanide complex, specifically europium (III). The motivation was that the chelates would accept additional donor atoms in the coordination sphere of the lanthanide, forming strong complexes with oxygen containing compounds. In other words, nucleophilic species could be separated from non-

nucleophilic species by formation of a complex. The non-nucleophilic compounds would be eluted normally, while the fraction containing nucleophilic compounds like aldehydes, ketones, alcohols, etc., complexed with the metal chelate, could be thermally dissociated and that fraction kept for subsequent analysis. This novel sorbent allowed analysis of specific classes of compounds and simplified what would otherwise have been very complex chromatograms. The last recommendation by these workers was the replacement of the costly lanthanide metal, europium, with lanthanum, based on experiments where the smaller lanthanide, lutetium, yielded identical results as with europium **[116]**.

The La (III) complex with the *p*-di(4,4,5,5,6,6,6-heptafluoro-1,3-hexanedionyl)benzene, (H_2dihed) fluorinated ligand **[117]** was later produced as previously suggested **[116]**, as were many other metal complexes in order to produce stationary phases with varying retention properties **[117]**.

More recently, work on these stationary phases was resurrected in order to apply them to the separation of a variety of explosive samples. These included TNT, 2,6-DNT, DMNB, TATP, and the nitrated esters, all of importance to this dissertation research. The idea was that these explosives, Lewis base analytes, would be strongly attracted to the Lewis acid polymer, the metal ß-diketonate stationary phase. The best retention was obtained with the La (dihed) chemistry, but some of the explosives were so strongly retained that they could not be eluted from the packed column. This was a consequence of using the fluorinated H_2 (dihed) ligand since its electron withdrawing inductive effects increase the metal center acidity, enhancing interaction with the weak Lewis base explosives **[118]**.

Since most of the retained species could be thermally desorbed from the metal ß-diketonate stationary phase, it was only logical to use this sorbent as a SPME phase. In simple terms, SPME in the fiber form, can be considered an inside-out chromatographic column and what likely further encouraged these researchers to pursue this application was the performance of La (dihed) in the packed form at retaining the volatile and semi-volatile explosives, volatile chemical signatures, and taggants that previous researchers have found success with while conducting SPME sampling (see Section 4.4.1). The La (dihed) SPME fibers produced, by dipping in a solution of the polymer in methanol or directly pasting it to the fiber with an epoxy, showed a 20 times enhancement in the detected amount of 2,4-DNT and 17 times enhancement in the detected amount of TNT following sampling/extraction from a large volume vessel (an explosives bunker), over the control PDMS fiber **[90]**. Demonstration of enhanced capture by this SPME fiber type is significant for two reasons: it improves the probability of extracting dilute amounts of these airborne compounds from large volume vessels, and may later prove, since it selectively extracts Lewis base analytes, to reduce or eliminate interferences from extraneous compounds in air.

Despite the promising data shown by the La (dihed) SPME fibers for improving explosives sampling, it is clear that this SPME phase does have room for improvement. First, the La (dihed) complex is hygroscopic and ligand hydrolysis is observed as artifacts of various hydrolysis products following desorption into the GC/MS instrument. It has a low operating temperature (175 °C) and lower reusability than conventional SPME fibers (20 times versus 100 times). The ligand hydrolysis was a result of adsorbed water on the

fiber reacting with the heat of the injection port and was likely exacerbated by the fact sampling was done on a rainy day **[90]**. This is an operational challenge since for a field sampling technique to be useful it must not be adversely affected by humidity or environmental conditions. The remaining issues seem to be largely caused by the La (dihed) coating not being covalently bound to the fiber substrate. The authors offer some possibilities for improving the attachment of the phase to the fiber **[90]**, like using sol-gel technology, but considering the structure of the complex this seems difficult at best.

4.3.3 Characterization of Polymer Products

4.3.3.1 Scanning Electron Microscopy

In scanning electron microscopy (SEM) a beam of energetic electrons is used to scan the surface of a solid in a raster pattern. As a result, several signals are produced that include: backscattered and secondary electrons, as well as other photons of varying energies. The backscattered and secondary electrons are the most commonly used signals in SEM surface analysis. When beam of electrons interacts with a solid sample, either elastic or inelastic scattering occurs **[119]**.

Elastic interactions affect the trajectory of the beam after surface interaction without significant reduction (<1 eV) in the energy of the electron beam. These interactions occur between the negative electron and the positive nucleus. Some of the electrons eventually lose energy by inelastic collisions and remain in the solid. Most electrons undergo numerous collisions but still exit from the surface as backscattered electrons **[120]**. The

exiting beam of backscattered electrons is much wider than the incident beam, reducing resolution in the image.

Inelastic scattering on the other hand, occurs when part or all of the energy of the electron beam is transferred to the solid sample, producing secondary electrons, from interactions between energetic beam electrons and valence electrons or weakly bonded conduction-band electrons in metals. Secondary electrons are emitted from the specimen with an energy of less than 50 eV **[121]**.

These signals are collected by a detector, converted to a voltage, which is then amplified. This amplified voltage hits a grid causing changes in the intensity of the spot of light. Thousands of these spots of different intensities create an image that corresponds to the sample topography. The image produced by backscattered signals provides information about topographical irregularities and changes in chemical composition, while secondary electrons provide information about surface characteristics **[122]**. For this research, SEM has been used to study the surface morphology of the polymer products developed, study their cross-sections for porous characteristics, and to determine their respective coating thicknesses.

4.3.3.2 ^{1}H Nuclear Magnetic Resonance Spectroscopy

^{1}H Nuclear Magnetic Resonance (^{1}H NMR) Spectroscopy is a method of measuring the absorption of radiofrequency radiation by hydrogen nuclei when these are subjected to an intense magnetic field. The spectra produced provide important information for analysts

conducting structure determination experiments since they can help elucidate the number and the environment of hydrogens attached to each carbon **[123]**.

4.3.3.3 Direct-Infusion Mass Spectrometry

Direct-Infusion mass spectrometry (DI-MS) enables the determination of the molecular weight of synthetic polymers and inorganic species **[124]**.Since the La (dihed) complex synthesized for the present work is both an inorganic compound as well as a synthetic polymer, DI-MS was used as one of several structure determination techniques. The DI-MS technique utilizes the atmospheric pressure ionization technique known as electrospray. The sample solution is pumped through a stainless steel capillary needle with a given flow rate (μL min^{-1}) maintained at several kV with respect to the cylindrical electrode surrounding the needle. The charged spray of droplets that results passes through a desolvating capillary. This is where the solvent is evaporated and charge is attached to the molecule. With further solvent evaporation, the droplets become smaller and their charge density greatly increases. Desorption of the ions into the ambient gas occurs **[119]**.

Electrospray is a soft-ionization technique such that large fragmentation does not occur. This is partly because other ionization techniques use volatilization, followed by an ionizing agent acting on the gaseous sample. These hard ionization techniques can damage thermally labile analytes or are irrelevant to the analysis of non-volatile substances. Electrospray is unlike these methods since it is a desorption technique whereby energy is introduced into the liquid sample so as to cause direct formation of gas phase ions. As a result, the spectra are simplified. This is especially desirable when

attempting to see the molecular ion alone and confirm the mass of the synthesized compound. Additionally, since multiply charged ions can also result, molecules with very large mass such as biomolecules, peptides, or large-chained polymers can be analyzed with a quadrupole mass spectrometer of limited mass range (1500-2000 a.m.u.) **[119]**.

4.3.3.4 Infrared Spectroscopy

Infrared (IR) spectroscopy, especially of the mid-IR spectral region from 4000 to 200 cm^{-1}, is used for organic analysis and structure determination of molecules that exhibit small differences in energy between several rotational and vibrational states. For absorption of infrared radiation, the molecule must undergo a net change in dipole moment as a consequence of its rotational and vibrational motion. Then, the electrical field of the infrared radiation can interact with the species and cause changes in the amplitude (or produce characteristic bands in the spectrum) of one of its vibrational or rotational motions **[119]**. In this study, infrared spectroscopy is used to aid in the structure determination of both the H_2dihed ligand and the La (dihed) complex following synthesis of these compounds.

4.4 Solid Phase Microextraction for Explosives and Illicit Drug Sampling

4.4.1 Explosives Sampling

The recovery of organic explosive residues of non-volatile PETN, RDX, and TNT **[125,126]** and of the homemade explosive TATP **[127]** has been demonstrated by SPME-GC/MS. For the extractions of PETN, RDX, and TNT, polyacrylate resin (PA) and polydimethyl siloxane (PDMS) were the fiber chemistries employed, with the former

being more effective. Heating of the sample at 100°C was necessary to promote the increase of the analyte concentration in the headspace.

For the recovery of TATP, the fiber chemistry PDMS/DVB was found to be more effective at extracting the target analyte than the conventional methods of post-blast debris extraction using adsorption by Amberlite XAD-7, which among other disadvantages, uses a solvent to extract the analyte **[127]**. Furton et al. tested HS and DI SPME techniques for the recovery of nitroaromatic explosives, using different types of SPME fibers analyzed by GC-ECD and HPLC **[128]**. Baez et al. optimized HS-SPME for sampling vapors emitted from TNT crystals buried in soil. Vapors of TNT and 2,4-DNT were predominant in the headspace under various meteorological conditions using SPME coupled to GC-ECD and TEEM (Tunable Electron Energy Monochromator) GC/MS **[61]**.

4.4.2 Drug Sampling

The sensitive analysis of illicit drugs from bodily fluids such as urine, serum, saliva and sweat was accomplished using direct immersion SPME. Commercial fibers and pre-treated chemically derivatized fibers were immersed inside the suspected media for efficient extraction **[129, 130, 131, 132]**.

A headspace SPME configuration has also been reported for the determination of cannabinoids and amphetamines from hair samples **[133, 134]**. Cannabinoids were also detected by SPME-GC/MS when the vapors emitted after the basic extraction of pre-treated head hair samples were sampled **[135]**.

The extraction of methamphetamine and impurities was improved by using HS-SPME instead of other liquid extraction techniques **[136]**. The amine salts of amphetamine related drugs were transformed into their volatile free bases using triethylamine. For improved chromatographic performance, the headspace above the drug was sampled by a SPME fiber previously derivatized with alkylchloroformates **[137]**.

These preceding examples were provided to demonstrate the utility of the SPME sampling technique in forensic analysis and its acceptance by researchers in the field.

CHAPTER 5. ION MOBILITY SPECTROMETRY

5.1 Theory of Ion Mobility Spectrometry

The differential velocities of gas phase ions in an electric field can be used to characterize chemical substances **[17]**. This is the basis of ion mobility spectrometry (IMS), the main analytical technique used in this research. Figure 11 shows a schematic of processes in IMS. In stand-alone IMS, sampling at security checkpoints involves standard operating procedures that include swiping the suspect area with a filter paper or a nylon cloth (among many other collection media) or vacuuming particles onto a Teflon membrane **[138]** to entrap the analytes of interest, but there are other methods of sample introduction.

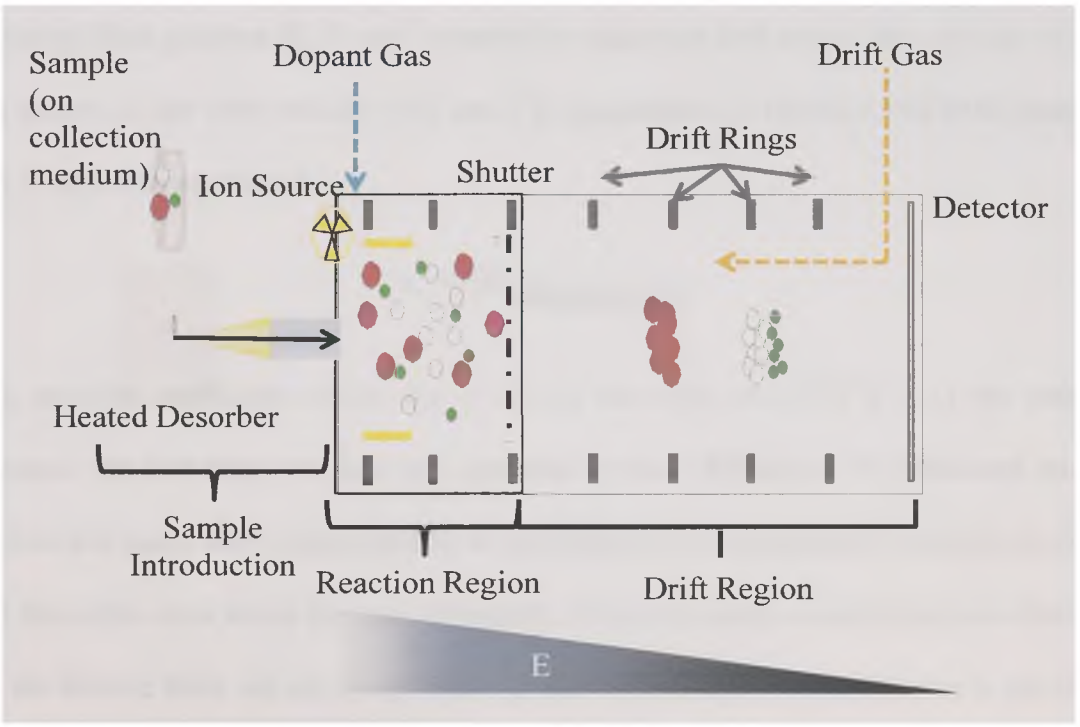

Figure 11. Schematic of Processes in an Ion Mobility Spectrometer [17].

In figure 11, the sample (on the collection medium), is introduced into the spectrometer as a vapor produced by thermal desorption from within a heated inlet at the head of the analyzer. Dried, filtered air sweeps the sample vapor into the reaction region where collisions with reactant ions (generated by a cascade of reactions β particles emitted from a ^{63}Ni ion source with purified air), enable positive or negative ionization of the sample based on the mode of the instrument. A dopant gas may be introduced into the reaction region to further promote ionization of the targeted analytes and prevent ionization of other substances not targeted for detection. Once the ions are generated, they are pulsed into the ionization region by an ion shutter, and move into the heated drift tube as a package of ions known as the ion swarm. The ion swarm is propelled through the drift tube, with a constant velocity towards the collector electrode, or the detector by an electrical field gradient (E, V cm^{-1}) created by sequential drift rings. The velocity of the ion swarm, or the drift velocity (vd), cm $s^{-1}$is proportional to the electrical field strength and is shown in equation 5:

$$v_d = KE \quad \textbf{(Equation 5)}$$

The mobility coefficient of the ion is K and has units of $cm^2V^{-1}s^{-1}$. As the swarm traverses the drift tube, the ions are separated by their differences in collisional cross-section and mass, with separation also being aided by a counter-flow of ambient air drift gas that helps slow down the ions differently. Residual sample neutrals are not affected by the electric field and are swept away by the counter-flow. The drift time is the time necessary for the ions to traverse the length of drift tube and reach the detector and is used to calculate the mobility coefficient, K, in equation 5, for the compound. This value

is normalized to 273K and 760 Torr, as in equation 6, resulting in a value with the same units, termed the reduced mobility K_0.

$$K_0 = K(\frac{273}{T})(\frac{P_{torr}}{760_{torr}}) \quad \textbf{(Equation 6)}$$

Based onK_0, compounds can be presumptively identified. When the ions collide with the detector they are neutralized, causing a current flow that is amplified and converted to a voltage (peak signal). The mobility spectrum, or plasmagram, displays the detected peaks, in a plot of the detector response (V, or another arbitrary unit) vs. drift time (ms) **[17]**.

5.1.1 Ion Chemistry

In IMS, the molecules of a sample chemically react with a pool of ions known as reactant ions to create product ions at atmospheric pressure that are subsequently detected. This reaction is observed in the mobility spectrum, by the decrease in intensity of the reaction ion peak with corresponding increase in the product ion peak. These product ions are characteristic of the compound(s) in the sample and have a reduced mobility, as do the reactant ion peak(s).

The reservoir of reactant ions are formed through series of ion-molecule reactions with nitrogen, oxygen, and water vapor in purified air to generate $H^+(H_2O)_n$ in the positive mode and $O_2^-(H_2O)_n$ in the negative mode.

In the positive polarity, proton transfer is the dominant reaction for the formation of product ions. The sample molecules M are ionized by colliding with the reactant ions

$(H^+(H_2O)_n)$ producing product ions that are stabilized by the displacement of water molecules as follows **[17]** in equation 7.

$$M + H^+(H_2O)_n \rightarrow MH^+(H_2O)_n \rightarrow MH^+(H_2O)_{n-x} + xH_2O \textbf{ (Equation 7)}$$

Sample + Positive reactant ion→ Cluster ion→ Product ion + Water

If the vapor concentration of a sample increases sufficiently, another sample molecule can attach to the product ion, also known as the protonated monomer, forming a proton-bound dimer, $M_2H^+(H_2O)_{n-x}$. When a proton bound dimer signal is observed in IMS, both the reactant peak and the protonated monomer peak intensities are reduced.

Product ions in the negative mode, are also formed by collision with the reactant ion, $O_2^-(H_2O)_n$ to form an adduct ion between the sample and hydrated O_2^- that is stabilized by collision with a third body, Z (shown in equation 8):

$$M + O_2^-(H_2O)_n \leftrightarrow [MO_2^-(H_2O)_n]^* + Z \leftrightarrow MO_2^-(H_2O)_{n-1} + H_2O + Z \textbf{ (Equation 8)}$$

Charge transfer (equation 9) and proton abstraction (equation 10) are additional pathways for product ion formation in the negative mode:

$$M + O_2^-(H_2O)_n \leftrightarrow [MO_2^-(H_2O)_n]^* + Z \leftrightarrow M^-(H_2O)_n + O_2 + Z \textbf{ (Equation 9)}$$

$$M + O_2^-(H_2O)_n \leftrightarrow [MO_2^-(H_2O)_n]^* + Z \leftrightarrow (M\text{-}1)^-(H_2O)_n + HO_2 + Z \textbf{ (Equation 10)}$$

The path to formation of product ions is dictated by the acidity of the protons. Adducts are more stable when the oxygen-hydrogen bond is comparatively strong (low acidity). An acidic proton will instead undergo proton abstraction since the O-H is weaker because of the increased bond length **[17]**.

Selectivity in IMS and formation of product ions can be promoted by the addition of a dopant gas in the reaction region (figure 11). In the negative mode, a chloride dopant is added to form long-lived chlorine adducts **[139]** and enhance the ionization of explosive compounds by simplification of the ionization route. That is because chloride is a single reactant ion as opposed to complicated reaction ion mixtures that are observed in air. As an example, the detection limits of EGDN were improved by using chloride dopant; reduced from 500 pg down for the EGDN*NO_3^- to only 30 pg for the EGDN*Cl^- adduct **[140]**. In the positive mode, ionization of sample molecules can be controlled/ enhanced by careful selection of a dopant gas possessing the appropriate proton affinity for proton transfer to proceed **[17, 141]**.

5.1.2 IMS Response

The response seen in IMS for product ions produced is dictated primarily by the strength of the ionization source. For instance, the maximum charge available for the creation of product ions in typical 63 Ni sources is an ion density of 10^9 to 10^{10} ions per cm^3s^{-1} **[17]**. This value is thought to be fixed temporally due to the comparatively slow kinetics for reactant ion formation as compared to the fast reactions of reactant ion consumption **[142]**.Once the reactant ion pool is consumed no additional product ion peak can be obtained. Care must be taken to prevent this scenario because once the reactant ion peak has been depleted, the calibrations conducted for the particular experiment are nullified. For these reasons, the linear dynamic range is limited in IMS, and it represents one of the disadvantages of this analytical technique.

5.2 Forensic Applications of Ion Mobility Spectrometry

Ion mobility spectrometry is the most prominent and successful technology for the detection of nitro-organic explosives in trace amounts from the surface of baggage in airports **[143]**. This success is attributed to the ability of the explosives to form stable negative product ions from the atmospheric pressure chemical ionization (APCI) reactions described in Section 5.1.1. This technology has also found its niche in the law enforcement community since it is routinely used by customs, police, and drug enforcement agencies to rapidly analyze trace amounts of illicit drugs. This popularity is due to the favorable response of the analyzers towards important nitrogen containing compounds of interest, such as cocaine and heroin, even in the presence of interferents **[144]**. Other reasons for the success of IMS for the detection of illicit contraband include: low detection limits (ppb to ppt range), detection under atmospheric conditions, rapid analysis on the order of seconds, low false positive rates, and ease-of use. Since ionization is conducted at atmospheric pressure, the need for complicated and bulky vacuum systems and purified gas tanks are eliminated, reducing the operational cost of IMS, as well as allowing ultra- portability. The use of IMS for security applications is staggering with over 15,000 instruments conducting over a million analyses per year **[17]**.

5.3 IMS Modifications to Improve Contraband Detection

The following is a summary of the research that has been conducted to improve the IMS detection of illicit drugs and explosives by improving the sample collection and detection probabilities.

5.3.1 Sampling Improvements

Improvements to the front-end of the IMS analyzer for efficient collection of illicit drugs and explosives and was the focus of the most recent Gordon Research Conference **[145]**. This is because reaching the full potential of field-portable IMS for effectively detecting explosives and illicit drugs at trace levels is hindered since the sampling technique relies on contact with particles. A tiny explosive or drug particle, either on a surface or in the air of a suspected area, may be missed while sampling or may not adhere to the collection surface **[146]**. Moreover, extraneous particles may overwhelm the detector's analytical response or may contaminate it through dusting. The commercial IMS instrument, General Electric Itemiser, employs a semi-permeable membrane **[147]** that allows sample vapors of drugs or explosives, obtained after thermal desorption of a sample swab, to enter the reaction region, but prevents the passage of inorganic material and water vapor into the instrument. This membrane is designed to help protect the instrument from dirty samples and field environments, and is not meant for preconcentration or actual sample collection.

The existing sample swabs provided by IMS manufacturers for particle swiping have been evaluated for their performance at trapping and effectively desorbing explosive particles into the instrument for analysis **[148]**. Recently, a patent application **[149]** has been submitted for a new type of surface swab, consisting of a bundle of fibers or strip of loop fasteners that enable the transfer of substances from the suspect surface. The particles become embedded in the gaps between the fibers or loops for and can be subsequently desorbed as usual. Even though continued efforts are directed at validating

and developing new sampling surfaces for collection of particulate matter, existing swabs have performed suitably for this purposes, although some better than others **[148]**. What is truly necessary is development and implementation of an effective sampling and preconcentration device that enables the collection of volatile chemical signatures for simplified introduction into the IMS analyzer.

Researchers have also attempted a sampling method for use in cargo containers that draws large volumes of air through treated filters, entrapping particles that are analyzed by a Gas Chromatography (GC)-IMS system following direct thermal desorption **[150]**. This is a cumbersome technique that requires significant modification of IMS instruments. It relies on the non-specific capture of particles, including dirt, dust and interferences in the hopes of trapping a tiny drug or explosive particle.

Vapor introduction is also possible by IMS by pumping air directly into the analyzer, but the volume of air it can accept is on the order of hundreds of mL **[48]**. However, this volume is mostly insufficient to representatively sample a suspected area for trace vapor concentrations without a much needed efficient, inexpensive, and an efficient and selective pre-concentration step becomes much needed. A stainless steel mesh preconcentrator **[151]** designed by Sandia laboratories, was fitted to these portable IMS analyzer in order to capture explosive particles and allow the remaining air to exit. The mesh is then flash heated to desorb the particles in seconds that were collected on the mesh and converts them to a vapor for IMS analysis. Sampling occurred for 5 to 30 s with times greater than 30 s causing what the researchers termed, "wash out" of the explosives from the mesh. There have been enhancements in the preconcentration of

particles of explosives, namely RDX, and drugs **[152]**, but again, the major drawback of this preconcentrator is that it relies on collecting particles and not the more prevalent volatile chemical signatures emitted from drugs and explosives. Furthermore, despite being named a preconcentrator, the device does not accumulate analytes over sampling times as little as 30 s.

The conversion of IMS instruments from particle samplers into vapor samplers is advantageous because sampling for the volatile chemical markers emanating from the parent explosives and drug compounds rather than sampling for particles themselves, can increase the probability of the detecting hidden drugs and explosives.

Considering the numerous benefits that SPME affords for the sampling of concealed drugs and hidden explosives, especially noting the enhancements in extraction efficiencies and consequences for increased detection capabilities of sampling for the associated volatile chemical markers, it is a reasonable tool for coupling to the front-end of IMS. The first SPME-IMS interface (*patent pending*) reported **[19]** was developed to allow the analysis of vapors rather than particles thereby improving the detection of illicit drugs, hidden explosives and taggants. The SPME-IMS method yielded limits of detection of the volatile chemical signatures 1-2 orders of magnitude lower than those of SPME-GC-MS **[19, 153, 154]**. Odor signatures of the illicit compounds of interest previously identified by canine trials and headspace analysis by SPME-GC-MS **[24, 27, 36, 63 ,64, 66]** have been successfully extracted from standards and real samples using SPME-IMS **[19, 59, 153, 154, 155, 156]**. The detection limits of instrumentation have been shown to reach sub-nanogram levels (e.g. 0.45 ng of piperonal using SPME-IMS) **[156]**.

This interface is designed as an add-on accessory for IMS and operates on the principle of a GC injection port, which enables efficient thermal desorption from a SPME fiber without damaging the fiber unlike previous attempts of placing the fiber directly into the desorber **[157]**. In this interface, an aluminum tube was machined to form a heated inlet with a septum and liner similar to that of a GC. Analytes desorb off the SPME fiber with ultra high purity helium carrier gas and the heat generated by a resistor. A Swagelok 1/8 inch union "t" is fitted onto the sample thermal desorption inlet of the IMS. This design is encouraging for the rapid implementation of this interface to the already large installed

base of IMS analyzers at ports of entry, airport screening checkpoints, etc. A thorough description of the SPME fiber interface is reported elsewhere **[19, 153, 154]**.

A SPME-IMS coupling has been devised that is based on the same transfer line/desorber concept as the one constructed by the Almirall group, but is used with a handheld IMS **[158]**. This system has the advantage of ultra-portability but does not yet address the need for sampling of large volumes.

Although these novel SPME-IMS interfaces improve upon conventional IMS analysis of drugs and explosives, they are limited by relying on modified-syringe geometry for sample introduction. Also, a recent review of numerous IMS sample introduction systems concluded that "SPME–IMS coupling cannot be deemed a robust system," **[159]** since the various fiber introduction interfaces may yield different analytical results.

A planar geometry for uniform SPME sample introduction in IMS can be explored since because unlike with GC-IMS does not suffer from restrictions of the volume of liquid sample injected, capillary column inner diameter, and stationary phase thickness that make a syringe injection system necessary.

Lastly, a microfabricated vapor concentrator **[160]** has been developed and shows preconcentration of TNT vapors and increases in sensitivities of one order of magnitude compared IMS analysis without the device. The materials used for fabrication of this preconcentrator, such as platinum, would make the device prohibitively expensive. The device also requires its own electrical power to operate so adapting it to existing IMS instruments would be cumbersome.

In summary, the development of a SPME extraction device of planar geometry, by exploiting the flexibility of various SPME configurations **[77]**, would allow direct desorption/ introduction of sample into the numerous commercial embodiments of IMS, while maintaining with low production and operational costs.

5.3.2 Operating Condition Optimization

Several of the volatile chemical signatures identified cannot be detected by IMS under default operating conditions. Lai, et al. systematically optimized IMS variables such as drift tube temperature, drift gas flow rate, sample gas flow rate, and dopant gas composition in both the positive and negative operating modes, using a Genetic Algorithm (GA) approach. Details on GA and its advantages over search approaches have been previously reported **[156]**.

Using the optimized operating conditions resulted in detection limits for methyl benzoate of only 0.23 ng by SPME-IMS, a compound that was previously impossible to detect using the installed manufacturer settings **[160]**.

CHAPTER 6. METHODOLOGY

6.1 Development of Planar SPME (PSPME) Devices for Static Extractions

The geometrical configuration of SPME was changed from cylindrical to planar in order to be easily adaptable to existing IMS desorbers and to increase the surface area and capacity for extraction of the targeted analytes. This change in geometry was achieved for static sampling by using microscope glass slides cut to the appropriate size as substrates for the subsequent absorptive/ adsorptive phase chemistries that would be attempted in the development of PSPME.

The phase chemistries used were chosen to resemble currently commercially available fiber types for comparison purposes between the planar and fiber geometries. Others were attempted to further improve upon commercial fiber chemistries in terms of durability, thermal resistance, capacity, and affinity for the targeted compounds.

6.1.1 Preparation of the Substrate

Prior to coating, 1 mm thick, pre-cleaned microscope slides (Chase Scientific Glass, Vineland, NJ), were cut into 3.81 cm × 2.54 cm pieces. The glass substrates were dipped individually into a 2:1 mixture of concentrated sulfuric acid (Fisher Scientific, Fair Lawn, NJ) and 30% hydrogen peroxide (Fisher Scientific, Fair Lawn, NJ) and placed in an oven at 90°C for 20 min. The solution was decanted and the substrates were rinsed thoroughly with 18 mΩ deionized water. Each substrate was dipped in 1M NaOH for 1 hr to expose the silanols on the glass surface. This was followed by thorough rinsing with deionized

water to ensure wettability (no beading of water on the glass surface). The substrates were placed in an oven at 120°C for 12 hr to dry.

6.1.2 Coating Techniques

The following section describes the two coating methodologies that were employed in these studies.

6.1.2.1 Dip-Coating

The dip coating process consists of 1) dipping (residence time), 2) withdrawal, and 3) solvent evaporation. The prepared substrates were immersed in the appropriate coating solution (~25 mL), contained in a 50 mL polypropylene disposable centrifuge tube (Fisherbrand, Fairlawn, NJ), and sealed tightly for a given amount of time. The substrate was withdrawn from the solution following the coating time period place in a 50 mL glass vial, 29 × 94 mm, 12 DR (Fisherbrand, Fairlawn, NJ). A schematic of the dip coating process is shown in figure 12.

The tight seal caps that are included with the glass vials were punctured in the center. These modified caps were used to seal the glass vials containing the newly coated substrates (including spin-coating, discussed in Section 6.1.1.2). The glass vials were then placed in the dessicator overnight (at least 12 hr). The subsequent treatments (if applicable) are described in later sections for each specific coating.

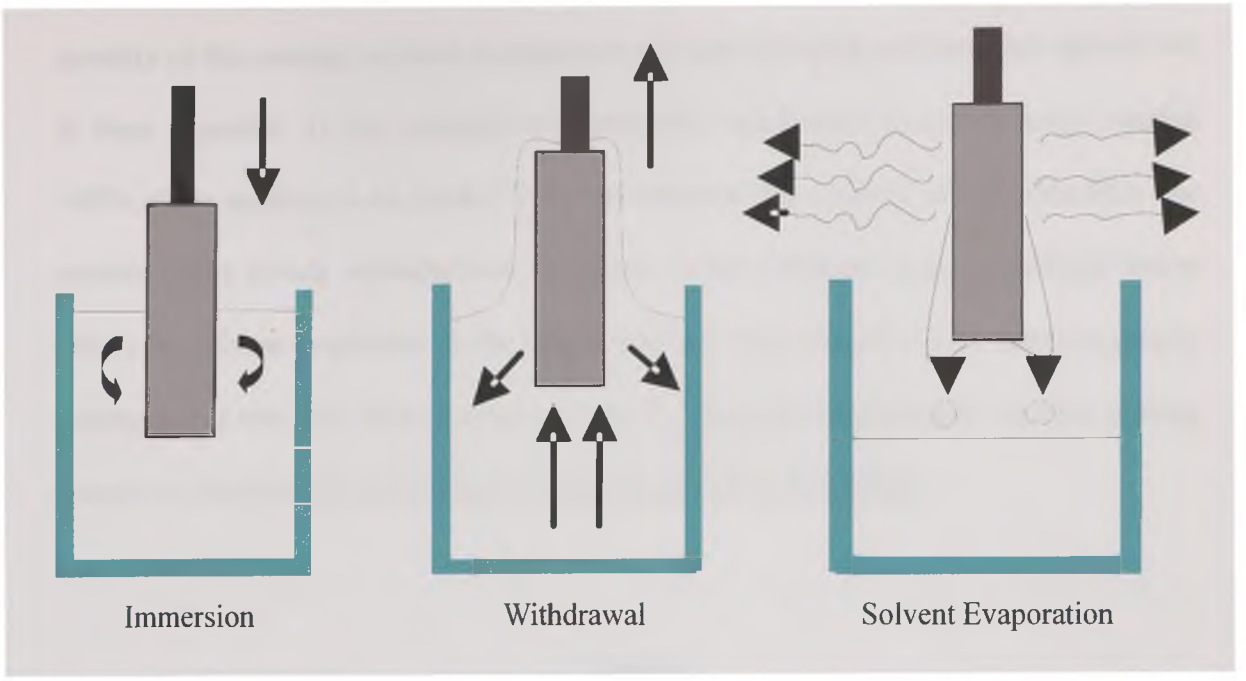

Figure 12. The Dip-Coating Process. Adapted from [161]

6.1.2.2 Spin-Coating

The spin-coating process figure 13 involves depositing an amount of coating solution on the prepared substrate. The substrate is accelerated to a certain velocity while the coating solution is spun-off leaving a thin film on the surface of the substrate. The spin-coater used in the development of PSPME is a model WS-400B-6NPP-LITE (Laurell Technologies Co., North Wales, PA) shown in figure 14.

The prepared substrate is placed on the vacuum chuck (with adapter if necessary). The vacuum is activated to hold the substrate in place. The coating solution is delivered to the substrate and the appropriate spin program is activated.

The stages of spin coating are as follows **[162]** and is illustrated in figure 13: 1) The polymer is applied in the form of a solution in the desired volatile solvent, then 2) a small

quantity of the coating solution is dispensed onto an activated substrate that spreads out to form a puddle. 3) The substrate is rotationally accelerated to a high speed causing ~90% of the solution to be ejected from the substrate immediately. 4) The thin film that remains flows slowly outward from the center of the substrate under centrifugal forces and 5) the solvent evaporates as the film is thinned. The viscosity of the solution greatly increases in a way that relative motion stops. 5) The spin program ends, and the coating process is completed by removing the residual solvent by heat **[162]**.

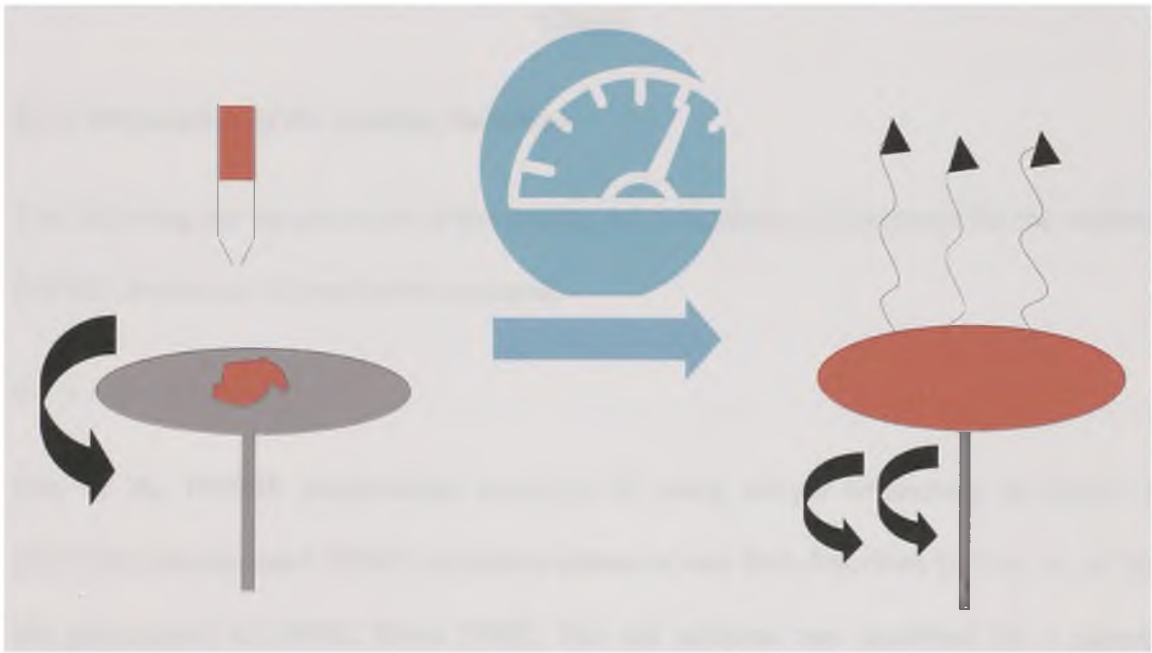

Figure 13. The Spin-Coating Process

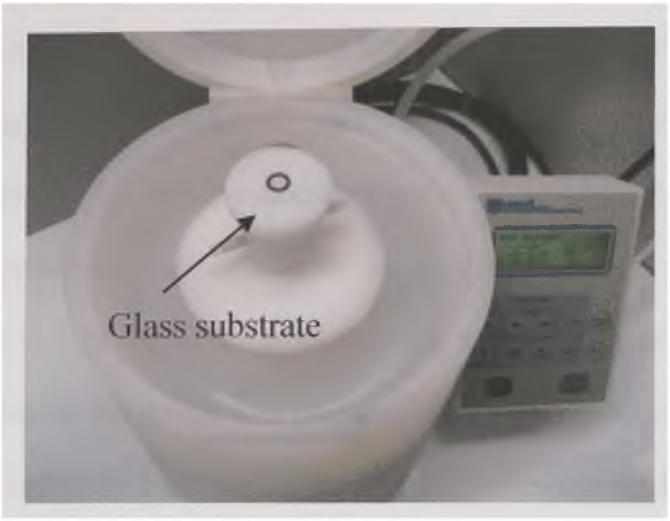

Figure 14. Image of the Spin Coater Used with the Glass Substrate in Place on the Chuck

6.1.3 Preparation of the Coating Solutions

The following are the protocols of the coating solutions that were prepared for the various PSPME devices developed in this research.

6.1.3.1 Sol-gel PDMS

One of the PSPME preparations consisted of using sol-gel technology to create a physically incorporated PDMS extraction phase as was first described by Liu, et. al for the preparation of SPME fibers **[105]**. The sol solution was modified for a planar geometry and prepared as follows: 6.40 g vinyl-terminated polydimethylsiloxane (vt-PDMS) (Gelest, Inc., Morrisville, PA) was dissolved in 8 mL of dichloromethane (DCM,Acros, New Jersey, USA); then 3.42 mL of methyltrimethoxysilane (MTMOS, $\geq$ 98%) (Fluka, Steinheim, Germany) and 1.67 g poly(methylhydrosiloxane) (PMHS) (Sigma-Aldrich, Inc., St. Louis, MO) were added, followed by 2.73 mL of trifluoroacetic

acid (TFA, 99 %, Acros, New Jersey, USA), (5% water, v/v). The solution was vortexed and allowed a 30 min stay. The prepared substrate was dipped in the solution for 1 h. The planar sol-gel PDMS SPME device was placed in the dessicator for 12 hr, followed by a 6 hr dip in dichloromethane. Gelation of the sol-gel PDMS PSPME device occurred by placing the device in a GC oven at 40 °C for 12 h. Conditioning of the sol-gel PDMS PSPME was as follows: the device was placed in a GC oven under nitrogen atmosphere at 120°C for 1 hr, 240°C for 1 hr, and 300°C for 3 hr. Following conditioning, the device was slowly cooled to room temperature to prevent cracking of the phase, a parameter **[100]** that is especially important to prevent when preparing sol-gel PDMS.

6.1.3.2 PDMS by a Chlorine-Terminated PDMS Route

A coating of PDMS was made on the prepared substrate by the chlorine-terminated PDMS route. This method consisted of spin-coating a prepared glass substrate with a 3:1 mixture of chlorine-terminated polydimethylsiloxane (Cl-PDMS) (Sigma-Aldrich, Inc., St. Louis, MO) and DCM. One mL of the coating solution was deposited on the substrate and the spin program, 1000 rpm for 60s, was activated. The PDMS planar SPME device was placed in a dessicator at room temperature for 12 hr followed by dipping in 18 mΩ deionized water to remove any excess hydrochloric acid that could result from the reaction. The PDMS PSPME device was placed in a GC oven at 40°C following the rinse with deionized water and was conditioned in the same manner as the sol-gel PDMS (Section 6.1.3.1).

6.1.3.3 Sylgard® 184 PDMS

The PDMS elastomer, Sylgard® 184 (Dow Corning, Inc., Midland, MI) was another coating chemistry employed. To obtain this coating, a 10:1 ratio of PDMS gel and the curing agent was mixed as described by the manufacturer **[163]**.

This polymer was first used to create explosive standards for LIBS experiments (unrelated to this research) that were being conducted by the U.S. Army Research Lab. Samples of the explosive Pentolite (TNT and PETN) and Composition C-4, were provided to us so that standards with concentrations of 0.0001, 0.001, and 0.01 g mL^{-1}, could be created onto glass and aluminum substrates. These substrates were prepared as described in Section 6.1.1. The standards were created by dispersing the solid Pentolite explosive in acetonitrile. The Composition C-4 explosive was mixed in hexane. The explosive dispersion was added to 3.2 mL PDMS, vortexed, and then 0.4 mL of the curing agent was added. One mL of solution was spin-coated onto the substrates using the following program: 5 seconds at 200 rpm, 3 seconds at 500 rpm, and 30 seconds at 4000 rpm. The standards were allowed to cure at room temperature overnight as per manufacturer recommendations. Blanks were produced in the same manner using both the glass and aluminum substrates but without the addition of explosives. Sylgard® 184 PDMS was also used for the experiments described in the next section.

6.1.3.4 Activated Charcoal/ Sylgard 184® PDMS

Activated charcoal (AC, Aldrich, Milwaukee, WI) was used as a substitute for costly Carboxen particles in the development of an AC/PDMS SPME phase. A mass of 0.5 g

activated carbon particles were mixed in a solution of 4 mL PDMS (0.5 mL of DCM added to reduce viscosity) mixed with 0.5 mL of curing agent. One mL of this solution was spin-coated onto per prepared glass substrate. The device was cured in 150 °C temperature for 15 min.

6.1.3.5 Activated Charcoal/Sol-Gel PDMS

For the formulation of AC/sol-gel PDMS, 5.15 g vt-PDMS was dissolved in 6.3 mL DCM. Volumes of 2.7 mL MTMOS and 1.3 mL PMHS were added to the mixture. A mass of 1.02 g AC was blended into the solution and the sol gel reaction was catalyzed by the addition of 2.1 mL TFA (5 % water, v/v). The solution was vortexed and allowed a 30 min stay. The solution was vortexed again after the 30 min stay and the prepared glass substrate was dipped for 30 min. The coating was treated as usual (Section 6.1.3.1) for the remaining steps.

6.1.3.6 La (dihed)

The synthesis of the H_2 dihed ligand, *p*-di(4,4,5,5,6,6,6-heptafluoro-1,3-hexanedionyl) benzene, has been described previously **[164]**, but the reaction was scaled down as follows. A 500 mL 3-neck round bottom flask (RBF) was dried and flushed with nitrogen and fitted with a reflux condenser a rubber stopper and a glass stopper. A magnetic stirrer was added to the (RBF). A mass of 6.676 g of sodium methoxide, pure, anhydrous powder (Acros Organics, New Jersey) was added to the RBF by opening the glass stopper. Diethyl ether, anhydrous, 99.7%+ (Sigma Aldrich St. Louis, MO) was added slowly through the rubber stopper while the RBF was in an ice bath and stirring, for a

total diethyl ether volume of 120 mL. The ice bath was removed and 10.7 mL of ethyl heptafluorobutyrate, 97% (Acros Organics, New Jersey) was added to the RBF while still stirring. A mass of 5 g of *p*-diacetylbenzene, 99% (Sigma Aldrich St. Louis, MO) was mixed with ~100 mL diethyl ether and this slurry was added to the RBF over the course of 45 min. Stirring was continued for over 1 hr. A 50:50 solution of HCl and 18 mΩ deionized water (total volume of 40 mL) was added to the solution in the RBF. The pH was checked (pH=2) and 60 mL deionized water was added. The solution was transferred to a separatory funnel, the ether layer was removed and evaporated using a Rotavap. The crude orange-yellow product was recrystallized three times from methanol. The crude product was dried overnight.

The synthesis of the La (dihed) complex was accomplished by following the procedure previously described **[117]**. A volume of 50 mL methanol, GC Resolv 99% (Fisher Scientific, Fairlawn, NJ), was heated in an Erlenmeyer flask containing boiling chips. A mass of 1.5 g of the H_2 (dihed) ligand was placed in a RBF with a magnetic stirrer inside. The hot methanol was pipetted into the RBF until the ligand dissolved, and while maintaining a 40 °C temperature from a water bath. A 1 mL 4M sodium hydroxide solution was added dropwise to the RBF. This neutralized solution was then added dropwise over 30 min to a solution of a mass of 0.825 g lanthanum (III) nitrate hexahydrate, 99.999 %, (Acros Organics, New Jersey) dissolved in 50 mL methanol. This solution was transferred to a 500 mL separatory funnel and added dropwise for 1 hr to 500 mL of vigorously stirred deionized water. Then, the solution was placed in an ice bath with continued stirring. Suction filtration was not effective to collect the solid

product; therefore the solution was heated for ~3hr and left on the bench overnight. The next day, the solid product was collected by suction filtration and dried in vacuo over P_4O_{10}.

The La (dihed) complex synthesized was coated on the surface of prepared glass, and PDMS and sol-gel PDMS PSME devices. A mass of 236 mg La (dihed) was dissolved in 50 mL methanol. This solution was poured into a glass thin layer chromatography (TLC) developing chamber with eight slots. The prepared glass (control), and PDMS and sol-gel PDMS PSME devices were dipped in the solution for 1 hr. Sol-gel PDMS and PDMS devices uncoated with La (dihed) were used for comparison purposes in subsequent experiments.

Temperature effects on the integrity of the La (dihed) layer on the coated devices were studied. The devices were each subjected to 10 minute exposures at 180, 225 and 300 °C temperatures and their surface characteristics were studied by scanning electron microscopy (described in Section 6.1.4.1).

Concentration of the La (dihed) and coating time effects on the extraction capabilities of La (dihed) PSPME devices were studied as well (described in Section 6.2.7); this required the preparation of the appropriate PSPME devices. The concentration studies involved dipping of the particular substrate for 1 hr. in 100, 200, and 300 mg La (dihed) in 50 mL methanol solutions. The 236 mg La (dihed) in 50 mL methanol was reused and served as a coating solution in the comparison. Sol-gel PDMS and PDMS SPME devices were each dipped in the various concentrations. The controls were 1) uncoated sol-gel PDMS and PDMS PSPME devices and 2) uncoated sol-gel PDMS and PDMS PSPME

devices dipped in methanol for 1 hr. The time studies were done by dipping the various substrates in a 200 mg La (dihed) in 50 mL methanol solution, for 30 min, 2hr, 1 hr, and 3 hr. Spin coating 1 mL of the coating solution at 1000 rpm for 1 min was also done and considered as t=0 min. The controls included dipping the sol-gel PDMS and PDMS PSPME devices in methanol for the longest time period in the study- 3 hr.

An alternative coating was made that physically incorporated La (dihed) into the sol-gel PDMS network. A mass of 0.0995 g of La (dihed) was dissolved in 1mL of methanol. Separately, 0.3085 g vt-PDMS was dissolved in 0.374 mL DCM. The La (dihed) solution was added to the vt-PDMS solution. Volumes of 0.164 mL and 80 μL of PMHS were delivered to the solution, followed by vortex mixing. A 5% TFA solution (0.138 mL) was added to the mixture followed by vortex mixing. The solution was left to stand 30 min. One 1 mL was deposited onto a prepared glass substrate and allowed to interact with the surface for 30 s. The spin program (200 rpm for 1 min.) was activated. The sol-gel/ La(dihed) PSPME device was placed in the dessicator for 12 hr, followed by a dip in DCM for 45 min. Gelation occurred as usual for sol-gel PDMS, 40 °C for 12 hr. Curing occurred in the GC oven at 120 °C under nitrogen atmosphere for 3 hr. The device was then placed in the dessicator for continued curing at room temperature for 48 hr.

A control sol-gel PDMS device was prepared by spin coating the sol solution without the addition of La (dihed) at 200 rpm for 1 min.

6.1.4 Characterization of Final PSPME Products

6.1.4.1 Scanning Electron Microscopy

The surface characteristics of the PSPME devices created, and coating thickness determinations were made using scanning electron microscopy (SEM). A Philips XL30 scanning SEM (FEI, Hillsboro, OR) was used at high vacuum. Both secondary electron and backscatter detection was used depending on the information that was desired. The sample preparation included gold coating the samples using a Hummer 10.2 Sputtering System (Anatech, LTD., Union City, CA).

6.1.4.2 IMS Plasmagram Blanks

For a PSPME device to be suitable for IMS analysis, the background produced following desorption of the newly created "blank" PSPME device following all appropriate conditioning procedures must be minimal or none. This was tested by desorbing the device(s), at the appropriate IMS desorption temperature.

6.1.4.3 Classical Methods

In the structure determination of the H_2 (dihed) ligand and La (dihed) complex several classical methods were first employed. The melting point was determined for both compounds. The solubility of these compounds in polar and non-polar solvents was also tested. Lastly, thin layer chromatography of the ligand and complex using a 200 μm thick HPK silica gel 60 A stationary phase (Whatman, Inc., Clifton, NJ) with a hexane: acetone (90:10) mobile phase was done.

6.1.4.4 Fourier Transform-Infrared Spectroscopy

Fourier Transform- Infrared (FT-IR) Spectroscopy was used in the structure determination of the ligand and metal complex. The samples were prepared as follows: 2mg of the solid compound was mixed with 200mg of potassium bromide, ground together in a mortar and pestle, and pressed into a pellet by applying a force of 6 ton $m^{-1}$for 5min.A Perkin Elmer Spectrum 2000 FT-IR Spectrometer (Waltham, MA) with an Nd-YAG 1064 nm laser was used for the analysis of the ligand and metal complex in the mid-infrared range (400- 4000 cm^{-1}) for 16 scans.

6.1.4.5 Direct Infusion- Mass Spectrometry

The determination of the molecular weights of both the ligand and the metal complex was conducted using direct infusion-mass spectrometry (DI-MS) with a Finnigan LCQ Deca XP Max instrument (Thermo Scientific, Waltham, MA). Solutions of the ligand and the metal complex with concentrations of 5 μg mL^{-1} were prepared in methanol. The solutions were filtered using a 0.45 μm pore size PTFE filter (Whatman, Inc. Clifton, NJ) before sample introduction. The operating conditions were as follows: positive and negative ionization, capillary voltage of 5 kV, 10 μL sample injection, 10:90 (water: acetonitrile) mobile phase with a flow rate of 0.5 mL min^{-1}, nitrogen sheath gas (30 unit flow), and an analysis temperature of 150 °C.

6.1.4.6 ^{1}H Nuclear Magnetic Resonance Spectroscopy

^{1}H nuclear magnetic resonance (^{1}H NMR) spectroscopy using a 400 MHx NMR (Bruker Spectroscopy, Madison, WI) was employed for the structure determination of both the ligand and the metal complex. The solvent used for the ligand was deuterated chloroform and for the metal complex the solvent was deuterated methanol- both from Cambridge Isotope Laboratories, Inc. (Andover, MA). The default number of scans, 16, was used for the analysis of both compounds but 160 scans were also taken of the metal complex. The experiments were done at room temperature for both compounds, but for the metal complex, an experiment at 50 °C was also conducted.

6.2 Validation Experiments for Static PSPME

The following experiments were conducted for testing of the preconcentration capabilities of the various PSPME devices that were developed in the static extraction sampling mode.

6.2.1 IMS Detection

In this study, two ion mobility spectrometers were used for the detection of the compounds of interest: a Smiths Detection IonScan 400B (Smiths Detection, Mississauga, ON, Canada) and a General Electric Ion Track Itemiser 2 (Wilmington, MA). For SPME fiber comparisons, the front end of the GE Itemiser 2 was coupled with a SPME interface designed by Perr, et al. **[19]**. The operating conditions for both standalone IMS instruments and the SPME-IMS interface are listed in Table 4.

Table 4. Operating Conditions of IMS Instruments and SPME-IMS Interface

Smiths IonScan 400B IMS Experimental Conditions	
Detection Mode	Explosives, taggants, and volatile chemical signatures, negative ion mode (-); volatile chemical signatures, positive ion mode (+)
Desorber Temperature (°C)	225 (-); 285 (+)
Drift Tube Temperature (°C)	115 (-); 235 (+)
Analysis Time (s)	10 (-); 8 (+)
Sample Flow (mL min^{-1})	300 (-); 200 (+)
Detector Flow (mL min^{-1})	351 (-); 300 (+)
Reagent Gas (Dopant)	hexachloroethane (-); nicotinamide (+)
GE Iontrack Itemiser 2 IMS Experimental Conditions	
Detection Mode	Explosives, taggants, and volatile chemical markers, negative ion mode (-)
Desorber Temperature (°C)	215
Drift Tube Temperature (°C)	180
Analysis Time (s)	7
Sample Flow (mL min^{-1})	1000
Detector Flow (mL min^{-1})	200
Reagent Gas	dichloromethane
SPME-IMS Experimental Conditions	
Interface Temperature (°C)	260 ± 1
Warm up time (hr)	1

6.2.2 Performance Comparison of the SPME Fiber, PDMS, and sol-gel PDMS PSPME Devices Using TNT as the Target Analyte

For static PSPME sampling, the device was suspended above the headspace of gallon or quart-sized cans (All American Containers, Miami, FL) depending on the specific experiment. The target analyte in a solution of known concentration was spiked into the can. The lid was immediately sealed with a rubber mallet. These cans were previously conditioned in an oven at 150 °C for over 24 hr to remove any volatiles from the cans themselves that may interfere with the extraction and analysis. Alternatively, sampling by the SPME fiber (100 μm PDMS, Supelco, Bellefonte, PA)was achieved by creating a hole in the lid of the can where an 11 mm stopper sleeve (Wheaton, Millville, NJ) could fit snuggly and through which the fiber SPME was inserted and exposed for sampling immediately after the sample had been spiked and the can was sealed.

6.2.2.1 Quantitation of TNT Using Response Curves

Standard solutions of 2,4,6-trinitrotoluene (TNT) (Cerilliant, Round Rock, TX) were prepared from a 1000 μg mL^{-1} stock solution in concentrations of 0.1, 0.2, 0.5, 0.8, 1.0, 2.5, 5.0, 10.0, and 240 μg mL^{-1} for the experiments with acetonitrile as the solvent (Fisher Scientific, Fair Lawn, NJ).Response curves for each IMS instrument were generated for TNT by spiking amounts of known concentration onto manufacturer provided filters (Smiths Detection, Mississauga, ON, Canada) and introducing them into the IMS in triplicate.

6.2.2.2 Determination of Equilibrium Extraction Time and Recovery

The determination of equilibrium time for the planar PDMS, planar sol-gel PDMS, and the PDMS fiber was determined as follows: 10 μL of 240 μg mL^{-1} TNT was spiked into quart cans and sampling at different time intervals was conducted with desorption into each IMS instrument. For the SPME fiber sampling, only analysis by the GE Itemiser 2 was possible since there is no currently machined SPME-IMS interface for the Smiths 400B. For calculating recovery, different concentrations of TNT were spiked and sampled at the equilibrium time for each SPME device. All extractions were conducted in triplicate.

6.2.2.3 Extraction Efficiency Experiments at Equilibrium

For comparison of extraction efficiency of the fiber and planar SPME devices, different volumes of a 5 μg mL^{-1} TNT solution were spiked into quart cans and sampled at the appropriate equilibrium times with detection by the GE Itemiser 2. All extractions were conducted in triplicate.

6.2.2.4 Study of TNT Adsorption to Vessel Walls

Both quart and gallon-sized cans were studied to test the effects of possible TNT adsorption to the surface of the sampling vessels used in these studies. Quart and gallon-sized cans were studied. A volume of 10 μL of 240 μg mL^{-1} TNT in acetonitrile was spiked into the appropriate sized cans. Sampling by the sol-gel PDMS PSPME device was conducted in the closed system as previously described (Section 6.2.2), for different time intervals.

6.2.3 Comparison of Sol-Gel PDMS PSPME and Fiber SPME for Sampling Piperonal

The following experiments were conducted on the volatile chemical signature of MDMA, piperonal, in order to determine and compare the extraction capabilities of both the fiber and planar SPME devices. The method development for the field sampling and detection of actual MDMA drug cases by PSPME-IMS is also described.

6.2.3.1 Gas Chromatography- Mass Spectrometry (GC/MS)

A Varian 3400cx gas chromatograph Saturn 2000 ion trap mass spectrometer (Walnut Creek, CA) was used for quantitation of the mass detected following a SPME fiber extraction. The conditions were as follows for both SPME and liquid injection: injection temperature of 280 °C, 1 mL injection volume for liquids, sample split of 20:1, and the column flow of 1.0 mL min^{-1} of helium. A Varian WCOT CP Sil 8 CB column was used with the following specifications: 50 m length, 95% PDMS, 5% diphenyl stationary phase and a 0.25 mm inner diameter. The temperature program was as follows: begin at 40 °C, hold1 min, ramp to 110 °C at a rate of 10 °C min^{-1}, hold 0.4 min, then ramp to 250 °C at a rate of 25 °C min^{-1} and hold for 2 min. The ionization was turned off from 0 min to 6 min (to eliminate thesolvent peak), then from 15 min to16 min to eliminate peaks due tocolumn bleed since the peak of interest elutes at 13.762 min.

6.2.3.2 IMS Operating Conditions

For the IMS detection of piperonal, it was necessary to change the manufacturer operating parameters for the Itemiser 2 instrument as described in the literature **[156]** from those shown in Table 4. The optimized operating conditions are as follows:

1) positive ion mode 2) nicotinamide reagent (dopant) gas, 3) drift tube temperature of 80 °C, 4) sample flow of 500 mL min^{-1}, and 5) detector flow of 350 mL min^{-1}.

6.2.3.3 SPME-IMS Sampling

A volume of 10 μL of a 1000 μg mL^{-1} solution of piperonal, 99 %(Sigma-Aldrich, St. Louis, MO) was spiked into a 15 mL glass vial (Supelco, Bellefonte, PA) fitted with an 18 mm polypropylene hole cap with PTFE/silicone septa. The vial was closed tightly and sealed with parafilm. The headspace in the vial was allowed to equilibrate for 24 hr prior to static SPME fiber sampling for subsequent introduction into the GC-MS and the IMS (via the SPME-IMS interface). The SPME fiber used in this study was a 100 μm PDMS fiber (Supelco, Bellefonte, PA).

For determining the equilibrium extraction time for the PDMS fiber in this static sampling scenario the vial was sampled for various times with the PDMS fiber and introduced into the IMS instrument.

Then, in order to determine the amount of time it takes to actually reach equilibrium in a vial, the same amount of piperonal was spiked in the vial and sampled at different times after sealing, for the amount the previously determined equilibrium extraction time.

6.2.3.4 SPME-IMS Quantitation

A response curve was generated for piperonal by GC-MS by using solutions prepared in a concentration range of 1-50 μg mL^{-1} from a stock solution of 1000 μg mL^{-1}. The equation of the best-fit line from this analysis was used to correlate the mass of piperonal introduced to the GC-MS with the signal output.

The mass loadings of piperonal on the PDMS fiber were calculated by statically sampling a vial at equilibrium as was done in Section 6.2.3.3. The same time intervals were used to sample the vial followed by desorption of piperonal from the fiber by injection into the GC/MS.

6.2.3.5 SPME-IMS Limit of Detection (LOD) and Linear Dynamic Range (LDR) Determinations

The method LOD was determined as the minimum amount of piperonal that would produce a signal at least the average of the blank plus three times its standard deviation. The LDR was determined by identifying the largest range of points on the response curve where a linear correlation existed between the mass of piperonal introduced and the IMS response.

6.2.3.6 Piperonal IMS Response Curve

The piperonal standard solutions were made from a stock solution of 1000 μg mL^{-1} piperonal in DCM. A volume of 2 μL each of 1, 2, 5, 8, and 10 μg mL^{-1} concentrations of piperonal were spiked onto filters (Smiths Detection, Mississauga, ON, Canada) and analyzed by the Itemiser 2 IMS for analysis of the piperonal monomer. Since piperonal has been reported to produce a proton-bound dimer at high concentrations **[156]** a second response curve was generated for this ion species, with the lowest concentration being the first observance of dimer formation. A volume of 2 μL each of 30, 40, 50, 100, 130 and 150 μg $mL^{-1}$of piperonal, diluted from the 1000 μg mL^{-1} stock, was also spiked onto filters and analyzed by IMS. Triplicate analyses of each concentration were conducted and a response curve was generated by plotting mass (typically in the ng range) versus

the cumulative signal output. From the equation of the best-fit line, the mass detected by IMS following sampling using the fiber SPME and the PSPMEwas calculated.

6.2.3.7 Method Development for PSPME-IMS of Piperonal

The determination of equilibrium extraction times for the sol-gel PDMS PSPME device and SPMEPDMS fiber was as follows: 100 μL of 100 μg mL^{-1} piperonal solution was spiked into gallon cans and sampled at different time intervals from 3 to 10 min. Once each sampling was complete, the PSPME device was removed and introduced into the Itemiser 2 IMS via the sample desorber. The PSPME device was conditioned in a GC oven at 150 °C and a blank of the PSPME device was obtained prior to each sampling. After sampling with the fiber, it was removed and the analytes introduced into the IMS by thermal desorption via the SPME-IMS interface.The fiber was conditioned in the injection port of the GC at 250 °C and a blank of the fiber was obtained prior to each sampling.

A comparison of the extraction efficiency of piperonal by both SPME types was conducted under strict experimental conditions by sampling for only 6 min at a sampling distance of 20 cm from the emitting source, 2 and 5 μg spikes (100 μL spikes each of 20 and 50 μg mL^{-1} piperonal, respectively, in DCM).

6.2.3.8 Sampling Real MDMA Cases at a Local Crime Laboratory

Five (5) tablets known to contain MDMA were placed in quart-sized cans, sealed and allowed to stand for 48 hr to ensure equilibrium extraction conditions. Sol-gel PDMS

PSPME devices were then used to sample the headspace for the following time intervals: 0.5, 1, 3, 5, 8.5, 9.5, 11, and 12 min. In a separate experiment, the extraction efficiency of both the PSPME and the fiber SPME were tested in relation to the number of tablets in the can. Cans containing 1, 3, 5 and 10 MDMA tablets were sampled by both the SPME fiber and PSPME for 15 min, allowing for 30 min equilibration between the sample and the headspace between analyses. This experiment was conducted in triplicate for the PSPME device and in duplicate for the fiber. The results from these two experiments dictated the best sampling parameters for further blind tests involving suspected MDMA cases. For the final on-site experiment, six actual drug cases were selected, some containing MDMA (confirmed by GC/MS) while others did not contain the drug. Five tablets of each suspected drug case were allowed to equilibrate inside a quart-sized can overnight, followed by 15 min extraction time and IMS analysis. The composition of the drug cases was revealed only after the SPME-IMS and PSPME-IMS results were reported.

6.2.4 Performance of PSPME for Other Volatile Chemical Signatures

A qualitative, proof of concept, experiment was conducted to evaluate the extraction capabilities of sol-gel PDMS PSPME for other volatile chemical signatures. This was tested by extracting the compound of interest diluted in acetonitrile, from a quart can with the sol-gel PDMS SPME device for a given sampling time. The compounds studied were: 2,4-DNT, 4-nitrotoluene (4-NT), a taggant, and cyclohexanone (Fisher Scientific, Fair Lawn, NJ). The 2,4-DNT and 4-NT were obtained in small amounts from a local law enforcement agency and diluted to the appropriate concentrations. Extraction of these

compounds preceded analysis by the IonScan 400B IMS according to the operating conditions in Table 1, in the negative mode, except cyclohexanone which was detected in the positive ion mode.

6.2.5 Performance of PSPME for the Smokeless Powder Volatile Chemical Signatures

Quantitative studies of the smokeless powder volatile chemical signatures, 2,4-DNT (in the negative polarity), and DPA and EC (in the positive polarity) were conducted using the Smiths 400 B IMS.

6.2.5.1 Smokeless Powder Volatile Chemical Signature IMS Response Curves

Standard solutions of the solid smokeless powder odor signatures, 2,4-DNT, EC, and DPA (Aldrich, St. Louis, MO) were prepared in acetonitrile, or hexane for 2,4-DNT. The 2,4-DNT calibration solutions originated from a 1000 ug mL^{-1} stock and consisted of the following concentrations: 5.0, 8.0, 10.0, 25.0, 50.0, 100, 250, 500, and 750 ug mL^{-1} in hexanes. The EC solutions were prepared from a 5 μg mL^{-1} stock solution in concentrations of 0.1, 0.5, 0.9, and 1.0 ug mL^{-1}. Solutions of DPA were diluted from a 500 ug mL^{-1} stock solution to concentrations of 1.0, 5.0, 10.0, 25.0, 40.0, 50.0 ug mL^{-1}. A volume of 1 μL each of the listed concentrations was spiked onto manufacturer provided filters (Smiths Detection, Mississauga, ON, Canada) and analyzed by the IonScan 400B IMS with the operating conditions listed in Table 4 except that the desorption temperature in the negative ion mode was raised to 300 °C for improved desorption of 2,4-DNT.

6.2.5.2 Concentration Study for 2,4-DNT

The analysis of 2,4-DNT in solution by IMS was studied in depth by testing various solvents (acetonitrile, methanol and hexane). Concentration effects on product ion formation were monitored by spiking increasing concentrations on manufacturer provided swabs and analyzing the swabs by IMS. These tests were conducted since, under certain conditions the IMS alerted for TNT instead of 2,4-DNT.

6.2.5.3 Determination of Equilibrium Extraction Time

The determination of equilibrium time for the planar sol-gel PDMS PSPME device was determined as follows: 10 μL of 100 μg mL^{-1} 2,4-DNT in hexane, 10 μL of 100 μg mL^{-1} DPA in acetonitrile, and 10 μL of 25 μg mL^{-1} EC were each spiked into individual quart cans and sampled at different time intervals followed by desorption of the PSPME into the IonScan 400B IMS instrument.

6.2.5.4 Sampling of Unburned Smokeless Powders

Four unburned commercial smokeless powders were used in this study: H322 (Hogdon, Shawnee Mission, KS), 4198 (IMR, Shawnee Mission, KS), Red Dot (Alliant Powder, Radford, VA), and Unique (Alliant Powder, Radford, VA).The sol-gel PDMS PSPME device was suspended above the headspace of a quart can. A mass of 100 mg of smokeless powder was placed in the can. The lid was immediately sealed with a rubber mallet and static sampling occurred for 1 hr. followed by desorption of the device into the IonScan 400 B IMS. Sampling was done both in the positive ion mode, targeting DPA and EC, and in the negative ion mode targeting 2,4-DNT.

6.2.6 PSPME Static Sampling of TNT from a Large Volume Vessel

A particle free hood (Labconco, Kansas City, MO) with the following dimensions: 18.75 in. depth, 30.5 in. height, and 49 in. depth, was used as the sampling area (see Figure 15). A mass of 2.0350 g of Pentolite (50:50 PETN:TNT) was placed in a plastic petri dish (Fisher Scientific, Fair Lawn, NJ) on one side of the hood. The sol-gel PDMS PSPME device was placed on the opposite side of the hood. The hood was enclosed with a sheet of plastic and sampling took place for 24 hr. The next day, the PSPME device was desorbed into the IonScan 400 B IMS for analysis.

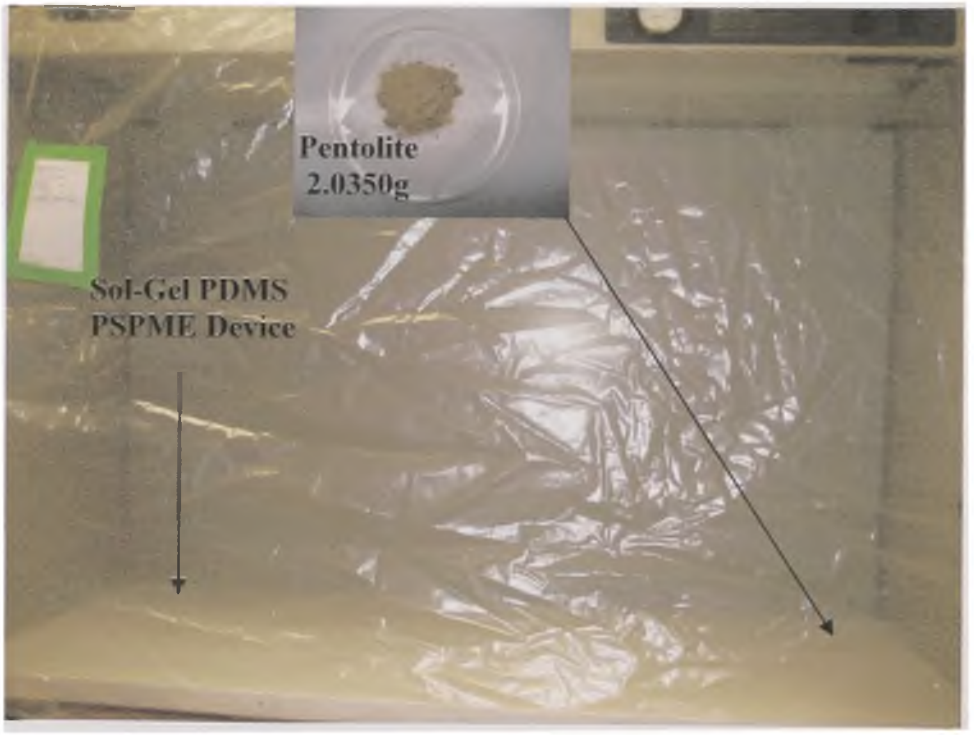

Figure 15. Large Volume Static Sampling for TNT from Pentolite

6.2.7 Comparison of Planar La (dihed) SPME Devices with Control Planar Sol-gel and PDMS Devices for the Extraction of TNT and 2,4-DNT

6.2.7.1 Aging Study

The PSPME devices made by dipping PDMS, sol-gel PDMS and prepared glass in 236 mg of La (dihed) dissolved in methanol were tested in comparison to uncoated PDMS and sol-gel PDMS PSME devices in terms of extraction and aging capabilities.

A 10 μL spike of 240 μg mL^{-1} TNT in acetonitrile into a quart can was sampled at room temperature under static, closed system conditions for 30 min by the PSPME device. Immediate IMS analysis of the PSPME device followed sampling. The same was done for 2,4-DNT (10 μL, 240 μg mL^{-1}) in hexane. The IMS conditions for all the La (dihed) PSPME devices developed were the same as those listed in Table 4 for the IonScan 400 B in the negative ion mode except that the desorption temperature was reduced to 180 °C.

The same experiments were repeated but instead of immediate analysis, the PSPME devices were removed from the quart cans and left outside in ambient laboratory conditions to study the effect aging has on trapping. The PSPME devices were analyzed by IMS after 30 min of being outside of the sampling vessel.

6.2.7.2 Coating Study

The various La (dihed) devices prepared as described in Section 6.1.3.6 for studying the effects of concentration of the metal complex and coating time were tested for their extraction capabilities. The targeted analytes were 2,4-DNT and TNT and sampling

occurred in the same manner as described in Section 6.2.7.1 followed by immediate IMS analysis.

6.2.7.3 La (dihed)/ Sol-gel PDMS

The completed PSPME device was introduced into the IMS for analysis of the background.

6.3 Development of Dynamic PSPME

In the process of developing dynamic planar SPME, substrate candidates were subjected to the typical surface preparation techniques, solvents, and temperatures that would be encountered by the final dynamic PSPME device. These substrates included: a fiberglass screen (Phifer, USA), the fiberglass manufacturer provided explosives filter (Smiths Detection, Mississauga, ON), and glass fiber filter circles (G6, Fisherbrand, Pittsburgh, PA).

6.3.1 Preparation of Dynamic PSPME Devices

Prior to coating, glass fiber filter circles (G6, Fisherbrand, Pittsburgh, PA) were cut down to 3.1 cm in diameter. The surface of the glass fiber filter circles was activated for coating as described in Section 6.1.1. A sol-gel PDMS solution was prepared in the following quantities: 2.060 g vt-PDMS was dissolved in 8 mL of DCM; then 1.10 mL of MTMOS and 0.5351 g PMHS were added, followed by 0.875 mL of TFA (Acros) (5% water v/v). The solution was vortexed and allowed a 30 min stay. The prepared glass fiber filter circle was placed atop a cut glass slide held by vacuum on the chuck of a model WS-400B- 6NPP-LITE spin-coater (Laurell Technologies, North Wales, PA). One mL of the

coating solution was deposited on the glass fiber filter circle and the spin program, 1000 rpm for 60 s, was activated. The newly coated substrate was placed in the dessicator for 12 h, dipped for 1.5 hr in DCM and gelated for 12 hr in an oven at 40 °C. The dynamic PSPME device was then placed in a GC oven in a nitrogen atmosphere at 120 °C for 1 hr, 240 °C for 1 hr, and 300 °C for 3 hr, for conditioning and to complete the curing process.

6.3.2 Coating Method Development

The following is a description of the optimization methodology used to arrive at the final coating procedure described in Section 6.3.1. First, following each step that involved deionized water washing, the glass fiber filter surface was tested for neutral pH using the appropriate litmus paper, blue or red (Fisher Scientific, Fair Lawn, NJ). The spin coating program was varied as follows: 0 (dip-coated), 200, 1000 and 2000 rpm for 1 min. For the 0 rpm data point, the prepared substrate was dipped in the sol solution and removed instantly. Then, the various products (for each spin program) were subjected to the dynamic PSPME sampling of 2,4-DNT from the headspace of the Hogdon 322 smokeless powder. A mass of 100 mg of smokeless powder was placed in a quart can and sealed for 2 hr. The can was opened and sampled dynamically with a PSPME device (described in Section 6.3.3) for 1 min. The dynamic PSPME devices were desorbed into the IonScan 400 B IMS for analysis. To study the extraction of TNT, a volume of 10 μL 240 ug mL^{-1} TNT in acetonitrile was spiked into a quart can, sealed overnight, and sampled by the dynamic PSPME devices for 1 min. Following sampling, the devices were analyzed by IMS.

6.3.3 Characterization of Final Dynamic PSPME Devices

Blanks of the final dynamic PSPME were taken by IMS (conditions listed in Table 2) to determine if the background was suitable prior to any extraction.

The surface characteristics of the dynamic PSPME devices created, and coating thickness determinations were made using a Philips XL30 scanning SEM (FEI, Hillsboro, OR) at high vacuum. Both secondary electron and backscatter detection were used depending on the information that was desired. The sample preparation included gold coating the samples using a Hummer 10.2 Sputtering System (Anatech, LTD., Union City, CA). For the SEM characterization of the samples spun at different speeds a reference Al stub was covered in a drop of sol solution and cured. The stub was also gold coated prior to SEM analysis.

6.3.4 Handheld Sampler

A handheld vacuum (Remote DC Sampler, Smiths Detection, Smiths Detection, Missausaga, ON) was the device used to pump sample air through the dynamic PSPME device and the manufacturer provided filters (Smiths Detection, Missausaga, ON). A schematic of the handheld vacuum showing introduction of the sampling media is shown in figure 16.

To determine the flow rate of air that is pumped while sampling, the dynamic PSPME device is placed in the slot of the handheld vacuum as shown in figure 16 and the pump was turned on. The air speed at the head of the nozzle was measured with an EA-3010U handheld anemometer (La Crosse Technology, La Crosse, WI). The same was done for

the manufacturer provided filter. The sampling of the appropriate emitting source (described in Sections 6.3.5.2 and 6.4.5) is accomplished as shown in Figure 17 with both the dynamic PSPME devices and the manufacturer provided filters.

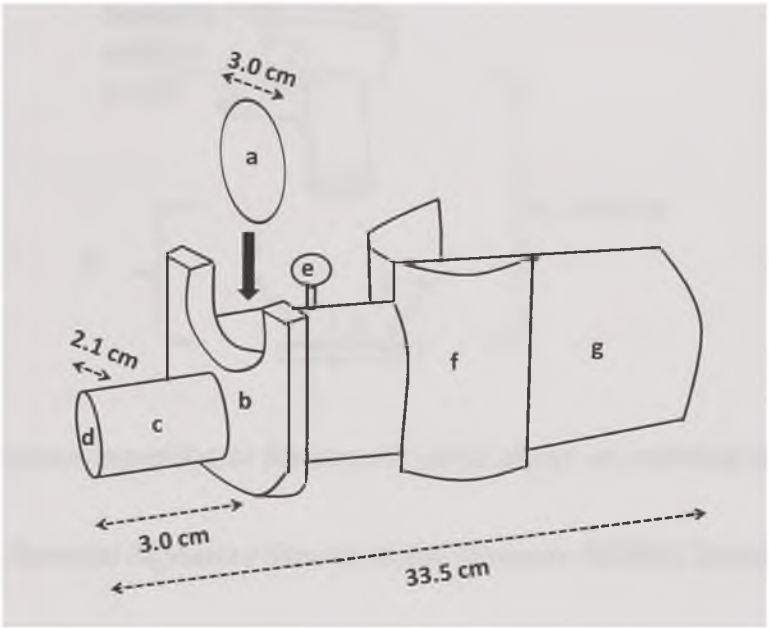

Figure 16. Dynamic Sampling by Dynamic PSPME and Manufacturer Provided Filters: a)the sampling medium, b) slot for sampling medium, c) nozzle length, d) nozzle width, e) release knob (keeps collection media in place during sampling), f) added funnel accessory prevent air flow from disturbing the sample, g) pump [165]

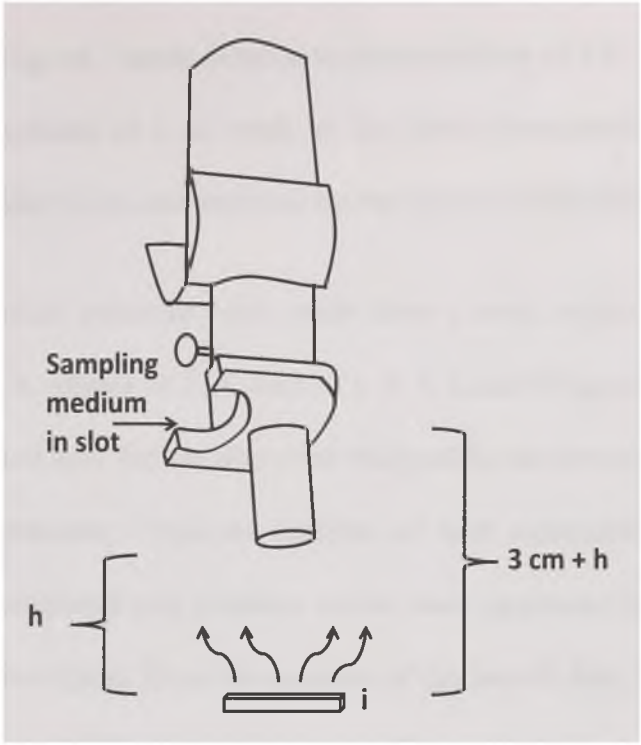

Figure 17. Dynamic sampling at distance (h (cm)) above an emitting source (i) [165]

6.3.5 Volatile Chemical Signature Standards for Dynamic PSPME Sampling

The following section lists the standards that were used to quantitate the mass detected by IMS following dynamic PSPME sampling.

6.3.5.1 Spike on Manufacturer Provided Filters

Standard solutions of TNT were diluted from a 1000 ug mL^{-1} certified standard solution (Cerilliant, Round Rock, TX) to concentrations of 0.1, 0.2, 0.5, 0.8, 1.0, 2.5, 5.0, and 10.0 ug mL^{-1} in ACN, while 2,4-DNT calibration solutions originated from a 1000 ug mL^{-1} stock and consisted of the following concentrations: 5.0, 8.0, 10.0, 25.0, 50.0, 100, 250, 500, and 750 ug mL^{-1} in hexanes. The EC solutions were prepared from a 5 µg mL^{-1} stock solution in concentrations of 0.1, 0.5, 0.9, and 1.0 ug mL^{-1}. Solutions of DPA were

diluted from a 500 ug mL^{-1} stock solution to concentrations of 1.0, 5.0, 10.0, 25.0, 40.0, 50.0 ug mL^{-1}. A volume of 1 μL each of the listed concentrations was spiked onto manufacturer provided filters and analyzed by the IonScan 400B IMS.

The piperonal standard solutions were made from a stock solution of 1000 μg mL^{-1} piperonal in DCM. A volume of 2 μL each of 1, 2, 5, 8, and 10 μg mL^{-1} concentrations of piperonal were spiked onto Teflon filters and analyzed by the Itemiser 2 IMS for analysis of the piperonal monomer. Triplicate analyses of each concentration for the suite of compounds were conducted and response curves were generated by plotting mass (ng) versus the cumulative signal. From the equation of the best-fit line, the mass detected by IMS for each compound following dynamic sampling, with the novel PSPME device and the manufacturer provided filter, was calculated in the ng range.

Blanks of the manufacturer provided filters were taken by IMS prior to spiking and before all subsequent experiments. The filters were only used one-time and they were stored/ sealed in metal cans supplied by the manufacturer until use.

6.3.5.2 Controlled Odor Mimic Permeation Systems (COMPS)

The COMPS standards were created as previously reported in the literature**[50]**using piperonal (100 mg), and they were for the first time created for the compounds, Pentolite (3 g), 2,4-DNT (3 g), DPA (100 mg), and EC (100 mg). The 0.076 m x 0.076 m 2 mil low-density polyethylene (LDPE) bags used were from Uline (Waukegan, IL). The compound was placed in the bag and distributed evenly. As much air as possible, was removed from the bag and then it was heat-sealed.

For each compound studied, COMPS standards were prepared in triplicate for statistical purposes and were allowed to stand under ambient conditions. The mass of the bags was recorded for up to 28 consecutive days. The average value and standard deviation for each triplicate set was determined. The average value (grams) was plotted vs. time (days) to determine the rate of mass lost each day, derived from the best-fit lines for the linear and exponential form (for piperonal only), respectively. From this data, the dissipation rate of the compound through the LDPE bag per second was determined and thus the maximal mass available for dynamic sampling by the PSPME device and manufacturer provided filter is known for a given sampling time.

6.4 Validation Experiments for Dynamic PSPME

Table 5 shows the operating conditions of the IMS instruments used for the dynamic PSPME validation experiments. Also, related information about each particular volatile chemical signature is included in this table.

Table 5. Detection of Volatile Chemical Signatures from Real Case Samples Using Dynamic PSPME–IMS [165]

IMS Operating conditions	IonScan 400B (#1)		Itemiser 2 (#2)
Polarity	Positive (+)	Negative (-)	Positive (+)
Desorber Temperature (°C)	250	300	215
Drift Tube Temperature (°C)	235	115	80
Sample Flow (mL min^{-1})	200	300	500
Drift Flow (mL min^{-1})	351	351	350
Reagent Gas	Nicotinamide	Hexachloroethane	Nicotinamide

Analyte	Piperonal	2,4-DNT	DPA	TNT	EC
IMS Instrument/ polarity	#2 / (+)	#1 / (-)	#1 / (+)	#1 / (-)	#1 / (+)
K_0 ($cm^2/V \times s$)	1.51	1.57	1.61	1.45	1.24
Drift time (ms)	8.3	11.8	11.0	12.8	14.4
Vapor pressure (Torr)	1.0 @ 87 °C	1.1 $x10^{-4}$ @ 25 °C	6.4$x10^{-4}$ @ 25 °C	4.5 $x10^{-6}$ @ 25 °C	N/A

6.4.1 Dynamic PSPME Retaining Capability Studied By Analyte Solution Spiking

The dynamic PSPME device was spiked with 2 μL of standard solution, with a concentration resulting in a mass within the response curve linear range of each compound, and was placed in the handheld vacuum. The concentrations were 0.25, 1, 5,

15 and 20 ug mL^{-1} for piperonal, 2,4-DNT, DPA, TNT, and EC, respectively. The pump was turned on for various times (s) to determine at what point, if any, the IMS signal would diminish following desorption of the dynamic PSPME device. The same was done using the manufacturer provided filters for comparison purposes. The measurements for each analyte were performed in triplicates. Controls with consisted of spike the analyte solution on the surface of the sampling media and aged (no pumping applied) for 60-70s.IMS blanks of both the manufacturer provided filters and dynamic PSPME devices were taken before sampling.

6.4.2 Dynamic PSPME Retaining Capability Studied By COMPS Vapor Source

Each COMPS device was placed in a particle-free hood (Labconco, Kansas City, MO) and sampled for 30 s at different heights by turning on the vacuum with the dynamic PSPME device in place (figure 17). Once the optimum sampling height was determined, the COMPS devices were then sampled at that height for different times. Following each sampling, the dynamic PSPME device was analyzed in the appropriate IMS instrument. The manufacturer provided filter was also used at the same sampling conditions for comparison. The COMPS devices were allowed a 30 minute stay in between each sampling. All the optimization measurements were performed in triplicates and with the appropriate blanks prior to sampling.

6.4.3 Dynamic PSPME LOD

The detection limits for the targeted compounds using the complete dynamic PSPME-IMS method were estimated. The method is considered as three consecutive steps:

dynamic sampling, desorption and detection. Accumulative extraction of the total mass of analyte onto the absorbent phase of the novel device that is above the IMS analysis LOD, is expected to alarm. The sensitivity of the PSPME-IMS method was estimated for each of the tested volatile chemical signatures in this study, considering a 10 s sampling time (total air volume of 3.5 L) as applicable to real case scenarios, 100% efficient absorption on the substrate and complete IMS desorption.

6.4.4 Application of Dynamic PSPME- IMS for Screening of Illicit Compounds

The dynamic PSPME device was tested on the headspace of illicit compounds with parameters designed for difficult sampling conditions in the field.

The high explosive, Pentolite, was tested, in triplicate, by placing 100 mg of solid into a quart-sized can and sealing it for 1 hr, opening it and sampling with dynamic PSPME for 30 s by lining up the base of the nozzle (Figure 16, c) with the top of the quart-sized can. Following sampling, the dynamic PSPME device was desorbed into the IMS for analysis of the targeted compound, TNT.

The illicit drug MDMA was sampled and analyzed on-site a local crime laboratory. The examiner at this agency prepared three quart-sized cans, each containing 5 tablets of suspected drugs from actual cases, for sampling with dynamic PSPME in a blind study. The cans were sealed for 15 min and sampled for only 10 s, followed by IMS analysis. A blank can (containing no tablets) was also sampled. This MDMA study was also done in triplicate.

Lastly, of the four smokeless powders (low explosives), the two previously reported to contain 2,4-DNT in their headspace by SPME- gas chromatography- mass spectrometry (SPME-GC-MS) **[59]**, Hogdon H322 and IMR 4192, were tested. A mass of 100 mg of each powder was placed in a quart-sized can, sealed 30 min, opened, and sampled for 30 s, followed by IMS detection targeting 2,4-DNT in the negative polarity. The Red Dot powder was reported to contain both EC and DPA in the headspace **[59]**, while the remaining 3 powders all contained DPA. These four powders were sampled dynamically, targeting DPA, and DPA and EC in the Red Dot case by IMS. For IMS detection of DPA and EC in the positive polarity from the headspace of the smokeless powders, the same mass (100 mg) was introduced into a quart-sized can as when targeting 2,4-DNT, but they were sealed overnight, opened and sampled dynamically for 1 minute.

CHAPTER 7. RESULTS AND DISCUSSION

7.1 Development of PSPME Devices for Static Extractions

Modification of the fiber SPME geometry to a planar geometry greatly increased the surface area for extraction as is depicted in figure 18.

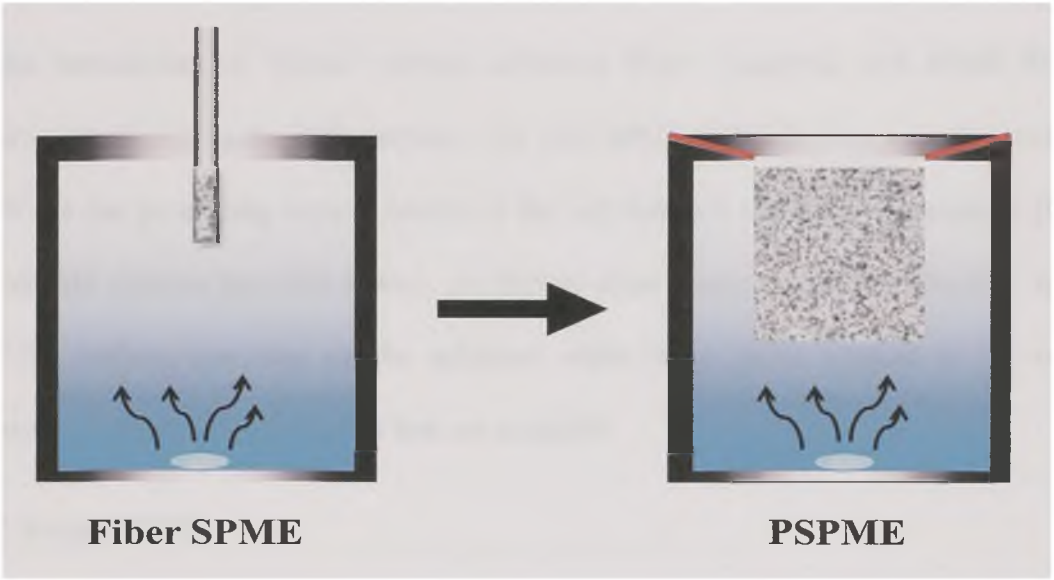

Figure 18. Fiber to Planar SPME

The thinnest SPME coating available for a cylindrical fiber is 7 μm while the thickest is 100 μm. This equates to a surface area of the fiber from 0.45 mm^2 to 10.47 mm^2. The planar SPME (PSPME) surface area ranges from 500 mm^2 to 1000 mm^2. The ideal surface area for the commercial embodiment of the PSPME device will be 792 mm^2 for a disk that is 32 mm in diameter.

As a result of this increase in surface area, the capacity is also further increased because the volume of the phase is greater. The thickest commercially available SPME fiber has a volume of only 1.03 mm^3 while the planar sol-gel PDMS discussed (Section 7.1.1) has a

volume of 165 mm^3. The change in SPME to a planar geometry thus greatly increases the possibility of absorbing volatile chemical signatures even in difficult field sampling scenarios.

Another consequence of the change in geometry is that the PSPME device can be directly introduced into the sample desorbers of commercial IMS instruments already designed for the introduction of "planar" sample collection filters. Sampling with SPME fibers requires interfacing to the IMS detector. The first SPME-IMS interface was designed to attach via the protruding sample nozzle of the GE Iontrack Itemiser 2 instrument **[19]**. Not all IMS systems have this feature, yet they do share planar sample introduction. With PSPME, uniform sampling can be achieved while being easily adapted to the wide variety of commercial instruments that are available.

7.1.1 Sol-gel PDMS

Sol-gel PDMS has been previously used to coat SPME fibers **[105]** because of the high thermal stability and strong bonding of the phase to the surface for longer lifetime of the extraction device. This same chemistry has been used as the extraction phase of the planar SPME device but has been modified for the difference in geometry. Sol-gel is defined as a colloidal suspension that is gelled to form a solid. The sol-gel process starts with hydrolysis of the precursor, MTMOS, which is catalyzed by TFA, and its polycondensation. This creates a polymeric network that is anchored to the glass surface since the silanol groups on the glass surface also participate in the condensation reactions. The last step is the cross-linking of the vinyl group of the PDMS during curing **[105]**.

For creation of the sol-gel PDMS PSPME devices, dip-coating was determined to be the best route when compared to spin coating. In dip coating, the activated substrate is immersed in a homogeneous polymer solution, at room temperature. While dipping, there is a residence time whereby the compounds that would eventually form the coating interact with the activated surface. Specifically for sol-gel processes, during withdrawal of the substrate from the polymeric solution, the liquid film on the substrate becomes a gelatinous coating upon coming into contact with the ambient atmosphere above the coating solution. There are many simultaneous processes, as illustrated in figure 19 taking place including: gelation (or connection of the particles that have condensed) and aggregation of these particles in preparation for gel formation. Meanwhile, solvent evaporation, gravitational draining, and continued condensation reactions are occurring. It is also important to note that the sol becomes dilute upon withdrawal of the substrate, and as a result, sol solutions as coatings can only be used once.

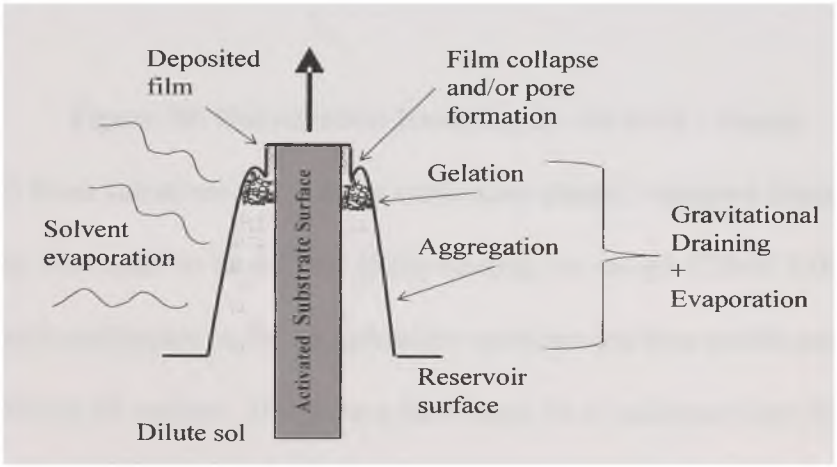

Figure 19. Sol-gel: Dip-coating Processes. Adapted from [100]

These processes help determine the final sol-gel film thickness. Other parameters that affect the film thickness are viscosity, withdrawal speed, oxide concentration of the

solution and heating temperature and time. Increased viscosity, withdrawal speeds and/or oxide concentration in the sol solution yield large film thickness. Inversely, since gels are porous they are sintered with heating; high heat and prolonged temperatures result in thinner films. Solvent evaporation occurs over time once the coated substrate is removed completely from the coating solution and can be aided by heat, which in turn also helps cross-link (chemically bond) the substrate and the polymer. Additionally, -M-O-M'- bonds may be formed as a result of dehydration (see figure 20), while subsequent heating can change the film to glass or ceramic depending on the tailored temperature for the desired effect **[100]**.

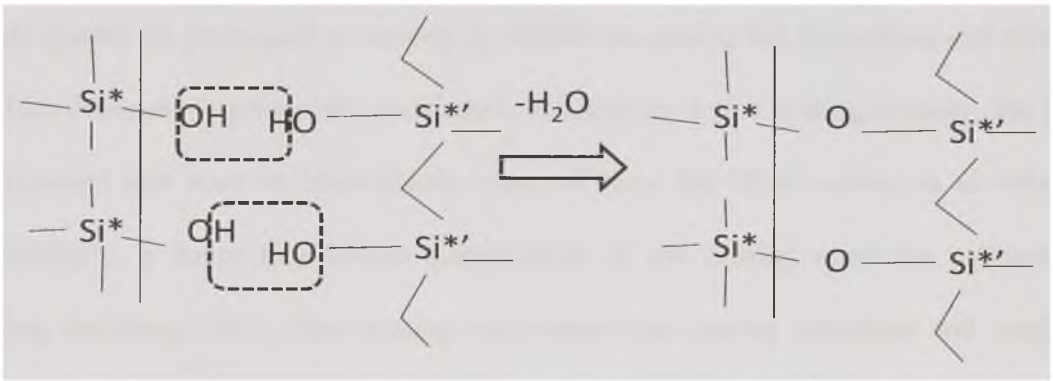

Figure 20. Dehydration Resulting in –M-O-M'- Bonds

(*-Si from substrate, *'-Si from stationary phase). Adapted from [100]

Spin-coating was found to be inferior to dip-coating for sol-gel PDMS PSPME since the surface silanols participate in the condensation reactions and thus enable anchoring of the sol-gel PDMS to the surface. This means there must be a residence time for the reaction. A possible solution was to deposit the solution on the prepared substrate, allow surface tension to keep the solution on the surface such that there is longer than instantaneous interaction of the sol solution with the activated surface. This unfortunately was not possible since DCM, the solvent system used in this reaction is so volatile it evaporates in

an uncontrolled fashion, causing premature gelation, and when the spin program is activated, chunks of gel are spun off leaving a rough surface, not the desired uniform surface with a controlled film thickness. Leveling of paint is affected negatively by surface tension gradients that arise partly from solvent evaporation **[166]**. Introducing the parameter of allowing a residence time, would defeat the purpose of using spin-coating for providing level coatings. Another idea was to change DCM as the solvent system but in sol-gel processes, solvent filled pores are created, and the solvent must be removed in a timely fashion. First, the swelling properties of the film would change and thus affecting particle size and uniformity. If a less volatile solvent were used, then curing would greatly be prolonged to remove it, further decreasing the throughput and altering the film thickness as previously mentioned. When using a spin coating strategy, the fluid is deposited and must be immediately spun off since the DCM solvent is so volatile. Additionally, a factor that affects planarization of the coating upon the substrate is coating shrinkage **[167].** Spin-coating exacerbates the coating shrinkage and cracking problem since the rotational acceleration that causes spin off also aids in solvent evaporation parallel to the substrate surface. For dip coating, it was observed that drying perpendicular to the substrate surface was more likely.

Imaging by SEM was used to characterize the sol-gel PDMS PSPME devices developed in this research. The sol-gel PDMS coating thickness and surface are shown in figures 21A and 22B, respectively. Note the highly packed and uniform nanoparticles evident on the surface (figure 22B). The coating thickness was determined to be ~ 168 μm.

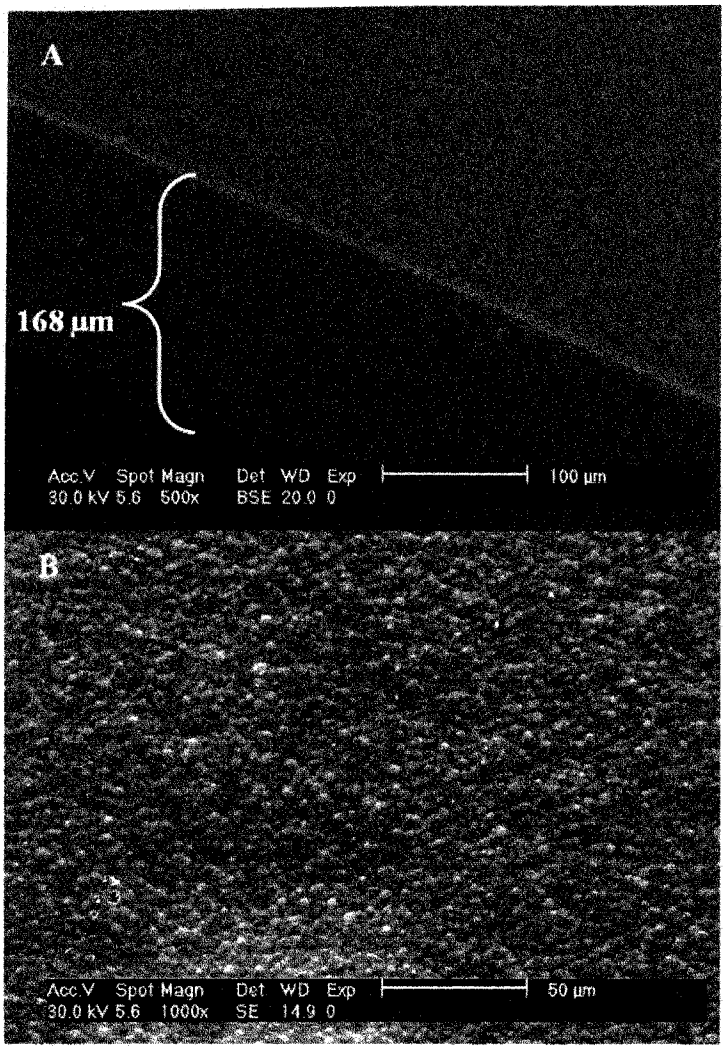

Figure 21. The Sol-gel PDMS PSPME Device A) coating thickness B) surface characteristics [168]

7.1.2 PDMS PSPME Via a Chlorine-terminated PDMS Route

Coating of the planar PDMS PSPME device was achieved by spin-coating chlorine-terminated PDMS onto a glass substrate with exposed silanol groups on the surface (from the surface activation procedure). A bimolecular nucleophilic substitution reaction (S_N2)

occurs where the exposed silanol group reacts with the chlorine moiety of the PDMS, liberating HCl and covalently binding PDMS to the glass.

Spin coating was much more desirable as a coating strategy for several reasons. First, with spin coating, only 1 mL of coating solution is required for creating a thin film upon the chosen substrate. Compared to the 25 mL of coating solution required per sol-gel PDMS PSPME device, using only 1 mL of raw materials is much more economical, especially in the development stages when a raw material is limited, as is the case with the La (dihed) powder that has been synthesized in this research (Section 7.1.5). Secondly, the spin coating process is much faster, 1 min compared to 1 hr in the case of sol-gel PDMS. During spinning, flow of the coating solution and drying of the solvent occurs simultaneously **[162]**. For these reasons there is higher throughput with spin coating for creating the extraction devices than with dip coating. Thirdly and most important, with spin coating there is higher reproducibility in final film thickness and uniformity. This is largely the result of the elimination of human error since in dip coating the withdrawal rate can affect the final film thickness. The greater the speed of withdrawal, the greater the film thickness produced **[100]**. By using the Laurell spin coater (in these experiments), the solution is spun off with both consistent and accurate acceleration and spin (accuracy better than 1 rpm **[169]**) for an given time span. Specifically, since solvent evaporation is such an important parameter, a hole on the lid of the spin coater used in this work was covered while the spin program is activated.

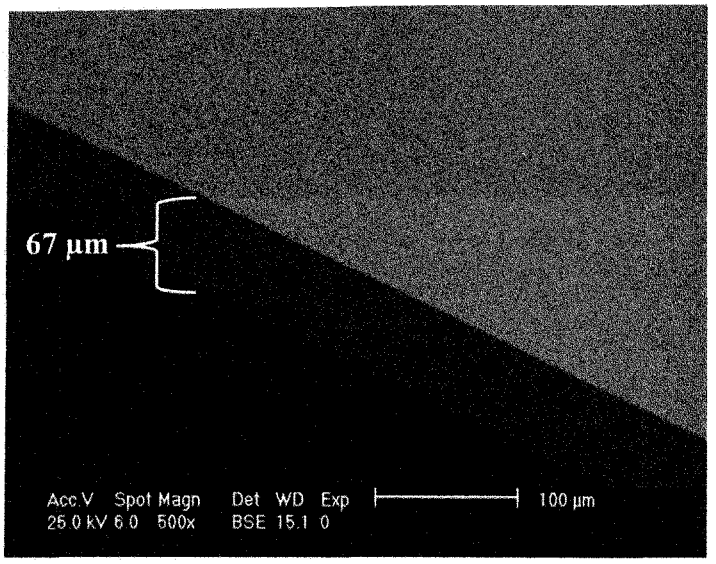

Figure 22. Surface and Coating Thickness of the PDMS PSPME Device [168]

An SEM image of the PDMS surface is shown in figure 22. The coating thickness was determined to be ~ 67µm.

7.1.3 Sylard® 184 by Dow

Sylgard® 184 PDMS was used in the coating of activated glass and aluminum. The requested concentrations of explosives in the polymer (by the U.S. Army Research Laboratory) were calculated according a 100 µm coating obtained by utilizing the spin program, 5 seconds at 200 rpm, 3 seconds at 500 rpm, and 30 seconds at 4000 rpm. Figure 23 is an image of the final standards intended for LIBS experiments, of RDX and Pentolite on aluminum and glass targets.

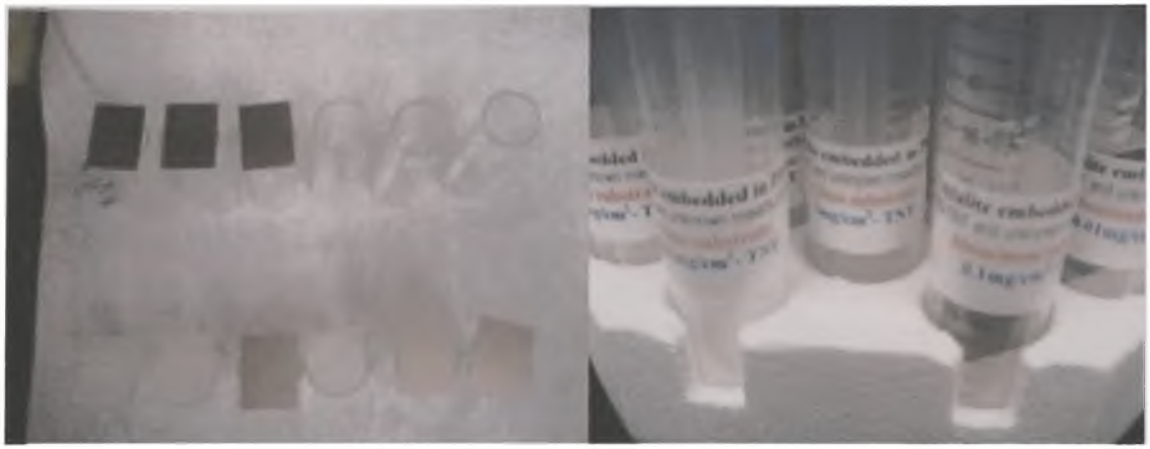

Figure 23. Explosive Standards for LIBS Experiments in Sylgard® 184 PDMS

There were several spin programs attempted in order to produce a coating 100 μm thick. Figure 24 is an SEM image of the coating produced by the appropriate spin program. The visual defect along the coating thickness is the result of a combination of the high viscosity of the final Sylgard PDMS polymer and the SEM sample preparation technique (smashing of the glass coated sample to produced glass fragments).

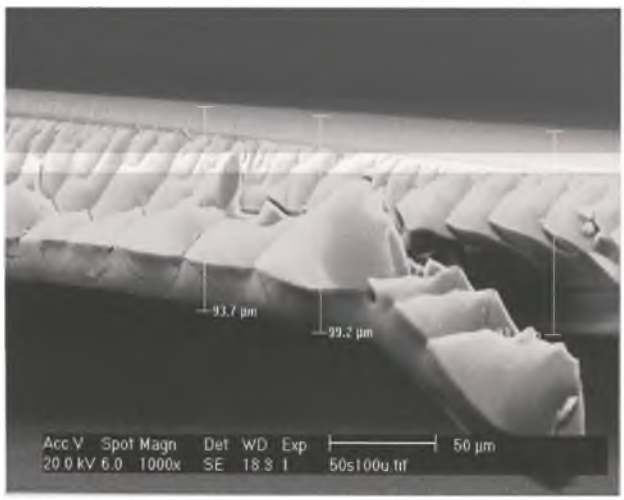

Figure 24. Coating Thickness of Sylgard 184 ® PDMS on Glass. Spin program: 5 seconds at 200 rpm, 3 seconds at 500 rpm, and 30 seconds at 4000 rpm

Sylgard® 184 PDMS was not considered suitable as an option for a PDMS absorptive phase for SPME because of the low maximum temperature (200 °C) **[170]** that would affect IMS desorption and since it is not covalently bound to the substrate as are the sol-gel PDMS and PDMS (chlorine-terminated route) SPME phases.

7.1.4 Activated Charcoal in PDMS Formulations

A modified carboxen/ sol-gel PDMS coating was attempted by substituting activated charcoal for the carboxen particles. A commercial carboxen (CAR)/ PDMS fiber was imaged using SEM (figure 25) in order to determine the particle size of the carboxen.

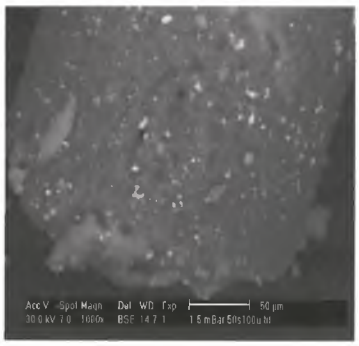

Figure 25. SEM Image (Low Vacuum) of CAR/ PDMS Fiber

Backscatter detection in low vacuum (LV), with no conductive coating, was used to see differences in composition. The lighter spots on the image represent the carboxen particles. The average size of these particles was determined to be 14.1 um. The activated charcoal that would be used in the activated charcoal/ PDMS coatings was also imaged, revealing irregularly shaped particles that also varied significantly in size (see figure 26).

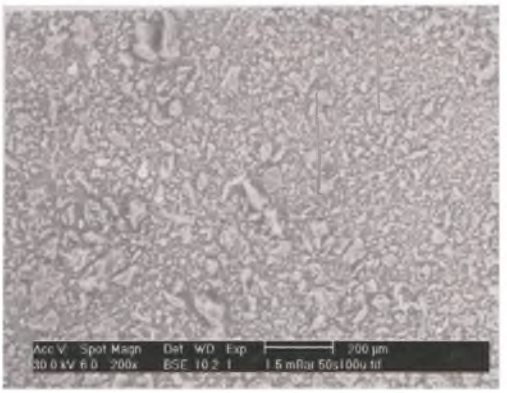

Figure 26. SEM Image (LV) of Activated Charcoal Particles

The activated charcoal particles were embedded in two PDMS formulations, sol-gel PDMS and Sylgard 184® PDMS, and were used to dip coat the activated glass slides.

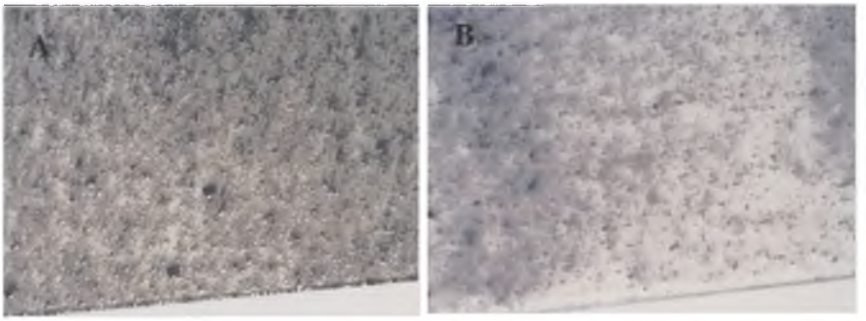

Figure 27. Activated Charcoal/ PDMS PSPME Devices. A) AC/ Sylgard® 184 PDMS B) AC/ sol-gel PDMS

Since commercial CAR/PDMS fibers require high desorption temperatures (up to 310 °C) **[171]** to remove adsorbed analytes, it was thought that by incorporating the activated carbon particles with sol-gel PDMS would afford added thermal stability enabling IMS desorption at 300 °C. The AC/ Sylgard PDMS served as a control for determining the

appropriate coating parameters when activated charcoal is used, but was this device not intended for eventual use with IMS due to its low maximum operating temperature.

The surfaces of the final PSPME devices are pictured in figures 27A and 27B. There is appreciable surface roughness on both devices, and in figure 27B, the cloudy surface characteristic of a sol-gel PDMS device indicates proper physical incorporation of the activated charcoal particles. Preliminary extractions with TNT resulted in minute amounts of TNT detected and unsuitable desorption profiles even at 300 °C desorption. Therefore, further experimentation with these coatings was abandoned.

7.1.5 La (dihed)

7.1.5.1 Structure Determination

First, the ligand, *p*-di (44,5,5,6,6,6-heptafluoro-1,3-hexanedionyl)benzene, H_2 dihed, was synthesized. The structure of the ligand is shown in figure 28 showing both the enol and keto tautomers of this ß-diketonate.

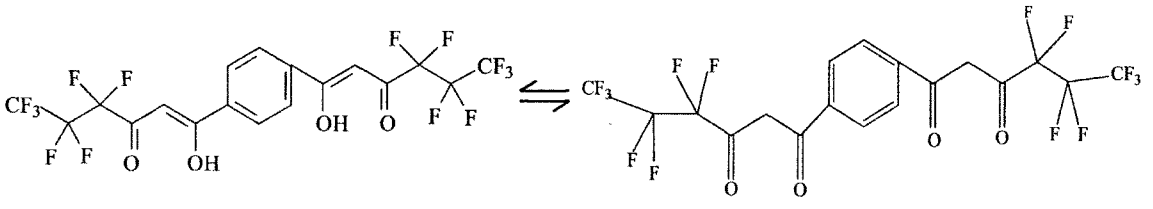

Figure 28. Ligand Structure Showing Enol and Keto Tautomers of H_2 (dihed): *p*-di(4,4,5,5,6,6,6-heptafluoro-1,3-hexanedionyl)benzene ($C_{18}H_8O_4F_{14}$)

Following synthesis of the ligand, analysis by ^1H NMR was done in order to elucidate its structure. Figure 29 is the spectrum of the ligand in deuterated chloroform.

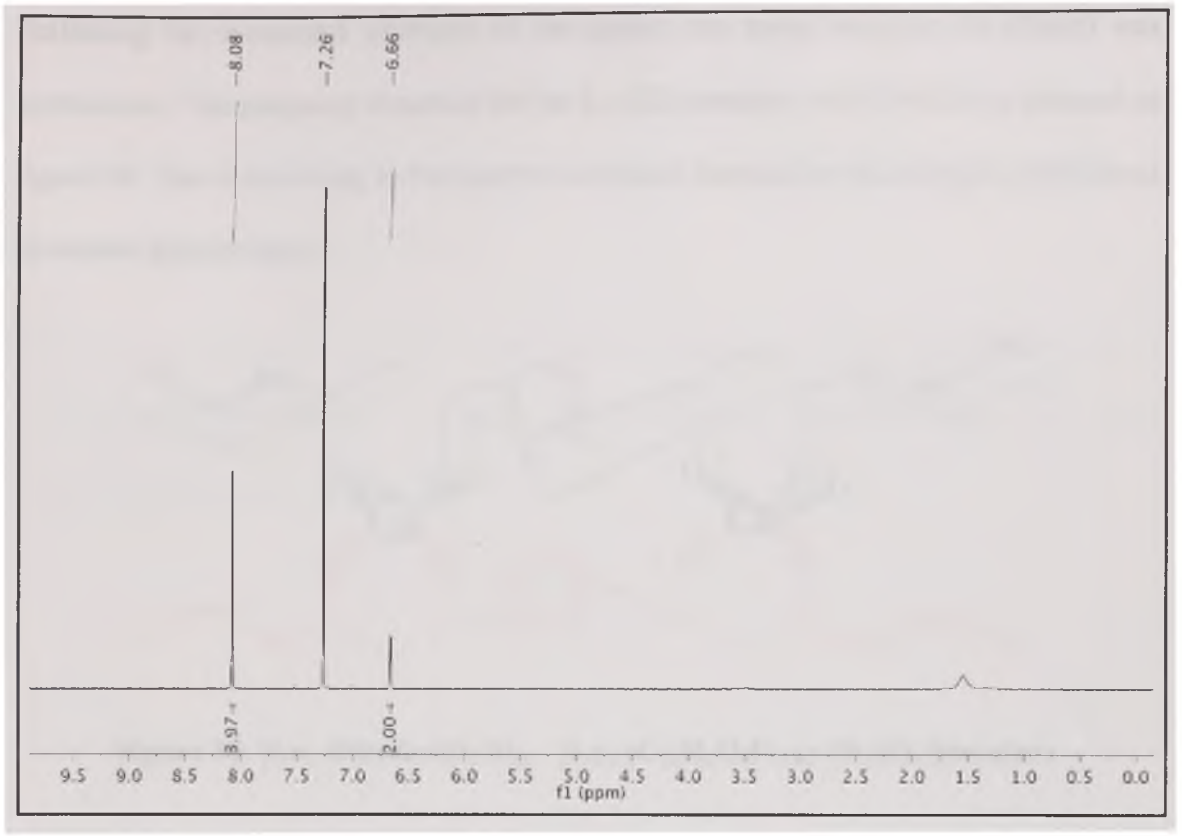

Figure 29. ^{1}H NMR Spectrum of the H_2 (dihed) ligand

The peak at 1.6 ppm represents traces of H_2O in the deuterated chloroform. The two vinyl hydrogens are represented at 6.7 ppm with a peak area of 2. The peak at 7.2 ppm is from the solvent. The peak at 8.1 represents the four aryl hydrogens with a peak area of 4, which is as expected- double the peak area of the vinyl hydrogens.

In non-polar solvents it is generally accepted that the enolic form is favored, and that simultaneous conjugation and chelation through hydrogen bonding is responsible for the stability of the enol tautomers. Enolization is also known to increase when the ligands are fluorinated or contain an aromatic ring **[172]**, as is the case with the H_2 (dihed) ligand.

Following the successful synthesis of the ligand, the metal complex La (dihed) was synthesized. The proposed structure for the La (III) complex with dihed is as pictured in figure 30. This is according to the reported chemical formula for this complex **[117]** from elemental analysis data.

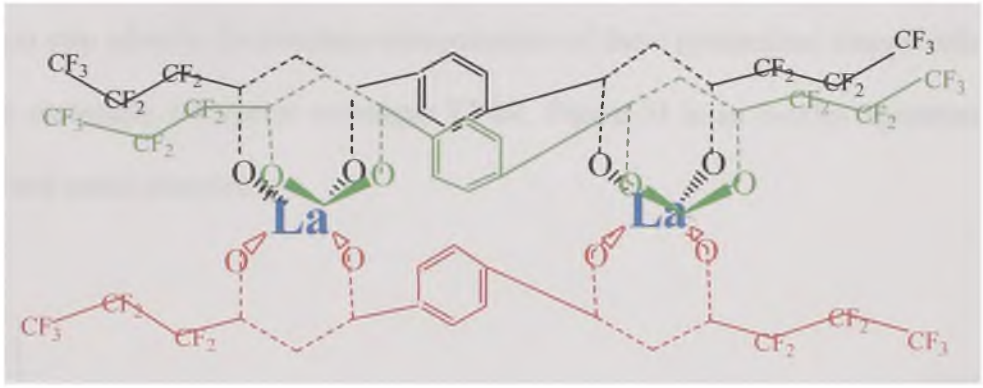

Figure 30. $[La_2\ Dihed_3 \cdot 4H_2O]_n$, $[La_2\ (C_{18}H_6O_4F_{14})_3 \cdot 4H_2O]_n$ Structure

The elemental analysis was consistent with a ratio of two lanthanum ions to three ligands as is shown in figure 30. This is because the metal ions in the ß-diketonate polymers are coordinatively unsaturated and will bond to suitable electron pair donors **[117],** in this case the carbonyl oxygens.

Following this synthesis, classical methods of structure determination were used for the ligand and the complex. The melting point of the ligand was found to be 144-146 °C which is close to the literature value of 146-147 °C **[164]**. In the melting point determination of La (dihed), at 300 °C there was no melting but the compound turned a brownish color. This is consistent with the literature, which reports that at 300 °C there was slight discoloration with no melting **[117]**. Solubility tests were also conducted whereby the ligand was soluble in non-polar solvents like chloroform and DCM and the

complex was soluble in polar solvents such as methanol. Lastly, TLC was done of both the ligand and the complex in a (hexane: acetone 90:10) mobile phase. The R_f values were 0.68 and 0.51 for the ligand and the complex respectively. There was only one spot per lane suggesting single products.

The next step taken in the structure determination of these synthesized compounds was to use the molecular absorption technique FT-IR. Figure 31 is an overlay spectrum of the ligand and metal complex.

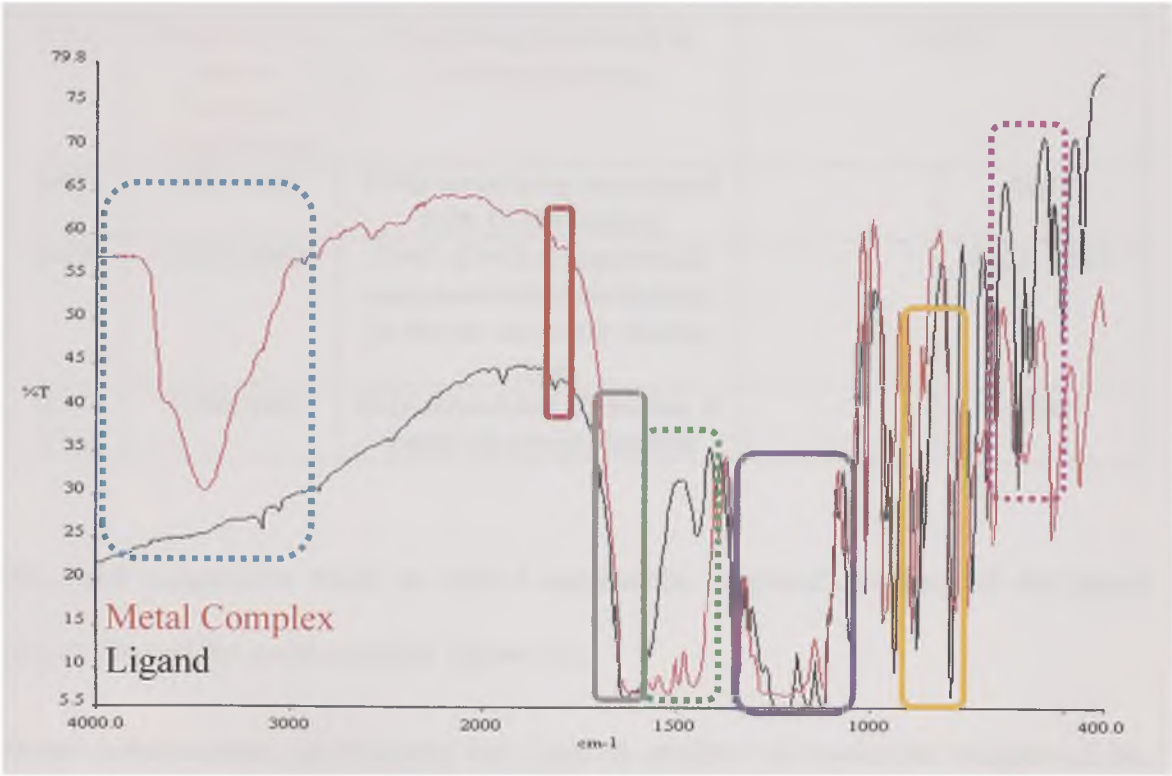

Figure 31. Overlaid IR Spectra of H_2 (dihed) and the La (dihed) Complex

The differences in the two spectra and regions of interest are highlighted in figure 32 with the corresponding interpretations listed in table 6.

Table 6. IR Band Interpretation

Ref.	Wavenumber (cm^{-1})	Group	Ligand	Complex
[173]	800-900	1,4 di-substituted aromatic benzene	793, 865, 881	784,867,893
[170, 174]	1050-1250	CF_2	1056, 1123	1055,1119
	1350	CF_3	1352	1346
[170]	1580-1640	Broad band due to intra-molecular hydrogen bonding stabilized by resonance. This is characteristic of the enol-keto tautomers	1600-1630	
[171]	Shift of C=O due to halogen substitution	Fluorines linked α/β to carbonyl group	1815	
[169]	1425-1489	C=O stretching associated with C-H bending	-	1495
[169]	1520, 1580	C=C, C=O symmetrical, unsymmetrical stretching in the six member chelate ring	-	1523, 1563
[171, 175]	3100-3600	O-H stretching vibration at water of crystallization	-	3446

The band assignments listed on table 6 support the proposed structures of the ligand (figure 29) and the metal complex (figure 31).

Direct infusion-mass spectrometry was used to confirm the molecular weights of the ligand and the complex. Figure 32 is the negative ion mass spectrum of the ligand.

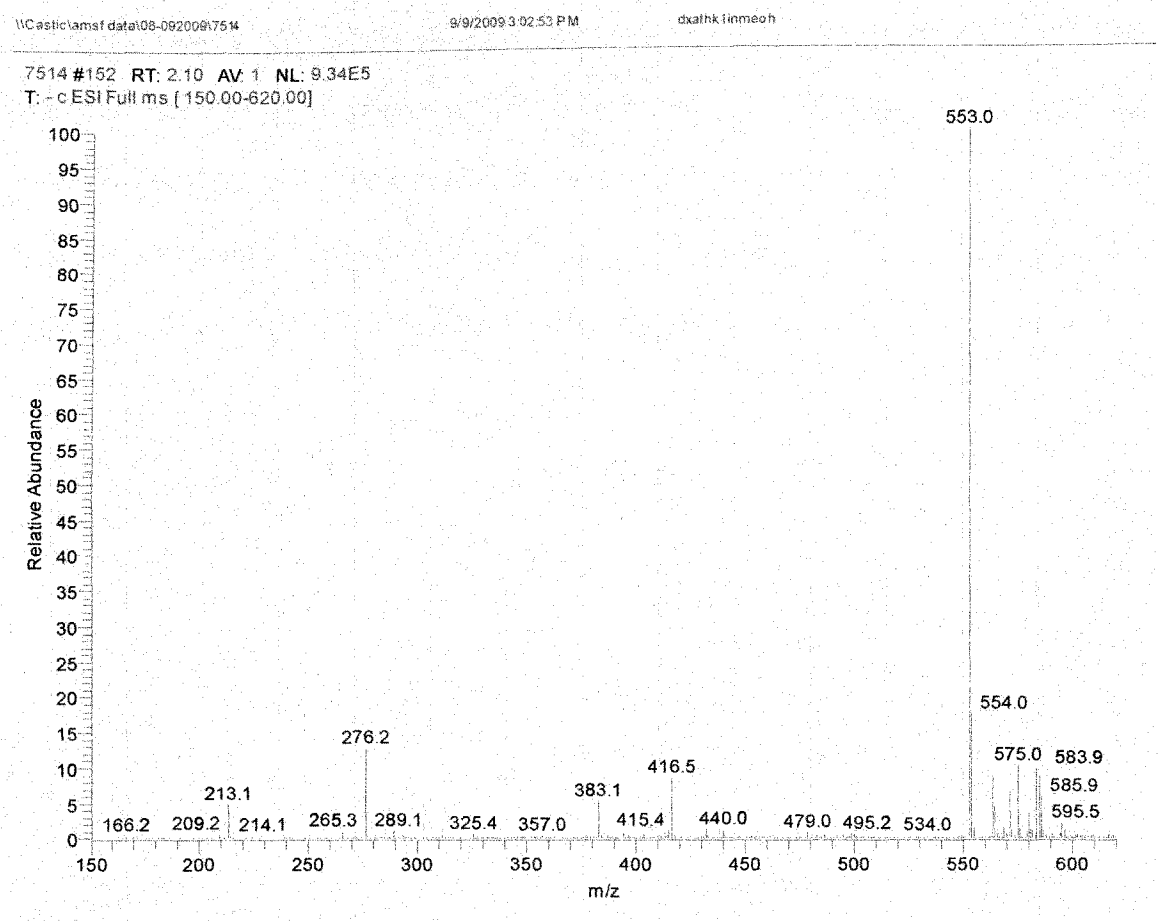

Figure 32. Negative Ion Mass Spectrum of H_2 (dihed) Ligand

The base peak (relative intensity 100 %, y-axis) is at 553 m/z (x-axis). This is the $[M-H]^-$ molecular ion of the ligand, which has a molecular weight of 554 a.m.u. The determination of the molecular weight of the complex was not so straightforward. Figure 33 is the negative ion mass spectrum of the complex.

The fragment of 553 m/z, is the peak with the second highest intensity and is likely the result of the $[Ligand-H]^-$. The peak with greatest intensity is likely the ligand with an attached sodium ion. At the higher mass range there are many peaks, but no fragment stands out. A zoom of this spectrum is shown in figure 34. There is no definitive peak in

this mass range either. This may be so because the complex is a polymer with each monomer having a molecular weight of 1934 a.m.u. (without counting the coordinated water molecules) and 2006 a.m.u. counting these. The mass range of the mass spectrometer is only 2000 a.m.u. If the presence of doubly charged ions is considered there are still no characteristic fragments other that the [Ligand-H]$^-$ ion seen in figure 33.

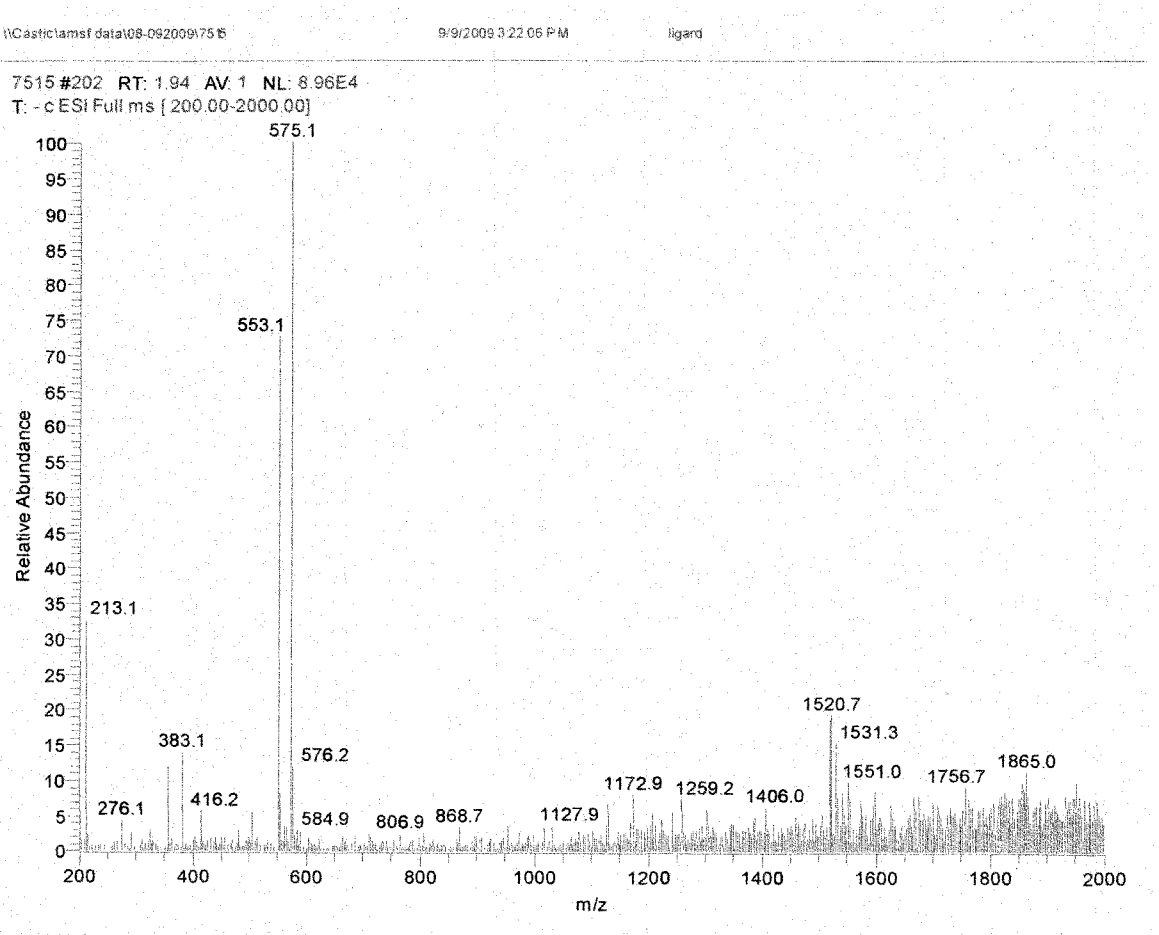

Figure 33. Negative Mass Spectrum of the La (dihed) Complex

The final steps used to characterize the La (dihed) complex involved the use of ^{1}H NMR. It is generally accepted that ^{1}H NMR of compounds containing paramagnetic metals such as La, is impossible **[176]**. This is because paramagnetic compounds have disordered,

permanent magnetic moments even in the presence of an applied field from, for example, an NMR magnet. Despite this, the NMR experiment was conducted to see if there could be any useful information gained, as there are a growing number of researchers attempting to obtain useful NMR spectra from paramagnetic complexes **[176]**.

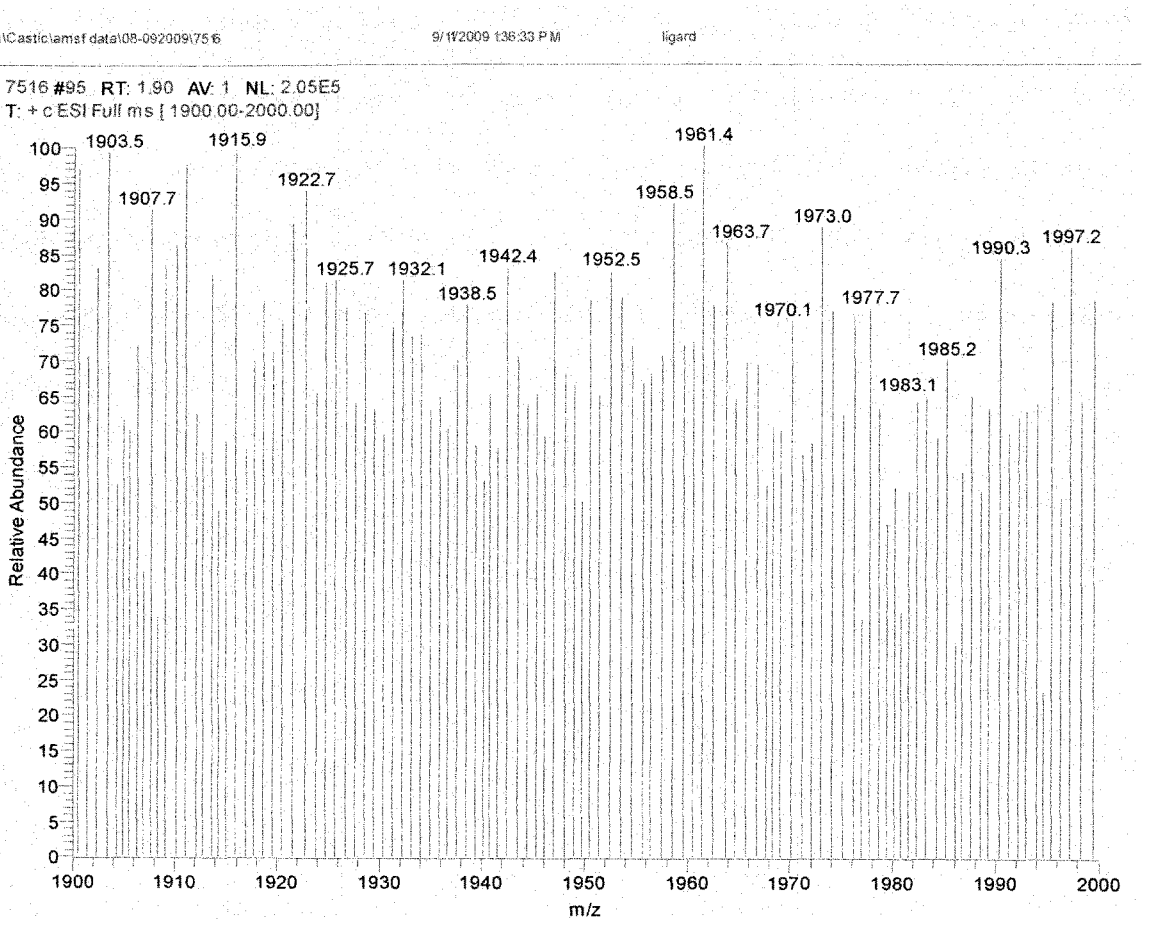

Figure 34. Negative Mass Spectrum of the La (dihed) Complex from 1900-2000 m/z

Figure 35 is the ^{1}H NMR spectrum of the La (dihed) complex in deuterated MeOH. This spectrum was taken using 160 scans in order to improve the signal-to-noise ratio. It is obvious that the spectrum is much different than that of the ligand. What is encouraging is the presence of line broadening since this likely due to the presence of a paramagnetic

metal. The three areas that have broad peaks indicate they are connected to a compound bound to a paramagnetic metal. The fact that some not all peaks are broad, is a good indication that the metal is bonded and not a free species. The sharp peaks with chemical shifts at 1.3, 2, and 2.5 ppm are likely interferences resulting from the synthesis, since these peaks are sharp. The broad peak at 2.6-2.8 ppm can be due to coordinated water. The peaks at 3.3-3.5 ppm and 2.8-5.0 ppm are from the solvent, deuterated methanol, as indicated by the large peak areas (48 for each). The broad peak at 6.2-6.4 ppm may be the hydrogen in the chelate aromatic ring. Lastly, the peaks at 7.7-8.2 ppm may be aryl protons and/or indicate possible residues of the ligand plus two mixed complexes or an unsymmetrical complex.

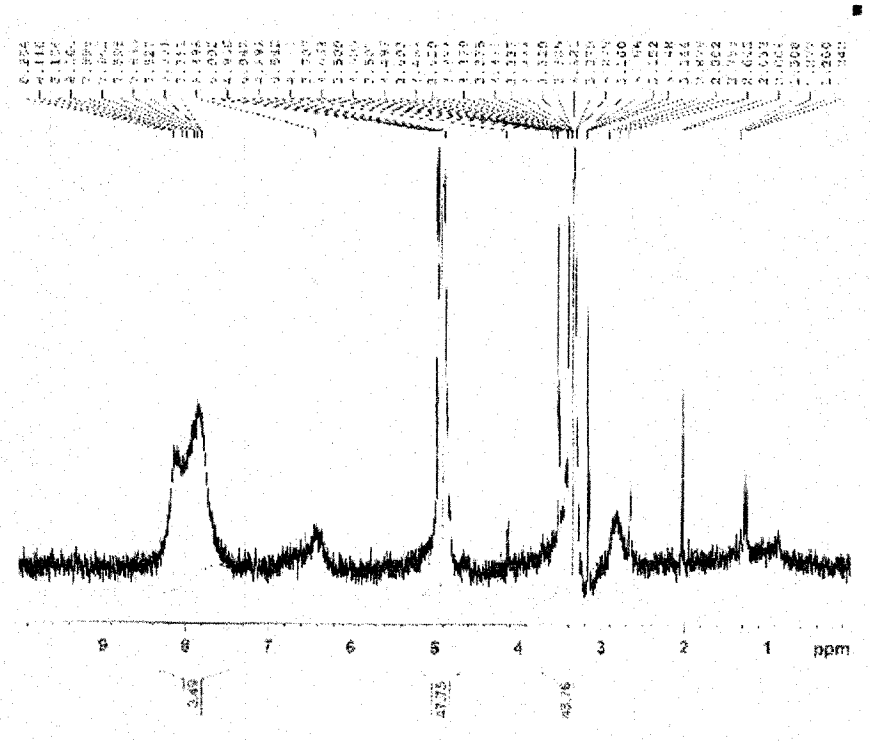

Figure 35. ^{1}H NMR (160 scans) of the La (dihed) Complex

The peaks at 7.7-8.2 ppm warranted further exploration since they could be 2 or 3 unresolved peaks due to the line broadening effect. This was studied by conducting a high temperature (50 °C) ^{1}H NMR experiment since raising the temperature might help better arrange the disordered magnetic moments that causes the line broadening and because there is a known temperature dependence of paramagnetic shifts **[176]**. The intent was to raise the temperature just below the boiling point of methanol, but the instrument only allowed analysis up to 50 °C. The resulting spectrum is shown in figure 36. It is evident that the overall noise was reduced and that there are 2 true peaks at 7.7-8.2 ppm. This means that the third sharp peak in this region was just noise and not indicative of free ligand.

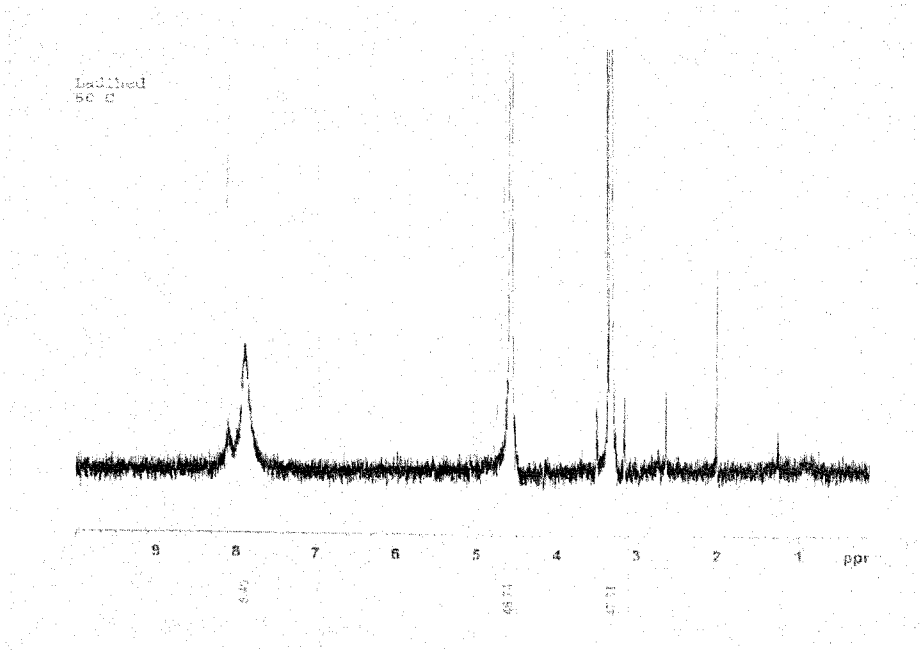

Figure 36. ^{1}H NMR of the La (dihed) Complex at 50 °C

The broad peak at 6.2-6.4 ppm disappeared in the high temperature spectrum and did not return when the room temperature spectrum was taken following the experiment. At this point this behavior is not clear and further supports the idea that ^{1}H NMR, at least one-dimensional ^{1}H NMR is not suitable for the analysis of paramagnetic complexes, other than to indicate the presence of a paramagnetic metal from observed line broadening. Furthermore, lanthanide ß-diketonate complexes are used as shift reagents in NMR because they induce changes in the chemical shifts of protons close to an electronegative substituent with a lone pair **[177]**, like carbonyls and alcohols. This further complicates the analysis since it is not known if the peaks observed are shifted from the accepted chemical shifts in the literature.

The structure of the ligand was confirmed by ^{1}H NMR, DI-MS, FT-IR and other classical methods. Although the molecular weight of the La (dihed) polymer could not be confirmed by DI-MS there were differences in the spectrum such as more peaks at higher mass range and a base peak that differed by 22 a.m.u. with the 553 a.m.u. peak that is likely the fragment [Ligand-H]$^+$. Furthermore, the IR band assignments strongly suggest the structure. In Table 6, the last three band assignments indicate the presence of the six-member chelate ring and coordinated water along with the other band assignments that confirm the presence of the ligand in the complex. Lastly, from the ^{1}H NMR data, the presence of a bonded paramagnetic metal is confirmed. Including the results of the classical methods of structure determination such as melting point, solubilities and differing R_f values, adds confidence that the products were synthesized successfully.

7.1.5.2 La (dihed) SPME Coatings

Following the synthesis of the complex, experiments were conducted to coat the surfaces of activated glass, PDMS (made by the chlorine-terminated PDMS route), and sol-gel PDMS. This was achieved by dipping the substrates in a solution of 236 mg of complex in 50 mL of methanol for 1 hr. The procedure published previously for the coating of SPME fibers called for instantaneous dipping and withdrawal of the fiber into 236 mg of complex dissolved in 1 mL of methanol **[90]**. This extraordinarily large concentration did not seem feasible so the concentration was reduced and the dipping time was extended in order to promote adhesion of the La (dihed) complex to the various surfaces. Despite the dilution the solution was still a bright yellow color. The drying and conditioning procedures for the devices were followed as reported.

Since the low operating temperature of La (dihed) coatings is known **[90]** an experiment was conducted to monitor the effects of temperature on the La (dihed) coated devices by SEM imaging. The various devices were exposed to 10 min of 180, 225, and 300 °C temperatures. The devices withstood the 10 min exposure to 180 °C without any visually apparent defects on the surface. Following exposure to 225 °C for 10 min, there was some yellow powder left on the container meaning the La (dihed) coating, at least partially, was removed from the surface. Lastly, only 10 min of 300 °C caused significant charring of the device, turning it into a brownish color consistent with the results of the melting point determination.

Following the temperature experiments, the samples of the various La (dihed) PSPME devices were prepared and analyzed by SEM. Figure 37 includes the SEM images

obtained for the control, La (dihed) coated on activated glass. It is evident that the superficial features, the spots with holes in the center and the more subtle bubbles that range in size from 2-4 μm are reduced with increasing temperature. The presence of these features may be crucial to the extraction enhancements observed when using La (dihed) over PDMS fibers. Next, figure 38 includes the SEM images for the La (dihed) coated over PDMS. The SEM images reveal a viscous film when the La (dihed) coats the PDMS phase. This is consistent with the "glassy" film reported for the SEM images of the La (dihed) coated over a commercial PDMS fiber **[90]**. Again, it is clear in these images that the features originating from La (dihed) are diminished with increasing temperatures.

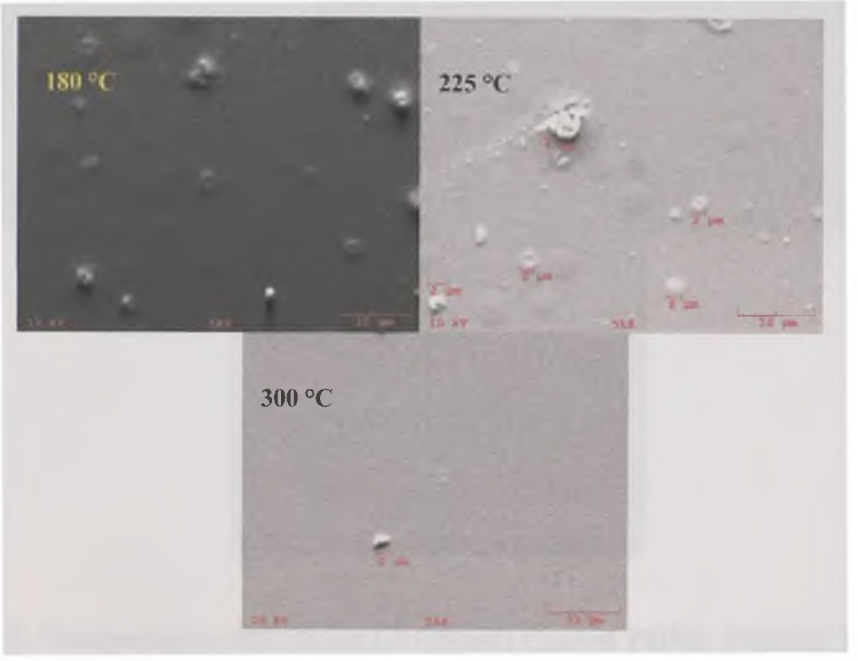

Figure 37. Temperature Effects on Control La (dihed) PSPME Devices

Figure 39 includes the SEM images of the devices that were coated with La (dihed) over a sol-gel PDMS base. The La (dihed) solution coats the sol-gel PDMS particles

efficiently. This is observed when comparing the SEM image of a sol-gel PDMS devices and the La (dihed) coated device. After exposure at 225 °C for 10 min, pores begin to appear in the La (dihed) coated sol-gel PDMS device. This may have implications for greater surface area & trapping by exposing the SG particles underneath the La (dihed) coating. At 300 °C,the La (dihed) was removed completely from the surface leaving behind only the original sol-gel PDMS particles. These results reveal that La (dihed) surface coatings are extremely susceptible to heat. This is an issue for efficient IMS desorption and thus builds a case for enhancing the thermal stability of these coatings.

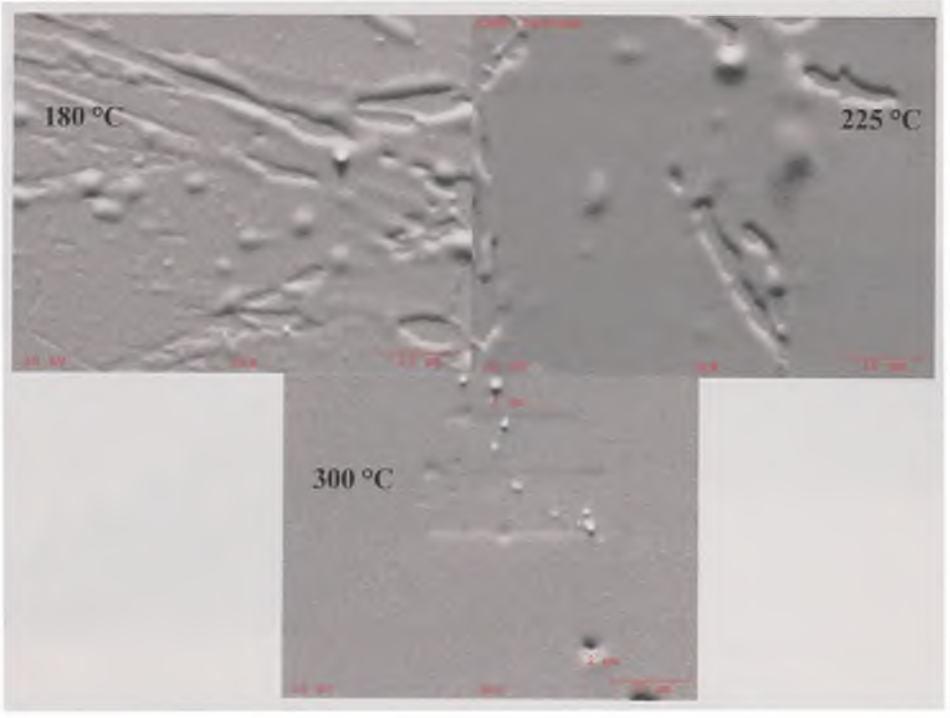

Figure 38. Temperature Effects on La (dihed) Coated PDMS PSPME Devices

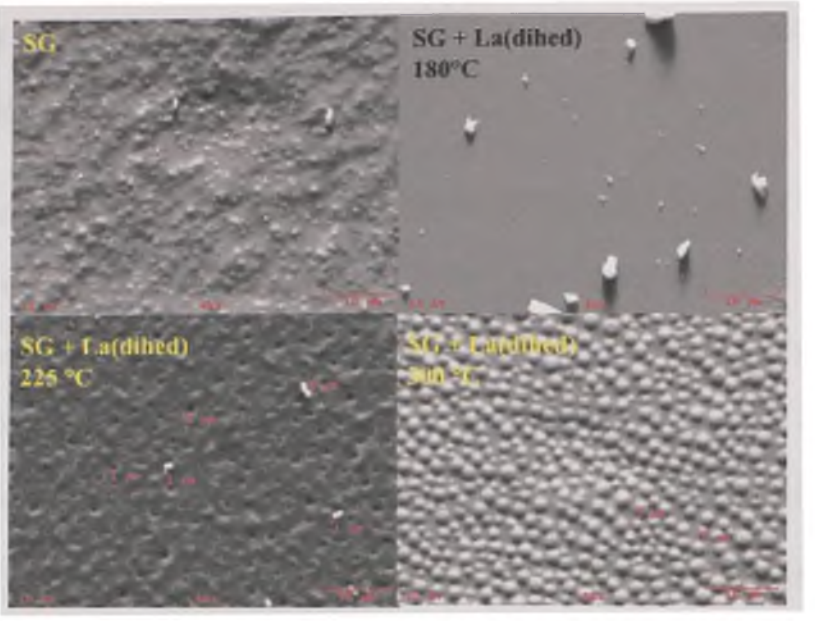

Figure 39. Temperature Effects on La (dihed) Coated Sol-gel PDMS Devices

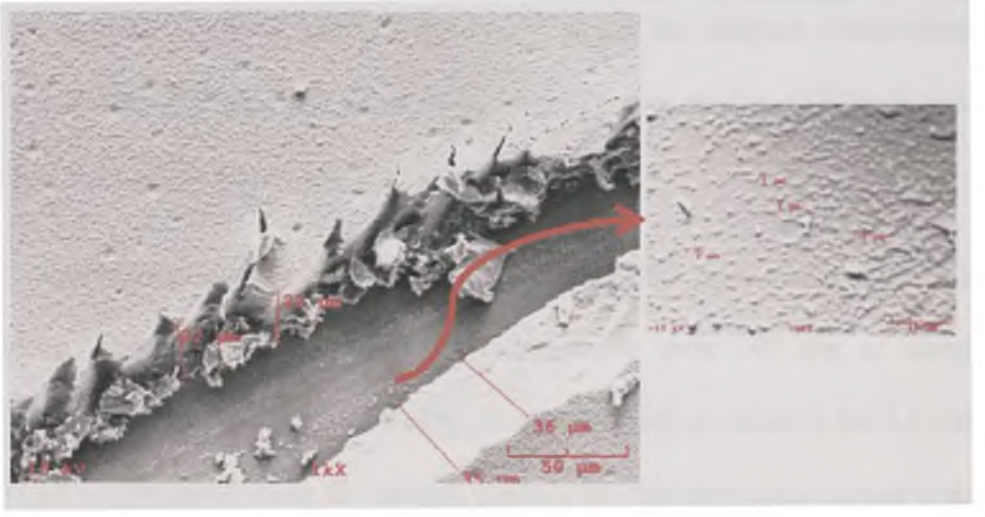

Figure 40. Coating Thickness of La (dihed)

During the SEM imaging experiments, a crack was located on one of the devices (La (dihed) coated over sol-gel PDMS) that was exposed to 10 min at 225 °C. This crack revealed a layer of La (dihed) with an average thickness of 30 µm. Underneath, the sol-

gel coating is evident from the particle presence (see figure 40). This indicates that the coating procedure produces a suitable coating thickness of at least 30 μm.

Given the negative effects of temperature, evident from the SEM analysis and humidity **[90]** on La (dihed) coatings, incorporation of the La (dihed) into a sol-gel network, known to be extremely thermally resistant, was pursued. Since the complex (figure 31) has no available sites such an exposed –OH group with which to bond to a sol-gel active stationary phase, a La (dihed) sol-gel reaction aimed at chemically binding the polymer to the substrate, is not feasible. Instead, it was thought that by introducing a solution of the La (dihed) complex at the appropriate step in the sol-gel PDMS reaction, the La (dihed) component of the phase would be protected from heat and humidity while maintaining its absorptive capabilities. In an ideal planar SPME phase, the analytes would absorb into the sol-gel PDMS coating and be strongly retained due to the additional host-guest interactions the La (dihed) component would afford.

The La (dihed) component in 1 mL of methanol was added prior to catalysis of the sol-gel reaction. There were problems encountered since even 100 mg of complex in methanol was difficult to dissolve. Initially, it was intended to dissolve the La (dihed) in only 100 μl of methanol since the solvent system for this particular sol-gel reaction is DCM. Once the solution was added to the sol-gel components prior to catalysis there were visible particles of un-dissolved La (dihed) powder. The mixture was heated in a water bath at 40 °C to homogenize the solution. The sol-gel reaction was conducted as normal. During the 30 min stay, two phases were observed from the mixture of DCM and methanol. The solution was vortexed and then deposited on the activated substrate. Since

sol-gel has been shown to require dip-coating, it was intended to deposit the sol solution and allow interaction with the surface for some time prior to spin off. Immediately upon deposition though, the solution started to gelate/ cure so within 30 s the solution was spun off using a slower 200 rpm program for 1 min. A control sol-gel device was prepared in the same manner without addition of La (dihed) powder. The devices were cured at lower than normal temperatures as described in Chapter 6. Figure 41 shows pictures of the sol-gel PDMS device (A) and the La (dihed)/ sol-gel PDMS device (B) that were created by this process. Granted, both surfaces hardly look uniform but these were not coated under optimal conditions of dip-coating. This was not done since dip coating would have required a much greater mass of La (dihed) powder than was available for testing and development purposes. What is encouraging is that the coating of the La (dihed) even seems more uniform than that of the sol-gel PDMS that experienced significant coating shrinkage and cracking. There is build up of coating solution evident on the four corners of the substrate meaning if spin-coating were continued to be used, a much faster spin speed would be necessary to reduce this effect.

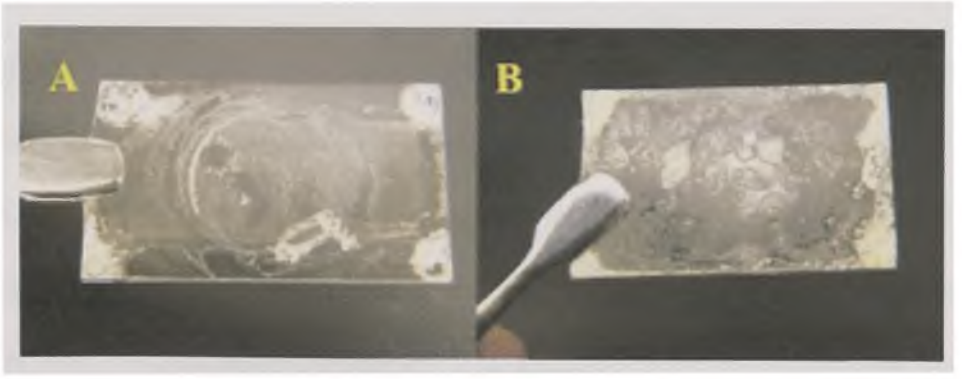

Figure 41. Images of the Sol-gel PDMS PSPME Device (A) and La (dihed)/ PDMS PSPME Device (B). Spin coating: 200 rpm for 1 min.

The next step was to determine if these devices, although not uniformly coated, were suitable for subsequent extractions. The devices were desorbed into the Ionscan IMS and the background produced was analyzed. Figure 42 shows the IMS plasmagram of the blank La (dihed)/ sol-gel PDMS device.

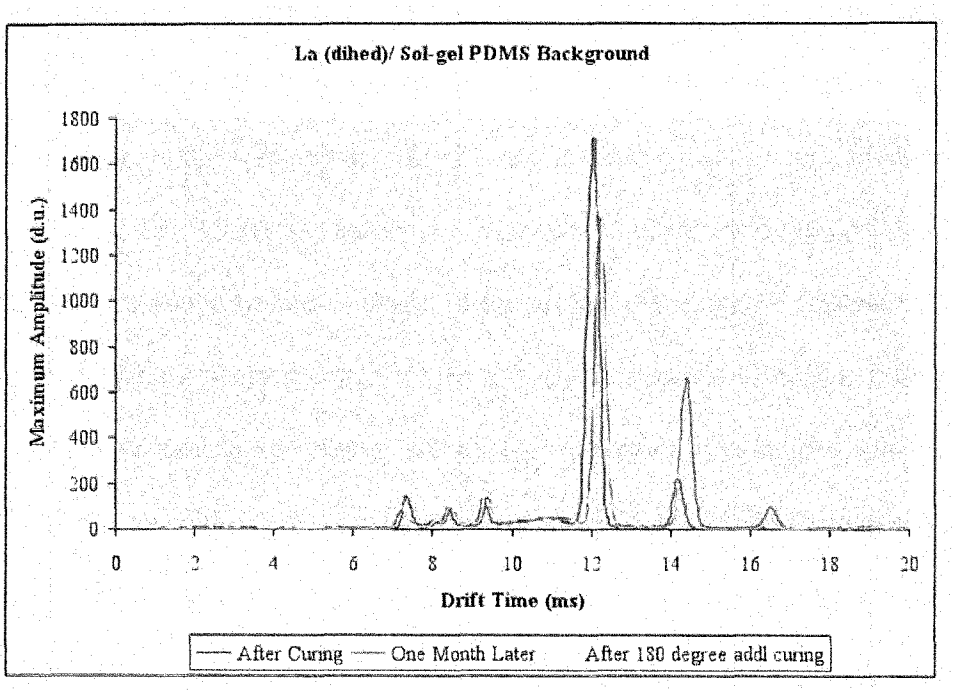

Figure 42. Plasmagrams of the Blank La (dihed)/ Sol-gel PDMS PSPME Device

The large peak at 12 ms is problematic since it interferes with the position of the 2,4-DNT peak and depletes the pool of reactant ions available for the formation of product ions. The peak at 12 ms is often seen when the substrate was not washed sufficiently well with deionized water in the surface activation stages although this is not likely in this particular case. It could also be attributed to trapped solvent or many other factors during the coating process. The device may not have been properly cured since the conditioning program was 150 °C for only 2 hr, followed by room temperature curing for 48 hr.

Further curing was done about after 1 month of the device being in the dessicator since a reanalysis of the background still showed the peak as in figure 43. The device was then heated for another 2 hr at 150 °C and no La (dihed) powder was observed on the vial containing the device meaning that temperature for that time did not affect the integrity of the coating. The IMS background still showed these peaks without any reduction in intensity. The next steps were heating at 180 °C for 2 hr, which left then corners of the device a brownish tinge. Reanalysis still showed the same background. Heating for an additional 6 hrs at 150 °C did not reduce the background either. It is thought that because the La (dihed) was added before catalysis of the sol-gel reaction, the solvent filled pores that were created were likely blocked by the presence of the La (dihed) and this did not allow the solvent to be released during drying. This is further complicated since methanol was used and has a relatively higher boiling point than DCM. Further experimentation is suggested that involves optimizing a sol-gel reaction with ethyl acetate as the solvent system, then adding the La (dihed) after the TFA has been added into the mixture. Despite these seemingly negative results, the positive outcomes are that prolonged curing at 150 °C does not seem to affect the integrity of the coating. Furthermore, the peak at 12 ms can be removed through diligent coating method optimization, as has been done before. This of course does mean additional La (dihed) must be synthesized. Lastly, a recent publication has detailed the impregnation of La (dihed) into glass filter for use with IMS **[118]**. This product produced a large, unidentified peak (above 1000 d.u. for just one scan) at 16 ms. These workers made no attempt to increase the thermal stability and decrease the hygroscopicity of the La (dihed) as this research has attempted to do.

7.1.6 Summary of PSPME Devices Developed

In summary, the PSPME devices that were developed successfully were: PDMS (via a chlorine-terminated route), sol-gel PDMS, and the activated glass, PDMS, and sol-gel PDMS coated with La (dihed). The explosives standards were also considered a success although they were not intended for extractions. The activated charcoal substitute for carboxen was considered a success in terms of incorporating the activated charcoal into the sol-gel PDMS and Sylgard 184 PDMS polymers, but did not enhance the detection outcomes for the model compound TNT. Lastly, incorporation of La (dihed) into a sol-gel network warrants continued efforts since it has implications for improving the stability of such as successful absorbent in the extraction of 2,4-DNT and TNT, two compounds of great interest for security applications.

7.2 Validation Experiments for Static PSPME

The following are results and discussion of the experiments that were conducted to test the capabilities of PSPME-IMS for the enhanced extraction of volatile chemical signatures and detection as compared to fiber SPME-IMS.

7.2.1 Performance Comparison of the SPME Fiber, PDMS, and Sol-gel PDMS PSPME Devices Using TNT as the Target Analyte

7.2.1.1 Quantitation of TNT Using Response Curves

Response curves of TNT for each IMS instrument were generated and the equations of the linear regression lines for the Ionscan 400B (equation 11) and the Itemiser 2 (equation 12) are shown below:

$$y = 1769.9x + 390.29, r^2 = 0.9678$$ **(Equation 11)**

$$y = 1131.2x + 2517.5, r^2 = 0.9944$$ **(Equation 12)**

From the equation for the best-fit line, the amount extracted by each SPME device can be calculated in the nanogram range.

7.2.1.2 Determination of Equilibrium Extraction Time and Recovery

Since SPME is an equilibrium technique, experiments were conducted to determine the minimum sampling time required to obtain the highest IMS signal for each SPME device. A 10 μL spike of a 240 μg mL^{-1} solution of TNT was introduced into a quart-sized can and sampled for different time intervals by each SPME device and subsequently desorbed into the IonScan 400B IMS (for the planar geometry) or the Itemiser 2 IMS (for the fiber geometry) to determine the equilibrium time. All sampling time increments were repeated in triplicate, each with fresh spikes into new quart cans each time. The resulting equilibrium curves are shown in figure 43. In figure 43A, it is evident that equilibrium is reached at about two hr for the sol-gel PDMS PSPME device. The equilibrium time for the PDMS PSPME device was reached by 40 min (figure 43B). The PSPME devices both performed better than the fiber PDMS SPME, which required over 10 hr of sampling time to reach equilibrium as shown in figure 43C. Since 10 hr of sampling is not practical and in order to compare the three types of SPME devices for extraction efficiency and speed of analysis, the sampling time for the PDMS fiber was thus conservatively set at 3 hr. The speed with which the planar PDMS reached equilibrium with the sample when compared to sol-gel PDMS PSPME can be due to the difference in coating thickness and

the sol-gel network. Sol-gel PDMS and PDMS PSPME devices reached equilibrium with TNT in the headspace faster than the fiber because of the increased surface area of the planar geometry. Longer sampling times are better suited for sampling cargo containers during transport. For applications that require short sampling times, it is important to note that sufficient sampling can be achieved at pre-equilibrium conditions and still obtain an appreciable signal by IMS. For the minimum sampling times in figures 43A and 43B for the sol-gel PDMS and PDMS PSPME devices respectively, the signals for TNT obtained are above the detection limits when solving for equation 11. Additionally, when comparing the results displayed in figures 43A and 43B, PDMS PSPME is more efficient than sol-gel PDMS PSPME at extracting in shorter times, yet for sol-gel PDMS PSPME, the signal is greater (13,000 d.u. versus 8,000 d.u. at their respective equilibrium times) under the same experimental conditions. As such, PDMS PSPME would be more useful for applications that require higher throughput while the sol-gel PDMS PSPME device is recommended for applications that can accommodate longer sampling times.

Table 7 shows the instrumental detection for TNT if introduced into the IMS instruments following a liquid spike with a known concentration. The Ionscan 400B instrument can detect 30 pg and the Itemiser 2 can detect 1 ng, which is consistent with the manufacturer specifications. The amount required for instrumental detection is much higher for the Itemiser 2 because the desorber is a heated slot that is open to the surroundings when compared to the desorber in the Ionscan 400B sample desorber, which is an enclosed heated port resulting in more efficient transfer. Table 7 also shows the minimum amounts of TNT that can be spiked in a quart can (with the associated uncertainty), sampled at

equilibrium, and detected by each IMS instrument used in this study. These values are recoveries calculated from the appropriate response curve equations (11 and 12).

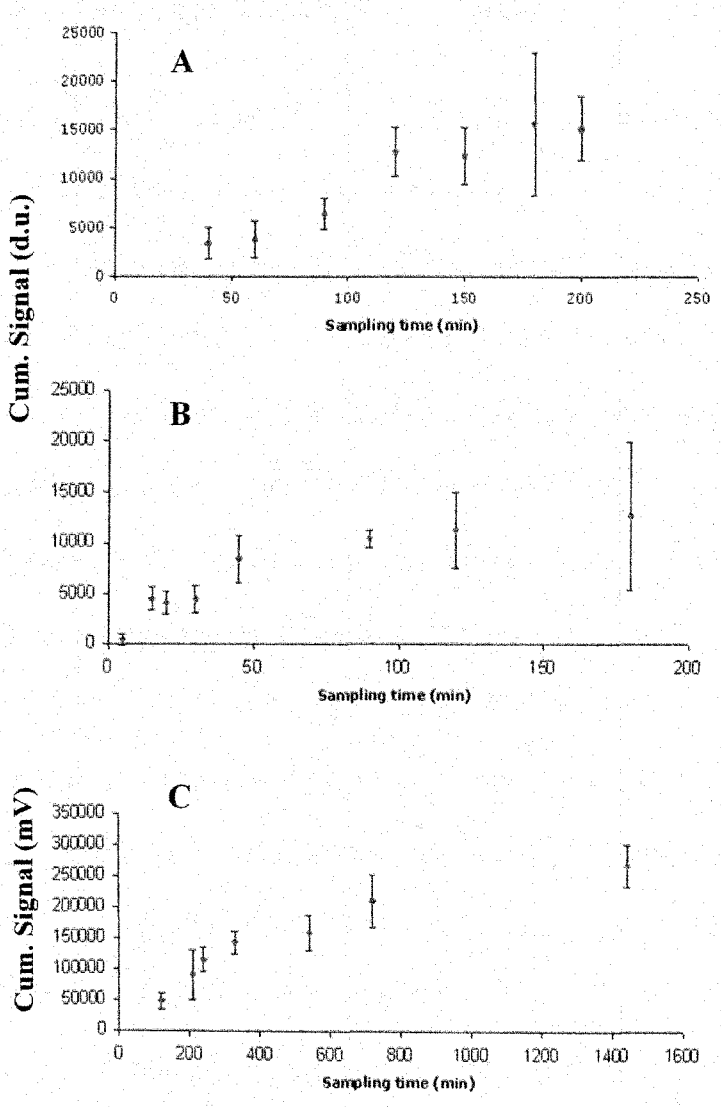

Figure 43. Equilibrium Extraction Time Curves for A) Sol-gel PDMS PSPME B) PDMS PSPME and C) PDMS SPME fiber [168]

For those samples that contain mass loadings that are close to the instrumental limit of detection, a large uncertainty in the amount of mass recovered is expected. The sol-gel PDMS PSPME has a higher calculated recovery of TNT for both instruments than the PDMS PSPME with respect to the amount initially spiked.

Since a SPME-IMS interface is available for the Itemiser 2 instrument, the minimum amount of sample that must be spiked in a quart can in order to be detected is 25 ng. Table 7 shows that both the fiber geometry SPME and the PDMS PSPME require a 25 ng TNT spike in a can, yet an alert for TNT from the Itemiser 2 instrument was obtained following the headspace extraction of only a 10 ng TNT spike in a quart can using the planar PDMS SPME. Since the signal obtained was less than the y-intercept in the equation from the Itemiser 2 response curve for the PDMS PSPME (equation 12), an actual recovery could not be calculated for the spiked amount. For this same reason, in order for the recovery of TNT by the sol-gel PDMS PSPME device using the Ionscan 400B to be reported, a spike greater than 2 ng in a can is required. Despite this, the instrument still reports an alert for an extraction of a 2 ng spike. Interestingly, when the same low mass (25 ng) of TNT is spiked into the quart cans for sampling with both fiber and the planar PDMS for comparison, the recovery by the planar PDMS is enhanced by almost a factor of 10 over the SPME fiber. In fact, both planar SPME devices afford the user greater recoveries than fiber SPME-IMS (a consequence of the improved extraction efficiency), an improvement since the advent of SPME-IMS, a technique that has itself greatly improved the detection limits as compared to particle analysis **[19]**.

Table 7. Recovery of TNT Calculated from Response Curves [168]

	Ionscan 400B		Itemiser 2	
Sample Introduction Method	Amount spiked	Calculated Recovery from Response Curve	Amount spiked	Calculated Recovery from Response Curve
Liquid spike on paper	30 pg	alert	1 ng	alert
Planar sol-gel PDMS	5 ng	0.34±0.14 ng*	8 ng	2.21±1.5 ng
Planar PDMS	8 ng	0.18±0.17 ng	25 ng	2.54±2.0 ng†
Fiber SPME	N/A‡	N/A‡	25 ng	0.32±0.80 ng

*alarms with as low as a 2 ng spike
†alarms with as low as a 10 ng spike
‡there is no SPME-IMS interface for the Ionscan 400B

7.2.1.3 Extraction Efficiency Experiments at Equilibrium

A comparison of the extraction efficiency of all three SPME devices at their respective equilibrium times, with detection by the Itemiser 2 instrument, was conducted and the results are shown in figure 44. The x-axis displays the different amounts of TNT spiked into a quart can for each extraction and the y-axis shows the amount detected by the IMS after desorption of the particular SPME device. The range of mass of TNT spiked was between 25 and 500 ng. In all cases, the planar sol-gel PDMS extracted more mass of the initially spiked sample. This can be due to the greater coating thickness and the porous sol-gel network. The PDMS PSPME-IMS response for TNT was greater than the PDMS SPME fiber response except at the 25 ng spike. This can be attributed to the closed nature of the sample introduction for the SPME-IMS interface as compared to the Itemiser 2 desorber that is used for the PSPME devices which is open and can lead to some loss. The PDMS PSPME device is 1.3 times more efficient than the PDMS SPME fiber and the sol-gel PDMS PSPME device is 3.8 times more efficient than the PDMS fiber when

just averaging the extraction efficiencies of each respective planar SPME device over the fiber PDMS SPME for the small masses of TNT (25 ng-500 ng) spiked in the cans. There is an obvious trend for increasing extraction efficiencies for both planar devices over the fiber geometry when more mass is available for sampling. That is a result of the 50 to 100 times surface area increase and the at least 16 times capacity increase of the planar geometry over the fiber geometry. Thus, when sampling in real case scenarios where much more mass is available in the headspace, the improvements over fiber SPME are expected to be even more significant.

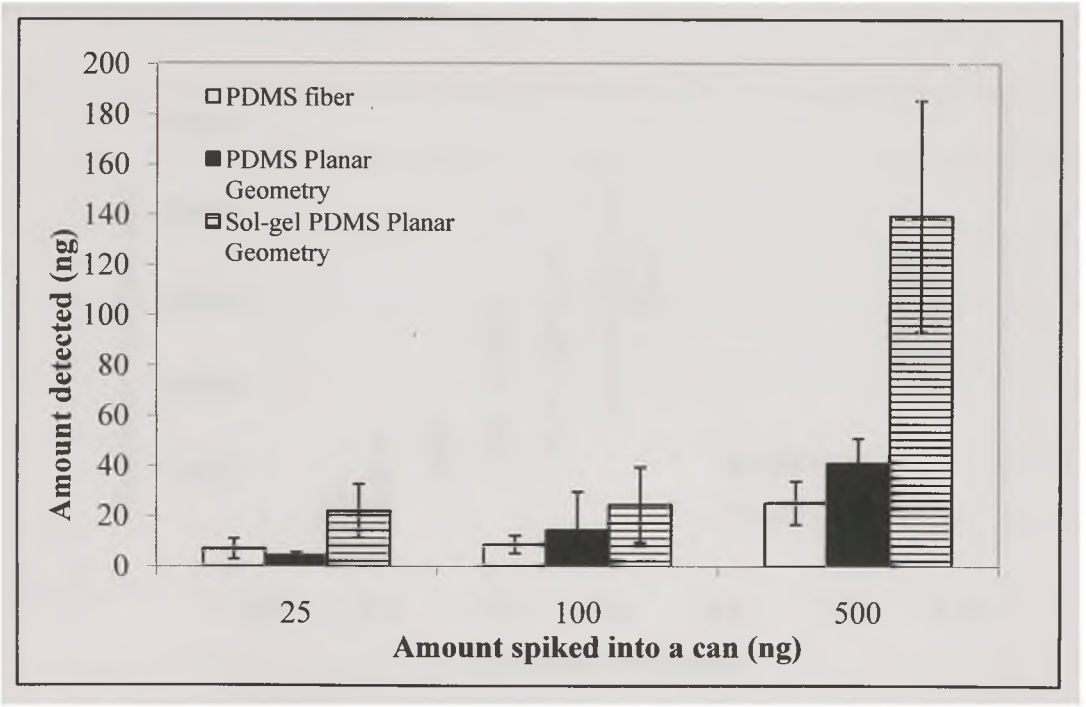

Figure 44. Extraction Efficiencies of the Three SPME Devices Tested for TNT [168]

7.2.1.4 Study of TNT Adsorption to Vessel Walls

Since the TNT used in the previous studies was spiked directly to the metal cans, both quart and gallon-sized cans were studied to test the effects of possible TNT adsorption to

the surface of the sampling vessels used in these studies. If there were appreciable adsorption to the walls the effects would be noticeable from the results of extractions from the gallon can because of its higher surface area compared to the quart can. According to SPME theory, once equilibrium conditions are reached, the mass extracted by a SPME device would be the same regardless of the sample vessel volume. In figure 45, the results of these tests are shown. Although the vessel with smaller volume, the quart can, does reach equilibrium faster than the gallon can, the signals obtained at equilibrium, 2 hr versus 3 hr, are not significantly different. This means that adsorption of TNT to the sample walls is negligible.

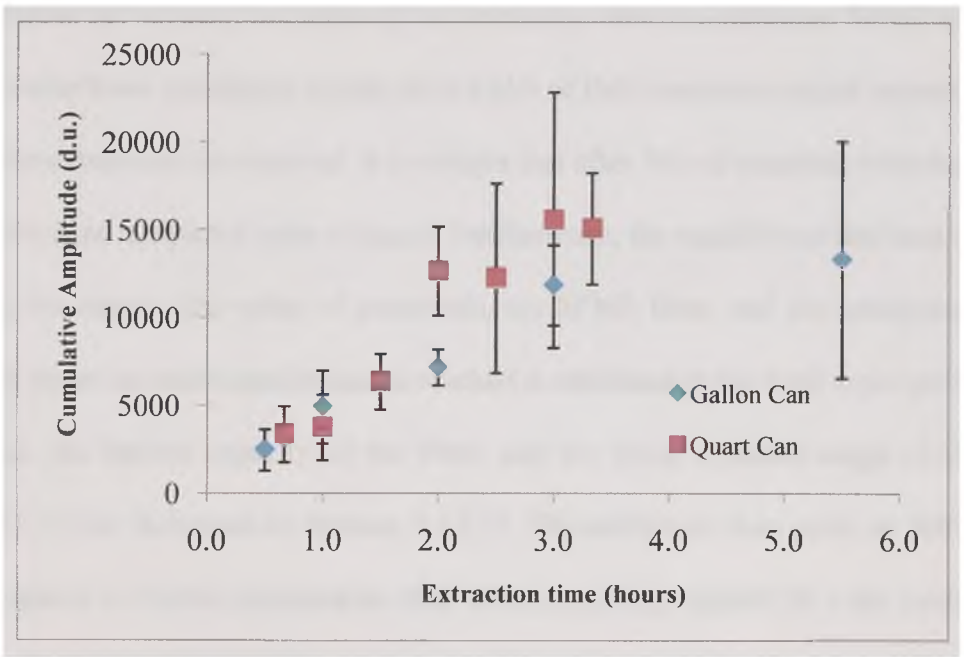

Figure 45. Effects of Adsorption of TNT to Vessel Walls. Conditions: 2.4 µg TNT spike into the cans, extraction with sol-gel PDMS PSPME at room temperature until equilibrium is reached.

7.2.2 Comparison of Sol-Gel PDMS PSPME and Fiber SPME for Sampling Piperonal

The following are results and discussion of experiments that were conducted on the volatile chemical signature of MDMA, piperonal, in order to determine and compare the extraction capabilities of both the fiber and planar SPME devices. The results of the method development for the field sampling and detection of actual MDMA drug cases by PSPME-IMS are also discussed.

7.2.2.1 SPME-IMS Sampling

A vial containing a saturated headspace of piperonal was sampled in a static configuration for various time intervals to determine what the minimum SPME sampling time is under these conditions. Figure 46 is a plot of IMS maximum signal intensity (mV) versus the extraction time interval. It is evident that after 30 s of sampling with the SPME fiber there is no additional gain of signal. Furthermore, the equilibrium has been reached between the sample (the spike of piperonal), the SPME fiber, and the headspace in the vial. The speed at which equilibrium is reached is attributed to the high vapor pressure of piperonal, the limited capacity of the fiber, and the linear dynamic range of the IMS detector (further discussed in Section 7.2.2.3). The additional data point at 300 s, or 5 min, is added to further demonstrate that when sampling beyond 30 s the analyst still obtains the maximal signal. Since the sampling occurs in a tightly sealed system this also shows that no analyte is lost even when sampling for extended periods of time, or in other words, the equilibrium extraction time stays the same. It is advantageous that only 30 s of sampling is necessary for this compound and we show by the coupling of SPME to bench-top IMS (7 s analysis time), that this method is promising for field applications

much like canine detection in terms of total sampling and analysis time, although it is important to reiterate the sampling mode differs between canines and SPME; canines sample the air dynamically while SPME, in this setup was done statically in a sealed vial.

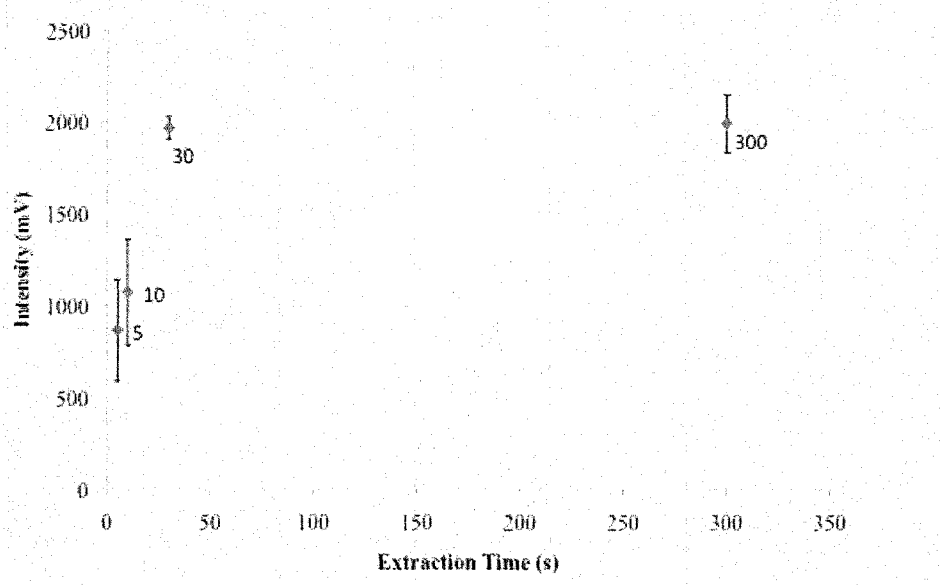

Figure 46. Piperonal Extraction Time Curve [50]

The time necessary for piperonal to reach equilibrium, meaning a saturated headspace, within the vial under these closed and static experimental conditions, was determined by sampling at various time increments (10 s, 60 s, 480 s, and 1260 s), for the equilibrium extraction time which was determined to be 30 s. The time for equilibrium in the vial to be established was determined to be essentially instantaneous (figure 28). This is not surprising considering the volatility of piperonal. Piperonal has a high vapor pressure of 1.0 mmHg at 87 °C. To ensure this equilibrium remained constant, results for long time increments (21 min) in relation to the time necessary to reach equilibrium were recorded (figure 47).

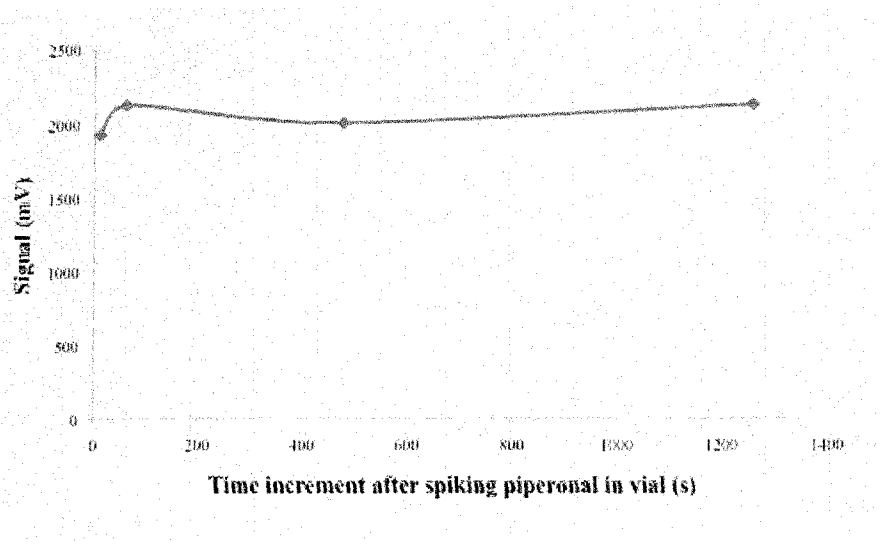

Figure 47. Equilibrium Time Curve for Piperonal

7.2.2.2 SPME-IMS Quantitation

In order to quantitate the mass loading of piperonal on the PDMS fiber, the same static sampling conducted for subsequent analysis by SPME-IMS is also done for analysis by SPME-GC-MS. First a calibration curve was generated, by introducing increasing concentrations of piperonal by liquid injection into the GC/MS then plotting the peak area (counts) versus the mass of piperonal (ng) introduced after taking into account the appropriate split.

The equation of the best-fit line produced (equation 13), is used for determining the mass corresponding to a peak area obtained following any other GC-MS analysis conducted including SPME-GC-MS.

$$y=285450x - 34811,\ r^2=0.9911 \quad \textbf{(Equation 13)}$$

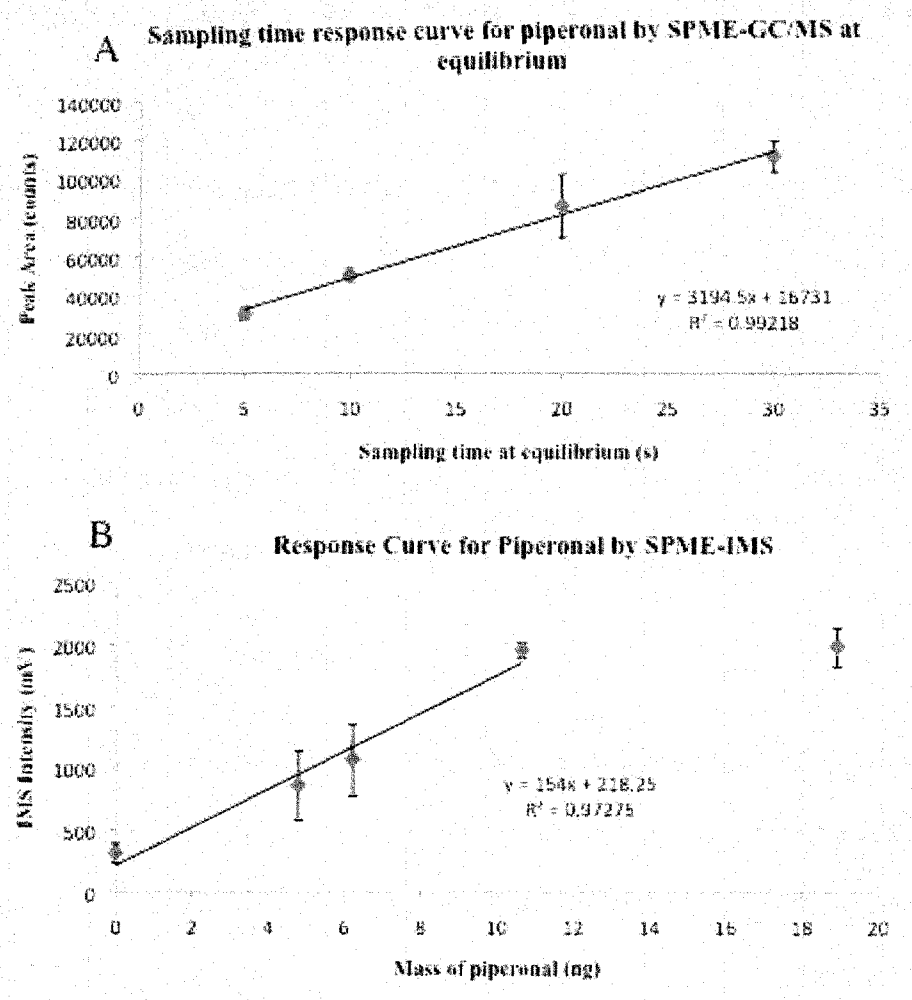

Figure 48. A) GC-MS Response Used for B) SPME-IMS Quantitation [50]

Figure 48A is a plot showing the response by SPME-GC/MS for piperonal at each respective sampling time with equilibrium conditions in the vial. This information is used to calculate and plot the mass introduced into the IMS by the same sampling scheme (Figure 48B).

7.2.2.3 SPME-IMS Limit of Detection (LOD) and Linear Dynamic Range (LDR) Determinations

The method LOD was determined as the minimum amount of piperonal that produces a signal at least the average of the blank plus three times its standard deviation. This resulted in 2.1 ng of piperonal as the SPME-IMS LOD. The line of best fit in Figure 48B relates to the LDR of IMS for piperonal, determined to be 2.1- 11 ng since this is the largest range of points on the response curve (Figure 48B) where a linear correlation, r^2=0.9727, exists between mass of piperonal and SPME-IMS response.

7.2.2.4 Piperonal IMS Response Curve

Quantification of piperonal detected by IMS following absorption on each device matrix, SPME fibers and PSPME, was enabled by the use of response curves obtained by adding freshly prepared standard solutions onto manufacturer provided filters followed by IMS analysis. In this study two separate complementary response curves, each for a different product ion, monomer and dimer, served for quantitation of the detected piperonal under the same IMS operating conditions. As the vapor concentration of the analyte increases in the IMS ion source, a protonated monomer product ion first appears, with a corresponding loss in the reactant ion intensity. With further increase in the analyte concentration, a second product ion (protonated dimer) appears through a stepwise clustering phenomenon at the expense of both the reactant ions and the monomer product ions **[17]**.

The monomer response curve (Figure 49A) exhibited linear regression in the range of 2-20 ng for piperonal with a limit of detection (LOD) of 2 ng mainly due to high background level. In positive mode and in low temperature IMS operation, the ionization of gaseous molecules is facilitated. The precision of the monomer analysis method varied from 50% for close to the LOD concentrations to 2% for the highest concentration in this dynamic range.

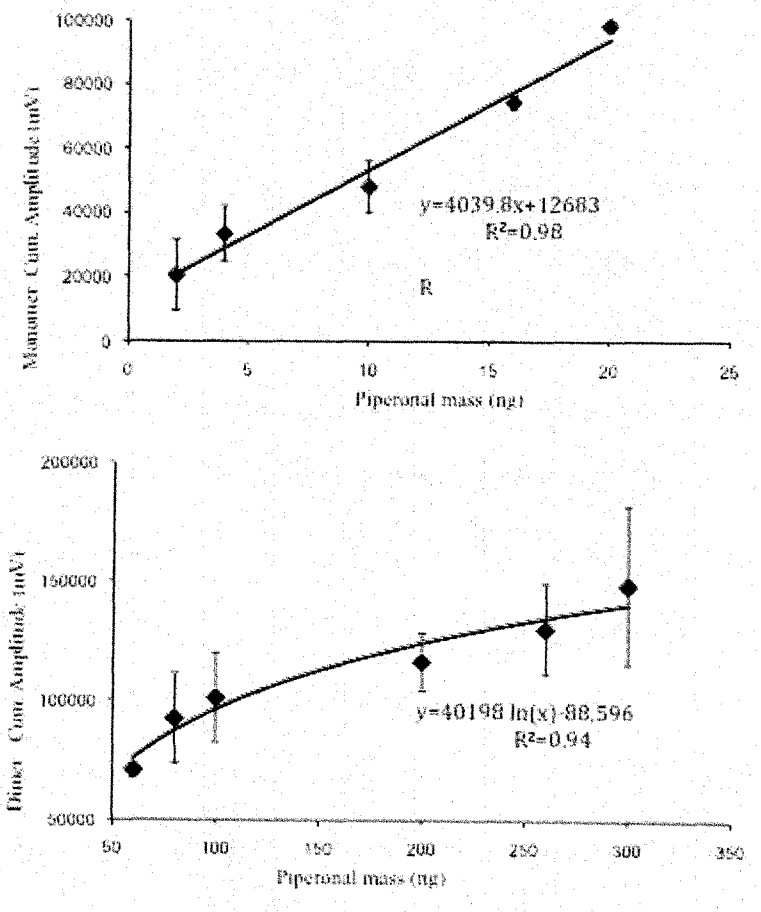

Figure 49. IMS Response Curves for the Piperonal A) Monomer and B) Dimer Product Ions [178]

The response curve for the dimer product ions was also determined for use in the quantification of the total detected piperonal amounts emitted from the MDMA tablets. The response curve obtained for the dimer exhibited a logarithmic regression curve in the range of 60-300 ng for piperonal (Figure 49B). The intensity response is expressed in logarithmic format and was previously demonstrated by Eiceman et al. for better categorization of different molecule classes, mainly at low temperature drift tube analyses **[179]**.

7.2.2.5 Method Development for PSPME-IMS of Piperonal

Both devices, PSPME and SPME fiber, were introduced into gallon-sized cans, spiked with 100 µL of a high concentration piperonal solution, 1000 µg ml^{-1} (100 µg piperonal), for a 10 min extraction time, and analyzed immediately by IMS. The plasmagrams shown in Figure 50 demonstrate the results obtained from headspace sampling using both devices. The ion peak for piperonal is found at a drift time of 8.3 ms and the reduced mobility valueof the product ion is K_0=1.51 $cm^2V^{-1}s^{-1}$ **[156]**. A significantly higher cumulative intensity is observed for all the scans of the piperonal peak as well as for the highest signal peak when sampling the headspace using PSPME in comparison to the SPME fiber. At higher concentrations, the observed decrease in peak intensity for the monomer shown for PSPME corresponds with the formation of a proton-bound dimer ion. Both the higher monomer response as well as the formation of a dimer measured by the PSPME device confirms the higher piperonal extraction efficiency over the SPME fiber.

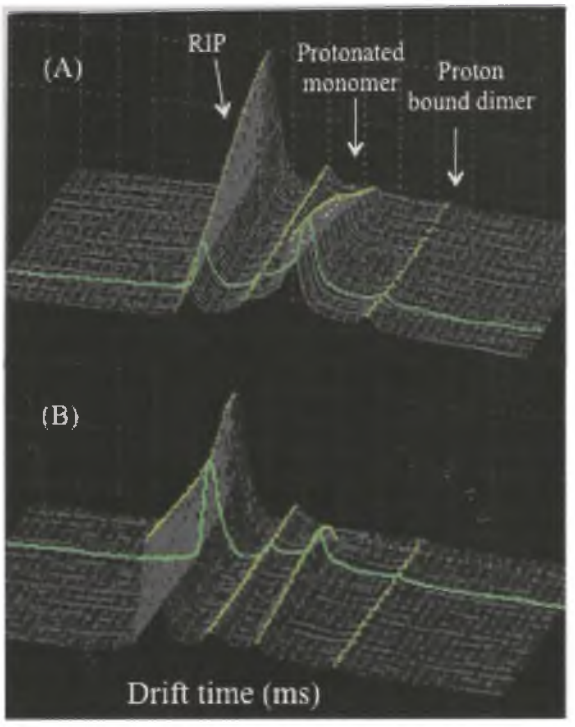

Figure 50. Piperonal Detected Following Extraction with A) the PSPME Device and B) the SPME Fiber [178]

Ideally, spiking a known mass of analyte dissolved in a volatile solvent inside a closed container can produce a headspace with the maximum concentration being the mass of the spiked compound divided by volume of the headspace but in practice, lower concentrations should be expected. Uncontrolled processes of unspecific adsorption/absorption to surfaces are expected to decrease the available amount of the spike. The experimental parameters can influence the distribution coefficient of the analyte fraction absorbed or remaining in the vapor. Sampling of the headspace created by spiking standard mixtures (including a solvent) with SPME likely resulted in solvent molecules adsorbing/absorbing into the fiber. The volatility of thetarget compound and solvent, the sampling time and/or the sampling temperature may also result in some

displacement of the target compounds by solvent molecules thus decreasing the extraction efficiency of a specific target analyte. When considering the capacity of the specific SPME device, greater solvent effects are encountered when sampling with the fiber compared to the PSPME device. In the case of sampling MDMA tablets from an actual case with the PSPME device, solvent effects can be minimized when compared to sampling dilute standard solutions of piperonal, but may be replaced by other overwhelming volatile components emitted from the MDMA tablets depending on manufacturing procedures for the illicit drug.

The mass detected by IMS versus extraction time was tested and evaluated by sampling lower concentrations of piperonal, 100 μL of a 100 μg mL^{-1} solution (10 μg piperonal), using both devices. The devices were allowed to sample the vapors for different extraction times immediately following the spike of piperonal into the can that ranged from 3 to 10 min. The results obtained are demonstrated in Figure 51 and represent the equilibrium curve for piperonal. Overall, a consistent increase in the intensity response was measured with both devices along the complete time range tested for extraction. The increasing trend in responses with time can be explained either by built-up vapor concentration inside the cans and/or gradual vapor absorption onto the devices. However, at all times tested, the PSPME device resulted in higher cumulative response intensity in comparison to the SPME fibers. Using the experimental conditions described above, in the shortest extraction time (3-4 min), the detection of piperonal was only achieved when the PSPME device was used. Identical measurements with a SPME fiber yielded no response, indicating lower extraction capability of the SPME fiber. The signal measured

on PSPME at extraction times longer than 10 min was outside the linear dynamic range for the monomer product ion. The decrease in the response peak at 12 min extraction time was accompanied by the formation of the dimer product ion peak. The increase in the response intensity using both devices showed similar slope at the extraction time range of4 min to 10 min. These results suggest similar profile absorption kinetics on both devices under these experimental conditions. The overall amounts of piperonal detected were very low with maximum recovery of 0.3% of the original mass spiked for a 10 min PSPME extraction. Considering an equilibrium process with SPME and the volatility of piperonal, this outcome is not surprising and could be attributed also to one or more of the following: (a) high affinity of the piperonal molecules to the PSPME coating followed by an inefficient desorption stage at the IMS inlet (b) displacement of the piperonal molecules from the coating by solvent molecules (c) non-specific adsorption of piperonal onto the container surface; (d) preference of piperonal molecules to remain in the headspace rather than partition into the coating or in other words, piperonal may have a small K_{fh} (partition coefficient between the SPME phase and the headspace phase) in this experimental setup. In regards to assumption (a), it has been experienced that piperonal samples extracted by the PSPME device produce a signal even at the second thermal desorption, although smaller than the first, while the piperonal on the fiber is completely desorbed after the first introduction into the IMS inlet. This is attributed to the higher mass loadings on the PSPME device as compared to the fiber SPME. The amounts of piperonal detected for the second desorption are not demonstrated in Figure 51 since the evaluation of PSPME device as a PSPME-IMS coupled method was planned

to follow the recommended operating procedure of the instrument with one desorption only.

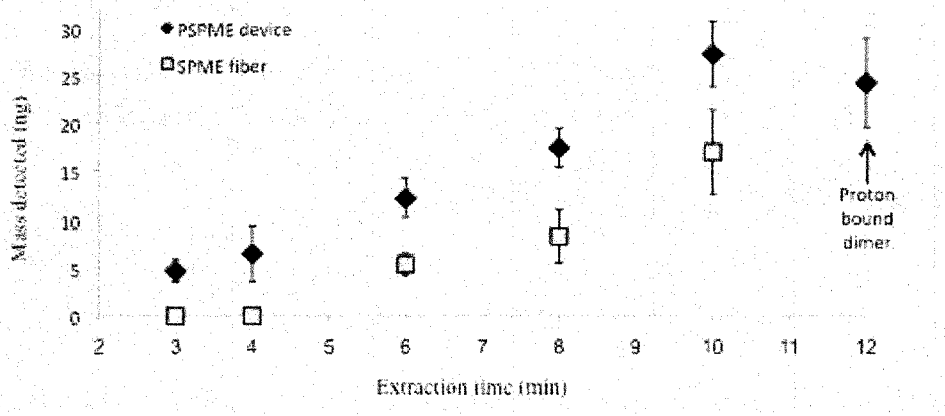

Figure 51. Equilibrium Extraction Curves for Piperonal by the PSPME Device and the SPME Fiber [178]

Table 8 lists the mass detected by IMS after extraction using both devices when sampling very low concentrations of piperonal close to IMS detection limits. A volume of 100 µL of 50 µg mL^{-1} and 20 µg mL^{-1} of piperonal solution (5 µg and 2 µg piperonal) were spiked into gallon-sized cans for 6 min of extraction time. Under these conditions, no piperonal alert could be achieved using the SPME fibers for sampling for either concentration tested. In contrast, using PSPME devices recorded positive piperonal alerts for all measurements. An average amount of 4 ng piperonal was detected following absorption onto the PSPME phase in a 6 min extraction for a 5 µg spike of the compound of interest. The absorbed average amount (n=3) was found to be twice the amount of the method LOD's. This result is also correlated to the absorbed average amount, 4.7 ng, measured for 10 µg piperonal in a 3 min extraction, as presented in Figure 51. Similar

average amounts measured in both experiments demonstrates that the equilibrium concentration had been reached in less than 3 min, leaving the extraction time as the dominant parameter for increased recovery.

Table 8. Extraction Efficiencies Measured by PSPME Device and SPME Fiber Inside Gallon-Sized Cans Containing 2 µg and 5 µg of Piperonal [178]

	PSPME device		SPME fiber	
Mass of piperonal spiked (µg)	2	5	2	5
Mass of piperonal detected (ng)	1.5±1.1	4±0.4	ND*	ND*

*ND- Not Detectable

The amount detected under the same conditions, following absorption from a 2 µg spike of piperonal, was slightly below the LOD analysis method. Extrapolated quantification at this concentration range yielded an average sampled amount of only 1.5 ng piperonal on the PSPME phase. Nevertheless, this amount generated a signal significantly greater than the PSPME blank samples, mainly the result of lower background levels attained for the PSPME device than for IMS filters which were used for piperonal response curves. The repeatability between the 3 replicate experiments was found to be low as expected in correlation with the measured deviation determined for the LOD concentration of the IMS analysis method.

Theoretically, from the complete evaporation of a spike without any kind of unspecific adsorption processes, the maximum piperonal concentration inside of a gallon-volume container can be calculated. Practically, the vapor concentration is expected to be much lower. Applying this conservative calculation, the LOD's for PSPME-IMS and SPME-IMS could both be estimated from the minimal theoretical concentration, which was

possible to be measured by each device. A calculated LOD of 2.5 μg L^{-1} obtained for the SPME-IMS complete method, while a significantly lower LOD of 0.5 μg L^{-1} was obtained for the PSPME-IMS novel method. Both LOD's were determined by the 6 min extraction time measurements.

This section summarized a stepwise evaluation of the PSPME-IMS method performance for the detection of piperonal vapors emitted from standard solutions. At all stages, the PSPME-IMS technique showed a strong advantage over SPME-IMS in terms of enhanced capacity and higher sensitivity.

7.2.2.6 Sampling Real MDMA Cases at a Local Crime Laboratory

The PSPME-IMS method was used to presumptively identify MDMA tablets from real cases using piperonal as the target odor signature for detection. In the headspace above MDMA tablets, although no additional solvents were used in the dilution, other possible volatile interferences, as well as trace amounts of processing solvents may still be present following synthesis. In contrast to the finite source of piperonal vapors generated from dilute solutions of the analyte in a volatile solvent, MDMA tablets can be considered as continuous vapor source of piperonal during timed experimental measurements.

A preliminary experiment with MDMA tablets aimed to determine the equilibrium time, the minimum extraction time that is required to obtain the highest extraction efficiency, was done. This experiment was conducted by introducing five MDMA tablets originating from the same case, of 1.5 g total average weight, to each quart can for 48 h to equilibrate. The results are demonstrated in Figure 52. The x-axis displays the extraction

times, from 30 seconds up to 15 min, and the y-axis demonstrates the cumulative amount detected by the IMS. Two peaks had been analyzed for piperonal at these experiment conditions at all extraction times. The earlier peak, at 8.3 seconds drift time, is determined to be the monomer product ions and the delayed peak, at 9.8 seconds drift time, represents the dimer product ion. Consistent detection of the dimer product ions at all extraction time points signaled high extraction efficiency for these conditions. The steep short increase from 30 seconds to 1 min stabilized at a constant response for the monomer product ions for all extraction time measurements, from 1 min up to 12 min, indicating its saturated detection level. At 15 min extraction time a small decrease in efficiency was measured. However, the initial small dimer product ions detected already for the minimal extraction time of 30 seconds, was followed by consistent increments with the lengthening of the extraction times, yielding for 15 min the highest response. It could be assumed that extraction times longer than 15 min will yield higher extraction efficiencies. Despite this, an extraction time of 15 min was chosen as the extraction time for all MDMA tablets experiments ahead, in order to enable large-scale measurements in a reasonable time duration.

The extraction efficiency of the PSPME device was evaluated versus tablets quantity. Different quantities of MDMA tablets 10, 5, 3 and 1 tablet, all originating from the same case, were added to the quart cans and sealed for 24 h to equilibrate. The headspace generated inside was sampled by suspending the PSPME devices, and for comparison the SPME fibers, for 15 minute extraction times. The results are illustrated in Figure 53.

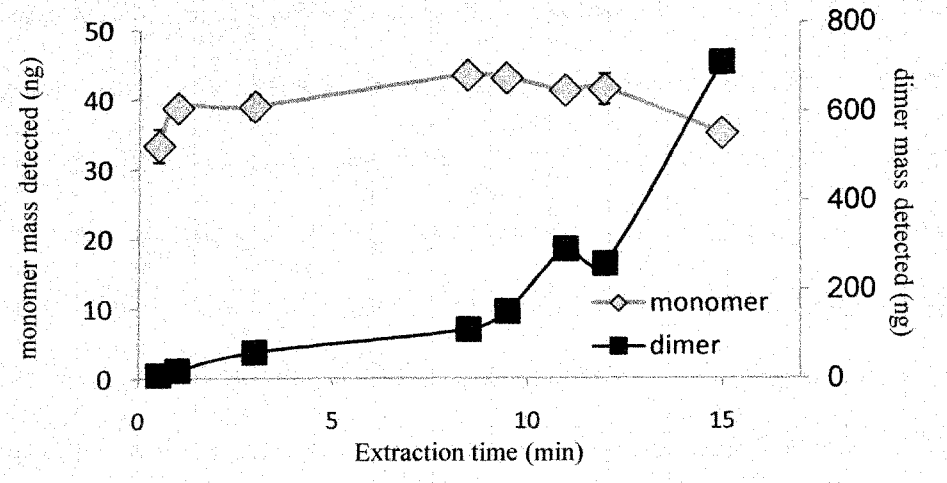

Figure 52. Extraction Time Curves Generated Using Confirmed MDMA Tablets [178]

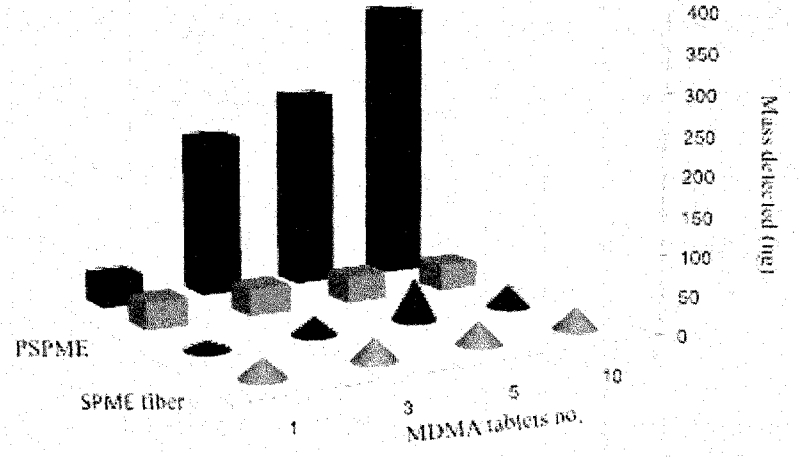

Figure 53. Response v. Number of MDMA Tablets Sampled [178]

Detectable levels of piperonal from the headspace generated by only 1 tablet were achieved by extracting with either device, with higher amounts detected from higher quantities of tablets. Extraction by either device yielded dimer product ions accompanied

by monomer product ions. However, overall consistently higher extraction efficiencies were measured with the PSPME device than for the SPME fibers under all experimental conditions, both for the monomer and dimer product ions. Saturated levels of monomer productions were analyzed following absorption by PSPME device by sampling the headspace generated from only 1 tablet, while with SPME fibers, saturated monomer product ion levels were observed with five MDMA tablets under the same experimental conditions. Despite the steep increase in the dimer product ions detected by sampling with the PSPME device from 1 and 3 tablets, the response continued to increase moderately when sampling 5 and 10 tablets, demonstrating the high capacity of the PSPME device. Under the same conditions for the SPME fibers, the increased response detected for the dimer product ions from 1 to 5 tablets was followed by a significant decrease in signal when sampling the headspace generated from 10 tablets. Despite the high concentrations of piperonal measured for 1 and 3 tablets, it was determined that for further experiments 5 tablets would be used in each can just in case the emitting source (the seized tablets) would contain lower amounts of MDMA or in case un-fresh samples were encountered.

The PSPME-IMS method was tested for analysis of suspected MDMA tablets, with evidence seized from six different real cases scenarios, at a local crime laboratory. The results obtained by both devices for each suspected case are demonstrated in Figure 54. Sampling and IMS analysis of the headspace generated inside the cans, each from a different suspected case, using PSPME and SPME fibers, both indicated positive for MDMA tablets for cases 3, 4, 5 and 6. Even though high responses of monomer and

dimer product ions were detected by both devices for these cases, even higher response for the dimer product ions were obtained with the PSPME devices over the fibers, demonstrating its higher extraction capacity. Moreover, higher repeatability between replicate measurements obtained with PSPME devices for all cases than with the commercial SPME fibers.

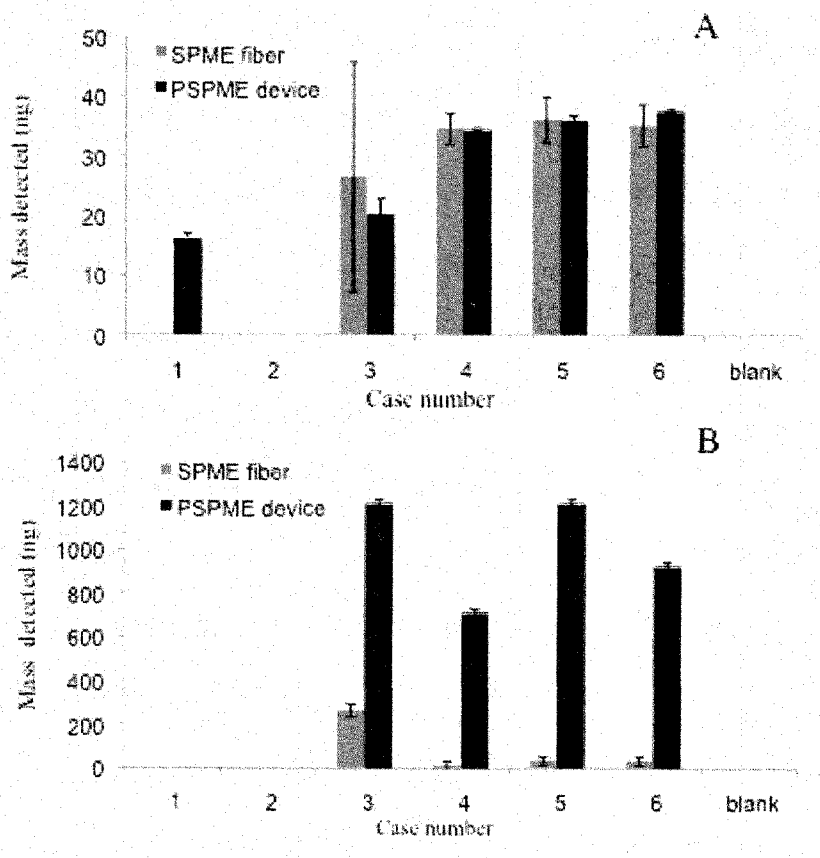

Figure 54. Blind Case Study Results for A) Monomer and B) Dimer Product Ions [178]

No piperonal vapors were detected in the headspace generated from case 2, using either device for sampling. The forensic examiner later confirmed from GC/MS data that case 2

was negative for MDMA. No piperonal vapors were extracted from the headspace generated by case 1 tablets when only using SPME fibers as the sampling device. Following these SPME fiber results, the suspected tablets of case 1 could be considered as a negative MDMA case. Alternatively, sampling case 1 under the same conditions as the fiber, by using the novel PSPME device, enabled clear detection of piperonal vapors. Even though lower amounts were detected for this case compared to the four other positive cases, consistent undeniable IMS peaks of the monomer product ions were obtained, confirming these tablets as a case positive for MDMA. Detection using the PSPME-IMS method for all tested cases corresponded with the crime laboratory's GC-MS data in this blind study test. Sample preparation followed by GC-MS analysis according to protocols performed by the crime laboratory confirmed the suspected tablets from all the cases, excluding case 2, were positive for MDMA. Case 2 was the only case confirmed as negative for MDMA by crime laboratory. Case 1 according to GC-MS analysis had a significantly lower concentrations of MDMA in the tablets analyzed compared to tablets from the positive cases 3 to 6. This is significant because, although SPME-IMS is a proven sensitive method for the detection of piperonal, if sampling had only been done with the SPME fiber, then case 1 would have been incorrectly deemed negative. This highlights the capabilities of the PSPME device in even the most difficult of cases.

7.2.3 Performance of PSPME for Other Volatile Chemical Signatures

Other volatile chemical signatures that have been identified as emanating from explosives were also sampled by sol-gel PDMS PSPME. Of the compounds studied, only

cyclohexanone, an odor signature of RDX, was analyzed in the positive mode. The rest of the compounds: 2,4-DNT (an odor signature of TNT and cast explosives) and 4-NT (a taggant) were analyzed in the negative polarity. Figure 55 displays plasmagrams that show that the PSPME device is capable of absorbing a sufficient amount of the analytes of interest for detection by IMS (2,4-DNT, 4-NT, and cyclohexanone, respectively). These plasmagrams represent the segment in the analysis with the highest signal for the target analytes. For figures 55 (A and B), the peak at 11.3 ms is the calibrant, 4-nitrobenzonitrile (K_0= 1.7 $cm^2V^{-1}s^{-1}$). The peaks from the reactant hexachloroethane are at 7.1 ms and 8.1 ms (K_0= 2.6 $cm^2V^{-1}s^{-1}$and K_0= 2.3 $cm^2V^{-1}s^{-1}$, respectively) and the oxide ion peak is at 8.4 ms (K_0= 2.2 $cm^2V^{-1}s^{-1}$). The peaks to the left of the calibrant peak are present before IMS analysis begins, but are depleted during the analysis and peak formation. In figure 55A, the 2,4-DNT signal (K_0= 1.6 $cm^2V^{-1}s^{-1}$) has a drift time of 11.8 ms. Figure 55B shows the plasmagram for the extraction of 4-NT, with a peak differing from the blank at 12.8 ms. In figure 55C, the peak at 9.6 ms in the positive polarity is the reactant ion peak nicotinamide (K_0= 1.9 $cm^2V^{-1}s^{-1}$). It is also interesting to note that for just a 1 hr extraction of such a highly volatile compound as cyclohexanone (4.35 Torr @ 25 °C, (K_0= 1.5 $cm^2V^{-1}s^{-1}$)) for which the smallest amount (10 μg) in a can is sampled, a detectable peak is found at 11.7 ms (figure 55C).

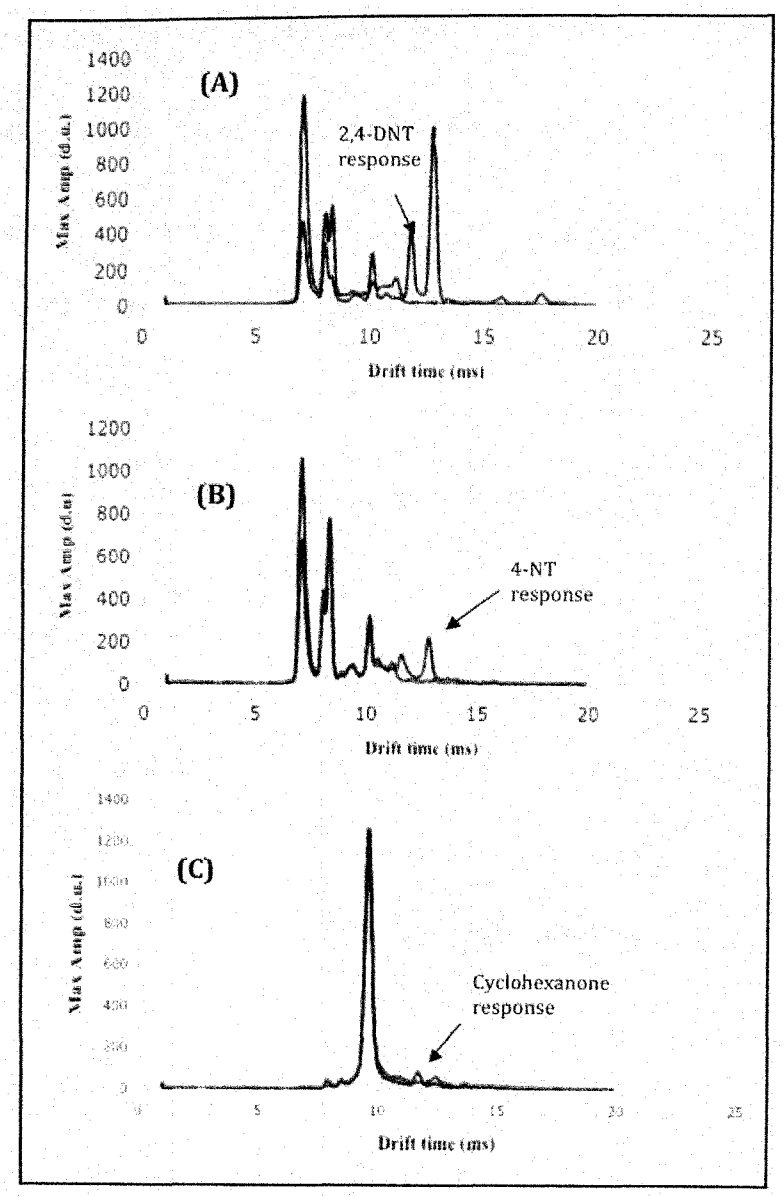

Figure 55. PSPME-IMS of the Volatile Chemical Signatures 2,4-DNT, 4-NT, and Cyclohexanone [168]

7.2.4 Performance of PSPME for the Smokeless Powder Volatile Chemical Signatures

7.2.4.1 Smokeless Powder Volatile Chemical Signature IMS Response Curves

Response curves of the smokeless powder odor signatures, DPA, 2,4-DNT, and EC were generated for quantitation following PSPME-IMS analysis. The response curve for DPA is shown in figure 56.

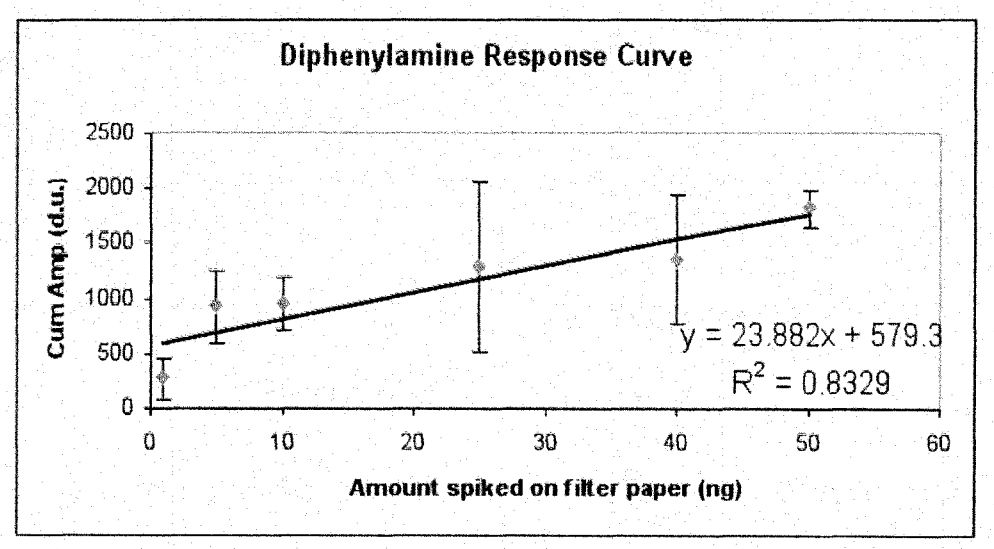

Figure 56. DPA Response Curve

Generation of the response curves for 2,4-DNT (figure 57) and EC (figure 59) proved to be more complicated. The only way to produce a response curve for 2,4-DNT was by using hexane, a solvent that is much more volatile than acetonitrile and is thus more compatible with the volatility of 2,4-DNT. In this manner, both hexane and 2,4-DNT are vaporized nearly at the same time rather than the 2,4-DNT being volatilized prior to the solvent in which case less and inconsistent amounts of 2,4-DNT arrive at the detector.

This is a result of the 2,4-DNT desorbing only until later scans such that the full amount of 2,4-DNT was not detected before analysis was complete.

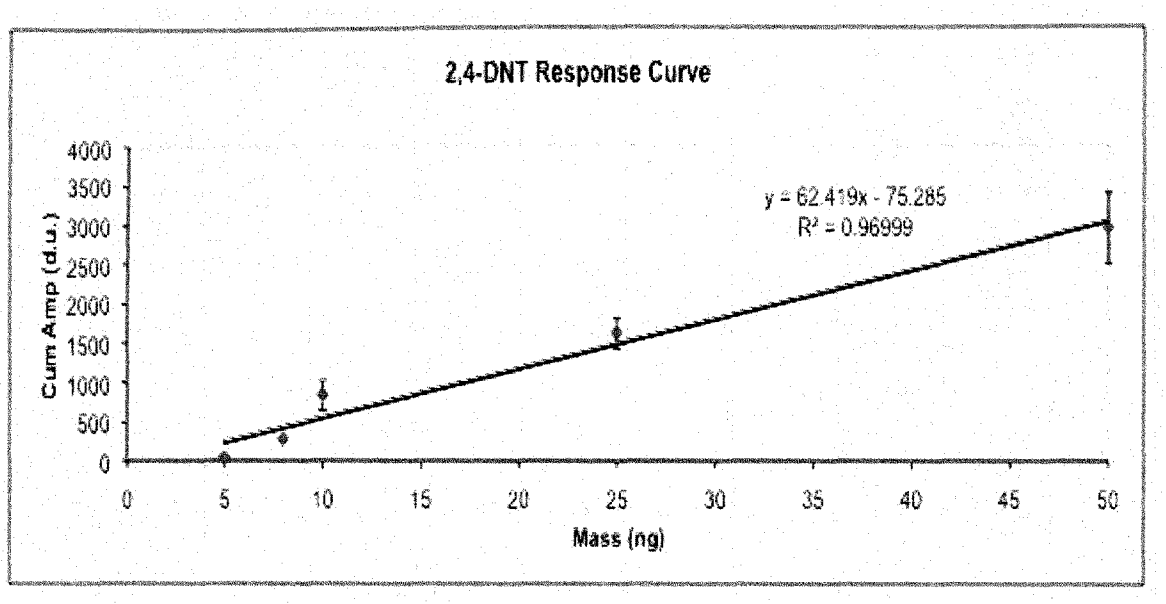

Figure 57. 2,4-DNT Response Curve

Since it was determined that solvent affected 2,4-DNT IMS analysis, a study was conducted on three likely IMS compatible solvents that ranged in boiling point and polarity. The results of the maximum and cumulative amplitudes for two mass loadings of 2,4-DNT in different solvents on a manufacturer provided filter is shown in figure 58. The highest maximum amplitude is indicative of the best desorption profiles, since it is amplitude of the scan with highest signal that alerted for 2,4-DNT out of all the other scans. The cumulative amplitude is the sum of all the scans in which the compound alerted during IMS analysis and indicates the highest total mass of the compound being detected. It is clear in figure 58, that analysis of 2,4-DNT in hexane provides the highest and most reproducible maximum and cumulative signals at both concentrations.

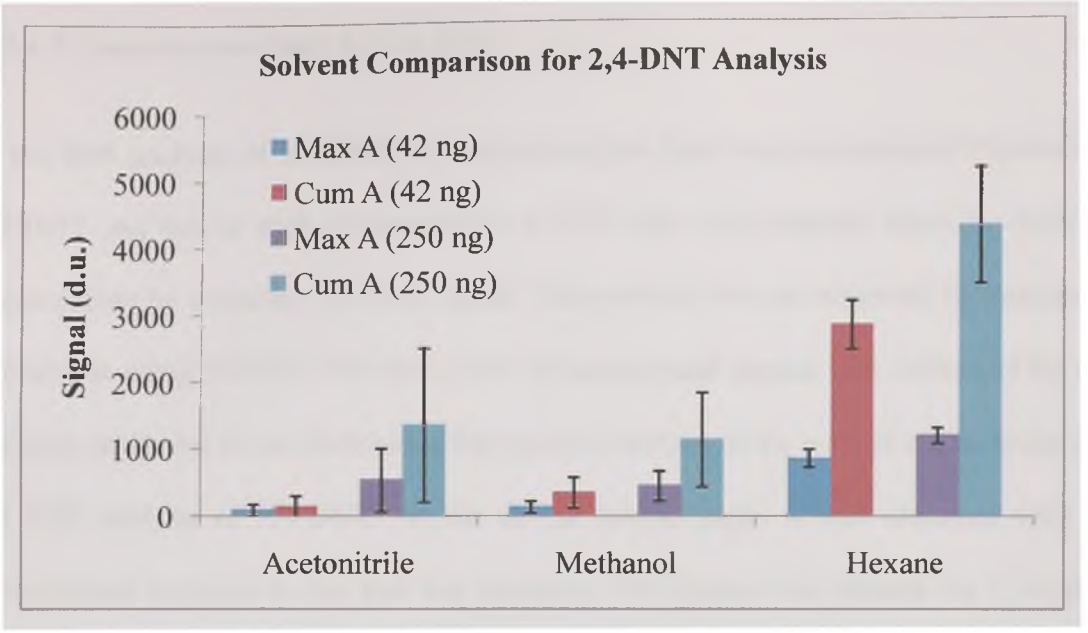

Figure 58. IMS Analysis: 1 µl of 42 and 250 ppm 2,4-DNT (n=5) in Different Solvents Spiked on Manufacturer Provided Filters

The response curve of EC (figure 59) was also problematic due to the small linear dynamic range for detection of this compound by IMS, between 0.5- 1 ng.

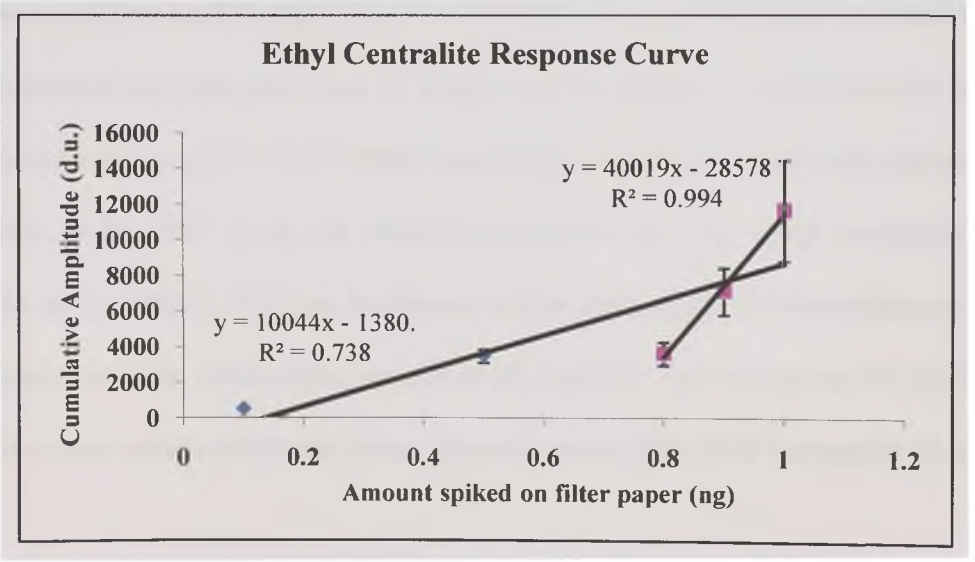

Figure 59. EC Response Curve

7.2.4.2 Concentration Study for 2,4-DNT

In the IMS analysis of 2,4-DNT it was noticed that there was inconsistent detection of 2,4-DNT and that at high concentrations a TNT alert was obtained either by itself or accompanied by a smaller 2,4-DNT signal. This problem was not observed for headspace extractions using PSPME. The first issue of inconsistent signals was addressed by the previous study and it was determined that proper selection of the solvent was necessary in the IMS analysis of 2,4-DNT. As far as the second peak, it was observed with an accompanied decrease in the first ion intensity. The product ion formed for 2, 4-DNT these reported IMS conditions is the $(M-H)^-$ ion **[143]**. By observing the baseline of the plasmagram and studying the locations of the two peaks, it is clear there is a conversion of the ions in the drift tube to a secondary form. The peak for the second ion was similar to the peak obtained for TNT and thus caused an IMS alert. This phenomenon was observed previously but it was demonstrated that the second peak for 2, 4-DNT seen at high concentrations and the peak for 2, 4, 6- TNT were not the same ion species. They also speculated that this peak may be due to the formation of a dinitrobenzyl anion at high concentrations of 2, 4-DNT **[180]**. Regardless, since the second peak appears at the drift time of the TNT peak, an important explosive, it may cause confusion in the detection of 2, 4-DNT. This can be minimized by heading the recommendations of this study which include: when using standards of 2,4-DNT, use hexane as the solvent and keep the concentration within the linear dynamic range of the IMS instrument (figure 57).

7.2.4.3 Determination of Equilibrium Extraction Time

The determination of equilibrium extraction times for the smokeless powder volatile chemical signatures was done by sampling spikes of 10 μL of 100 μg mL^{-1} DPA in acetonitrile, and spikes of 10 μL of 25 μg mL^{-1} EC in their respective quart cans using PSPME as the extraction media for different time intervals. The equilibrium extraction curve was impossible to generate for 2,4-DNT using PSPME since is absorbed so strongly to the SPME phase that more than 6 desorptions into IMS were required in order to obtain a blank. The sum of these desorptions did not seem a valid method of quantitation since additional loss to the surrounding environment was likely in between desorptions. This was exacerbated by the fact that the slide remained hot in between each thermal desorption and uncontrolled loss of analyte could be assumed. Therefore, the equilibrium curves for only EC and DPA are shown in figure 60. After 30 min of sampling, equilibrium is reached for EC while DPA requires about 1 hr.

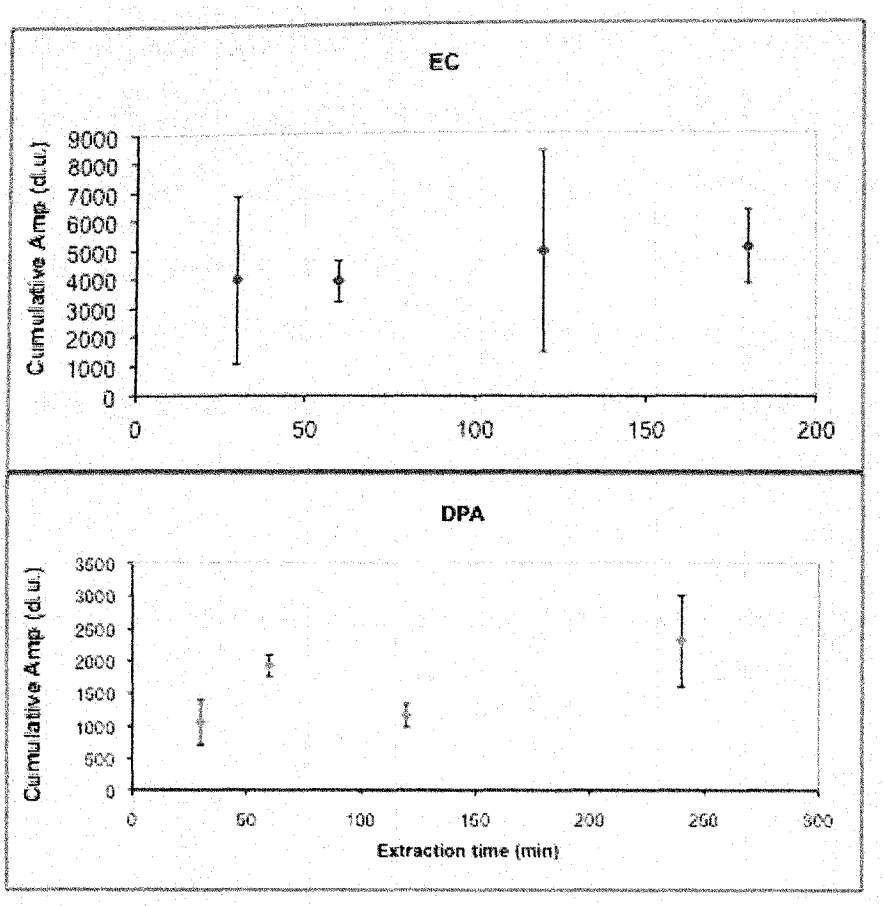

Figure 60. Equilibrium Curves for EC and DPA

7.2.4.4 Sampling of Unburned Smokeless Powders

Four brands of smokeless powders were sampled statically in a closed system at room temperature with the PSPME in order to target the volatile chemical signature DPA. The results of the mass of DPA detected from the headspace of the smokeless powders by PSPME-IMS are shown in figure 61. They were calculated according to the response curve shown in figure 56. Static sampling occurred for only 1 hr from the headspace generated from 100 mg during that time in a quart can. The only powder that did not alert to DPA was IMR 4198 although it has been reported that this powder contains DPA from

SPME fiber-GC-MS data **[59]**. These experiments were done of 100 mg of the powders in a 15 mL vial as opposed to a quart-sized can, allowed to equilibrate then sampling took place. These experiments described herein were intended for the rapid extraction and detection of volatile chemical signatures from larger volumes. Had a comparable experiment been done, it is likely that IMR 4198 would have alerted resulting in even higher mass detected compared to SPME-IMS, by virtue of the higher capacity of the PSPME device.

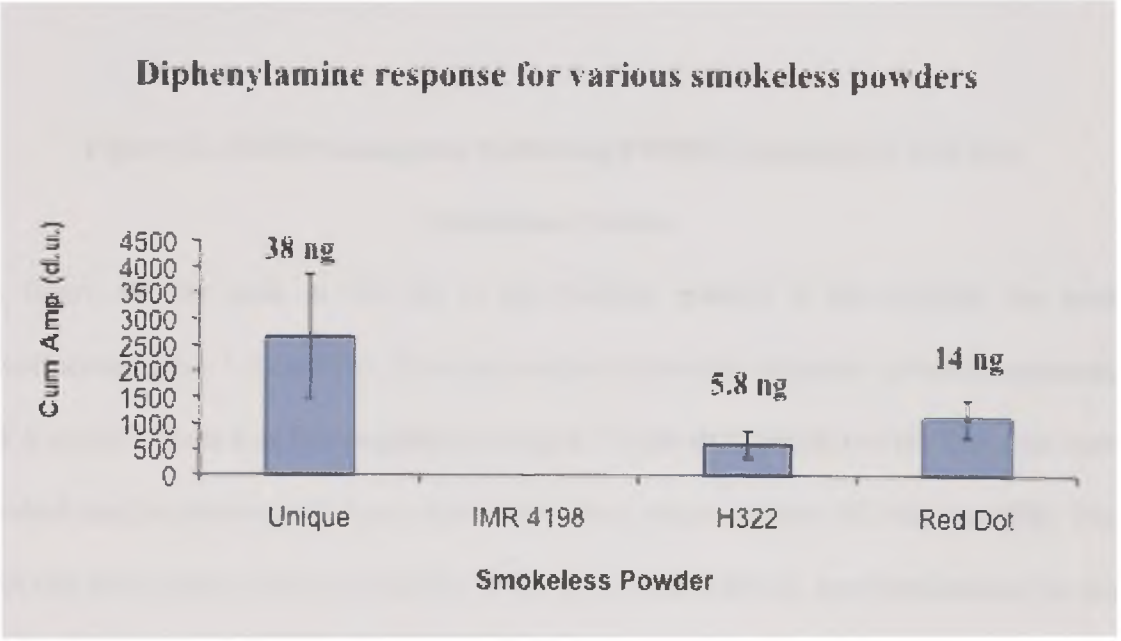

Figure 61. Mass Detected of DPA from Smokeless Powders Using PSPME-IMS

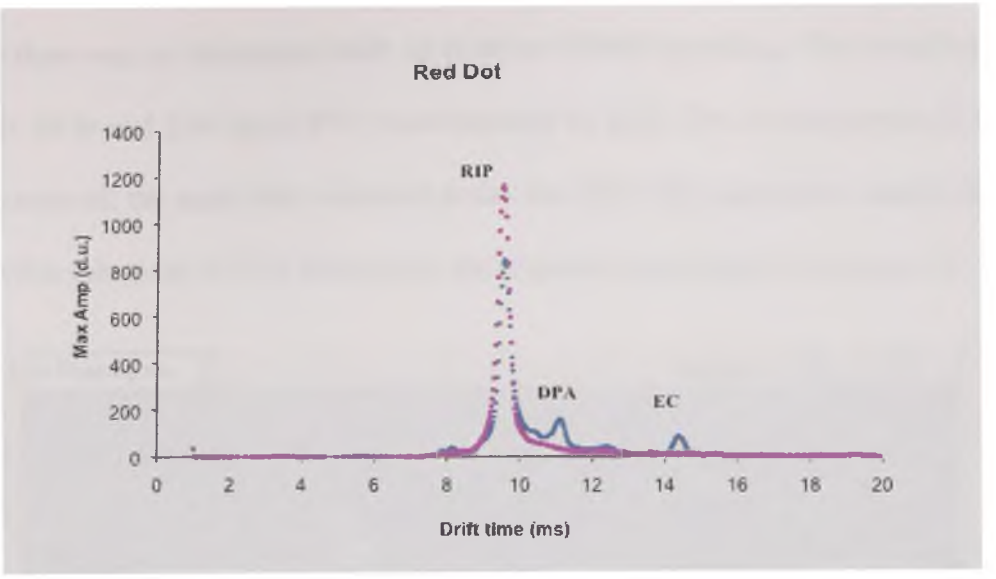

Figure 62. IMS Plasmagram Following PSPME Sampling of Red Dot Smokeless Powder

In figure 62, the peak at 9.6 ms in the positive polarity is the reactant ion peak nicotinamide (K_0= 1.9 cm^2/Vs). This plasmagram shows the detection of two compounds, DPA and EC, from Red Dot smokeless powder. This is only powder of the four that were studied that has been reported to contain both these compounds by GC-MS data **[59]**. The fact that both peaks were seen in IMS, with considerable signals, has implications for the multi-channel detection of smokeless powders by PSPME-IMS.

7.2.5 PSPME Static Sampling of TNT from a Large Volume Vessel

Figure 63 shows the 3-D plasmagram of the extraction of TNT from (~2 g) Pentolite in a large volume area, a sealed hood, at room temperature. Pentolite contains 50:50 PETN: TNT, therefore the maximum amount of TNT available for extraction was 1 g. The introduction of the PSPME sampling device and the explosive took place at the same

time so there was no headspace built up prior to PSPME sampling. The sampling took place for 24 hr and 2.96 ng of TNT were detected by IMS. The circled portion in figure 63 represents all the scans that contained peaks for TNT. The cumulative amplitude was converted to this mass of TNT detected by the response curve listed in equation 11.

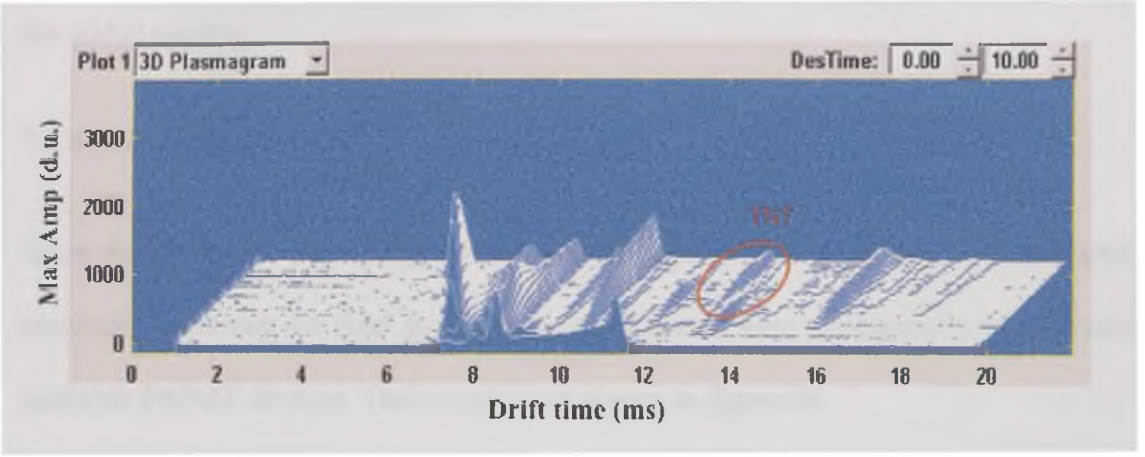

Figure 63. 3-D IMS Plasmagram for the Static Large Volume Sampling of TNT

The results of these experiments provide motivation for the development of a PSPME device that allows dynamic sampling. In this manner, the explosive would be detected in shorter sampling times since mass transfer would be aided by fluid flow, making the sampling of large volume containers for contraband by sampling volatile chemical signatures feasible.

7.2.6 Comparison of Planar La (dihed) SPME Devices with Control Planar Sol-gel and PDMS Devices for the Extraction of TNT and 2,4-DNT

The following includes results and discussion of experiments using La (dihed) coated PSPME devices aimed at comparing the extraction and aging capabilities resulting from the added coating.

7.2.6.1 Aging Study

Since the ability of a sampling device to retain absorbed analyte until it is analyzed is especially important for field applications, experiments were conducted to test the all the available PSPME devices. These results are shown in figure 64.

For the detection of TNT, the control + La (dihed) PSPME showed the best desorption characteristics since it produced the highest maximum amplitude (data not shown). This is not surprising since the analyte only has to be desorbed from the La (dihed) layer not an additional sorbent. Furthermore, in figure 44, the La (dihed) + sol-gel PDMS PSPME device retained 32% of the TNT after 30 min aging. For 2,4-DNT, La (dihed) + sol-gel PDMS retained 23% after 30 min aging. It is interesting to note that, without the La (dihed) coating, the absorbed 2,4-DNT and TNT were lost completely from the plain sol-gel PDMS and PDMS PSPME devices after only 30 min of aging. This makes the case for using La (dihed) as a coating to improve retention by PSPME.

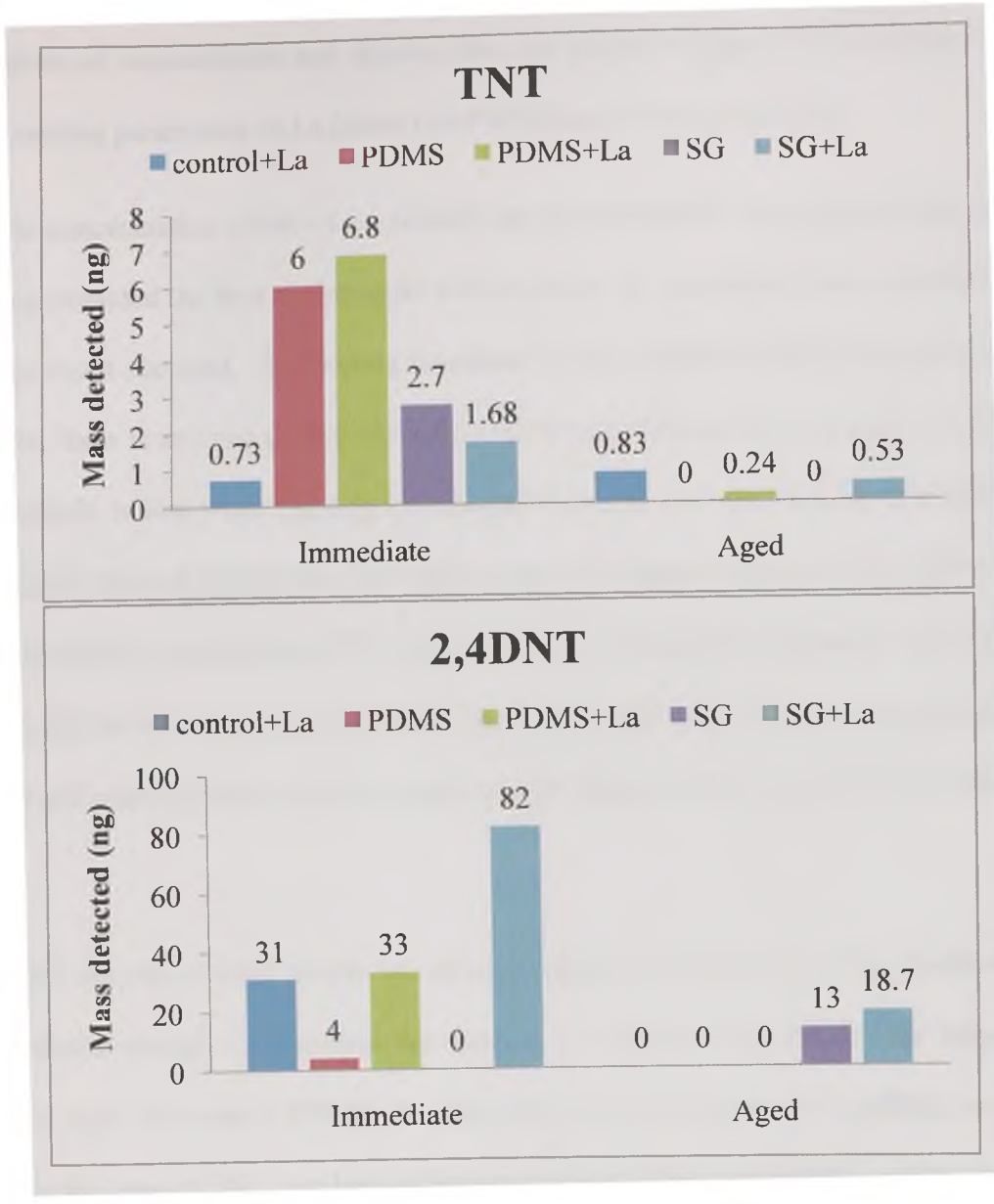

Figure 64. Results for the Aging of 2,4-DNT and TNT

7.2.6.2 Coating Study

The next study was conducted to determine the best coating parameters for La (dihed) on sol-gel PDMS and PDMS PSPME devices. The results of the extraction and immediate analysis of 2,4-DNT and TNT by sol-gel PDMS coated with La (dihed) with varying

conditions of concentration and dipping time are shown in figure 65. The results for the same coating parameters of La (dihed) on PDMS are shown in figure 66.

For the concentration effect of La (dihed) on sol-gel PDMS, the highest concentration 300 mg provided the best response for both analytes. In conducting these experiments, a curious result occurred. By dipping the control sol-gel PDMS PSPME device in MeOH for 1 hr, there is an even greater extraction efficiency obtained than by using La (dihed). This benefit is lost when dipping in methanol for 3 hr. For the coating time effect, by dipping for 1hr and patting the slide with a tissue, the highest response for 2,4-DNT, even considering the concentration effect and the effect of dipping in methanol, was obtained. This could be since by patting the slide, the LA (dihed) particles were adhered better to the sol-gel coating below and makes the case for incorporating sol-gel and La (dihed) in situ.

For TNT the spin coated results are missing since this slide broke. The results do not demonstrate enough justification for coating La (dihed) onto PDMS for immediate analysis since the control PDMS provides even greater response for 2,4-DNT, or nearly equal in the case of TNT. For both substrates, sol-gel PDMS and PDMS, and the analytes 2,4-DNT and TNT, shorter dipping time increased extraction efficiency.

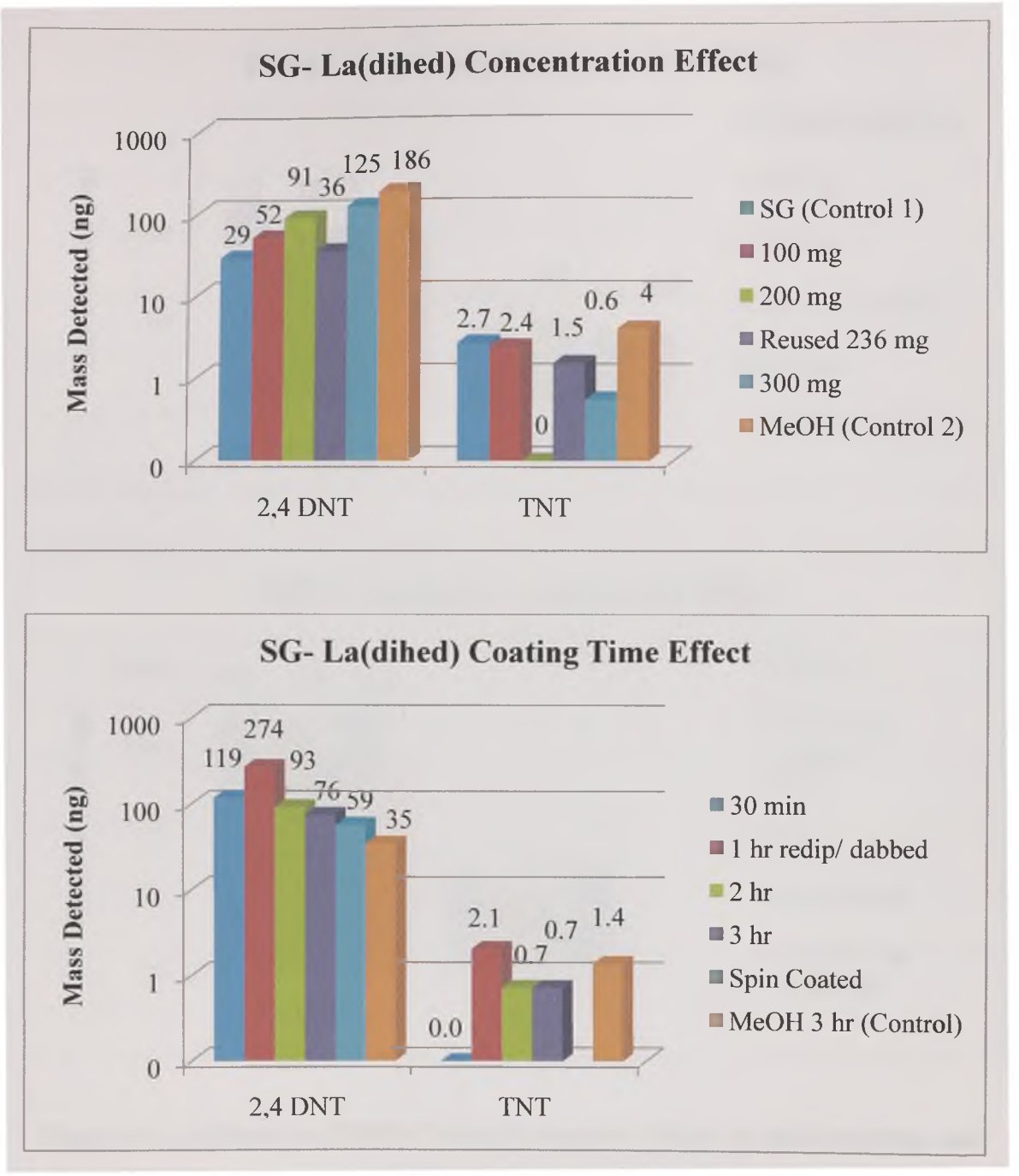

Figure 65. La (dihed) on Sol-gel PDMS Coating Parameter Effects on the Extraction and Detection of 2,4-DNT and TNT

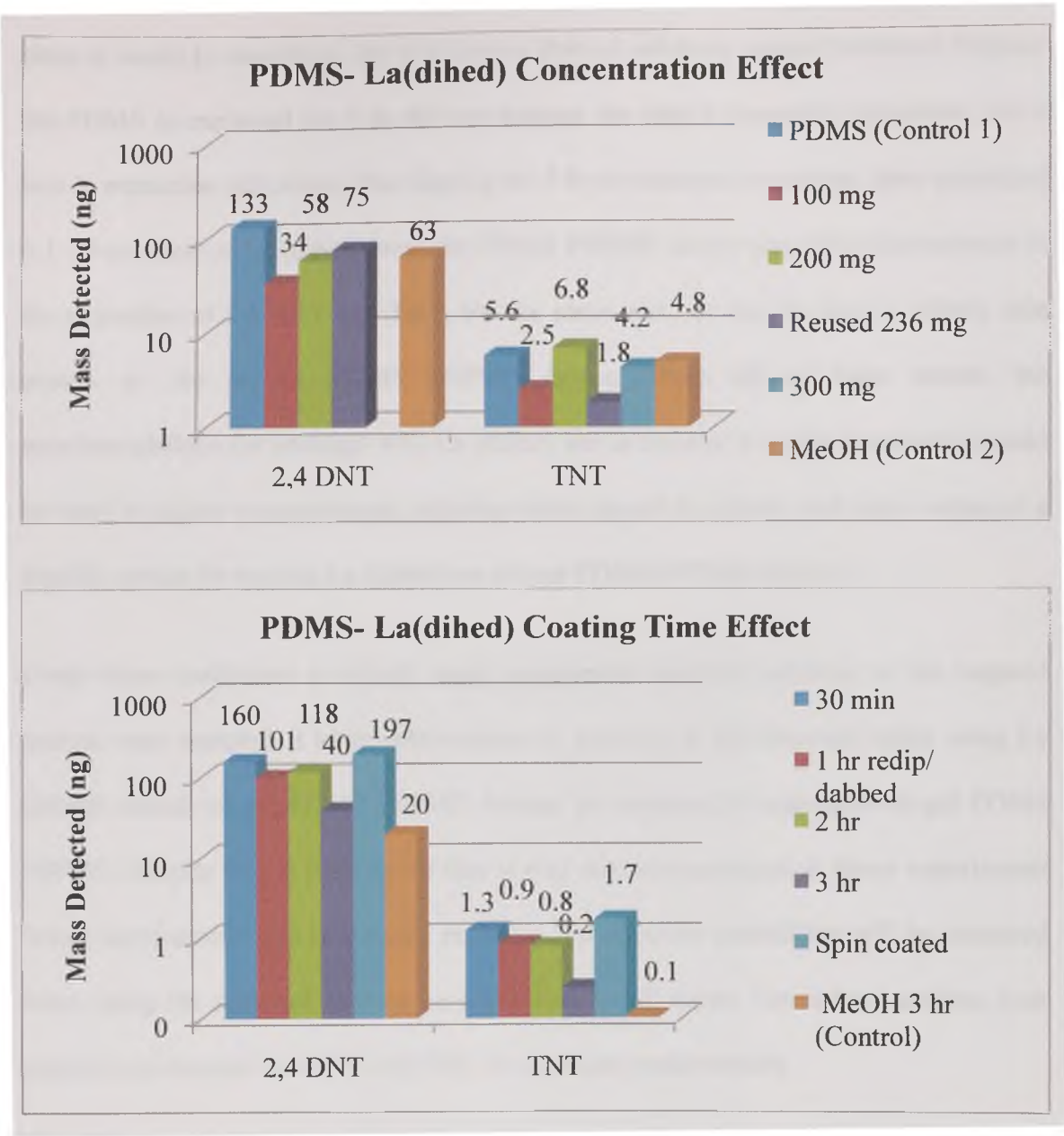

Figure 66. La (dihed) on PDMS Coating Parameter Effects on the Extraction and Detection of 2,4-DNT and TNT

It also seems in both La (dihed) coated sol-gel PDMS and PDMS, for the extraction of both analytes, higher La (dihed) concentration increases affinity. It is difficult to conclude if reusing the La (dihed) solution for dipping is acceptable. This parameter was tested

since it would be beneficial, but it is known that sol solutions cannot be reused. Dipping the PDMS in methanol for 1 hr did not damage the slide's absorptive properties, but a loss in extraction efficiency after dipping for 3 hr in methanol is evident. Spin coating of a 1 ml solution of La (dihed) over the PDMS PSPME device provided enhancement in the extraction of 2,4-DNT and TNT, but the same was not true for the La (dihed) spin coated on the sol-gel PDMS PSPME device. From all of these results the recommendations for coatings with La (dihed) are as follows: La (dihed) solution should be used in higher concentrations, dipping times should be shorter and spin coating is a feasible option for coating La (dihed) on sol-gel PDMS PSPME devices.

Under these conditions in which single component standard solutions of the targeted analyte were sampled, a large enhancement in recovery is not observed when using La (dihed) coated sol-gel PDMS PSPME devices as compared to uncoated sol-gel PDMS PSPME. Despite this, it is expected that in real case scenarios and in future experiments where interferences will be present, recovery and detection capabilities will be enhanced when using the selective coating La (dihed) as it will attract Lewis base analytes (our targeted compounds 2,4-DNT and TNT for example) preferentially.

7.3 Development of Dynamic PSPME

The development of dynamic PSPME was enabled mainly by the selection of glass fiber filters (G6, Fisherbrand, Pittsburgh, PA) as the substrates, as opposed to the glass slides used in the static PSPME devices. These glass fiber filters have a reported temperature limit of 500 °C by the manufacturer, which is well above the maximal IMS desorption

temperatures of 300 °C. The substrate surface withstood the corrosive activation procedure, unlike other candidate substrates like the fiberglass screen in figure 67, and was covalently bound to a sol-gel PDMS solution. By spin-coating the glass fiber filters, not only was the coating solution spread by centrifugal forces, but it was also absorbed throughout the thickness of the glass fiber filter. This sol–gel PDMS coating was previously used as the extraction phase of static PSPME because of its high thermal stability and strong bonding of the polymer to the surface resulting in a longer lifetime of the extraction device. Additionally, the sol-gel nanoparticles afforded additional surface area beyond simply changing the geometry from a fiber to a planar configuration.

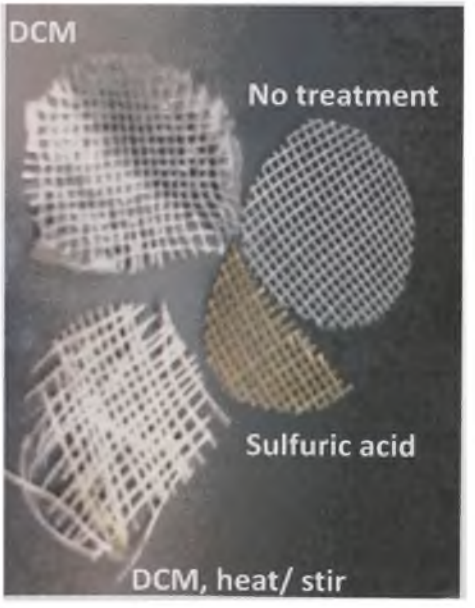

Figure 67. Fiberglass Screen Exposed to Various Corrosive Procedures

7.3.1 Coating Method Development

The spin program in the coating procedure was optimized to be 1 mL of sol-gel PDMS solution statically deposited onto the prepared substrate and spinning at 1000 r.p.m. for 1 min. The tested spin speeds were 2000 rpm, 1000 rpm, and 200 rpm.

The final PSPME devices weighed 0.1472 g, 0.1594g, and 0.2205 g, respectively. This is as expected because with a slower spin speed more of the coating solution remains on the substrate due to the lessening of centrifugal forces. The SEM images confirmed an increased amount of sol-gel nanoparticles on the product resulting from slower spin speeds. Figure 68 show SEM images of a control experiment for this question. Sol-gel PDMS was deposited into an Al stub and the glass filter was dipped in the sol solution. These represent a spin= 0 rpm data point. The results show a high concentration of micron-sized particles on both substrates.

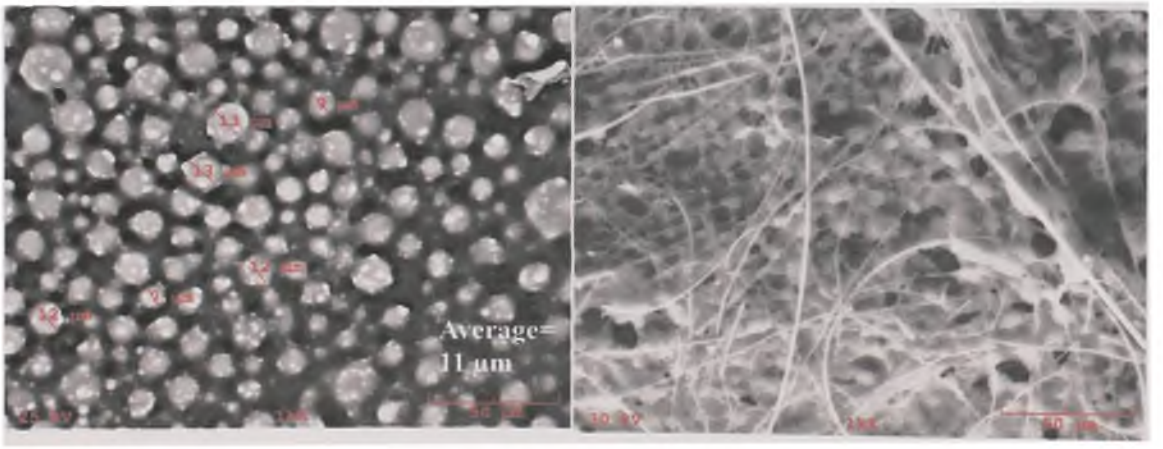

Figure 68. SEM Images of Sol-gel PDMS on Different Substrates: a) 10 uL sol solution deposited on Al stub b) prepared glass fiber filter substrate dipped in sol-solution 1 min.

Figure 69 includes the SEM images of prepared glass fiber filters coated under the various spin programs. It is clear that with increasing spin speed there is a loss of the nanoparticles and there is even a reduction in their size.

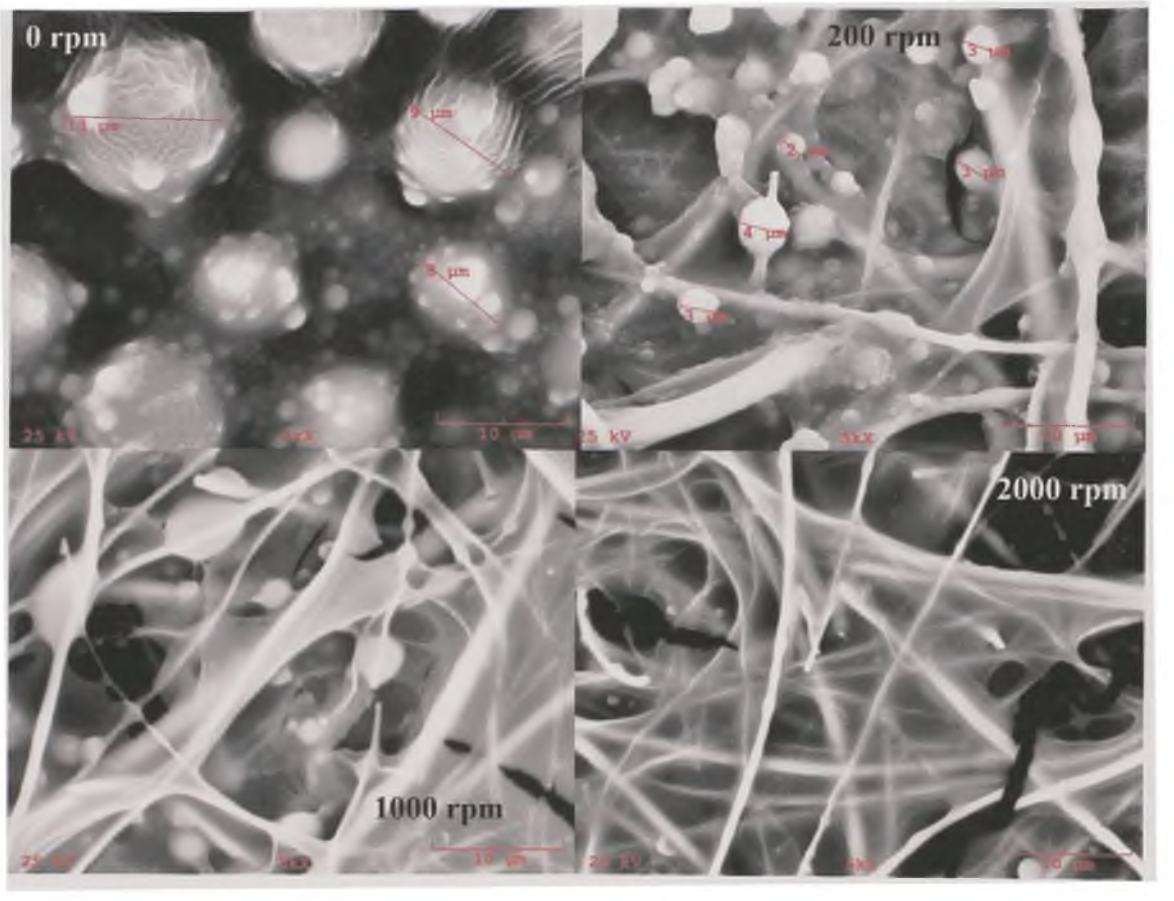

Figure 69. Spin Speeds Tested by Deposting 1 mL of Coating Solution on Substrate and Spinning for 1 min at 0, 200, 1000, and 2000 rpm

When comparing the final products by extracting the headspace of the Hogdon H322 smokeless powder containing 2,4-DNT, and spikes of TNT in solution, the 1000 rpm product resulted in consistently higher peak intensities, cumulative peak intensities of immediate and aged samples (figure 70), and lower background signal (figure 71). This

means that a maximal amount of sol-gel nanoparticles present is not necessarily the best for extraction efficiency, but rather there is an optimal concentration range of nanoparticles for use in dynamic PSPME.

An additional study was conducted to test the aging of TNT directly spiked on the substrates created using the different spin speeds with comparison to spikes on manufacturer provided filters (figure 72). As expected the 200 rpm dynamic PSPME retained TNT the best because of the greater presence of sol-gel nanoparticles, but the 1000 rpm still performed suitably, still retaining a portion of the TNT after 30 min of aging.

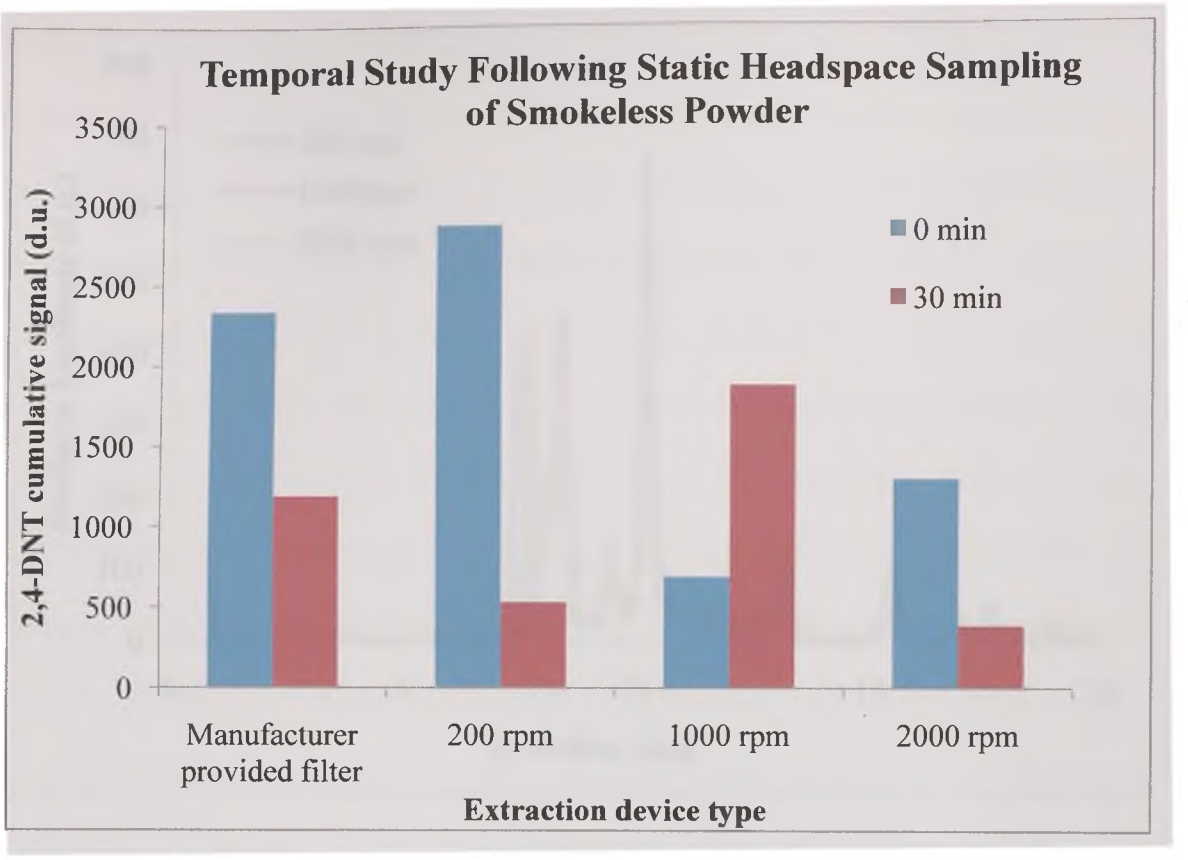

Figure 70. 100 mg of Hogdon H322 Smokeless Powder- Immediate or Aged: Qt. can, 30 minute stay, extraction for 30 min at room temperature, IMS analysis either t=0 or t=30 min after extraction

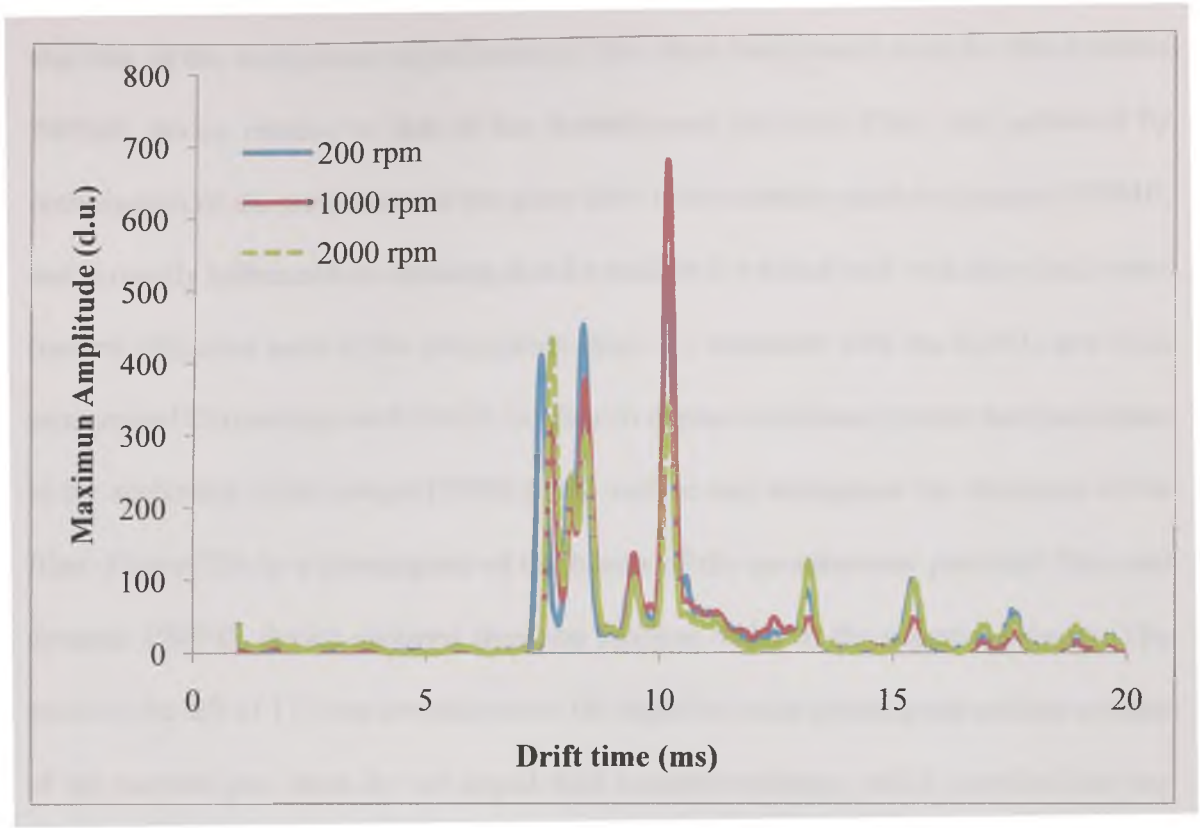

Figure 71. IMS plasmagram of Backgrounds Obtained From Blank Dynamic PDMS Devices Created Using Various Spin Programs

The substrate preparation procedure was also optimized in order to minimize the background to the levels seen in figure 71 and to minimize the yellowish tinge and sometimes burned appearance that was observed at times following curing and conditioning.

The IMS backgrounds in the IonScan 400B (+/- polarities) and the Itemiser 2 (+ polarity) obtained for both the dynamic PSPME filter and manufacturer provided filter are shown in figure 73 (A-C). Low background signal for the sampling media used in IMS is desirable to diminish the effects of any competitive ionization between the analyte signal

and that of the background signal peak(s). The clean background seen for the dynamic PSPME device relative to that of the manufacturer provided filter, was achieved by optimization of the preparation of the glass fiber filter substrate used in dynamic PSPME, and is mainly influenced by ensuring that the surface is washed well with deionized water (neutral pH) after each of the preparation steps: 1) treatment with the H_2SO_4 and H_20_2 mixture and 2) treatment with NaOH in order to expose the silanol groups that participate in the anchoring of the sol-gel PDMS to the surface and throughout the thickness of the filter. Figure 73A is a plasmagram of the blanks of the manufacturer provided filter and dynamic PSPME device obtained from the IonScan 400B in the negative polarity. The peaks to the left of 11.3 ms are inherent to the negative mode plasmagram and are a result of the reactant gas, clean dry air doped with hexachloroethane, which provided the two peaks at (K_0= 2.60 and 2.32cm^2 V^{-1} s^{-1}) and the O_2^- peak (K_0= 2.22 cm^2 V^{-1} s^{-1}). The calibrant (cal) peak is from 4-nitrobenzyl nitrile (K_0= 1.65 cm^2 V^{-1} s^{-1}). To the right of the calibrant peak it is evident that the manufacturer provided filter produces a large peak at 16 ms when desorbed. This can suppress the signal of the analytes targeted in the negative mode in this IMS instrument since it will compete with the analyte for the pool of reactant ions. The three minor peaks (13.4, 15.6, and 17.7 ms, all with intensities below 50 d.u.) for the dynamic PSPME device do not interfere with the drift times of 2,4-DNT (11.8 ms, K_0= 1.57 cm^2 V^{-1} s^{-1}) and TNT (12.8 ms, K_0= 1.45 cm^2 V^{-1} s^{-1}). Figure 73B is a plasmagram of the blanks of the manufacturer provided filter and the dynamic PSPME device obtained from the IonScan 400B in the positive polarity. It is immediately evident that the trace of the dynamic PSPME device represents a much cleaner background than that of the manufacturer provided filter. The reactant ion peak (RIP),

also the calibrant (Cal) is nicotinamide (K_0= 1.86 cm^2 V^{-1} s^{-1}), has a much higher intensity for the dynamic PSPME which translates to a larger pool of reactant ions to produce product ion peaks. The depletion of the RIP evident from the plasmagram of the manufacturer provided filter is likely due to the background peaks seen in this trace. In the positive polarity, this study targeted DPA (K_0= 1.61 cm^2 V^{-1} s^{-1}) and EC (K_0= 1.24 cm^2 V^{-1} s^{-1}). The background shown in figure 73C resulted from IMS analysis using the Itemiser 2. The RIP is nicotinamide at a drift time of 5.4 ms. There is no major difference observed between each trace. Piperonal is detected at 8.3 ms (K_0= 1.51 cm^2 V^{-1} s^{-1}).

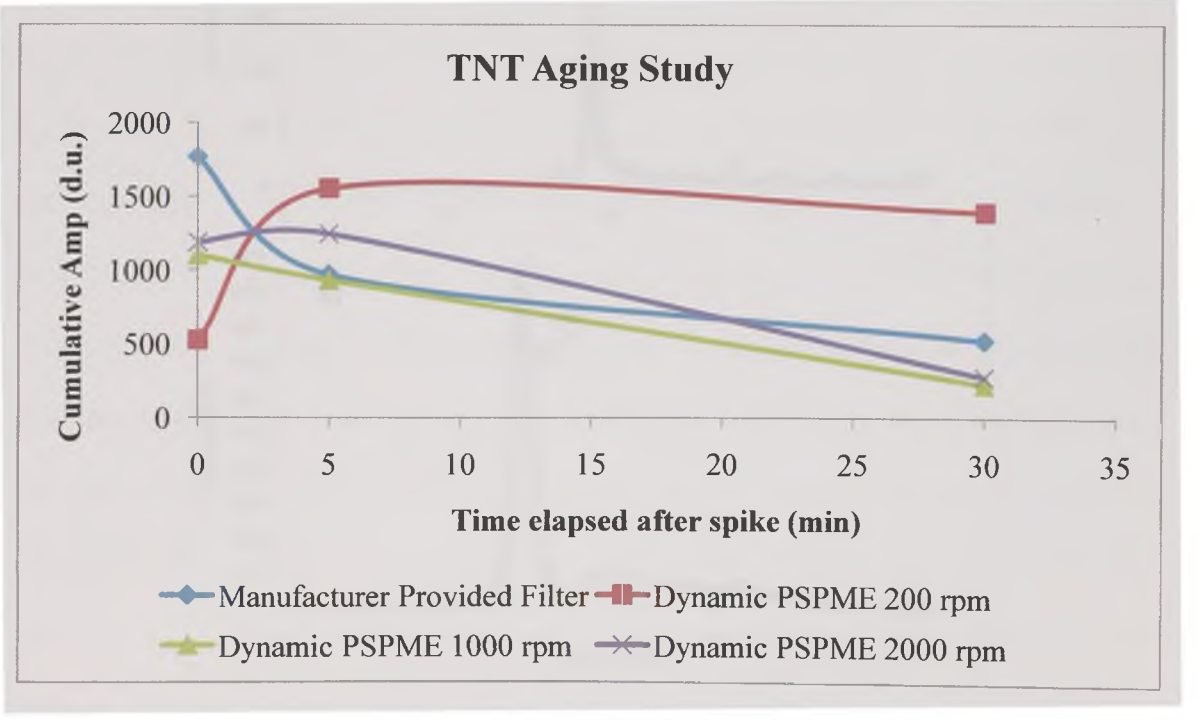

Figure 72. Aging Study of TNT in ACN on the Surface of Manufacturer Provided Filters and Dynamic PSPME Devices Created Using Various Spin Programs

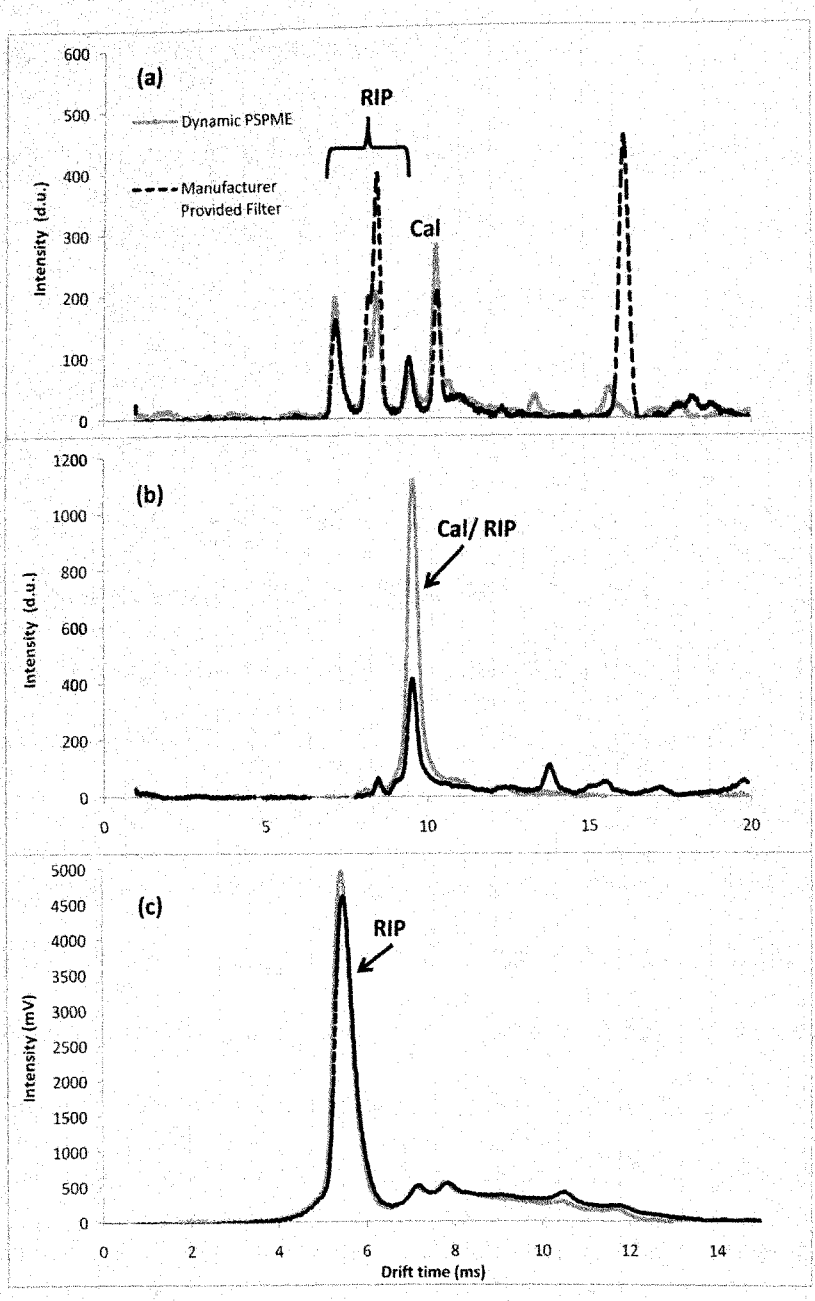

Figure 73. IMS Plasmagrams of Both the PSPME Device and Manufacturer Filter Blanks. IonScan 400B in negative polarity (a); IonScan 400B in positive polarity (b); Itemiser2 in positive polarity (c) [165]

7.3.2 Characterization of Final Dynamic PSPME Devices

The surface and cross-section of both the uncoated glass fiber filter and the dynamic PSPME device were characterized by SEM. Figure 74a displays the cross section of the glass fiber filter with a thickness of ~280 μm while figure 74b is that of the dynamic PSME device (thickness ~324 μm). This represents a 44 μm increase in thickness of the glass fiber filter following coating with sol-gel PDMS using the spin-coating program described in the Methods section. The porous nature of the dynamic PSME device is evident from the cross-section seen in figure 74b. This porosity provides additional surface area and capacity since more sites for partitioning/ absorption of analyte onto the extraction phase are available. This is expected to result in enhanced extraction efficiency and sensitivity in SPME-IMS. Additionally, improved desorption profiles compared to static PSPME are expected since: 1) the thickness of the dynamic PSPME device coating is much smaller, ~44 μm, as compared to 170 μm for static PSPME and 2) because the dynamic PSPME device allows flow through the sample media, it can take advantage of the suction/ sample flow of IMS instruments, that besides the high temperature of desorption, helps direct the analyte from the dynamic PSPME device into the IMS analyzer. Figure 74c and 74d display surface images of the uncoated glass fiber filter and dynamic PSPME device, which demonstrate retention of the porous properties in dynamic PSPME even after coating and final curing of the device.

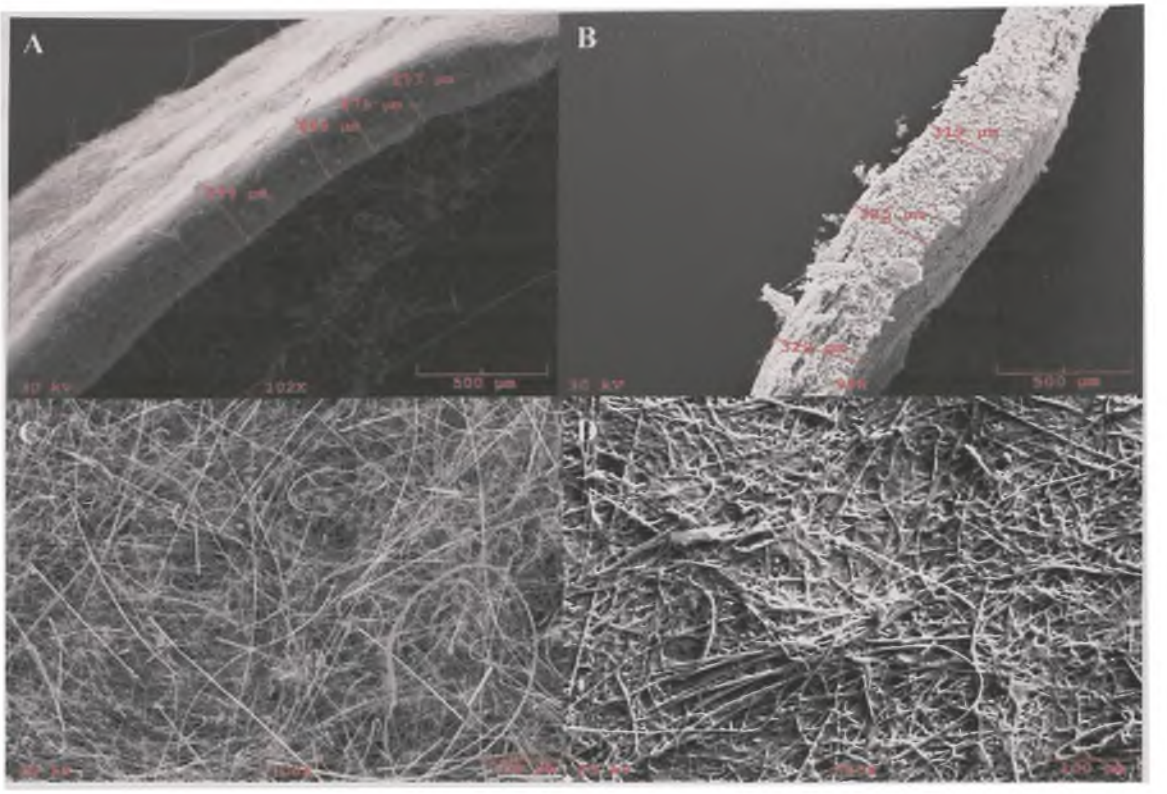

Figure 74. SEM Images of the Glass Fiber Filter and the Dynamic PSPME Device: the surface (c & d), and cross section (a & b), of the original substrate, the glass fiber filter (a & c) and the dynamic PSPME device (b & d) [165]

The dynamic PSPME device is placed in the slot of the handheld vacuum and the pump is turned on. The average air speed at the head of the nozzle was measured to be 0.5 m s^{-1} with a EA-3010U handheld anemometer (La Crosse Technology, La Crosse, WI). When sampling was done using the manufacturer provided filter, the air speed was measured to be an average of 1.3 m s^{-1}. The volumetric flow rate, Q, or the volume of fluid that passes through a surface (m^3 s^{-1}), is defined in equation 14 as:

$$Q = A \times v \times \cos\theta \quad \textbf{(Equation 14)}$$

where A is the area of surface (0.03 m), v is the velocity at the head of the nozzle (0.5 m s^{-1} for dynamic PSPME and 1.3 m s^{-1} for the manufacturer provided filter), and θ is the angle away from the perpendicular direction to A (in this case it is θ°). The values for the volume of air sampled per unit time, result in 0.35 L s^{-1} for dynamic PSPME and 0.92 L s^{-1} for the manufacturer provided filter. The resistivity encountered by using the dynamic PSPME device when compared to the manufacturer provided filter, evident from the 3-fold greater volume of air sampled for the former, is not surprising because of the durable, heat resistant, rugged sol-gel PDMS coating of the PSPME device that allows 100 times of use as other PDMS SPME devices, unlike the one-time use designated for these manufacturer provided filters. The handheld vacuum was chosen as the pump for these experiments since it represents a common and readily available accessory for sampling particles that can typically accompany the sale of commercial IMS and the training/use by security screeners.

7.3.3 Volatile Chemical Signature Standards for Dynamic PSPME Sampling

7.3.3.1 Spike on Manufacturer Provided Filters

Standard solutions of piperonal, 2,4-DNT, DPA, TNT and EC, were spiked onto the surface of both the dynamic PSPME and manufacturer provided filters, followed by analysis with the appropriate IMS instrument. Corresponding and reproducible cumulative signals (n=3, low SD see figure 76) were obtained from both filters for the standard solutions of most compounds proving their calibration with the Teflon manufacturer provided filter valid for further quantitation. Piperonal was dissolved in

DCM while DPA, TNT and EC were all dissolved in ACN, as described in the Methods section. An exceptional result was obtained for the compound 2,4-DNT. This compound was dissolved in hexane, a solvent with comparable volatility to 2,4-DNT, but when spiked over the dynamic PSPME surface yielded a response curve (equation 15) that underestimated the mass of 2,4-DNT detected following vapor sampling due because of the interaction of hexane with the sol-gel PDMS phase (almost instantaneous solvent evaporation). However, the generation of 2,4-DNT standard solutions on the manufacturer filters provided response curves for quantitation purposes.

$$y = 89.511x + 524.29, r^2 = 0.9846 \quad \textbf{(Equation 15)}$$

Table 9 summarizes the response curves determined for all target compounds by using the manufacturer provided filter for further quantitation in this study. All response curves exhibited a linear regression over the tested dynamic range. The results, including the r^2 values, are shown in Table 9 along with the IMS linear dynamic range (LDR) and minimal detection limit (MDL). Typical LDR's of one order of magnitude characterized these response curves. Standard solutions of piperonal, 2,4-DNT, DPA, TNT and EC, were analyzed individually using the appropriate IMS instrument. The response curves exhibited a linear regression over the tested dynamic range. Quantitation of TNT in a broader dynamic range of two orders of magnitude was enabled by determining two linear dynamic ranges along the low (0.025- 1 ng) and high (0.2-8 ng) concentrations, yielding for this compound the lowest LOQ and MDL of 0.025 ng. Two linear dynamic ranges can often been seen in IMS analysis since the pool of reactant ions available to yield product ions is temporally fixed. Because the kinetics of reactant ion formation are

much slower than reactant ion consumption, when higher concentrations are introduced, the reactant ion pool becomes depleted much faster than it can be regenerated, resulting in product ion signals that are lower than expected **[142]**. The signal/noise ratio obtained for the LDR's lowest concentration of piperonal, TNT and 2,4-DNT confirmed their LOQ as their MDL, while for the other analytes, lower LOD's than LOQ's are expected. Extrapolation for the minimal signal/noise ratio (S/N≥3) yielded estimated MDL's of 0.05 ng and 2 ng as detected masses of EC and DPA, respectively.

It is important to note that liquid spikes on a substrate do not necessarily desorb in the same fashion as absorbed vapor or swipe deposition, but this is remedied by using the cumulative amplitude, the sum of all the peak amplitudes that alert for the compound in IMS. Given complete desorption of the standard, meaning the signal returns to baseline before analysis ends, quantitation is possible because there is a specific instrumental response for a given mass introduced into the IMS.

Table 9. IMS Analysis Response Curves [165]

Analyte	Slope	Y Intercept	r^2	LDR (ng)	MDL (ng)
Piperonal	4039.8	12683	0.98	2-20	2
2,4-DNT	62.42	-75.28	0.97	5-50	5
DPA	23.88	579.3	0.83	5-50	2
TNT	1769.9	390.29	0.99	0.2-8	0.025
	2531.6	36.62	0.99	0.025-1	
EC	11097	-1275.1	0.90	0.1-1	0.05

7.3.3.2 Controlled Odor Mimic Permeation Systems (COMPS)

The COMPS devices made for each targeted compound were weighed over the course of 28 days (see Figure 75) to observe the mass loss as a result of the permeation of the compounds through the LDPE bags. In Figure 75, the mass of Pentolite remains the same throughout the 28 days (r^2=0.2581). There is no correlation between day and mass, in other words, there is essentially no permeation of any component of Pentolite through the LDPE bag. Since TNT possesses an appreciable vapor pressure (4.5×10^{-6} Torr @ 20 °C), it was expected to be able to escape from its mixture with the PETN and other components of the Pentolite mixture. Solid TNT (pure) was not used in the COMPS devices, since it is controlled and only available in dilute certified standard solutions with concentrations of only up to 1000 $\mu g\ mL^{-1}$. The dissipation of 2,4-DNT was calculated to be 15 ± 0.2 ng s^{-1} which would result in a sufficient amount released into the air after

several seconds, to then be pre-concentrated by the dynamic SPME device and detected by IMS. The same is true for the rest of the compounds, DPA, EC and piperonal with linear dissipation rates of 7.64 $\pm$ 0.17 ng s^{-1}, 0.93 $\pm$ 0.09 ng s^{-1}, and 34.7 $\pm$ 0.5 ng s^{-1}, respectively. A general trend is observed with these COMPS devices; the higher the vapor pressure of the compound in the COMPS device, the faster is dissipates through the LDPE bag. The TNT in Pentolite is an exception due to competition it encounters with the compounds in the mixture for release into the headspace, but if the COMPS device were made with solid TNT alone, the resulting dissipation rate is expected to be between those observed for DPA and EC. As another note, due to the volatility of piperonal, this compound shows a tendency for exponential decay (exponential fit; r^2=0.9891) as is permeates through the LDPE over the course of 28 days. This translates to a half-life of about 15 days. Since the other compounds (DPA, EC, and 2,4-DNT) are losing compound every second, then with each passing time interval there is essentially less starting material to continue to lose mass from. This exponential decay behavior would likely be experimentally observed when measuring the mass loss for time periods much longer than 1 month. This was not studied since the COMPS bags were developed as a simple and inexpensive calibration device, and are only meant for use within the time used to calculate the reported permeation rate.

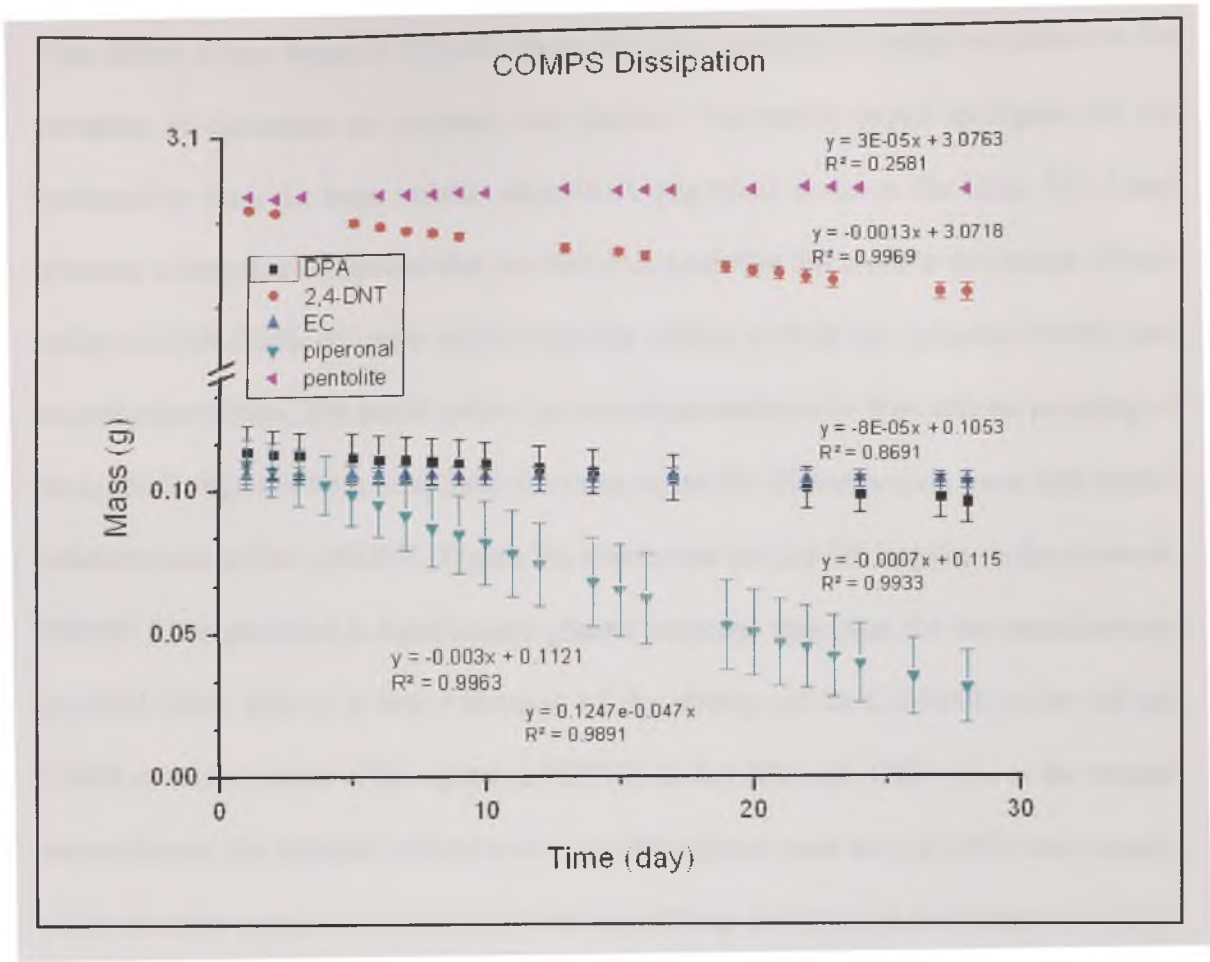

Figure 75. Dissipation Rates of Volatile Chemical Signatures in COMPS Devices [165]

7.4 Validation Experiments for Dynamic PSPME

7.4.1 Dynamic PSPME Retaining Capability Studied by Analyte Solution Spiking

The retention capability of the novel PSPME device for the pre-concentration of analytes sampled dynamically from air was studied first by directly spiking the standard analyte solution in a minimal solvent volume onto the substrate followed by clean air pumping.

The ability of the dynamic PSPME device to retain compounds when subjected to the pumping of increasing air volumes was studied. The results shown in Figure 76, are arranged by from the most volatile compound, piperonal, down to the least, EC. Equal amounts of targeted compound that resulted in a mass that fell close to the center of each analyte's LDR (Table 9), were spiked onto the surface of both the dynamic PSPME and manufacturer filters. The initial points, in immediate analyses (t= 0 s) with no pumping of air applied, originate from essentially the same signal for all compounds from both spiked substrates except for 2,4-DNT. Figure 76, shows that the 2,4-DNT spike on the dynamic PSPME filter provided a significantly greater response than that for the manufacturer provided filter. This is a first indication of the affinity of the 2,4-DNT to the sol-gel PDMS extraction phase of the dynamic PSPME device. The only difference in the sample preparation of the standard solutions was that the solvent used for 2,4-DNT was hexane, while the other compounds were dissolved in ACN, as described in the Methods section. Unlike ACN, the use of hexane enabled the generation of IMS response curve for 2,4-DNT quantification purposes. Another study **[59]**, suggested the hypothesis that 2,4-DNT desorbed slowly from surfaces preventing lower mass loadings from being detectable by IMS. Taking this into account, the dynamic PSPME device developed may also serve an additional purpose as an improved sampling surface for the calibration of IMS for 2,4-DNT, a compound that has proven difficult to introduce and reliably transport into the IMS reaction chamber. This extraction phase absorbs 2,4-DNT extremely well, retains it, and facilitates thermal desorption from the surface and by aid of the IMS sample tray flow.

Figure 76 clearly shows opposing trends for both the PSPME device and the manufacturer filter, while simulating dynamic sampling by pumping clean air through both substrates. After only a short time of pumping (10-15 s), an increased signal was obtained for all compounds spiked on the dynamic PSPME filter, while a large drop was measured for the manufacturer provided filter. Generally, while pumping air, unavoidable evaporation of the volatile solvent involved with the delivery of the analyte, is expected for both substrates. While significant co-evaporation of analyte was measured for the manufacturer provided filters, analytes were strongly retained on the adsorptive phase of the dynamic PSPME filter, confirming its efficient pre-concentration capability. The trend in increasing IMS signals measured for all compounds at only the shortest pumping time applied for the dynamic PSPME filters, when at least the same results as for t=0 were expected, can be explained. At t=0 s, since pumping is not applied, both the solvent and analyte are introduced into the IMS reaction chamber. The presence of the solvent in the reaction region can serve to cluster or solvate the reaction ions affecting both the thermodynamics and kinetics of ionization **[17]**. Since the available charge is shielded, the ionization of analytes becomes less favorable leading to diminished responses. Pumping for as little as 10 s aids in desolvation and maximizes interactions between the analyte and the reactant ions that lead to effective ionization.A study was conducted to evaluate the solvent effects encountered when attempting to quantitate extracted analytes by SPME using IMS and GC-MS response curves **[181]**. This study showed that by minimizing the solvent, from the μL range to the sub-nL range, both instrumentals responses were greatly enhanced.

The compounds, DPA, TNT, and EC are retained on the dynamic PSPME filter throughout the complete range of sampling time intervals, up to 70 s, as evidenced by the absence of signal decreases in these cases. The maximum sampling time, 70 s, was designated as a length of time that is amenable to field sampling and/or high throughput situations, allowing for multiple sampling before battery recharging or replacement is necessary. Piperonal signal increased up to 45 s of sampling time (Figure 76) after which the signal decreased 28 % from the initial amount. This is not surprising due to the volatility of piperonal and its tendency to remain in the headspace. Specifically, for the 2,4-DNT (Figure 76), after 30 s of pumping, there is some signal loss (2 % at 45 s), with 70 s of pumping causing the greatest signal reduction (33 %).

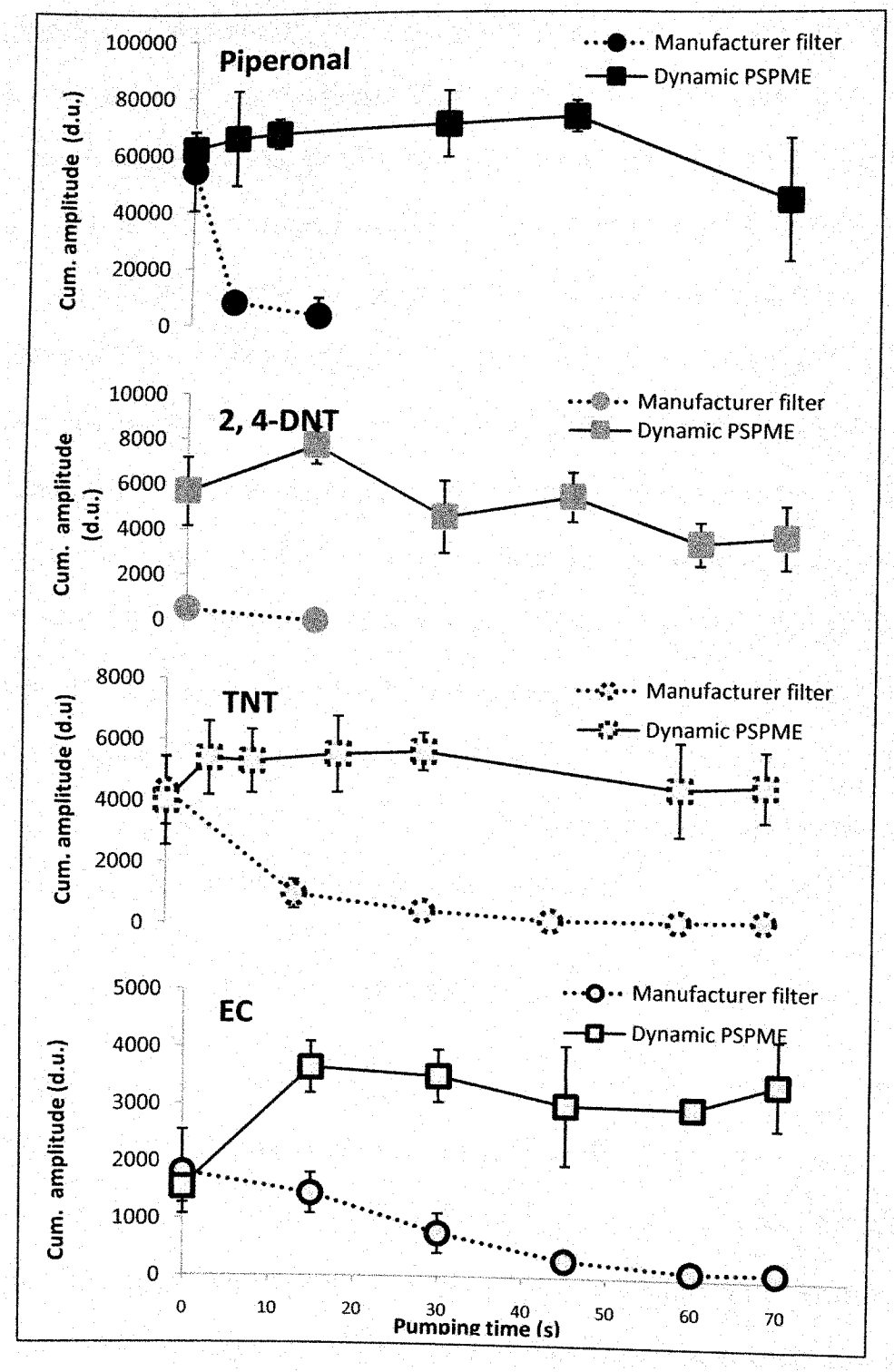

Figure 76. Retention Capability Study by Spiking Standard Solution of the Analytes onto the PSPME Surface Device Followed by Clean Air Pumping [165]

From Figure 76 it also evident that when spiking onto the manufacturer provided filter, pumping of only 15 s caused a large drop in retention for all the compounds, with the most being retained for EC (79%) and the least for 2,4-DNT (4%). The original designation of this filter is not for pre-concentration but rather for capturing particulate matter. There is no specific adsorptive/absorptive coating for collecting vapors as opposed to the dynamic PSPME device. The same would be concluded while analyzing the results taking into account total air volume sampled instead of pumping time. Even though the volume of air that was sampled is 3-fold higher for the manufacturer provided filter, when the sampling time is correlated with the appropriate sample volumes, dynamic PSPME still outperforms the manufacturer provided filter. For example, by comparing the 15 s sampling time for the manufacturer provided filter (13.8 L air sampled) with the 45 s sampling time for the dynamic PSPME device (15.75 L air sampled), the dynamic PSPME device still retains all of the starting compounds (100 % or greater), except 2,4-DNT which as previously mentioned, loses a mere 2%.

7.4.2 Dynamic PSPME Retaining Capability Studied by COMPS Vapor Source

The performance of the dynamic PSPME devices coupled to IMS analysis was estimated further by dynamic sampling of air containing the analytes. Controlled Odor Mimic Permeation Systems (COMPS) devices were used to generate vapor source of the tested analytes, which enabled quantitation of the maximum mass available in air for extraction. This was an alternate manner to simulate dynamic sampling in the field for detection of vapors emitted from drugs, high and low explosives in order to test the performance of dynamic PSPME device. The optimum sampling height was determined for 30 s of

pumping above the COMPS devices for each targeted compound. Sampling of piperonal, DPA, EC, and 2,4-DNT at the height of 10, 10, 5 and 5 cm, respectively, produced IMS responses within the linear dynamic range of each analyte. Figure 77 shows the pervasiveness of piperonal odor. This is indicated by the amount of piperonal that is detected reproducibly following dynamic PSPME sampling from even the farthest distance possible in the hood (40 cm high).

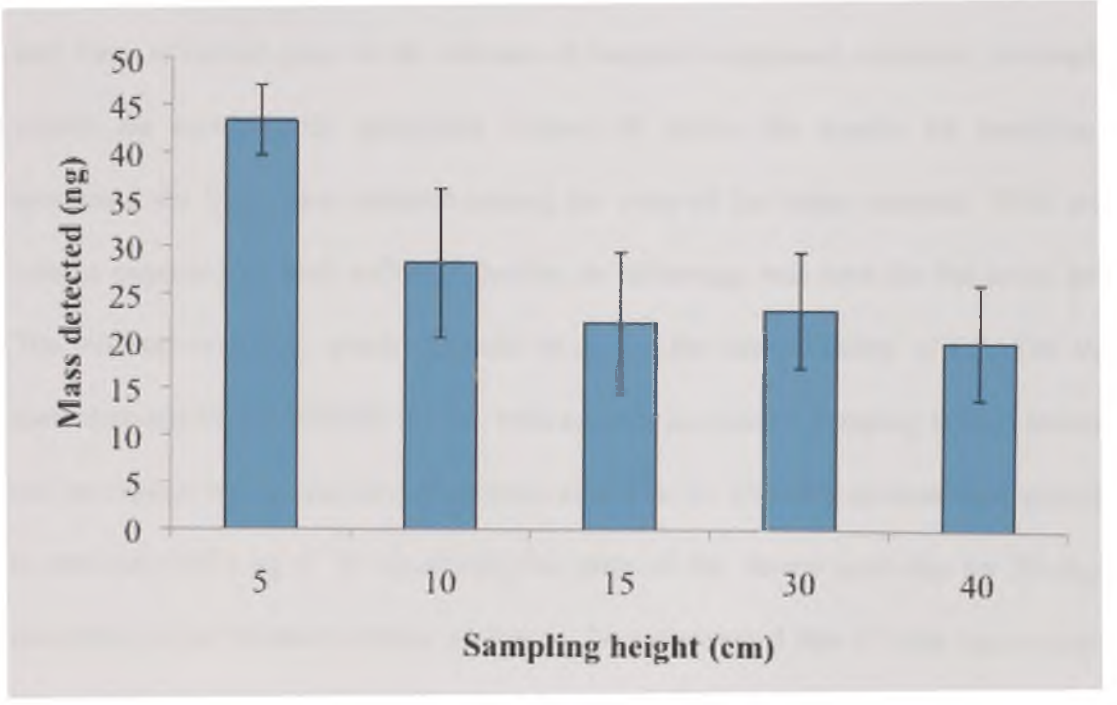

Figure 77. Mass of Piperonal Detected When Dynamically Sampling a COMPS Device for 30 s at Different Sampling Heights

At the selected sampling heights, the effect of pumping time was studied, and as with the retention capability study, the manufacturer provided filter was also tested for comparison purposes (Figure 78). It is key to note that on Figure 78, for the compounds,

piperonal, 2,4-DNT and DPA, there is an increasing trend of amount extracted versus the sampling time, demonstrating yet again the trapping capability of the dynamic PSPME device absorbent phase. Figure 78 depicts opposing results for the extraction of the same compounds using the manufacturer provided filter. No detectable amounts of DPA vapors were collected. Piperonal and 2,4-DNT were detected but at significantly lower masses. Moreover, those amounts collected remained constant regardless of sampling time. This demonstrates that the vapors sampled are being passed through this filter while pumping, and there is no net gain in the amount of targeted compound adsorbed, although the vapors are continuously generated. Figure 78 shows the results for sampling EC producing the least mass detected among the suite of the target analytes. With similar masses extracted by both collection media, no advantage was seen for the novel device. The minimal responses obtained could be due to the low volatility of EC. The steady mass detected by the PSPME device, with no gain in mass as pumping time is increased, can be explain by the analyte's dissipation rate. The EC COMPS devices were calculated to emit only 0.93 ng s^{-1} by measuring the mass of the device each day for 28 days as described in the Methods section. However, for a compound like EC that has a relatively low vapor pressure, this method of determining the dissipation rate may not directly correlate directly with seconds, thus not allowing steady and continuous generation of the vapors in this time scale. Evaluation of the PSPME device in sampling TNT vapors generated by COMPS bags was not possible since solid TNT (pure) was not available, and by using the only available source, Pentolite, no permeation through the LDPE bag was obtained. Overall, these results demonstrate the powerful pre-concentration power of

dynamic PSPME device desirable for rapidly (on the order of seconds) sampling trace amounts of volatile chemical signatures of illicit compounds in the field from air.

When considering extraction efficiency, or the mass detected divided by the mass available, the dynamic PSPME device performs much better than the manufacturer provided filter. The mass available is derived by the COMPS dissipation rates (ng s^{-1}) (Figure 75) multiplied by the sampling time (s) to give a total maximal mass available for extraction. For piperonal (Figure 78), 30-45s is required to extract the highest mass when considering only the sampling time, but when taking into account the mass of piperonal in air with every passing second, a sampling time of 15 s was the best, resulting in 4.9% extraction efficiency. Averaging the extraction efficiency for all sampling times, the dynamic PSPME device resulted in 3.4% versus 1% for the manufacturer provided filter. For 2,4-DNT, the average extraction efficiency was 3.1% and 0.42% for the dynamic PSPME device and the manufacturer provided filter, respectively. For DPA, detection was only possible with the dynamic PSPME device, whose best extraction efficiency was at 30 s, with an extraction efficiency of 12.4% (average of 6.3% for all sampling times).

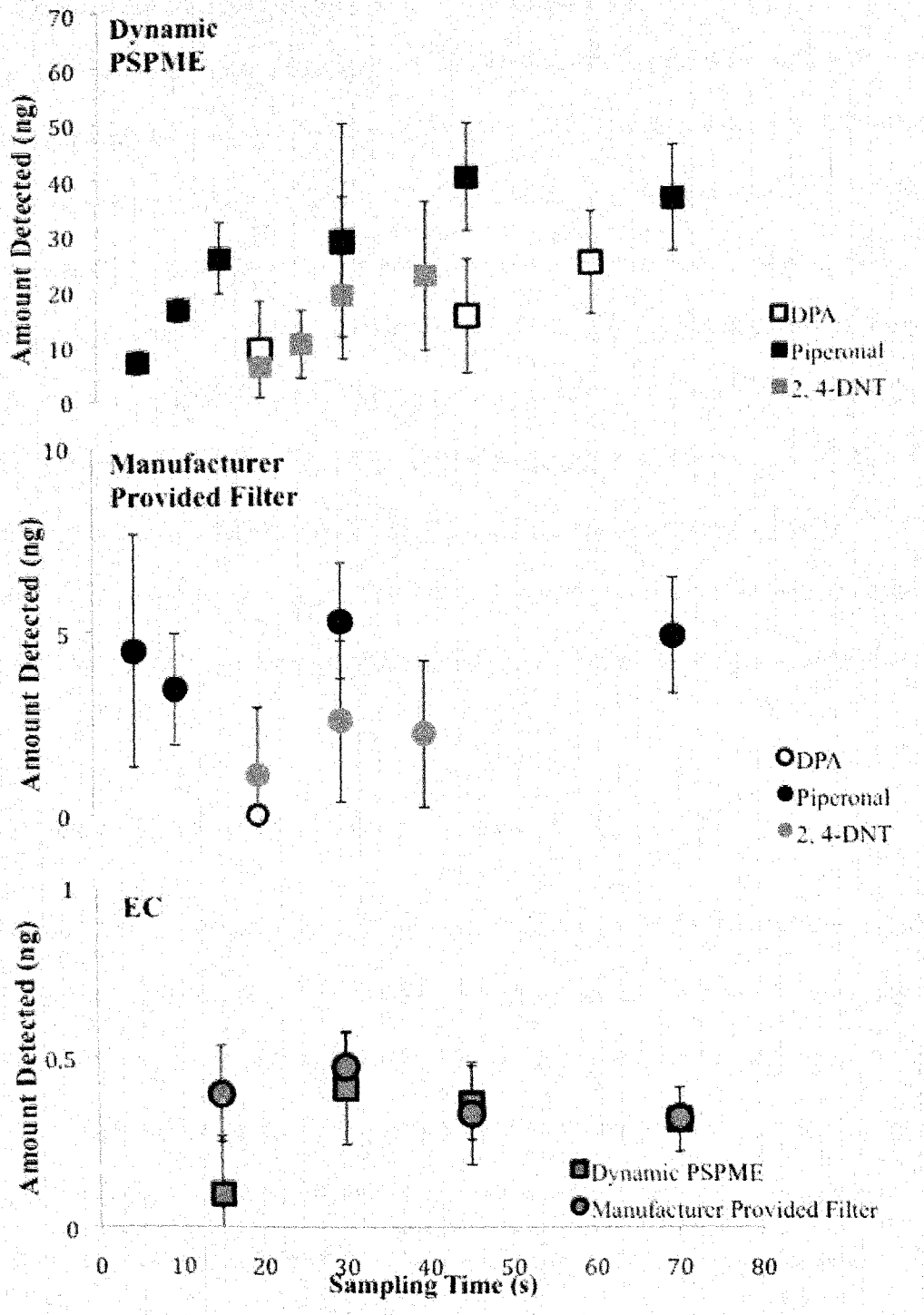

Figure 78. Retention Capability Study and Sampling Time Optimization by Dynamically Sampling Vapors of Analytes Emitted from COMPS Bags [165]

These large recoveries are a testament to the pre-concentration power of the dynamic PSPME device considering that sampling was conducted in an open laboratory clean bench on the scale of seconds. By employing a dynamic sampling scenario, the extraction device's mass uptake rate is increased and the boundary layer that has to be overcome in a static sampling scenario is decreased **[86]** thus allowing faster extractions. This, coupled with the large surface area of this porous dynamic PSPME device, provides greater capacity to capture a larger portion of the targeted analytes from air selectively. Another advantage of this selectivity is that artifacts that would cause competitive ionization in IMS, thus depressing signal of the target analyte, are not extracted/ detected from ambient air. Again, it is important to emphasize that the amounts detected also fell within the IMS LDR's for each compound, adding to the reliability of this quantification approach.

7.4.3 Dynamic PSPME LOD

The detection limits for the targeted compounds using the complete dynamic PSPME-IMS method were estimated. The method, based on three consecutive steps: dynamic sampling, desorption and detection, proved to be highly efficient in the first two stages with no virtually loss of sample, whereby determining the method's sensitivity became restricted by the third step, the IMS analysis. Accumulative extraction of a total mass of analyte onto the adsorbent phase of the novel device that is above the IMS analysis MDL is expected to alarm. The sensitivity of the PSPME-IMS method was estimated for each of the tested analytes in this study, considering a 10 s sampling time (total air volume of 3.5 L) as applicable to real case scenarios, followed by 100% efficient absorption on the

substrate and complete IMS desorption. The resulting LOD's, or the minimum amounts of target analyte that must be available in air for sampling, are as follows: 0.6, 1.5, 0.6, 0.01, and 0.02 ng L^{-1} for piperonal, 2,4-DNT, DPA, TNT, and EC, respectively.

7.4.4 Application of Dynamic PSPME- IMS for Screening of Illicit Compounds

The retaining capabilities obtained for the novel dynamic PSPSME device confirm its validity in detection of the target analytes from real case scenarios. The dynamic PSPME device was tested on the headspace of illicit compounds under conditions designed to simulate difficult sampling conditions in the field. These results along with the sampling conditions are listed in Table 10. Sample plasmagrams are shown in figure 79.

Suspected MDMA tablets were sampled and analyzed, in a blind study test, on-site at a local crime laboratory. Case 2 was negative for MDMA, by GC/MS, and this was corroborated by a negative response for piperonal by dynamic PSPME-IMS. Case 4 was positive for MDMA, from GC/MS data, and 40 ng of piperonal were detected by IMS following only 10 s extractions with 15 min of equilibration time. In the difficult scenario, case 1, minimal amounts of the MDMA drug were confirmed by GC/MS data, resulting in even less amounts of piperonal being present. Despite this, 11.7 ng of piperonal were detected from only a 10 s dynamic PSPME extraction in the first trial. Since 15 min was not a sufficient sealing time for such a small initial concentration of piperonal in the tablets to rebuild the headspace, no piperonal was detected for the two subsequent dynamic extractions. Because of time constraints related to sampling at this crime laboratory, the cans could not be sealed longer.

Table 10. Detection of Target Analytes from Real Case Samples Using the Dynamic PSPME–IMS Method [165]

Analyte	Emitting source		Source mass	Equilibrium time (h)	Pumping time (s)	Mass detected (ng)
Piperonal	Ecstasy tablets	Case 4 [178]	5 tablets (~1.5g)	24	10	40.0 ± 2
		Case 1 [178]				12
2,4-DNT	Smokeless Powder	IMR 4198	100mg	0.5	30	35.0 ± 11.5
		Hodgon H322				26.0 ± 14.0
DPA		Hodgon H322		24	60	38.0 ± 9.3
		IMR 4198				11.2 ± 2.5
		Unique				73.9 ± 13.4
		Red Dot				69.1 ± 18.6
EC		Red Dot		24	60	N/D

A mass of 100 mg of several brands of the smokeless powders (low explosives), were sealed in a quart can, opened, and sampled by dynamic PSPME. For 2,4-DNT detection in the negative polarity, only 30 min of sealing was required followed by 30 s of sampling dynamically in order to detect 35 ng from the IMR 4198 powder and 26 ng from the Hogdon H322 powder. This is significant, since in a previous study it was reported that although up to 41 ng of 2,4-DNT was detected by GC/MS following extraction from the headspace of 100 mg of these powders for 120 min in a 50 mL vial following equilibration, detectable amounts were not observed by SPME-IMS **[59]**. With dynamic PSPME, pre-equilibrium sampling of the same mass from a sample container with a volume 80-fold greater was possible in only 30 s resulting in the relatively same amount of 2,4-DNT being detected as by GC/MS.

In the positive polarity, the powders were sampled in a similar fashion except they were sealed overnight. DPA was detectable from the four powders following dynamic PSPME-IMS method (see Table 10), with lesser amounts detected from the powders that also contained 2,4-DNT. The smokeless powder Red Dot is known to contain both DPA and EC, but only DPA alarmed in this experimental scheme. As was shown in the COMPS sampling optimization, there was no accumulation of the EC on the dynamic PSPME even while sampling this compound alone. Additionally, the EC may in fact have been pre-concentrated, but its detection was likely inhibited by competitive ionization with DPA in the IMS ionization chamber. It is expected that in a sealed static sampling system using PSPME, or if a greater mass of the smokeless powders was used as is typical for improvised explosive devices (IEDs), then this compound would be detectable.

Additional research must be conducted to determine the optimal dynamic sampling parameters and IMS operating conditions to favor detection of the more discriminating compound, EC. Since smokeless powders are available in a variety of particle shapes, rods, discs, and balls, the difference in their surface area may affect the amount of the volatile chemical signature that is emitted into air. This phenomenon may inhibit an additive such as EC from being released despite that fact it is in the formulation, and should be investigated. In figure 80b a sample plasmagram from the dynamic sampling of an EC COMPS device for 30 s from 5 cm has been included. From these results, dynamic PSPME-IMS is a rapid and sensitive option for the detection of 2,4-DNT and DPA from a variety of smokeless powders, covering both IMS ionization polarities.

The high explosive, Pentolite, was sampled by the dynamic PSPME device targeting TNT. Although the COMPS device created for Pentolite showed no measurable dissipation, it was still sampled without the barrier of an LDPE bag expecting that the semi-volatile component, TNT would still be released. After sealing a small amount, 100 mg of this powder in a can for 1 hr and sampling only 30 s, an amount of 0.6 ng was detected by IMS, a value within the LDR.

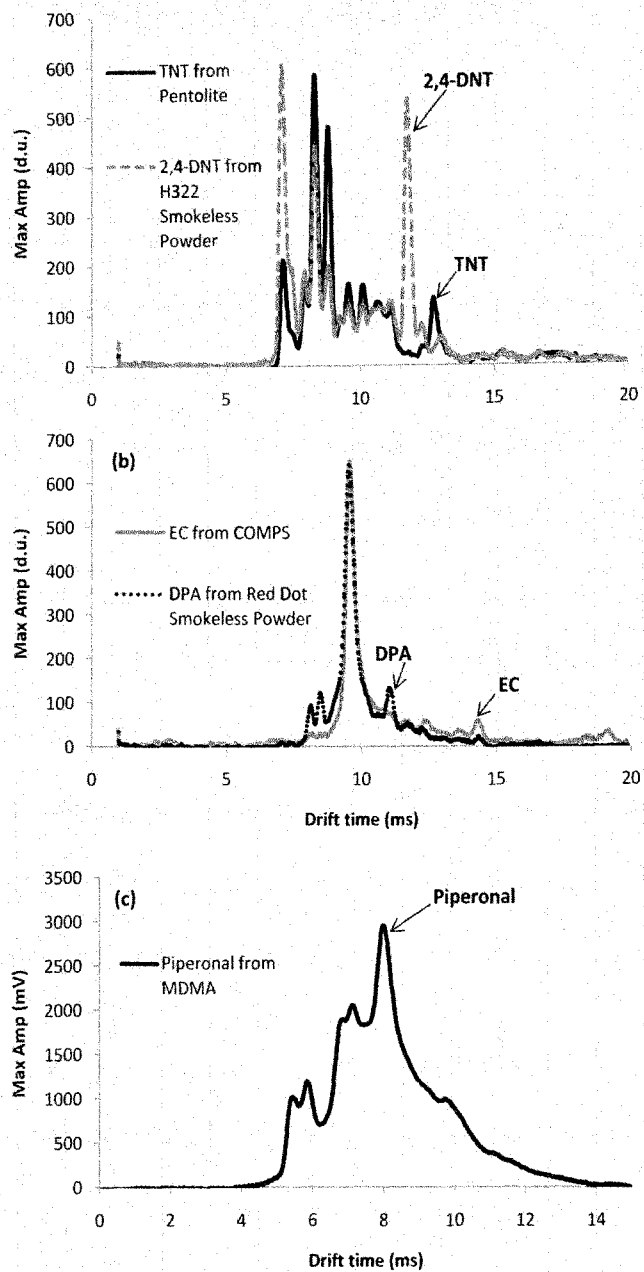

Figure 79. Sample IMS Plasmagrams Following Dynamic PSPME Sampling of Illicit Drugs and Explosives. a) TNT from Pentolite and 2,4-DNT from H322 Smokeless Powder, b) EC from COMPS and DPA from Red Dot Smokeless Powder, and c) Piperonal from MDMA [165]

CHAPTER 8. CONCLUSIONS

8.1 Static PSPME

This study has shown that by altering the widely-used SPME fiber type to a planar geometry SPME device, the surface area is greatly increased by a factor of 50 to 100 times. As a result, the capacity is also increased because the volume of the SPME phase is increased by a factor of at least 16 times over the fiber geometry. The use of PSPME for static sampling from closed systems enhanced analyte recovery at least 10 times when extracting even trace amounts. Another advantage is the decrease in equilibrium time required for extraction of TNT, from more than 10 hr down to 40 min, for example. Although sampling at equilibrium results in the highest signal, it has been shown that sampling at pre-equilibrium (on the order of min), does result in detectable signals. Because of the reduction in equilibrium time, faster on-site analyses can be conducted with this geometry when compared to fiber SPME.

When comparing two PSPME devices for the extraction of TNT, sol-gel PDMS takes longer to reach equilibrium than PDMS due to its increased capacity over PDMS PSPME, yet for shorter extraction times, PDMS produces a consistently higher signal. The PDMS PSPME device affords higher throughput with increased sensitivity at shorter extraction times, while sol-gel PDMS PSPME is designed for applications that can accommodate longer sampling times and require even higher sensitivity.

Extraction of more volatile compounds such as taggants (4-NT) and volatile signatures from their parent compounds (cyclohexanone from RDX, 2,4-DNT, etc.) has been shown

to be practical and effective when coupled with fast detection by IMS. In particular, the PSPME-IMS method was applied to the analysis of odor compounds from drugs at a local crime laboratory, where in a blind study of suspected MDMA tablets, 100 % correct detection of the target analytes was achieved in short sampling times (15 min). The SPME fiber-IMS method, although sensitive for the detection of piperonal, produced a false negative for one blind case that in fact had a minute concentration of MDMA. The extraction of piperonal with PSPME was enhanced over 600 times due to the capacity of PSPME that enabled quantitation of a dimer product ion peak seen at high concentration of piperonal. This peak was not seen in significant intensities when extracting by fiber SPME because capacity had been reached. The volatile chemical signatures of smokeless powders were also successfully extracted and detected using PSPME-IMS, where sampling of the standards proved difficult.

Alternate phase chemistries for static PSPME were also tested. Besides sol-gel PDMS, which demonstrated enhanced surface area and capacity from the presence of sol-gel nanoparticles, and PDMS that has fast absorption/desorption kinetics, selective coatings based on La (dihed) proved to enhance the extraction efficiency and retention of two important volatile chemical signatures, TNT and 2,4-DNT over sol-gel PDMS and PDMS PSPME devices. The results obtained provide motivation for continued work to further improve the thermal stability and reduce the hygroscopicity of the La (dihed) component by incorporation into a sol-gel network.

Finally, with PSPME, it is no longer necessary to fabricate an interface between SPME and each particular IMS instrument model since with the planar geometry of PSPME is

readily compatible with the already large installed base of IMS instruments. As a result, no significant modification of the security infrastructure should be necessary for implementation of PSPME for screening purposes.

8.2 Dynamic PSPME

The static PSPME pre-concentration device was improved by development of dynamic PSPME that enables rapid open air sampling of the volatile chemical signatures of drugs and explosives for direct introduction into existing IMS instruments. Dynamic PSPME is accomplished by use of a planar device that allows sampling of a large volume of air and has a high surface area for the capture and strong retention of these compounds from air. These attributes suggest dynamic PSPME as an exhaustive sampler, as opposed to the other SPME configurations that are generally considered as non-exhaustive, equilibrium-based sampling devices. This is advantageous when extracting trace amounts of volatile chemical signatures diluted in a large volume of air, as is the case when sampling in the field. Dynamic PSPME affords improved desorption profiles over static PSPME. This device was developed and optimized in a manner applicable to field sampling using an accessory, the handheld vacuum, as a portable, easy-to-use pump, that is already available and in use for the collection of particles.

The results obtained for the novel device demonstrate that even with a minimal amount of emitting source present, the dynamic PSPME-IMS method performs well as a rapid and sensitive screening tool applicable for field analysis.

Dynamic PSPME represents a significant improvement in detection of drugs and explosives via their volatile chemical signatures since it more closely resembles sampling by trained canines. Dynamic PSPME was tested on the same COMPS devices used to determine and calibrate canine sensitivity. This biological detector uses a dynamic sampling process to allow for rapid detection over a large search area. By coupling a sensitive, portable, and rapid dynamic sampling device (effective preconcentration of analytes present in air at the ppt level) with a sensitive (ng-pg detection limits) and rapid (ms response) detector, PSPME-IMS is one step closer to the gold standard in explosives and drug detection.

8.3 PSPME Terminology

It is important to emphasize that the PSPME devices developed in this research are based on the solid phase microextraction technique, with an alternative configuration. PSPME should not be thought of as an extension of solid phase extraction (SPE). SPE is a three-step process whereby the sample is passed through a sorbent bed and the sample is exhaustively extracted from the matrix to the sorbent material. In the second step, unwanted analytes (interferences) are removed from the sorbent by selecting an appropriate solvent/solution capable of desorbing the unwanted analytes. The desired analytes remain on the sorbent and then are washed out by another solvent/solution that is able to elute the desired analytes. This eluent can be concentrated to the desired volume by evaporation. SPME, on the other hand, is an equilibrium technique that employs a coating with a high affinity for the desired analytes. Mass transfer occurs upon contact with the sample, and the analytes are absorbed/adsorbed, depending on the phase

chemistry are subsequently introduced into the analytical instrument. There is no intermediate clean up step and SPME is a solvent-free technique. Additionally, SPME devices have an open bed structure relative to SPE devices where the sampling media (disks, packing, etc.) are packed into a cartridge. With SPME, the extraction phase is itself accessible for instrumental analysis.

The dynamic PSPME devices developed satisfy all these requirements. Extraction occurs when the device comes into contact with the sample (volatile chemical signatures in air), it has an open bed structure, no clean up is required, and the device has intimate and direct access to the instrumentation for desorption of the analytes from the extraction phase. Lastly, of the many configurations that SPME can take including fiber, vessel walls, disk/ membrane, etc, this is the first report of the planar configuration of SPME (high surface area) that allows both static and dynamic sampling (flow through and simultaneous extraction of volatile and semi-volatile compounds from air) for direct introduction into the IMS instrumentation. The work herein shows development of a novel PSPME device that allows air pumping, the dynamic sampling configuration of SPME, a considerable advancement since only static PSPME sampling was previously possible. Dynamic PSPME allows the open system sampling of air in seconds because of the reduction in boundary layer thickness resulting from constant agitation provided by pumping. The novel features of static and dynamic planar SPME, allow for the new acronym PSPME.

8.4 Implications of PSPME-IMS for Security

The advent of PSPME provides a much-needed rapid, sensitive and cost-effective pre-concentration and sampling device for security applications. First, this research has demonstrated that PSPME in both sampling configurations is effective at detecting drugs and explosives from large volume spaces. The PSPME device is operationally feasible since it is low cost, easy to use, reusable, and easily couples to existing IMS detectors. It is envisioned that the static PSPME devices can be placed inside cargo containers before transport in order to take advantage of the long dwell times during shipment, which can be up to 2 weeks. Then, upon arrival at port, IMS detectors, already in place, can be use to analyze the absorbed compounds on the devices. This would be a simple, non-intrusive and inexpensive way of helping to meet the screening of 100 % of cargo containers that could be implemented rapidly. A similar methodology could be extended to help meet the 100 % air cargo screening demand instead by using the dynamic PSPME method sampling near baggage much the same as canines are used. Additional applications of PSPME include medical screening for diseases from breath analysis and have yet to be explored.

8.5 Future Directions

Future work on PSPME would involve the development of alternate chemistries that provide more selectivity for the volatile chemical signatures even in the presence of interferents. The most obvious route is to continue to optimize the La (dihed) chemistry. Also, it was an unexpected result, but sol-gel dipped in methanol for 1 hr prior to

sampling increased extraction efficiency. Methanol is likely a porogenic solvent that further increases sites and surface area for absorption and this should be further explored.

In terms of dynamic PSPME, a net could be stamped out into a fiberglass filter, coated and, cured. This would allow sampling of a greater volume of air, which may help improve extraction outcomes.

Work on the field applications of static and dynamic PSPME should be continued. Cargo container sampling must be done to simulate conditions that the sampling devices would be subject to. The air around packaged explosives (military and improvised) must also be sampled, in conjunction with law enforcement, preferably with the dynamic PSPME since rapid sampling times would be required for this application. Lastly, in collaboration with military and law enforcement partners, the volatile chemical signatures of pre-blast and post detonation homemade explosive devices, made under different (illicit) protocols, must be determined by a confirmatory technique such as GC/MS. This would be followed by method development with PSPME-IMS.

REFERENCES

[1] Public Law 104-132, Antiterrorism and Effective Death Penalty Act of 1996; Section 603; April 24, 1996.

[2] Connelly, J.M.; Curby, W.A.; Fox, F.T.; and Hallowell, S.F. Detection of hidden explosives, In: *Forensic Investigations of Explosions*. Ed: Beveridge, A.D., 1998,Taylor & Francis, London, pp 45-74.

[3] Statement of the Sporting Arms and Ammunition Manufacturers' Institute in the H.R. 1710 (The Comprehensive Anti-Terrorism Act of 1995) hearings before the House Committee on the Judiciary, June 13, 1995, distributed to the committee on January 15, 1998.

[4] National Research Council. *Black and smokeless powders: technologies for finding bombs and the bomb makers,* 1998, National Academy Press, Washington, D.C.

[5] Public Law 110-53, 9/11 Act.; August 3, 2007.

[6] Air Cargo. http://www.tsa.gov/what_we_do/layers/aircargo/index.shtm, accessed January 4, 2010.

[7] Chris Strohm, U.S. Lacks Technology to Meet Air Cargo Screening Goal, March 19, 2009, http://gsn.ntl.org/gsn/nw_20090319_2186.php, accessed January 4, 2010.

[8] Container Security Initiative 2006-2011, U.S. CUSTOMS AND BORDER PROTECTION, Pub# 0000-0703 August 2006, Washington, D.C.

[9]Global Security Newswire, Napolitano Says U.S. Cannot Meet Cargo-Screening Goal, Thursday, December 3, 2009, http://www.globalsecuritynewswire.org/gsn/nw_20091203_5175.php, accessed January 4, 2010.

[10]Secure Freight Initiative, Department of Homeland Security, http://www.dhs.gov/files/programs/gc_1166037389664.shtm#2, accessed January 4, 2010.

[11]Lieberman, Collins React to Limited Progress on 100 Percent Cargo Scanning at Foreign Ports, Senate Committee on Homeland Security and Governmental Affairs http://hsgac.senate.gov/public/index.cfm?FuseAction=Press.MajorityNews&ContentRecord_id=5105ac86-5056-8059-76ae-28516ab3dfac, accessed January 4, 2010.

[12] The U.S. Coast Guard Strategy for Maritime Safety, Security, and Stewardship Washington, D.C. Pub # 20593-0001, January 19, 2007.

[13] Drug Interdiction, http://www.uscg.mil/hq/cg5/cg531/drug_interdiction.asp, accessed December 1, 2009.

[14] Office of Law Enforcement (CG-531), http://www.uscg.mil/hq/cg5/cg531/Drugs/stats.asp, accessed December 1, 2009.

[15] MDMA (Ecstacy) Abuse. National Institute On Drug Abuse. Pub# 06-4728. National Institutes of Health, Washington, D.C., March 2006.

[16] Cole, M. D. *The Analysis of Controlled Substances*. 2003, John Wiley and Sons West Sussex, England.

[17] Eiceman, Karpas *Ion Mobility Spectrometry*, 2nd Ed. CRC Press, Boca Raton, 2005.

[18] Griffy, T.A. A model of explosive vapor concentration II, in *Proceedings of the Fourth International Symposium on the Analysis and Detection of Explosives*. Ed.: J. Yinon, 1992, Kluwer-Academic, New York, pp. 503-511.

[19] Perr, J.M., Furton, K.G., Almirall, J.R., *J. Sep. Sci.* 2005, *28*, 177.

[20] Akhavan, J. *The Chemistry of Explosives*. 2nd Ed., Royal Society of Chemistry, 2004.

[21] Bender, E.C. Analysis of Low Explosives. In: *Forensic Investigation of Explosions*; Ed.:Beveridge, A.D., 1998, Taylor & Francis, London, pp 343-385.

[22] Hopler, R. B. In: Forensic Investigation of Explosives; Beveridge, A.D., Ed.; Taylor & Francis: London, 1998, pp 1-13.

[23] Heramb, R.M.; McCord, B.R. The Manufacture of Smokeless Powders and their Forensic Analysis: A Brief Review, *Forensic Science Communications*, April 2002 Vol 4 (2). http://www.fbi.gov/hq/lab/fsc/backissu/april2002/mccord.htm, accessed January 23, 2010.

[24] Furton, K.J.; Myers, L.J. *Talanta* 2001, *5,* 487.

[25] Yinon, J. *Trends in Analytical Chemistry* 2002, *21,* 292.

[26] Conrad, F.J. *Nuclear Materials Management* 1984, *13*, 212

[27] Harper, R.J.; Almirall, J.R.; Furton, K.G. *Talanta 67 (2005) 313.*

[28] Beveridge, A.D. *Forensic Sci Rev* 1992, *4(17)*, 18.

[29] DEA Mission Statement, http://www.justice.gov/dea/agency/mission.htm, accessed Jan. 23, 2010.

[30] Public Law 91-513, Controlled Substances Act, October 27, 1970.

[31] Savelli, L. *Street Drugs.* Looseleaf Law Publications, Inc. Flushing, NY, 2008.

[32] Dejarme, L. E.; Gooding, R.E.; Lawhon, S. J.; Ray, P.; Kuhlman, M.R. *Proceedings of SPIE-The International Society for Optical Engineering* 1997, *2937*, 19.

[33] Methyl benzoate [93-58-3], http://www.thegoodscentscompany.com/data/rw1015011.html, accessed January 23, 2010.

[34] Poulsen, H.A.; Sutherland, G.J. *Sci. Justice*, 2000, *40*, 171.

[35] Moffat, A.C. *Sci. Justice* 2002, *42*, 55.

[36] Lorenzo, N.; Wan, T; Harper , R.J.; Hsu, Y.; Chow, M.; Rose, S.; Furton, K.G. *Anal Bioanal Chem* 2003, *376*,1212.

[37] Shulgin, A. T. *J Psychoactive Drugs* 1986, *18*, 291.

[38] Davis W. M.; Borne, R. F. *Substance Alcohol Actions/Misuse* 1984, *5*,105.

[39] O'Brien B.A.; Bonicamp J. M.; Jones, D. W. *J Anal Toxico* 1982, *l6*, 143.

[40] Braun U, Shulgin AT, Braun G *J Pharm Sci* 1980, *69*,192.

[41] Eckenrode, B.; Bartick, E.G.; Harvey, S.; Vucelick, M.E.; Wright, B.W.; Huff, R.A. *Forensic Science Communications* 2001, *3* (4), http://www.fbi.gov/hq/lab/fsc/backissu/oct2001/eknrode.htm, accessed January 24, 2010.

[42] Eliasson, C.; Macleod, N. A.; Matousek, P. *Anal. Chim. Acta* 2008, *607,* 50.

[43] Lewis, I. R.; Daniel, N. W., Jr.; Chaffin, N. C.; Griffiths, P. R.; Tungol, M. W. *Spectrochimica Acta, Part A: Molecular and Biomolecular Spectroscopy* 1995, *51A*(12), 1985.

[44] Shibamoto, K.; Katayama, K.; Fujinami, M.; Sawada, T. *Review of Scientific Instruments* 2003, *74*, 910.

[45] Heflinger, D.; Arusi-Parpar, T.; Ron, Y.; Lavi, R. *Optics Communications* 2002, *204*, 327.

[46] Rodacy, P. J.; Bender, S.; Bromenshenk, J.; Henderson, C.; Bender, G. *Proceedings of SPIE-The International Society for Optical Engineering* 2002, *4742*, 474.

[47] Jackson, P. Development of methods that detect and monitor environment munitions contaminants using plant sentinels and molecular probes. Report 1996, AD-A309 583, 23 pp.

[48] Settles, G.S. *J. Fluid. Eng.* 2005, *127*, 189.

[49] Johnston, J.M. Institute for Biological Detections Systems, Auburn University, Alabama, 1999.

[50] Macias, M.S.; Guerra-Diaz, P.; Almirall, J.R.; Furton, K.G. *Forensic Sci. Int.* 2010, *195*, 132-138.

[51] Gardener, J.W; Bartlett, P.N. Electronic noses and principles and applications, Oxford University Press, Oxford.

[52] Yinon, J. *Anal. Chem.* 2003, *75*, 99A.

[53] SWGDOG SC1i – Terminology, http://www.swgdog.org, accessed January 21, 2010.

[54] MacCrehan, W.A.; Bedner, M. *Forensic Sci. Int.* 2006, *163*,119.

[55] Northop, D.M.; MacCrehan, W.A. Smokeless Powder Residue Analysis by Capillary Electrophoresis, National Institutes of Justice, 1997.

[56] Wissinger, C.E.; McCord, B.R. *J. For. Sci.* 2004, *479*,168.

[57] West, C.; Baron, G.; Minet, J.J. *Forensic Sci. Int.* 2007, *166*, 91.

[58] Harper, R.J.; Almirall, J.R.; Furton, K.G. Improving the scientific reliability of biological detection of explosives by canis familiaris through active odor signatures and their implications, in: *Proceedings of the 8th International Symposium on the Analysis and Detection of Explosives*, Ottawa, Canada, 2004.

[59] Joshi, M.; Delgado, Y.; Guerra, P.; Lai, H.; Almirall, J. R. *Forensic Sci. Int.* 2009, *188*, 112.

[60] Jenkins, T. F.; Leggett, D. C.; Miyares, P. H.; Walsh, M. E.; Ranney, T. A.; Cragin, J. H.; George, V. *Talanta* 2001, *54*, 501.

[61] Baez, B.; Correa, S. N.; Hernandez-Rivera, S. P. *Proceedings of SPIE* 2005, *5794*(2), 1263.

[62] Lorenzo, N. *M.S. Thesis*, Florida International University, Florida 2002.

[63] Furton, K.G.; Hong, Y.; Hsu, Y.; Lue, T.; Rose, S.; Walton, J. *Journal of Chromatographic Science* 2002, *40,* 147.

[64] Aarons, J.N.; Furton, K.G. *Proceedings of the American Academy of Forensic Sciences,* Washington DC, 2008, pp. 52-53.

[65] http://www.arb.ca.gov/db/solvents/solvent_pages/Ketones-HTML/cylclohexanone.htm, accessed January 21, 2010.

[66] Harper, R.J. *Ph.D. Dissertation.* 2005, Florida International University, Miami, FL.

[67] Nelson, G.O. *Gas Mixtures: Preparation and Control*, CRC Press, Boca Raton, FL, 1992.

[68] Koziel, J. A.; Martos, P. A.; Pawliszyn, J. *J. Chromatogr. A* 2004, *1025*, 3.

[69] Antohe, B. V.; Hayes, D. J.; Ayers, S.; Wallace, D. B.; Grove, M. E.; Christison, M. Portable Vapor Generator for the Calibration and Test of Explosive Detectors. In *Proceedings of the 2009 IEEE International Conference on Technologies for Homeland Security*; 2009 May 11-12; Boston, MA.

[70] Pawliszyn, J., *Solid Phase Microextraction: Theory and Practice*, Wiley-VCH, New York, 1997.

[71] Pawliszyn, J.; Liu, S. *Anal. Chem.* 1987, *59*, 1475.

[72] Belardi, R.G.; Pawliszyn, J. *Water Pollut. Res. J. Can.,* 1989, *24,*179.

[73] Arthur, C. L.; Pawliszyn, J. *Anal. Chem.* 1990, *62*, 2145.

[74] Risticevic, S.; Niri, V. H.; Vuckovic, D.; Pawliszyn, J. *Anal. Bioanal. Chem.* 2009, *393*, 781.

[75] Kataoka, H. *Anal. Bioanal. Chem.* 2009, in press, DOI 10.1007/s00216-009-3076-2.

[76] Hakkarainen, M. Adv. Polym. Sci. 2008, *211*, 23.

[77] Pawliszyn, J. Solid Phase Microextraction, In: *Comprehensive Analytical Chemistry XXXVII* Ed: Pawliszyn, J. 2002.

[78] Baltussen, E., Sandra, P., David, F., Cramer, C., *J. Microcol. Sep.* 1999, *11*, 737.

[79] Soini, H.A., Bruce, E.K., Wiesler, D., David, F., Sandra, P., Novotny, M.V., *J. Chem. Ecol.* 2005, *31*, 377.

[80] Bruheim, I., Liu, X., Pawliszyn, J., *Anal. Chem.* 2003, *75*, 1002.

[81] Hinshaw, J.V. *LCGC NORTH AMERICA* 2003, *21*, 1056.

[82] Wercinski, S.A.S., Pawliszyn, J., in: Wercinski, S.A.S. (Ed.), Solid phase microextraction theory, *Solid phase microextraction: a practical guide*. Marcel Dekker, Inc., New York, 1999.

[83] Isetun, S.; Nilsson, U.; Colmsjo, A. *Anal. Bionanal. Chem.* 2004, *380*, 319.

[84] Isetun, S.; Nilsson, U. *Analyst* 2005, *130,* 94.

[85] Larroque, V.; Desauziers, V.; Mocho, P. *J. Environ. Monit.* 2006, *8*, 106.

[86] Augusto, F.; Koziel, J.; Pawliszyn. *Anal. Chem.* 2001, *73*, 481.

[87] Ramsey, S. A.; Mustacich, R. V.; Smith, P. A.; Hook, G. L.; Eckenrode, B. A. *Anal. Chem.* 2009, *81*, 8724.

[88] Shirey, R. E. *J. Chromatogr. Sci.* 2000, *38*, 270.

[89] Jiang, G.; Huang, M.; Cai, Y.; Lv, J.; Zhao, Z. *J. Chromatogr. Sci.* 2006, *44*, 324.

[90] Harvey, S. *J. Chromatogr. A* 2008, *1213*, 110.

[91] Dintith, J. Facts on File Dictionary of Organic Chemistry, 2004 Market House Books, New York, NY.

[92] Dale E. Niesz, "Ceramics", in AccessScience@McGraw-Hill, http://www.accessscience.com, DOI 10.1036/1097-8542.121000, accessed Jan. 13, 2010.

[93] Kumar, A.; Gaurav; Malik, A.K.; Tewary, D.K.; Singh, B. *Anal. Chim. Acta* 2008, *610*, 1.

[94] Rath, K. Novel materials from solgel chemistry. Lawrence Livermore National Laboratory, *ST&R*, May 2005, 24-26.

[95] Fang, L.; Kulkarni, S.; Alhooshani, K.; Malik, A. *Anal. Chem.* 2001, *79*, 9441.

[96] Liu, W.; Hu, Y.; Zhao, J.; Xu, Y.; Guan, Y. *J. Chromatogr. A* 2006, *1102*, 37.

[97] Sarwar, M.I.; Ahmad, Z. *Eur. Polym. J.* 2000, *36*, 89.

[98] Tilgner, I.C.; Fischer, P.; Bohne, F.M. Rehage, H. Maier, W.F. *Microporous Mater. 5*, 1995, 77.

[99] Schmidt, H. Thin Films, The Chemical Processing Up To Gelation, In: *Structure and Bonding 77, Chemistry, Spectroscopy, and Applications of Sol-gel Glasses*, Springer-Verlag, Berlin Eds. Reisfeld, R. and Jørgensen, C.K.1992, pp 119-151.

[100] Sakka, S.; Yoko, T. Sol-gel coating films and applications. In: *Structure and Bonding 77, Chemistry, Spectroscopy, and Applications of Sol-gel Glasses*, Springer-Verlag, Berlin Eds. Reisfeld, R. and Jørgensen, C.K.1992, pp 89-118.

[101] Chong, S.L.; Wang, D.; Hayes, J.D.; Wilhite, B.W.; Malik, A. *Anal. Chem.* 1997, 69, 3889.

[102] Mackenzie, J.D., in: Mark, J.E.; Lee, C.C.Y.; Bianconi, P.A. (Eds.), *Hybrid Organic-Inorganic Composites, ACS Symposium Series*, vol. 585, American Chemical Society, Washington, D.C., 1995, p. 227.

[103] Ligor, M.; Scibiorek, M.; Buszewski, B. *Micro. Sep.* 1999, *5*, 377.

[104] Liu, Y.; Shen, Y.; Lee, M.L. *Anal. Chem.* 1997, *69*, 190.

[105] Liu, M.; Zeng, Z.; Fang, H. *J. Chromatogr. A* 2005, *1076*, 16.

[106] Cai, L.; Gong, S.; Chen, M.; Wu, C. *Analytica Chimica Acta* 2006, *559*, 89.

[107] Z.Y. Wang, C.H. Xiao, C.Y. Wu, H.M. Han, *J. Chromatogr. A* 2000, *893*, 157.

[108] J.X. Yu, L. Dong, C.Y. Wu, J. Xing, *J. Chromatogr. A* 2002, *978*, 37.

[109] Springer, C.S.; Meek, D.W.; Sievers, R.E. *Inorg. Chem.* 1967, *6*(6), 1105.

[110]Charles, R.G.; Perrotto, A. J. *Inorg. Nucl. Chem.*, 1964, *26*, 373.

[111] Eisentraut, K.J.; Sievers, R.E. *J. Am. Chem. Soc.* 1965, *87*, 5254.

[112] Taketatsu, T.; Banks, C.V. *Anal. Chem.* 1966, *38*, 1524.

[113] Davis, T.S.; Fackler, J.P. *Inorg. Chem.* 1966, *5*, 242.

[114] Feibush, B.; Richardson, M.F.; Sievers, R.E.; Springer, C.S. *J. Amer. Chem. Soc.* 1972, *94*, 6717.

[115] Brooks, J.J.; Sievers, R.E. *J. Chromatogr. Sci.* 1973, *11*, 303.

[116] Picker, J.E.; Sievers, R.E. *J. Chromatogr.* 1981, *203*, 29.

[117] Wenzel, T.J.; Yarmaloff, L.W.; St. Cyr, L.Y.; O'Meara, L.J.; Donatelli, M.; Bauer, R.W. *J. Chromatogr.* 1987, *396*, 51.

[118] Harvey, S.D.; Ewing, R.G.; Waltman, M.J. *Int. J. Ion Mobil. Spec.* 2009, *12*, 115.

[119] Skoog, D.A.; Holler, J.F.; Nieman, T.A. *Principles of Instrumental Analysis*, 5th Ed. Tompson Learning, 1998, United States.

[120] http://www.mse.iastate.edu/microscopy/backscatter.html, accessed January 20, 2010.

[121] http://www.mse.iastate.edu/microscopy/secondary.html, accessed January 20, 2010.

[122] Trejos, T. SEM basic training: Philips XL 30. Florida International University, April 2007.

[123] Solomons, G.T.W.; Fryhle, C.B. *Organic Chemistry*, 8th Ed. John Wiley & Sons, Inc., 2004, New Jersey, United States.

[124] Hop, C.E.C.A, Bakhtiar, R. *J. Chem. Edu.* 1996, *73*, A118.

[125] Kirkbride, K.P.; Klass, G.; Pigou, P.E. *J Forensic Sci* 1998, *43*(1), 76.

[126] Jenkins, T.F., Leggett, D.C., Ranney, TA. Vapor signatures from military explosives: part 1. vapor transport from buried military-grade TNT. Washington (DC): U.S. Army Cold Regions Research and Engineering Laboratory; 1999: *Special Report No. 99-21.*

[127] Muller, D.; Levy, A.; Shelef, R.; Abramovich-Bar, S.; Sonenfeld, D.; Tamiri, T. *J. Forensic Sci* 2004, *49*(5), 935.

[128] K.G. Furton , J.R. Almirall, M. Bi, J. Wang, L. Wu, *J. Chromatogr. A.* 2000, *885*, 419.

[129] Yonamine, M.; Tawil, N.; Moreau, R. L. M.; Silva, O. A. *J. Chromatogr. B.* 2003, *789,* 73.

[130] Kenji, M.; Tetsuya, A.; Takeshi, K.; Masae, I.; Yoko, M.; Hideki, H.; Akira, I.; Osamu, S.; Hiroshi, S. *Japanese Journal of Forensic Toxicology* 2005, *23*(1), 33.

[131] Fucci, N.; De Giovanni, N.; Chiarotti, M. *Forensic Sci. Int.* 2003, *134*(1), 40.

[132] Follador, M. J. D.; Yonamine, M.; Moreau, R. L. M.; Silva, O. A. *J. Chromatogr. B.* 2004, *811*(1), 37.

[133] Frank, M.; Junker, H. P.; Lachenmeier, D. W.; Kroener, L.; Madea, B. *Journal of Analytical Toxicology* 2002, *26*(8), 554.

[134] Frank, M.; Junker, H. P.; Lachenmeier, D. W.; Kroener, L.; Madea, B. *J. Chromatogr. Sci.* 2002, *40*(6), 359.

[135] Rodrigues de Oliveira, D.; Yonamine, M.; Moreau, R. L. M. *J. Sep. Sci.* 2007, *30*, 128.

[136] Koester, C. J.; Andersen, B. D.; Grant, P. M. *J. Forensic Sci.* 2002, *47*(5), 1002.

[137] Brown, H.; Kirkbride, K. P.; Pigou, P. E.; Walker, G. S. *J. Forensic Sci.* 2003, *58*(6), 1232.

[138] Keller, T.; Keller, A.; Tutsch-Bauer, E.; Monticelli, F. *Forensic Sci. Int.* 2006, *161*, 130.

[139] Lawrence, A.H.; Neudorfl, P.; Stoneb, J.A. *Int. J. Ion Mobil. Spec.* 2001, *209*, 185.

[140] Lawrence, A.H.; Neudorfl, P. *Anal. Chem.* 1988, *60*, 104.

[141] Miki, A.; Keller, T, Regenschiet, P., Dirnhofer, R.; Tatsuno, M.; Katagi, M.; Nishikawa, M.; Tsuchihashi, H. *J. Chromatogr. B* 1997, *692*, 319.

[142] Young, D.; Thomas, C.L.P; Breach, J.; Brittain, A.H.; Eiceman, G.A. *Analytica Chimica Acta* 1999, *381*, 69.

[143] Ewing, R.G.; Atkinson, D.; Eiceman G.A. ; Ewing, G.J. *Talanta* 2001, *54*, 515.

[144] Fythce, L.M.; Hupe, M.; Kovar, J.B.; Pilon, P. *J Forensic Sci* 1992, *37*, 1550.

[145] Gordon Research Conference, Detecting Illicit Substances: Explosives & Drugs-Sampling, Signatures And Clutter: Unconventional And Novel Approaches To Age Old Problems (Les Diablerets, Switzerland) June 17, 2009.

[146] Verkouteren, J. R.; Coleman, J. L.; Fletcher, R. A.; Smith, W. J.; Klouda, G. A.; Gillen, G. *Meas. Sci. Technol.* 2008, *19*, 115101 (12pp).

[147] GE Product Literature, The science behind ion trap mobility spectrometry, http://tracedetection.net/Itemiser_White_Paper.pdf, accessed January 22, 2010.

[148] Mina, N.; Hernández, S.P.; Román, F.R.; Rivera, L.A. *Int. J. Ion Mobil. Spec.* 2001, *4*(1), 37.

[149] Patent Application. US20090249897A1 2009-10-08 Transfer of Substances Adhering to Surfaces Into a Detection Instrument.

[150] Greenberg, D., Grigoriev, A.G., James, R., Lynds, P., Nacson, S., in: Garbutt, D., Pilon, P., Lightfoot, P.(Ed.), *Proceedings of the 8th International Symposium on Analysis and Detection of Explosives* 2004, 55.

[151] Hunter, J. A. Baumann, M. J.; Carlson, D. L.; Lenz, M. C.; Hannum, D. W.; Mitchell, M.; Gladwell, T. S.; Hobart, C. G.; Anderson, R. J.; Denning, D. J.; Peterson D.J. SAND Report 2005-5916, 2005.

[152] Parmeter, J. E.; Eiceman, G. A.; Rodriguez, J. E. NIJ Report 602–00 Trace Detection of Narcotics Using a Preconcentrator/Ion Mobility Spectrometer System April 2001, Washington, DC.

[153] Perr, J.M., Furton, K.G., Almirall, J.R., *Proc. SPIE Int. Soc. Opt. Eng.* 2005, *5778*, 667.

[154] Perr, J., *PhD Dissertation*, Florida International University, Florida 2005.

[155] Lai, H.; Corbin, I.; Almirall, J.R. *Anal. Bioanal. Chem.* 2008, *392*, 105.

[156] Lai, H.; Guerra, P.; Joshi, M.; Almirall, J. R. *J. Sep. Sci.* 2008, *31*, 402.

[157] Orzechowska, G.; Poziomek E.J.; Tersol, V. *Analytical Letters*, 1997, *30*, 1437.

[158] Liu, X., Nacson, S., Grigoriev, A., Lynds, P., Pawliszyn, J., *Anal. Chim. Acta* 2006, *559*, 159.

[159] Arce, L., Menedez, M., Garrido-Delgado, R., Valcarcel, M. *Trends Anal. Chem.* 2008, *27*, 139.

[160] Martin, M.; Crain, M.; Walsh, K.; McGill, R.A.; Houser, E.; Stepnowski, J.; Stepnowski, S.; Huey-Daw, W.; Ross, S. *Sensors and Actuators B* 2007,*126,* 447.

[161] http://www.solgel.com/articles/Nov00/mennig.htm, accessed Spring 2006.

[162] Lawrence, C.J. *Phys. Fluids* 1988, *31*, 2786.

[163] Product Information: Dow Corning Sylgard 184 Silicone Elastomer. Report No. 10-1204A-01.

[164] Picker, J.E.; Sievers, R.E. *Journal of Chromatography*, 1981, *203*, 29.

[165] Guerra- Diaz, Patricia; Gura, Sigalit; Almirall, José R. *Ana.l Chem.*, in press, DOI 10.1021/ac902785y.

[166] Overdiep, W.S. *Prog. Org. Coating* 1986, *14*, 159.

[167] Gu, J.; Bullwinkel, M.D.; Campbell, G.A. *J. Electrochem. Soc.* 1995, *142*(3), 907.

[168] Guerra, Patricia; Lai, Hanh; Almirall, José R.. *J. Sep. Sci.* (2008), *31*, 2891-2898.

[169] Laurell Technologies, Certificate of Calibration, Spin Processor S/N 07265.

[170] Dow Corning Product Information. Sylgard 184 Silicone Elastomer. Ref no. 10-1204A-01

[171] Supelco Product Information. Solid Phase Microextraction Fiber Assemblies. 1999, T794123N.

[172] Mehrotra, R. C.; Bohra, R.; Guar, D.P. *Metal β-diketonates and Allied Derivatives.* Academic press, 1978.

[173] Silverstein, R.M. *Spectrometric Identification of Organic Compounds*, 5th edition, John Wiley & Sons, Inc. 1991.

[174] Nakanishi, K. *Infrared Absorption Spectroscopy*, 2nd edition, Holden-Day, Inc, 1977.

[175]Wang, R.; Li, J.; Jin, T.; Xu, G.; Zhou, Z.; Zhou, X. *Polyhedron* 1997, *16*(8), 1361.

[176] Walker, F.A. Advances In Single and Multi-Dimensional NMR Spectroscopy of Paramagnetic Metal Complexes. In: *Spectroscopic Methods in Bioinorganic Chemistry*, 1998, American Chemical Society, San Francisco, CA.

[177] Binnemans, K. Rare-Earth Beta-Diketonates. In: *Handbook on the Physics and Chemistry of Rare Earths.* Vol 35, Ed. Gschneider, K.A., et.al. 2005, Elsevier, 107.

[178] Gura, S.; Guerra-Diaz, P.; Lai, H.; Almirall, J.R. *Drug Testing and Analysis*, 2009, *1*, 355.

[179] Eiceman, G.A.; Nazarov, E.G.; Rodriguez, J.E. *Analytica Chimica Acta* 2001, *433*, 53.

[180] Spangler, G. E.; Lawless P. A. *Anal. Chem.* 1978, *50*(7), 884.

[181] Gura, S.; Joshi, M.; Almirall, J.R. Personal communication, 2009.

APPENDIX A STATIC PSPME

A.1 Substrate Preparation

Prior to coating, cut 1 mm thick, pre-cleaned microscope slides (Chase Scientific Glass, Vineland, NJ), into 3.81 cm × 2.54 cm pieces. Dip the glass substrates individually into a 2:1 mixture of concentrated sulfuric acid (Fisher Scientific, Fair Lawn, NJ) and 30% hydrogen peroxide (Fisher Scientific, Fair Lawn, NJ) and placed in an oven at 90°C for 20 min. Decant the solution and rinse the substrates thoroughly with 18 mΩ deionized water. Dip each substrate in 1M NaOH for 1 hr to expose the silanols on the glass surface. Thoroughly rinse with deionized water to ensure wettability (no beading of water on the glass surface). Place the substrates in an oven at 120°C for 12 hr to dry.

A.2 Sol-gel PDMS

Dissolve 6.40 g vinyl-terminated polydimethylsiloxane (vt-PDMS) (Gelest, Inc., Morrisville, PA) in 8 mL of dichloromethane (DCM, Acros, New Jersey, USA); then add 3.42 mL of methyltrimethoxysilane (MTMOS, ≥ 98%) (Fluka, Steinheim, Germany) and 1.67 g poly(methylhydrosiloxane) (PMHS) (Sigma-Aldrich, Inc., St. Louis, MO), followed by 2.73 mL of trifluoroacetic acid (TFA, 99 %, Acros, New Jersey, USA), (5% water, v/v). Vortex the solution and allowed a 30 min stay. Dip the prepared substrate in the solution for 1 h. Place the planar sol-gel PDMS SPME device in the dessicator for 12 hr, followed by a 6 hr dip in dichloromethane. Gelate the sol-gel PDMS PSPME device by placing the it in a GC oven at 40 °C for 12 h. The next step is conditioning the sol-gel PDMS PSPME as follows: place the device in a GC oven under nitrogen atmosphere at

120°C for 1 hr, 240°C for 1 hr, and 300°C for 3 hr. Following conditioning, cool the device slowly to room temperature to prevent cracking of the phase.

A.3 PDMS by a Chlorine-Terminated Route

Spin-coat a prepared glass substrate with a 3:1 mixture of chlorine-terminated polydimethylsiloxane (Cl-PDMS) (Sigma-Aldrich, Inc., St. Louis, MO) and DCM as follows: deposit one mL of the coating solution on the substrate and activate the spin program, 1000 rpm for 60s. Place the PDMS planar SPME device in a dessicator at room temperature for 12 hr then dip in 18 mΩ deionized water to remove any excess hydrochloric acid that could result from the reaction. Place the PDMS PSPME device in a GC oven at 40°C following the rinse with deionized water condition in the same manner as the sol-gel PDMS (Section A.2).

APPENDIX B DYNAMIC PSPME

Prior to coating, cut glass fiber filter circles (G6, Fisherbrand, Pittsburgh, PA) down to 3.1 cm in diameter. Activate the surface of the glass fiber filter circles as described in Section A.1. Prepare a sol-gel PDMS solution in the following quantities: 2.060 g vt-PDMS dissolved in 8 mL of DCM; then add 1.10 mL of MTMOS and 0.5351 g PMHS, followed by 0.875 mL of TFA (Acros) (5% water v/v). Vortex the solution and allow a 30 min stay. Place the prepared glass fiber filter circle atop a cut glass slide held by vacuum on the chuck of a model WS-400B- 6NPP-LITE spin-coater (Laurell Technologies, North Wales, PA). Deposit one mL of the coating solution on the glass fiber filter circle and activate the spin program, 1000 rpm for 60 s. Place the newly coated substrate in the dessicator for 12 h, dip for 1.5 hr in DCM and gelate for 12 hr in an oven at 40 °C. Place the dynamic PSPME device in a GC oven in a nitrogen atmosphere at 120 °C for 1 hr, 240 °C for 1 hr, and 300 °C for 3 hr, for conditioning and to complete the curing process.

VITA

PATRICIA DIAZ

May 26, 1983	Born Miami, Florida
2005	B.S. Chemistry, minor in Sociology and Anthropology, Florida International University, Miami, Florida
2008	1st Place (oral presentation) Graduate Students' Association Scholarly Forum, Chemistry/ Physics
2009	Kauffmann Doctoral Student Fellowship The Ewing Marion Kauffman Foundation and the Eugenio Pino Entrepreneurship Center at FIU
2009	American Association for the Advancement of Science Member
2009	Sigma Xi, The Scientific Research Honor Society Associate Member
2009	1st Place (oral presentation) Graduate Students' Association Scholarly Forum, Physics/ Chemistry
2009	Dissertation Year Fellowship The FIU University Graduate School
2009	FIU Board of Trustees, Selected Graduate Student Speaker Academic Policy Meeting and Full Board Meeting
2010	Winner (poster presentation) FIU Department of Chemistry, Graduate Student Recruiting Day

PUBLICATIONS

2008 Lai, Hanh; Guerra, Patricia; Joshi, Monica; Almirall, Jose R. Analysis of volatile components of drugs and explosives by solid phase microextraction- ion mobility spectrometry. *Journal of Separation Science* (2008), *31(2),* 402-412.

2008 Guerra, Patricia; Lai, Hanh; Almirall, José R. Analysis of the volatile chemical markers of explosives using novel solid phase microextraction coupled to ion mobility spectrometry. *Journal of Separation Science* (2008), *31*, 2891-2898.

2009 Almirall, Jose; Perr, Jeannette; Guerra, Patricia. Method and apparatus for extraction, detection, and characterization of vapors from explosives, taggants in explosives, controlled substances, and biohazards. U.S. Pat. Appl. Publ. (2009), 12pp., Cont.-in-part of U.S. Ser. No. 630,559.

2009 Joshi, Monica; Delgado, Yisenny; Guerra, Patricia; Lai, Hanh; Almirall, José R. Detection of odor signatures of smokeless powders using solid phase microextraction coupled to an Ion Mobility Spectrometer, *Forensic Science International* (2009), *188*, 112-118.

2009 Gura, Sigalit; Guerra-Diaz, Patricia; Lai, Hanh; Almirall, José R. Enhancement in sample collection for the detection of MDMA using a novel planar SPME (PSPME) device coupled to ion mobility spectrometry (IMS), *Drug Testing and Analysis*, [invited article, cover page article] (2009), *1*, 355-362.

2010 Macias, Michael M.; Guerra-Diaz, Patricia; Almirall, José R.; Furton, Kenneth G. Detection of piperonal emitted from polymer controlled odor mimic permeation systems utilizing Canis familiaris and solid phase microextraction-ion mobility spectrometry, *Forensic Science International*, (2010), *195*, 132-138.

2010 Guerra- Diaz, Patricia; Gura, Sigalit; Almirall, José R. Dynamic Planar Solid Phase Microextraction (PSPME)- Ion Mobility Spectrometry (IMS) for Rapid Field Air Sampling and Analysis of Illicit Drugs and Explosives, *Analytical Chemistry*, in press, DOI 10.1021/ac902785y.

PRESENTATIONS

2006 Poster "Portable Raman Spectroscopy for Narcotics Detection," American Academy of Forensic Sciences 58th Annual Meeting, *Young Forensic Scientist Poster Session*, (International)

2006 Poster "Detection of Explosives Using Volatile and Semi-Volatile Chemical Markers by SPME-IMS," Explosives Detection Conference sponsored by TSWG (Technical Support Working Group), (National)

2006 Poster "Detection of Explosives Using Volatile and Semi-Volatile Chemical Markers by SPME-IMS," 15th International Conference on Ion Mobility Spectrometry, (International)

2007 Poster "New SPME coatings for explosives detection by ion mobility spectrometry (IMS)," American Academy of Forensic Sciences 59th Annual Meeting, (International)

2007 Poster "A novel solid phase microextraction geometry for explosives detection by ion mobility spectrometry," Nanoelectronic Devices for Defense and Security (NANO-DDS) Conference, (National)

2008 Oral "Demonstration of the utility of a planar geometry SPME device for use with ion mobility spectrometers," American Academy of Forensic Sciences 60th Anniversary Meeting, (International)

2008 Oral "Planar SPME-IMS for the detection of threat agents," Florida Annual Meeting and Exposition (FAME) sponsored by the American Chemical Society, (Regional)

2009 Oral "High-volume dynamic sampling using planar SPME coupled with IMS for the detection of explosives," American Academy of Forensic Sciences 61st Annual Meeting, (International)